

CARPATHIAN-BALKAN GEOLOGICAL ASSOCIATION  
XVI CONGRESS

**Field Trip Pre1**  
**TRANSSECT THROUGH THE CENTRAL EASTERN ALPS**  
Coordination: Franz Neubauer & Johann Genser  
24 August – 29 August 1998



AUGUST 30<sup>th</sup> to SEPTEMBER 2<sup>nd</sup>, 1998  
Geocenter, University of Vienna,  
Althanstraße 14,  
1090 Vienna, AUSTRIA

Geological Survey of Austria  
Austrian National Committee of Geology  
Geological Society of Austria  
Austrian Academy of Sciences



## Preface

The excursion "Transect through central Eastern Alps" is aimed to provide an overview of the principal structural units of Alps. The geology of Eastern Alps made much progress during the last two decades. New stratigraphic, geochronological, petrological and structural data significantly changed models on the evolution of the Eastern Alps. Among these, the evidence of Meliata-type deep sea sediments within the Northern Calcareous Alps is of prime importance. Consequently, the Eastern Alps represent an important link between the geology of the Western Alps and the Carpathian-Balkan-Dinaric chains. The latter chains appear to be clues for understanding of the Alps. Furthermore, quantitative modelling presents new insights on possible processes which were considered separately until now. E.g., there are good arguments that pressure-temperature-deformation-time paths from metamorphic sequences are the expression of the same lithospheric-scale processes as basin subsidence.

The first part of the Field Guide presents some introductory papers, the second part descriptions of stops. The excursion will present some classical outcrops from various tectonic units and many new data. The organizers of the excursion like to express their thanks to companies which are giving access to their quarries: Fa. Hatscheck (Gmunden), Leube (St. Leonhard), Fa. Kiefer (Fürstenbrunn). The organizers gratefully acknowledge the efforts of coworkers including PhD and MSc students which contributed to the field guide. These are: Dr. Robert Handler, Dr. Hans-Peter Steyrer, Dr. Xianda Wang, Dr. Franz Nemes, Dr. Joachim Schweigl and Stefan Freimüller.

Much of the work presented in this Field Guide "Transect through central Eastern Alps" has been supported by Austrian research funding agencies. We acknowledge support by grants P9918-GEO and 10,506-GEO of the FWF and grant 4786 of the 'Jubiläumsfonds der Österreichischen Nationalbank to F.N., and of J0814-GEO and P12,777-GEO to JG.

Salzburg, August 1998

Franz Neubauer and Johann Genser



Carpathian-Balkan Geological Association, XVI Congress	Field Guide "Transect through central Eastern Alps"	p. 2	Salzburg - Wien, 1998
--	---	------	-----------------------

## Table of contents

	Page
The structure of the Alps: an overview ( <i>by F. Neubauer, J. Genser, R. Handler and W. Kurz</i> )	7
Stratigraphy and hydrocarbons in the molasse foredeep of Upper Austria and Salzburg ( <i>by H. Polesny</i> )	25
Late orogenic rebound and oblique Alpine convergence: new constraints from subsidence analysis of the Austrian Molasse basin ( <i>by J. Genser, S. Cloetingh and F. Neubauer</i> )	33
New $^{40}\text{Ar}/^{39}\text{Ar}$ and geochemical data from the Molasse zone ( <i>by D. Schneider, F. Neubauer, J. Gense, Handler and D. Topa</i> )	45
Petrography of sandstones of the Rhenodanubian Flysch Zone of the Salzburg Region ( <i>by F. Neubauer and R. Handler</i> )	49
The Rhenodanubian/Helvetic thrust wedge in the Attersee to Traunsee region ( <i>by St. Freimüller, F. Neubauer and J. Genser</i> )	53
Deformation phases and age data of the Austro-Alpine-Penninic plate boundary, Eastern Tauern Window ( <i>by J. Genser</i> )	65
Middle and Upper Austroalpine units of Gurktal Mountains/Nock region ( <i>by F. Neubauer, B. Koroknai, J. Genser, R. Handler and D. Topa</i> )	85
Transect through central eastern Alps: Description of stops ( <i>by J. Genser, F. Neubauer, St. Freimüller, R. Handler, B. Koroknai, D. Mader, F., Nemes H. Polesny, J. Schweigl, H.P. Steyrer, X. Wang</i> )	102



Carpathian-Balkan Geological Association, XVI Congress	Field Guide "Transsect through central Eastern Alps"	pp. 7 - 24	Salzburg - Wien, 1998
--	--	------------	--------------------------

## **The structure of the Alps: an overview**

**F. Neubauer<sup>1</sup>, J. Genser<sup>1</sup>, R. Handler<sup>1</sup> and W. Kurz<sup>2</sup>**

<sup>1</sup> Institut für Geologie und Paläontologie, Hellbrunnerstr. 34, A-5020 Salzburg, Austria.

<sup>2</sup> Institut für Geologie und Paläontologie, Heinrichstr. 26, A-8010 Graz, Austria

### **Abstract**

New data on the present structure and the Late Paleozoic to Recent geological evolution of the Eastern Alps are reviewed mainly in respect to the distribution of Alpidic, Cretaceous and Tertiary, metamorphic overprints and the corresponding structure. Following these data, the Alps as a whole, and the Eastern Alps in particular, are the result of two independent Alpidic collisional orogens: The Cretaceous orogeny formed the present Austroalpine units *sensu lato* (including from footwall to hangingwall the Austroalpine *s. str.* unit, the Meliata-Hallstatt units, and the Upper Juvavic units), the Eocene-Oligocene orogeny resulted from continent-continent collision and overriding of the stable European continental lithosphere by the Austroalpine continental microplate. Consequently, a fundamental difference in present-day structure of the Eastern and Central/Western Alps resulted. Exhumation of metamorphic crust formed during Cretaceous and Tertiary orogenies resulted from several processes including subvertical extrusion due to lithospheric indentation, tectonic unroofing and erosional denudation. Original paleogeographic relationships were destroyed and veiled by late Cretaceous sinistral shear, and Oligocene-Miocene sinistral wrenching within Austroalpine units, and subsequent eastward lateral escape of units exposed within the central axis of the Alps along the Periadriatic fault system due to the indentation of the rigid Southalpine indenter.

### **Introduction**

Facts and models on Alpine geology made rapid progress during the last decades, mainly due to detailed paleogeographical, structural, petrological and geochronological investigations. These, together with deep reflection seismic profiling allowed new insights into the present-day structure and triggered new models which fundamentally changed ideas on Alpine geology (e.g., NICOLAS ET AL., 1990; PFIFFNER, 1992; PFIFFNER et al., 1997).

This review intends to synthesize principal structural data of the Eastern Alps in respect to the distribution of Alpine metamorphism. The review also includes some redefinitions of paleogeographic and tectonic units exposed within the Eastern Alps that appear to be necessary according to the present state of data. The time scale calibrations follow that of the Paleozoic and early Cenozoic by Gradstein and Ogg (1996) of the Mesozoic proposed by Gradstein et al. (1994), and of the Paratethyan Oligocene-Neogene proposed by Rögl (1996).

Aspects of the tectonic evolution Eastern Alps were reviewed in JANOSCHECK and MATURA (1980), OBERHAUSER (1980, 1995), TOLLMANN (1977, 1986, 1987), FRANK (1987),

THÖNI AND JAGOUTZ (1993), FROITZHEIM et al. (1996), EBNER (1997) and FAUPL (1997). The evolution of the pre-Alpine basement is reviewed in VON RAUMER and NEUBAUER (1993).

### **Tectonic units**

The Alps are divided in a geographical sense into the E-trending Eastern Alps and the arc of the Western Alps, divided by the meridional Rhine valley south of the Bodensee and its southward, meridional extension. Eastern and Western Alps display fundamentally different geological structure (see below), geological development and in part a distinct geomorphology. The most prominent mountain peaks are along the central axis in the Eastern and Swiss Central Alps, and more internally located in the Western Alps forming here an asymmetric topographic profile. East of the Tauern window area, the topography gradually changes from high elevations into the Neogene Pannonian basin with its plains and a very low elevation above sea level (Fig. 1).

The Alps as a whole include the following tectonic units from footwall to hangingwall, respectively from N to S, and NW to SE (e.g., DAL PIAZ, 1992; DEBELMAS, 1997; TRÜMPY, 1980, 1997a, b; TOLLMANN, 1977; FRANK, 1987; FAUPL, 1997) (Figs. 1, 2, 3):

(1) The stable respectively south- and eastwards flexured European continental lithosphere which also carries the late Eocene to Neogene Molasse basin, the northern peripheral foreland basin; and the Swiss-French Jura, an externally located thin-skinned fold-and thrust belt (e.g., TRÜMPY, 1980, 1997a, b);

(2) the Dauphinois/Helvetic units, a thin-skinned fold and thrust belt, that nearly exclusively comprise Late Carboniferous to Eocene cover sequences detached from the European lithosphere and the External massifs which constitute pre-Alpine basement rocks and Helvetic, Late Carboniferous to Cretaceous cover sequences (DEBELMAS et al., 1983);

(3) the Valais units which represent the infilling of a mainly Cretaceous rift zone on attenuated continental to likely oceanic crust (PFIFFNER, 1992);

(4) the Briançonnais units which represent a microcontinent rifted off from stable Europe during opening of the Valais trough;

(5) the Piemontais units with oceanic lithosphere in the Western Alps; the Glockner ophiolitic nappe exposed within the Tauern window and its correlatives exposed in other windows along the central axis of the Eastern Alps, the Ybbssitz ophiolite (DECKER, 1990; SCHNABEL, 1992) and overlying flysch sequences as well as the Rhenodanubian flysch zone with remnants of a trench filling alone without any substrate may represent part of this zone. The Valais, Briançonnais and Piemontais units are conventionally combined to Penninic units also assigned as North, Middle and South Penninic units, respectively;

(6) the Austroalpine s. str., a continental unit which includes remnants of a Triassic passive continental margin which originally faced towards the Hallstatt-Meliata ocean (e.g., LEIN, 1987) and a Jurassic passive continental margin which faced towards the Penninic (Piemontais) oceanic tract;

(7) the Hallstatt-Meliata units with its remnants of the infilling of a small oceanic trough and the adjacent distal continental margins;

(8) the Upper Juvavic unit that exclusively comprises late Paleozoic to Mesozoic cover sequences of a passive continental margin;

(9) and finally, the Southalpine unit juxtaposed along the Periadriatic Fault to the Austroalpine units s. str.. The Southalpine unit is another continental unit that is largely similar to the Austroalpine unit s. str.. The Southalpine unit is considered to represent the northern extension



of the stable Adriatic microplate which also includes the Po plain and the adjacent Adriatic Sea (e.g., CHANNEL et al., 1979).

The Alps are sometimes divided into external, sedimentary, unmetamorphic units and internal units dominated by highly deformed metamorphic rocks. This division applies well in Western Alps. There, the *external zones* include : (1) the Dauphinois-Helvetic zone comprising External basement massifs and their Late Carboniferous to Mesozoic cover, and Mesozoic-Cenozoic cover sequences separated into so-called Subalpine massifs. Both basement and cover massifs are clearly allochthonous in the Swiss Western Alps; and, more internally located, (2) the Ultradauphinois-Ultrahelvetic zone.

In the Eastern Alps, the external zones are small and include the Helvetic/Ultrahelvetic zones, the latter imbricated with the Rhenodanubian Flysch zone, a Penninic unit. From a structural point of view, the Northern Calcareous Alps also belong to unmetamorphic external zones.

The Southalpine unit is considered as the southern external retro-arc orogenic wedge within the Alpine orogenic system (e.g., DOGLIONI and FLORES, 1997; SCHMID et al., 1996).

Compared with previous interpretations, the Ybbssitz ophiolite and the subdivision of the previous Austroalpine units into three different tectonic units are introduced. In this paper, we limit the use of the Austroalpine unit (s. str.) to the pile of nappes of continental origin in the footwall of remnants of the Hallstatt-Meliata oceanic and transitional continental cover sequences (see below). Consequently, the overlying Upper Juvavic units derive from a separate continental unit and are excluded from the Austroalpine units s. str.. For further details, see SCHWEIGL and NEUBAUER (1997).

In terms of metamorphism, these units display fundamental differences. The Austroalpine s.str., Meliata-Hallstatt and Upper Juvavic units display Cretaceous-age metamorphism all over the Alps, the Penninic and Helvetic units Eocene to Oligocene regional metamorphism. The Southalpine units are unmetamorphic except narrow zones adjacent to the Periadriatic fault which display an anchi- to epizonal Cretaceous and Oligocene metamorphic overprint (LÄUFER et al., 1997; RANTITSCH, 1997).

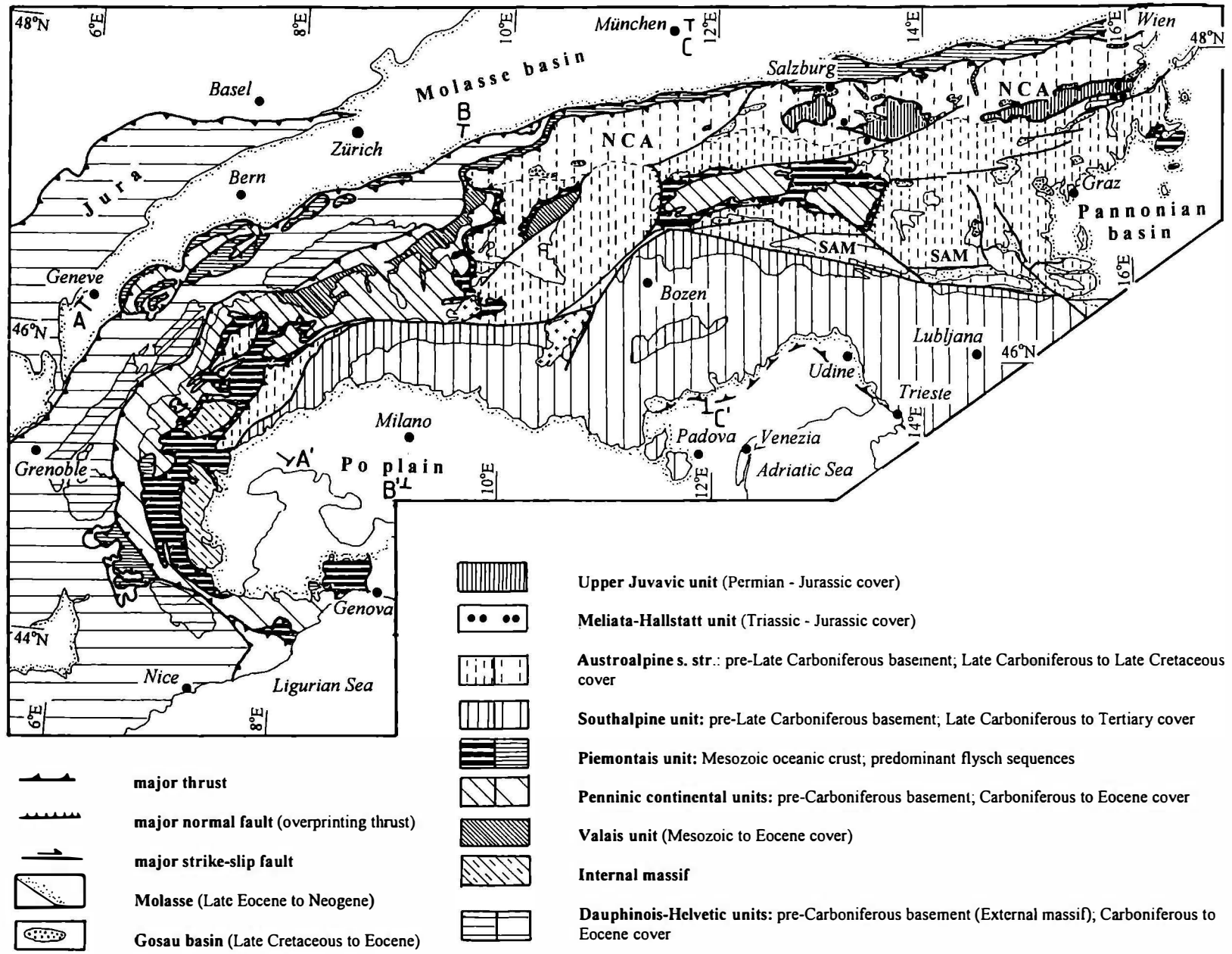
### **Europe-related, Helvetic and Penninic continental, units**

The Penninic continental units are exposed within the Tauern window within the so-called Venediger nappe and the overlying Riffel-Modereck nappe complex (e.g., KURZ et al., 1998b, and references therein). The basement is composed of the Habach-Storz Groups with Late Proterozoic to Early Paleozoic island arc successions, the Stubach Group, an Early Paleozoic back arc ophiolite, and widespread Variscan granite suite, collectively known as Central Gneisses. The Central Gneisses are exposed within several structural domes along the central structural axis of the antiformal Tauern window. The cover sequences include fossil-bearing Carboniferous sequences exposed in the western Tauern window, minor Permian and Triassic sequences, and thick Jurassic-Cretaceous sequences exposed within the Silbereck, Hochstegen and Kaserer Groups (e.g., LAMMERER, 1986; Kurz et al., 1998b).

### **Penninic ophiolites**

In the Eastern Alps, the Glockner ophiolite is considered to represent the extension of the Penninic units of the Western Alps. Penninic oceanic sequences of the Eastern Alps are exposed within the Engadin, Tauern, and Rechnitz windows (e.g., HÖCK and KOLLER, 1989; KOLLER and HÖCK, 1989).

Fig. 1. Simplified tectonic map of the Alps (modified after BGI et al. (1989)).



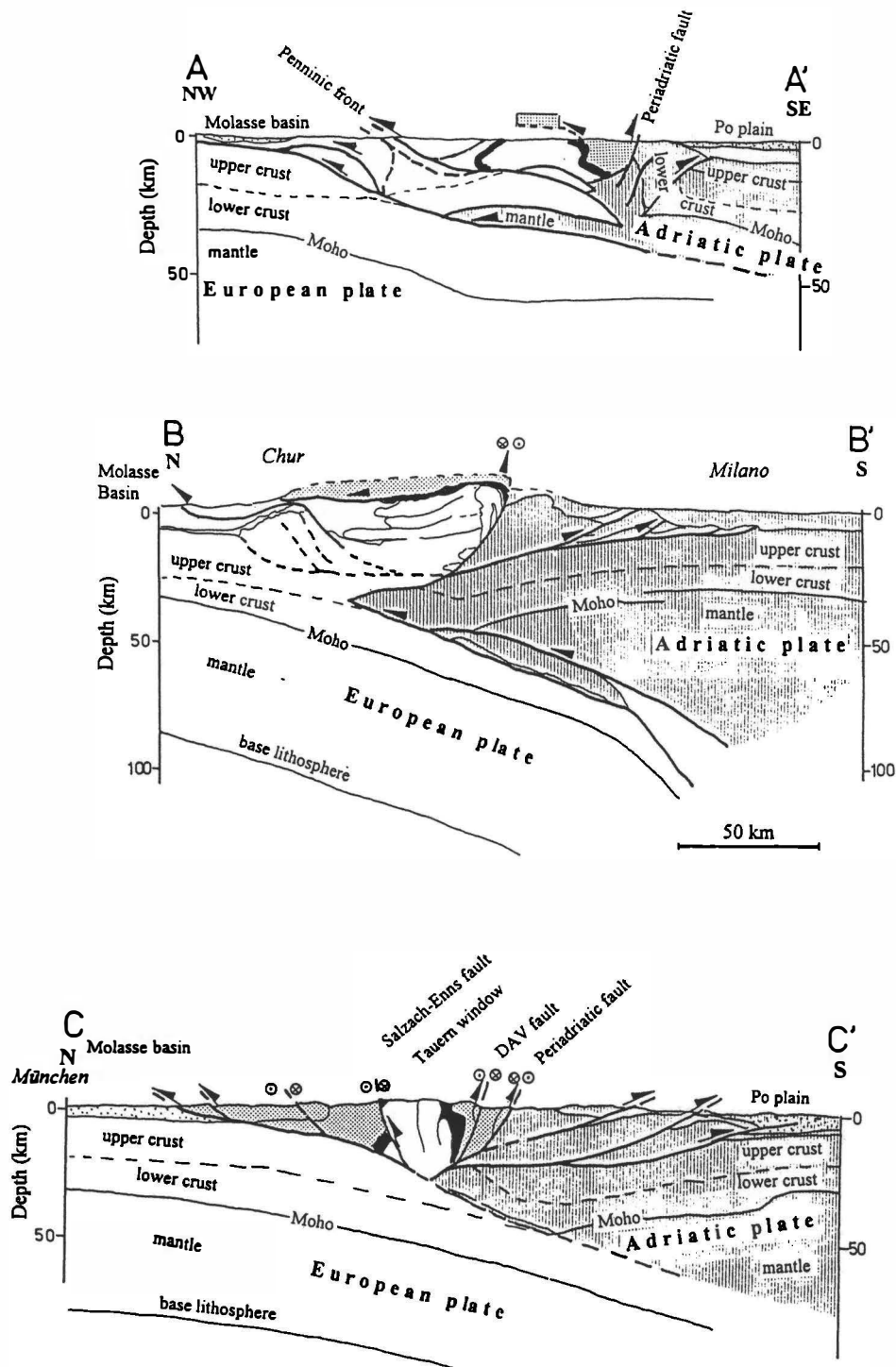
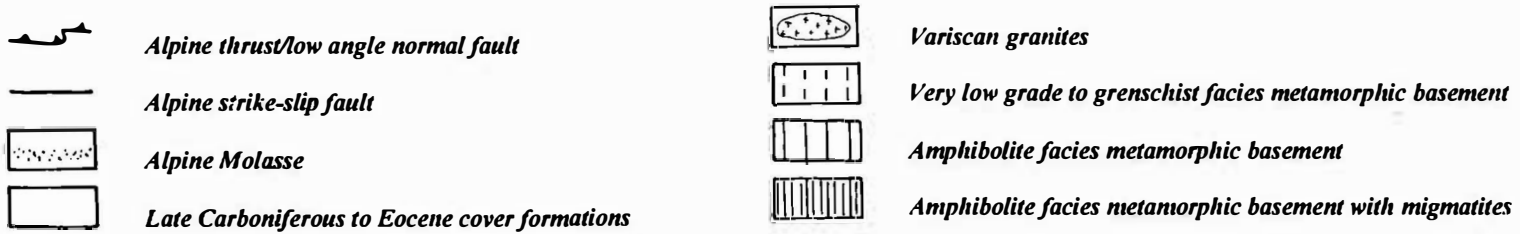
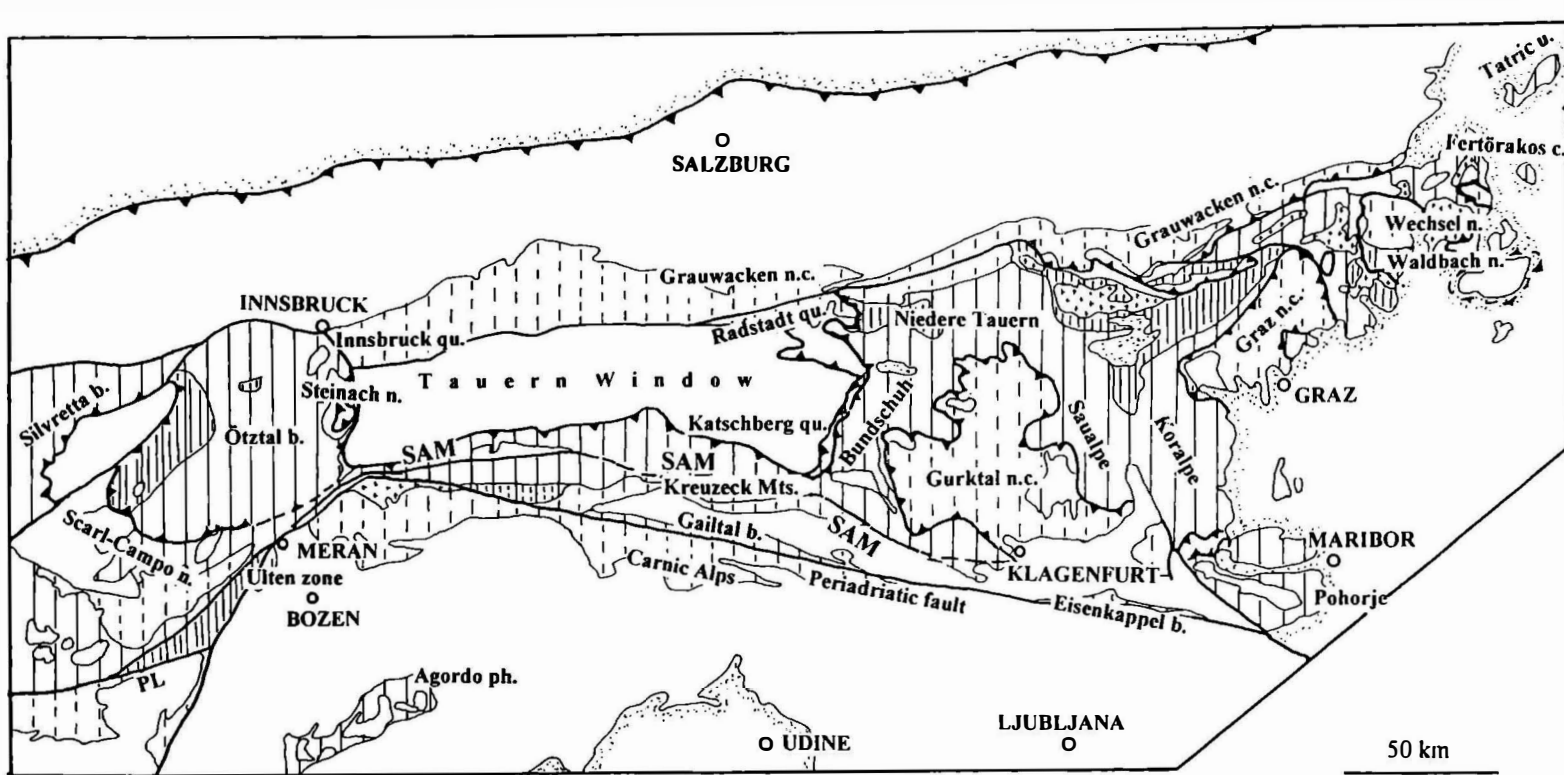


Fig. 2. Three transects of the Alps: a - Transect of the Western Alps (simplified after NICOLAS et al., 1990 and ROURE et al., 1990); b - transect across the eastern Central Alps (after SCHMID et al., 1986); transects of Western and eastern Central Alps are based on deep seismic reflection profiling; c - transect across the Eastern Alps (modified after LAMMERER and WEGER, 1998, and ROEDER, 1980, and extrapolating the structures of section b towards the east.

Fig. 3. Map of Austroalpine units sensu lato and Southalpine units of the Eastern Alps displaying extent of pre-Alpine metamorphism in basement units.



In the Engadin window, the Idalpe ophiolite is a well-preserved ophiolite with an only weak metamorphic overprint (e.g., KOLLER and HÖCK, 1990). The Glockner nappe of the Tauern window represents a dismembered ophiolite and the sedimentary infilling, mainly calcic schists, laid down on top of it (HÖCK and MILLER, 1987). The Rechnitz window group exposes ophiolitic successions with serpentinites, prasinites, and carbonate schists within two nappes, an upper ophiolite nappe with serpentinites at the structural base, and a lower nappe which includes carbonate schists and carbonate olistostromes (Köszeg conglomerate) (KOLLER, 1985).

### **Austroalpine unit s.str.**

The Austroalpine s. str. represents a continental, basement-cover, thick-skinned nappe pile which received its essential internal nappe structure during the Cretaceous orogenic events (e.g., RATSCHBACHER, 1986; DALLMEYER et al., 1998). They can be divided basically into the Central Eastern Alps with dominant basement sequences and Northern Calcareous Alps with predominant Permo-Cenozoic cover sequences (Fig. 4, 5). Although fiercely discussed (CLAR, 1973; FRANK, 1987; TOLLMANN, 1987), subdivision into Lower, Middle and Upper Austroalpine nappe complexes is easily applicable over large portions of the Austroalpine nappe pile which is bounded to the south by the SAM (southern limit of Alpine metamorphism; see below). The Lower Austroalpine nappe complex includes units exposed along the southwestern margin of Eastern Alps (e.g., Err-Bernina and Campo nappes), the Innsbruck-Reckner and Radstadt nappes around the Tauern window, and the Kirchberg-Stuhleck and Wechsel nappes along the eastern margin of the Eastern Alps, all having an originally northwestern paleogeographic position. The broadly developed Middle Austroalpine nappe complex extends from western to eastern margins of the Eastern Alps. The Upper Austroalpine nappe complex includes the Steinach nappe, the Grauwackenzone nappes and the overlying Tirolic and Bajuvaric nappes of the Northern Calcareous Alps, the Gurktal and Graz nappe complexes forming klippen, Grauwackenzone nappe complex and the overlying Northern Calcareous Alps along the northern leading edge of the Austroalpine nappe complex. These Upper Austroalpine units were derived from an originally southeastern paleogeographic position. The Middle Austroalpine units take, therefore, an intermediate paleogeographic position. The general nappe transport direction was towards WNW and N, respectively (RATSCHBACHER, 1986; KROHE, 1986).

The southern limit of Alpine (Cretaceous-age) metamorphism (SAM: term created by G. HOINKES) represents a c. east-trending system of polyphase faults which juxtaposes Austroalpine units with a strong, generally amphibolite and eclogite grade metamorphism to the north mostly against very-low grade Austroalpine units in the south. The SAM consists, from west to east, of the Peio-, Passeier-Jaufen-, Defreggen-Antholz-Vals- (DAV), Isel-, Zwischenbergen-Wöllatratzen-, Ragga-Teuchl-, Siflitz-, and Viktring fault zones. Western sectors of the SAM represent a zone of important, mostly Oligocene sinistral strike-slip displacement with an oblique-slip component. The eastern sectors (east of the Isel fault) represents a zone of Late Cretaceous sinistral strike-slip shear with a subordinate normal component, too. No large-scale nappe structures within Austroalpine units exposed within the SAM and the Periadriatic fault are preserved except flower structures related to the Periadriatic fault.

The composition and evolution of the Austroalpine basement units is not considered here in detail. However, it must be noted that each Alpine nappe comprises a basement that differs from under- and overlying basement units in composition, age and degree of pre-Alpine

tectonothermal events (NEUBAUER and FRISCH, 1993; NEUBAUER and SASSI, 1993; SCHÖNLAUB and HEINISCH, 1993). E.g., the Upper Austroalpine units comprises continuous fossiliferous Ordovician to early Carboniferous sequences affected by a late Variscan and/or Cretaceous metamorphic overprint. In contrast, the Middle Austroalpine units comprise exclusively medium-grade metamorphic basement that only minor successions represent correlatives of Ordovician to Carboniferous sequences.

Cover sequences deposited on the Austroalpine basement include a nearly continuous, conformable Late Carboniferous to early Late Cretaceous succession of rift, carbonate platform and shelf margin and later pelagic formations. The principal rift phase occurred during the Permian and resulted in rapid tectonic subsidence during the Triassic, where a passive continental margin was formed opposing the Meliata-Hallstatt ocean towards the SE (e.g., LEIN, 1987; SCHWEIGL and NEUBAUER, 1997) (Fig. 4, 5). A second, Jurassic rift phase created the Piemontais oceanic basin by rifting off the stable European continent, and another passive continental margin facing towards NW. Resulting structures along this passive margin are halfgrabens filled with escarpment breccias. Asymmetric simple shear is supposed to lead to exhumation of subcontinental mantle lithosphere and the formation of the continental Margna, Hippold and the questionable Sesia extensional allochthons (FROITZHEIM and MANATSCHAL, 1996; HEIDORN, 1998).

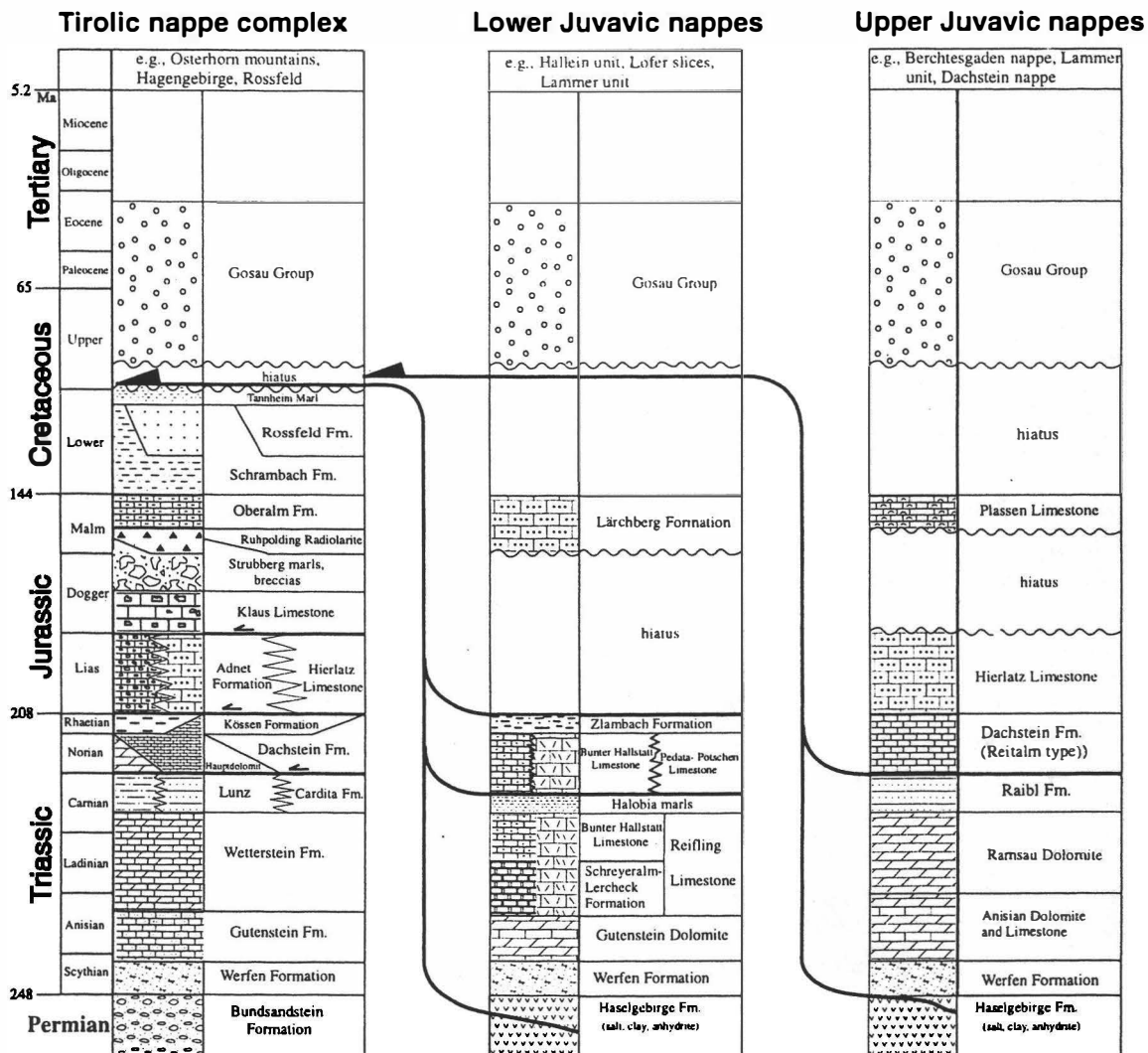
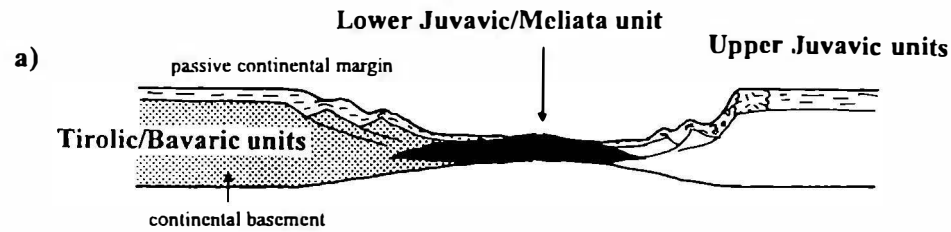


Fig. 4. Stratigraphic sections of units exposed within the Northern Calcareous Alps (from Schweigl and Neubauer, 1997).

## LATE TRIASSIC:



## EARLY CRETACEOUS:

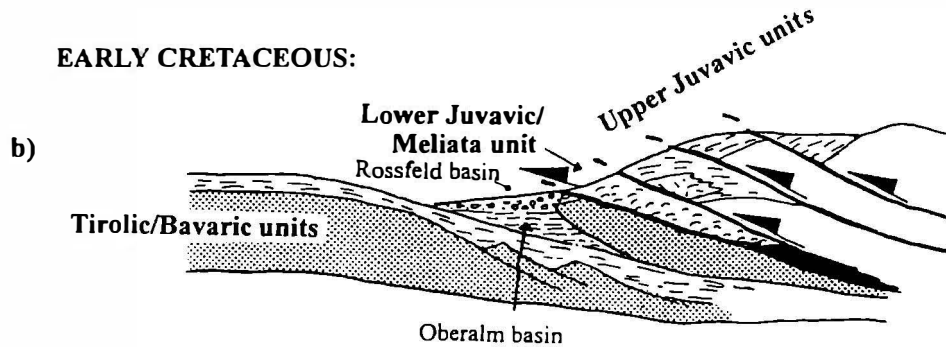


Fig. 5. Schematic (a) Late Triassic and (b) Lower Cretaceous paleogeography of Upper Juvavic, Meliata-Hallstatt and Austroalpine units *sensu stricto* (Tirolic/Bajuvaric units). (From Schweigl and Neubauer, 1997).

### Hallstatt-Meliata units

The Hallstatt-Meliata units comprise distal continental margin deposits (Hallstatt facies) (LEIN, 1987; MANDL and ONDREJICKOVA, 1991) and the recently detected oceanic sediments of Middle Triassic to Dogger age (KOZUR, 1991; MANDL and ONDREJICKOVA, 1991; KOZUR and MOSTLER, 1992). These include Middle and Late Triassic pelagic carbonates, Late Triassic radiolarites and Doggerian shales, volcanogenic greywackes and ashfall tuffs. Greywackes and tuffs indicate a volcanic source of subduction-related origin (NEUBAUER, unpubl. data).

Furthermore, salt melanges (Permian and Scythian strata) are often connected with the structural sole of the Hallstatt-Meliata unit generally interpreted to represent the primary lowermost sequence of this unit (KOZUR, 1991). If this is true, some doubts are apparent because of strong structural destruction of this unit. Anyway, the salt melange is connected with serpentinites, melaphyres and a few gabbro bodies. The melaphyres have an alkaline basaltic affinity (KIRCHNER, 1980). Gabbro and melaphyres appear to record some doubtful Permian ages. These rocks are interpreted, therefore, to record incipient Permian rifting (KIRCHNER, 1980).

### Upper Juvavic unit

Upper Juvavic units include a continuous Permian to Triassic section with some rare Jurassic sediments. The Upper Juvavic units form several large tectonic klippen on top of the Hallstatt-Meliata units within the eastern half of the Northern Calcareous Alps (Figs. 1, 4). The

sequences display remarkable differences to the Tirolic-Bajuvaric nappe complex, mainly including thick Late Triassic Norian reefs in the Upper Juvavic nappe in contrast to the Norian lagoonal Hauptdolomit facies and presence of Rhaethian reefs in the Tirolic-Bajuvaric nappe (SCHWEIGL and NEUBAUER, 1997). The Jurassic sequence is incomplete and only record some thin Liassic limestones and Malmian reefal limestone in the northwesternmost exposures.

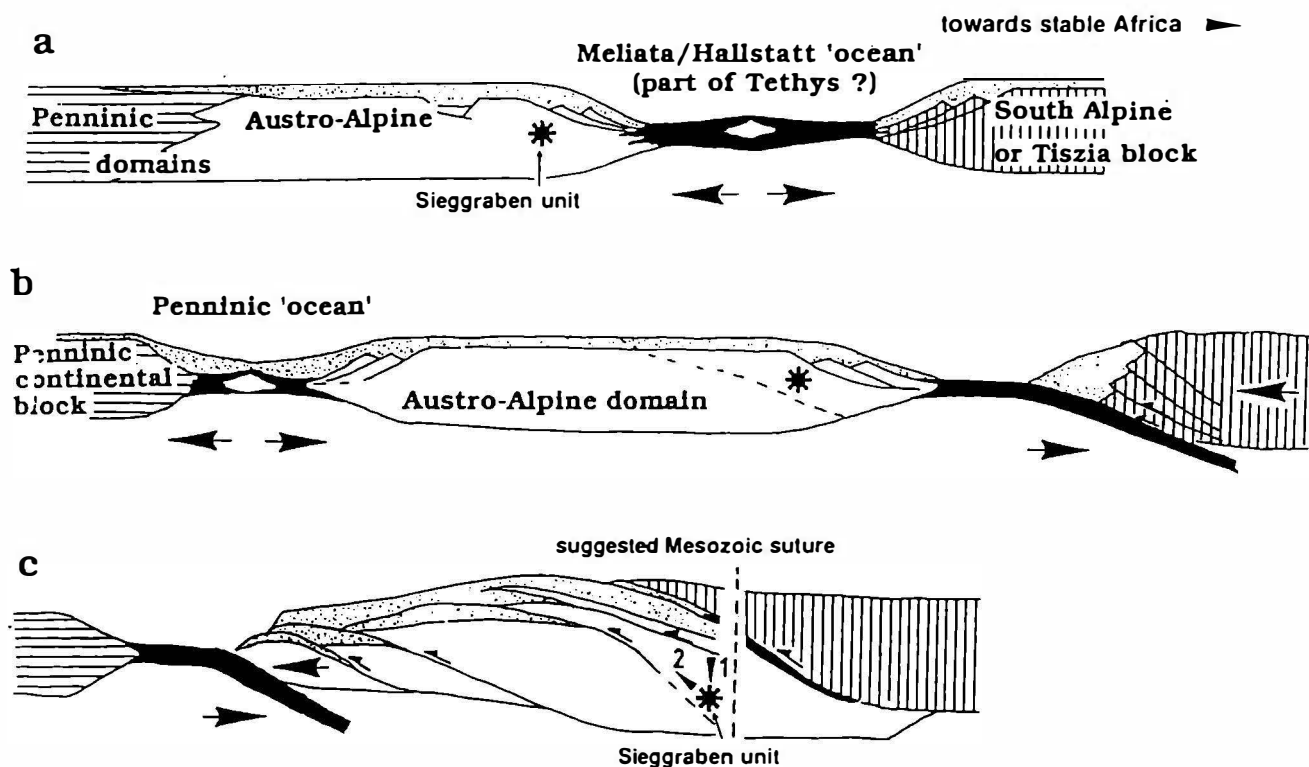


Fig. 6. Tectonic evolution of units exposed in the eastern Central Alps (modified after Neubauer, 1994).



## Southalpine unit

The Southalpine unit includes a continental basement exposed along the Periadriatic fault, and a continuous Late Carboniferous to Oligocene sequence. Two main rift phases affected the Southalpine unit: NW-SE extension during Permian resulted in the formation of a swell and high topography which governed deposition from Permian to Cenozoic. Permian magmatic underplating by mantle melts in the Ivrea zone (e.g., VOSHAGE et al., 1990) may have been associated with crustal extension. Progressive onlap of the Paleotethys (definition of the Tethys was by SUESS, 1887) from the SE reached the Carnic Alps during the Late Carboniferous, South Tyrol during the Late Permian, and the Lombardian Alps during the Middle Triassic. A strong tectonic subsidence phase during Middle Triassic times in eastern to central sectors of the Southern Alps was associated with magmatism in the central Southern Alps. A second rift phase during the Late Triassic to Early Jurassic mainly affected western sectors and resulted in formation of pronounced troughs, thinning of the crust and exhumation and cooling of middle crustal levels (e.g., BERTOTTI et al., 1993).

The deposition of the Late Cretaceous Lombardian flysch in the western Lombardian Alps with northern source heralds ongoing deformation which is not evidenced otherwise in Southern Alps. The structure of the Southern Alps is dominated by c. E-trending, top-S-directed thrusts which brought up basement rocks on top of cover (e.g., DOGLIONI and BOSSELLINI, 1987; CARMINATI et al., 1997). The earliest thrusts in the western Southern Alps were formed before intrusion of the Adamello (before ca. 42 Ma; BRACK, 1980). In eastern sectors, c. WNW-trending, SSW-directed structures were formed during the Paleogene, believed to represent a Dinaric trend (DOGLIONI and BOSSELLINI, 1987). These structures were overprinted by Oligocene to Recent structures which also involved the basement (CARMINATI et al., 1997).

## Tectonic evolution

In terms of metamorphism and associated deformation, the Alps are divided into three units: (1) The Austroalpine units s.l., Meliata-Hallstatt units, and Upper Juvavic units which were overprinted by Cretaceous deformation, W- to NW-directed, ductile thrusting; (2) the Penninic continental and oceanic units, and the Dauphinois-Helvetic units which were overprinted by Cenozoic metamorphism and associated N- to W-directed ductile deformation; and (3) Southalpine units which are largely unaffected by metamorphism except northernmost sectors adjacent to the Periadriatic fault and which were mainly deformed during Cenozoic, c. S-directed thrusting and shortening.

A model of the Triassic to Cretaceous tectonic evolution of units exposed in the eastern Central Alps is shown in Fig. 6. Essential arguments for an independent Cretaceous orogeny within Austroalpine units are: the Cretaceous age (c. 95-90 Ma; THÖNI and MILLER, 1997) of eclogite metamorphism with pressures of c. 18 kbar within Austroalpine basement units which argues for a subduction of continental crust; the superposition of Austroalpine continental crust by oceanic units exposed in the Western Carpathians and their Late Jurassic blueschist-facies metamorphic overprint (e.g., KOZUR, 1992; DALLMEYER et al., 1996; FARYAD and HENJES-KUNST, 1987); the sealing of early Late Cretaceous thrusts within Upper Austroalpine units in the Eastern Alps by Gosau (Late Cretaceous to Middle Eocene) basins which are associated with exhumation of deeply buried, continental metamorphic crust exposed in

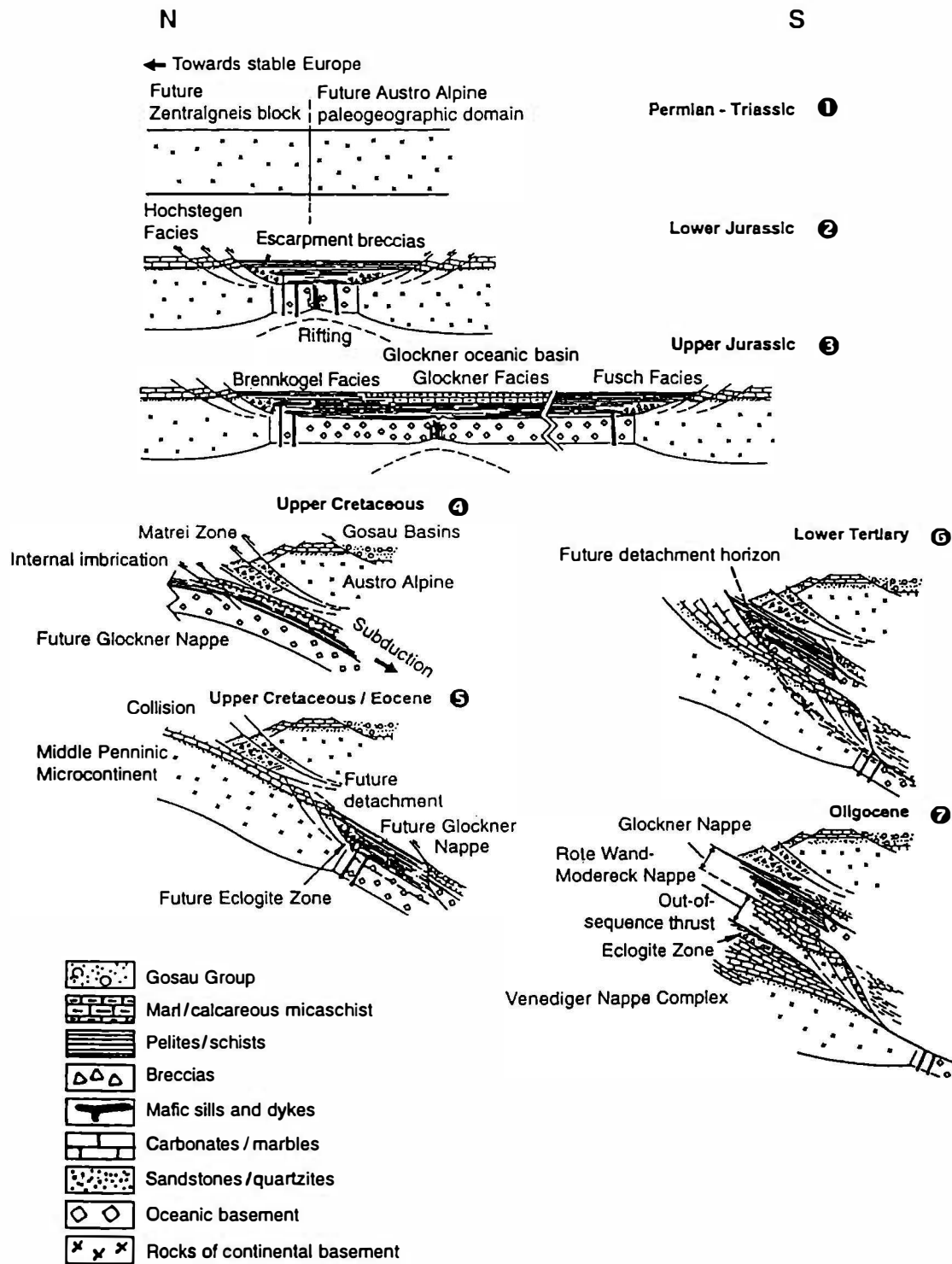


Fig. 7. Schematic tectonic evolution of Penninic units exposed in the Tauern window (from Kurz et al., 1998b).

present-day Middle Austroalpine units (NEUBAUER et al., 1995; FROITZHEIM et al., 1997). The internal ductile deformation of Austroalpine units stopped during the latest Cretaceous, and large portions were exhumed during the Paleogene to shallow crustal levels. Furthermore, the entire Austroalpine units were peneplained not later than the early Neogene, as it evidenced by the presence of large-scale peneplaine surfaces east of the Tauern window, some Oligocene and numerous Miocene sedimentary basins and early Tertiary apatite fission track ages (Hejl, 1997). The internal deformation, generally of transtensional and transpressional character, of these basins was always at shallow, brittle crustal levels. The preservation of these peneplains (and Eocene sedimentary sequences in some places) over the entire eastern sectors of the Eastern Alps excludes large vertical displacement in excess of c. 3 kilometres after the Eocene. A model displaying the tectonic evolution of Penninic units is shown in Fig. 7. Penninic units were overridden by the combined Austroalpine units *sensu lato* not before Paleogene because of the presence of Eocene pelagic limestones within Penninic successions exposed within the Engadin window (for reference, see OBERHAUSER, 1995), and the presence of Eocene blueschists within the ophiolitic Reckner nappe (Dingeldey et al., 1997). Initial thrust were directed towards the NNE (Genser, 1992; Kurz et al., 1998b) same as earlier NNE-directed subduction-related and decompressional fabrics within eclogites of the distal continental margin sequences of the Tauern window (Kurz et al., 1998a). Subsequent W-directed ductile deformation within the Tauern window was related to exhumation of previously buried Penninic sequences during the Oligocene and Neogene. Exhumation was due to indentation by the Southalpine indenter, tectonic unroofing along upper margins of Penninic sequences and eastwards escape of a tectonic wedge (Ratschbacher et al., 1991). The wedge is confined by sinistral wrench corridors to the N, including the Oligocene to Lower Miocene Salzach-Enns-Mariazell-Puchberg fault: RATSCHBACHER et al., 1991; WANG and NEUBAUER, 1998), the Miocene to Recent Mur-Mürz fault and the dextral Periadriatic fault to the S (Fig. 8). The Periadriatic also has an important stage of back-thrusting towards the S due to flake tectonics similar as found in the Western Alps (Fig. 2).

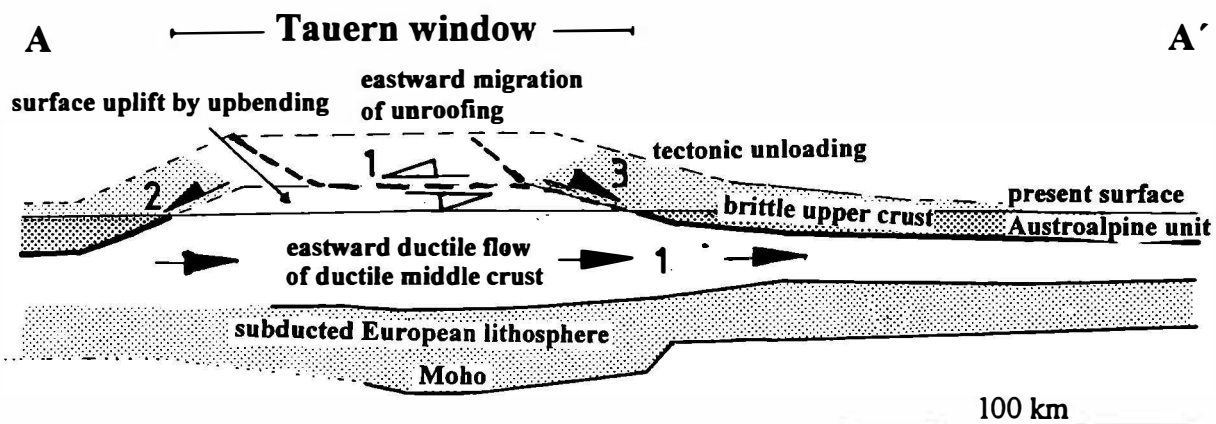


Fig. 8. Schematic evolution of escape tectonics and related phenomena (modified from Neubauer, submitted).

## References

- BEHRMANN, J. H. and RATSCHBACHER, L. (1989): Archimedes revisited: a structural test of eclogite emplacement models in the Austrian Alps. *Terra Nova* 1: 242-252.
- BERTOTTI, G., PICOTTI, V., BERNOULLI, D. and CASTELLARIN, A., 1993: From rifting to drifting: tectonic evolution of the South-Alpine upper crust from the Triassic to the Early Cretaceous. *Sed. Geol.*, 86, 53-76.
- BIGI, G., CASTELLARIN, A., CATALANO, R., COLI, M., COSENTINO, D., DAL PIAZ, G.V., LENTINI, F., PAROTTO, M., PATACCA, E., PRATURLON, A., SALVINI, F., SARTORI, R., SCANDONE, P. and VAI, G.B. (1989): Synthetic structural-kinematic map of Italy. C.N.R., Roma.
- BORSI, S., DEL MORO, A., SASSI, F.P., ZANFERRARI, A. and ZIRPOLI, G. (1978): New geopetrologic and radiometric data on the Alpine History of the Austridic continental margin south of the Tauern Window (Eastern Alps). *Mem. Ist. Geol. Mineral. Univ. Padova*, 32, 1-19.
- CARMINATI, E., SILETTO, G.B. AND BATTAGLIA, D. (1997): Thrust kinematics and internal deformation in basement-involved fold and thrust belts: The eastern Orobic Alps case (Central Southern Alps, northern Italy). *Tectonics*, 16, 259-271.
- CHANNELL, J.E.T., DÁRGENIO, B. and HORVATH, F., 1979: Adria, an African promontory in Mesozoic Mediterranean palaeogeography. *Earth Sci. Rev.*, 15, 213-292.
- CLAR, E. (1973): Review of the structure of the Eastern Alps. In: DE JONG, K.A. and SCHOLTEN, K., eds., *Gravity and Tectonics*. pp. 273-270, Wiley, New York.
- COWARD, and DIETRICH, D. (1989): Alpine tectonics - an overview, *in* Coward, M. P.; Dietrich, D.; and Park, R. G., eds., *Alpine Tectonics*: Geol. Soc. Spec. Publ. 45, p. 1-29.
- DAL PIAZ, G.V. (1992): *Le Alpi dal M. Bianco al Lago Maggiore*, 13 itinerari e 97 escursioni (2 vol.). *Soc. Geol. Ital.*, 311 + 209 p.
- DALLMEYER, R.D., NEUBAUER, F., HANDLER, R., FRITZ, H., MÜLLER, W., PANA, D. and PUTIS, M. (1996): Tectonothermal evolution of the internal Alps and Carpathians: Evidence from  $^{40}\text{Ar}/^{39}\text{Ar}$  mineral and whole rock data. *Eclogae geol. Helv.*, 89: 203-227.
- DALLMEYER, R.D., HANDLER, R., NEUBAUER, F. and FRITZ, H. (1998): Sequence of thrusting within a thick-skinned tectonic wedge: evidence from  $^{40}\text{Ar}/^{39}\text{Ar}$  and Rb/Sr ages from the Austroalpine Nappe Complex of the Eastern Alps. *J. Geol.*, 106: 71-86.
- DEBELMAS, J., ESCHER, A. and TRÜMPY, R. (1983): Profiles through the Western Alps. In : Profiles of orogenic belts, *Geodyn. ser.*, Am. Geophys. Union, 10, 83-96.
- DECKER, K. (1990): Plate tectonics and pelagic facies: Late Jurassic to Early Cretaceous deep-sea sediments of the Ybbsitz ophiolite unit (Eastern Alps, Austria). *Sed. Geol.*, 67, 85-99
- DECKER, K., FAUPL, P. and MÜLLER, A. (1987): Synorogenic Sedimentation on the Northern Calcareous Alps During the Early Cretaceous. In: Flügel, H. W. and Faupl, P., eds., *Geodynamics of the Eastern Alps*. Vienna, Deuticke, 126-141.
- DEWEY, J. F.; HELMANN, M. L.; TURCO, E.; HUTTON, D. H. W.; and KNOTT, S. D., 1989, Kinematics of the western Mediterranean. In: COWARD, M. P.; DIETRICH, D. and PARK, R.G., eds., *Alpine Tectonics*. Geol. Soc. Spec. Publ., 45, 265-283.
- DINGELDEY, CH., DALLMEYER, R.D., KOLLER, F. and MASSONNE, H.-J. (1997): P-T-t history of the Lower Austroalpine Nappe Complex in the "Tarntaler Berge" NW of the Tauern Window: implications for the geotectonic evolution of the central Eastern Alps. *Contrib. Mineral. Petrol.*, 129, 1-19.
- DOGLIONI, C. AND BOSELLINI, A. (1987): Eoalpine and Mesoalpine tectonics in the Southern Alps. *Geol. Rundschau*, 76, 735-754.
- DOGLIONI, C. and FLORES, G. (1997): Italy. In: MOORES, E.M. and FAIRBRIDGE, R.W., eds., *Encyclopedia of European and Asian regional Geology*, p. 414-435, Chapman & Hall, London.
- EBNER, F. (1997): Die geologischen Einheiten Österreichs und ihre Rohstoffe. *Archiv für Lagerstättenforschung*, 19, 49-229.

- FARYAD, S.W. and HENJES-KUNST, F. (1997): Petrological and K-Ar and  $^{40}\text{Ar}/^{39}\text{Ar}$  age constraints for the tectonothermal evolution of the high-pressure Meliata unit, Western Carpathians (Slovakia). *Tectonophysics*, 280, 141-156.
- FAUPL, P. (1997): Austria. In: MOORES, E.M. and FAIRBRIDGE, R.W., eds., *Encyclopedia of European and Asian regional Geology*, p. 51-60, Chapman & Hall, London.
- FLÜGEL, H.W. and FAUPL, P. (1987): *Geodynamics of the Eastern Alps*. Deuticke, Wien.
- FRANK, W. (1987): Evolution of the Austroalpine elements in the Cretaceous, in Flügel, H. W.; and Faupl, P., eds., *Geodynamics of the Eastern Alps*: Vienna, Deuticke, p. 379-406.
- FRISCH, W. (1979): The plate tectonic evolution of the Alps: *Tectonophysics*, 60, 121-134.
- FRITZ, H. (1988): Kinematics and geochronology of Early Cretaceous thrusting in the northwestern part of Graz (Eastern Alps): *Geodynamica Acta*, v. 2, p. 53-62.
- FROITZHEIM, N. and MANATSCHAL, G. (1996): Kinematics of Jurassic rifting, mantle exhumation, and passive-margin foremargination in the Austroalpine and Penninic nappes (eastern Switzerland). *Geol. Soc. Amer. Bull.*, 108, 1120-1130.
- FROITZHEIM, N., SCHMID, S.M. AND FREY, M. (1996): Mesozoic paleogeography and the timing of eclogite facies metamorphism in the Alps: A working hypothesis. *Ecl. Geol. Helv.*, 89, 81-110.
- FROITZHEIM, N., CONTI, P. and VAN DAALEN, M. (1997): Late Cretaceous, synorogenic, low-angle normal faulting along the Schlinig fault (Switzerland, Italy, Austria) and its significance for the tectonics of the Eastern Alps. *Tectonophysics*, 280, 267-293.
- FÜGENSCHUH, B., SEWARD, D. and MANCKTELOW, N. (1997): Exhumation in a convergent orogen: the western Tauern window. *Terra Nova*, 9, 213-217.
- GRADSTEIN, F.M. and OGG, J. (1996): A Phanerozoic time scale. *Episodes*, 19, 3-4.
- GRADSTEIN, F.M., AGTERBERG, F.P., OGG, J.G., HARDENBOL, J., VANVEEN, P., THIERRY, J. and HUANG, Z. (1994): A Mesozoic time scale: *J. Geophys. Res.*, 99, 24051-24074.
- HÄUSLER, H. (1987): The northern Austroalpine margin during the Jurassic: breccias from the Radstädter Tauern and the Tarntaler Berge. In: FLÜGEL, H.W. and FAUPL, P. (eds): *Geodynamics of the Eastern Alps*. Deuticke: Wien, 103-111.
- HEIDORN, R. (1998): Structural evolution at the Penninic to Lower-Austroalpine boundary, northwestern margin of the Tauern window (Tux mountains/Eastern Alps). Unpubl. MSc thesis, University of Salzburg, pp. 131.
- HÖCK, V. and KOLLER, F. (1989): Magmatic evolution of the Mesozoic ophiolites in Austria. *Chemical Geology*, 77, 209-227.
- HÖCK, V. and MILLER, Ch. (1987): Mesozoic ophiolitic sequences and non-ophiolitic metabasites in the Hohe Tauern. In: FLÜGEL, H. W. and FAUPL, P., eds., *Geodynamics of the Eastern Alps*. Vienna, Deuticke, p. 16-33.
- HSÜ, K. J. (1991): Exhumation of high-pressure metamorphic rocks. *Geology*, 19, 97-192.
- HUNZIKER, J. C., DESMONS, J. and MARTINOTTI, G. (1989): Alpine thermal evolution in the central and western Alps, in Coward, M. P.; Dietrich, D.; and Park, R. G., eds., *Alpine Tectonics*: *Geol. Soc. Spec. Publ.* 45, p. 353-367.
- HUNZIKER, J.C., DESMONS, J. and HURFORD, A. J. (1992): Thirty-two years of geochronological work in the Central and Western Alps: a review on seven maps. *Mémoires de Géologie (Lausanne)*, 13, 1-59.
- INGER, S. AND CLIFF, R. A. (1994): Timing of metamorphism in the Tauern Window, Eastern Alps: Rb-Sr ages and fabric formation: *J. metamorphic Geol.*, 12, 695-707.
- JANOSCHECK, W.R. and MATURA, A. (1980): Outline of the Geology of Austria. *Abh. Geol. Bundesanst.*, 34, 7-98.
- KIRCHNER, E. (1980): Vulkanite aus dem Permoskyth der Nördlichen Kalkalpen und ihre Metamorphose. *Mitt. Österr. Geol. Ges.*, 71/72, 149-162.
- KOLLER, F. (1985): Petrologie und Geochemie der Ophiolithe des penninikums am Alpenostrand. *Jb. Geol. Bundesanst.*, 128, 83-150.
- KOLLER, F. and HÖCK, V. (1990): Mesozoic ophiolites in the Eastern Alps. In: MALPAS, J., MOORES, E.M., PANAYIOTOU, A. and XENOPHONTOS, C. (eds.): *Ophiolites, Oceanic Crustal Analogues, Proceedings of the Symposium "TROODOS 1987"*, 253-263.

- KOZUR, H. (1992): The evolution of the Meliata-Hallstatt ocaen and its significance for the early evolution of the Eastern Alps and Western Carpathians: *Palaeogeogr. Palaeoclimat. Palaeoecol.*, v. 87, p. 109-135.
- KOZUR, H. and MOSTLER, H. (1992): Erster paläontologischer Nachweis von Meliaticum und Süd-Rudabanyaicum in den Nördlichen Kalkalpen (Österreich) und ihre Beziehung zu den Abfolgen der Westkarpaten.. *Geol. Paläont. Mitt. Innsbruck*, 18, 87-129.
- KRALIK, M., KRUMM, H. and SCHRAMM, J. M. (1987): Low grade and very low grade metamorphism in the Calcareous Alps and in the Greywacke. zone: Illite-crystallinity data and isotopic ages, *in* Flügel, H. W.; and Faupl, P., eds., *Geodynamics of the Eastern Alps*: Vienna, Deuticke, p. 164-178.
- KROHE, A. (1987): Kinematics of Cretaceous nappe tectonics in the Austroalpine basement of the Koralpe region (eastern Austria): *Tectonophysics*, 136, 171-196.
- KURZ, W., NEUBAUER, F. and GENSER, J. (1996): Kinematics of Penninic nappes (Glockner Nappe and basement-cover nappes) in the Tauern Window (Eastern Alps, Austria) during subduction and Penninic-Austroalpine collision. *Eclogae geol. Helv.*, 89, 573-605.
- KURZ, W., NEUBAUER, F. and DACHS, E. (1998a): Eclogite meso- and microfabrics: implications for the burial and exhumation history of eclogites in the Tauern Window (Eastern Alps) from P-T-d paths. *Tectonophysics* 285: 183-209.
- KURZ, W., NEUBAUER, F., GENSER, J. and DACHS, E. (1998b): Alpine geodynamic evolution of passive and active continental margin sequences in the Tauern Window (Eastern Alps, Austria, Italy): a review. *Geologische Rundschau*, 87, .
- LAGABRIELLE, Y. and POLINO, R. (1988): Un schéma structural du domaine des Schistes lustrés ophiolitifères au nord-ouest du massif du Mont Viso (Alpes Sud-Occidentales) et ses implications. *C.R. Acad. Sci. Paris* 306, ser. II, 921-928.
- LAMMERER, B., 1986. Das Autochthon im westlichen Tauernfenster. *Jb. Geol. Bundesanst.*, 128, 51-67.
- LAMMERER, B. and WEGER, M. (1998): Footwall uplift in an orogenic wedge: the Tauern Window in the Eastern Alps. *Tectonophysics*, 285, 213-230.
- LÄUFER, A.L., FRISCH, W., STEINITZ, G. and LOESCHKE, J. (1997): Exhumed fault-bounded Alpine blocks along the Periadriatic lineament: the Eder unit (Carnic Alps, Austria). *Geol. Rundsch.*, 86: 612-626.
- LEIN, R. (1987): Evolution of the Northern Calcareous Alps during Triassic times. *In*: Flügel, H.W.; and Faupl, P., eds., *Geodynamics of the Eastern Alps*: Vienna, Deuticke, p. 85-102.
- LINZER, H. G., RATSCHBACHER, L. and FRISCH, W. (1995): Transpressional collision structures in the upper crust: the fold-thrust belt of the Northern Calcareous Alps: *Tectonophysics*, 242, 41-61.
- MANCKTELOW, N. (1985): The Simplon line: a major displacement zone in the western Lepontine Alps. *Ecl. Geol. Helv.*, 78, 73-96.
- MANDL, G. W. AND ONDRELJOKOVA, A. (1991): Über eine triadische Teifasserfazies (Radiolarite, Tonschiefer) in den Nördlichen Kalkalpen - ein Vorbericht: *Jb. Geol. Bundesanst.*, 134, 309-318.
- NEUBAUER, F. (1994): Kontinentkollision in den Ostalpen. *Geowissenschaften*, 12, 136-140.
- NEUBAUER, F. and FRISCH, W., 1993: The Austroalpine metamorphic basement east of the Tauern window. - *In*: RAUMER, J.VON and NEUBAUER, F. (Eds.): *Pre-Mesozoic Geology in the Alps*. - Berlin (Springer), 515-536.
- NEUBAUER, F. and SASSI, F.P., 1993: The quartzphyllite and related units of the Austro-Alpine domain. - *In*: RAUMER, J.VON and NEUBAUER, F. (Eds.): *Pre-Mesozoic Geology in the Alps*. Berlin (Springer), 423-439.
- NEUBAUER, F., DALLMEYER, R. D., DUNKL, I. and SCHIRNIK, D. (1995): Late Cretaceous exhumation of the metamorphic Gleinalm dome, Eastern Alps: kinematics, cooling history and sedimentary response in a sinistral wrench corridor. *Tectonophysics*, 242, 79-89.
- NEUBAUER, F., GENSER, J., KURZ, W. AND WANG, X. (submitted): Exhumation of the Tauern window, Eastern Alps. *Phys. Chem. earth*.
- NICOLAS, A., POLINO, R., HIRN, A., NICOLICH, R. AND ECORS-CROP WORKING GROUP (1990). ECORS-CROP traverse and deep structure of the western Alps: a synthesis. *Mém. Soc. géol.*

- France N.S., 156: 15-27.
- OBERHAUSER, R. (1980): Das Unterengadiner Fenster. In: OBERHAUSER, R. (ed.): Der Geologische Aufbau Österreichs, Springer-Verlag Wien-New York, 291-299.
- OBERHAUSER, R. (1995): Zur Kenntnis der Tektonik und der Paleogeographie des Ostalpenraumes zur Kreide-, Paleozän- und Eozänzeit. *Jb. Geol. Bundesanst.*, 138, 369-432.
- PFIFFNER, A., LEHNER, P., HEITZMANN, P., MUELLER, ST. and STECK, A., eds. (1997): Results of NRP 20. 380 pp., Birkhäuser-Verlag, Basel Boston Berlin.
- PFIFFNER, O. A. (1992): Alpine Orogeny, in Blundell, D.; Freemann, R.; and Mueller, S., eds., *A Continent Revealed - The European Geotraverse*: New York, Cambridge University Press, p. 180-190.
- POLINO, R., DAL PIAZ, G.V. and GOSSO, G. (1990): Tectonic erosion at the Adria margin and accretionary processes for the Cretaceous orogeny of the Alps. *Mém. Soc géol. France N.S.*, 156: 345-367.
- RANTITSCH, G. (1997): Thermal history of the Carnic Alps (Southern Alps, Austria) and its paleogeographic implications. *Tectonophysics*, 272: 213-232.
- RATSCHBACHER, L. (1986): Kinematics of Austro-Alpine cover nappes: changing translation path due to transpression. *Tectonophysics*, 125, 335-356.
- RATSCHBACHER, L. and NEUBAUER, F. (1989): West-directed décollement of Austro-Alpine cover nappes in the eastern Alps: geometrical and rheological considerations, in Coward, M. P.; Dietrich, D.; and Park, R. G., eds., *Alpine Tectonics*: Geol. Soc. Spec. Publ. 45, p. 243-262.
- RATSCHBACHER, L., FRISCH, W., NEUBAUER, F., SCHMID, S. M. and NEUGEBAUER, J. (1989): Extension in compressional orogenic belts: The eastern Alps: *Geology*, 17, 404-407.
- RATSCHBACHER, L., FRISCH, W., LINZER, G. AND MERLE, O. (1991): LATERAL EXTRUSION IN THE EASTERN ALPS, PART 2: STRUCTURAL ANALYSIS. *TECTONICS*, 10, 25-271.
- RAUMER, J.VON and NEUBAUER, F., eds. (1993): *Pre-Mesozoic Geology in the Alps*. Berlin - Heidelberg - New York (Springer), pp. 677.
- RING, U., RATSCHBACHER, L., FRISCH, W., BIEHLER, D. and KRÁLIK, M. (1989): Kinematics of the Alpine plate-margin: structural style, strain and motion along the Penninic-Austroalpine boundary in the Swiss-Austrian Alps: *J. geol. Soc. Lond.*, 146, 835-849.
- RÖGL, F. (1996): Stratigraphic correlation of the Paratethyan Oligocene and Miocene. *Mitt. Ges. Geol. Bergbaustud. Österreich*, 41, 65-73.
- ROURE, F., POLINO, R. and NICOLICH, R. (1990): Early Neogene deformation beneath the Po plain: constraints on the post-collisional Alpine evolution. *Mém. Soc géol. France N.S.*, 156: 309-322.
- SCHMID, S.M., PFIFFNER, O.A., FROITZHEIM, N., SCHÖNBORN, G. AND KISSLING, E. (1996): Geophysical-geological transect and tectonic evolution of the Swiss-Italian Alps. *Tectonics*, 15, 1036-1064.
- SCHNABEL, G.W. (1992): New data on the Flsch Zone of the Eastern Alps in the Austrian sector and new aspects concerning the transition to the Flysch Zone of the Carpathians. *Cretaceous Research*, 13, 405-419.
- SCHÖNLAUB, H.P. and HEINISCH, H. (1993): In: RAUMER, J.VON and NEUBAUER, F. (Eds.): *Pre-Mesozoic Geology in the Alps*, p. 395-422, Berlin - Heidelberg - New York (Springer), .
- SCHÖNBORN, G. (1992): Alpine tectonics and kinematic models of the Central Southern Alps. *Mem. Sci. Geol.*, 44, 229-393.
- SCHWEIGL, J. AND NEUBAUER, F. (1997): Structural development of the central Northern Calcareous Alps: Significance for the Jurassic to Tertiary geodynamics in the Alps. - *Ecl. Geol. Helv.*, 60/2, 303-323.
- SPALLA, M.I., LARDEAUX, M., DAL PIAZ, G.V., GOSSO, G. and MESSIGA, B. (1996): Tectonic significance of Alpine eclogites. *J. Geodynamics*, 21, 257-285.
- THÖNI, M. and JAGOUTZ, E. (1992): Some new aspects of dating eclogites in orogenic belts: Sm-Nd, Rb-Sr and Pb-Pb isotopic results from the Austroalpine Saualpe and Koralpe type-locality (Carinthia/Styria, SE Austria). *Geochim. Cosmochim. Acta*, 56, 347-368.
- THÖNI, M. and JAGOUTZ, E. (1993): Isotopic constraints for eo-Alpine high-P metamorphism in the Austroalpine nappes of the Eastern Alps: bearing on Alpine orogenesis. *Schweiz. mineral. petrogr.*

- Mitt., 73, 177-189.
- TOLLMANN, A. (1977): Geologie von Österreich, Band 1. Wien, Deuticke, 766.
- TOLLMANN, A. (1987): The Alpidic evolution of the Eastern Alps, *in* Flügel, H. W.; and Faupl, P., eds., *Geodynamics of the Eastern Alps*: Vienna, Deuticke, p. 361-378.
- TOLLMANN, A., (1986): Geologie von Österreich, Bd.3: Vienna, Deuticke, 718 p.
- TRÜMPY, R. (1960): Paleotectonic evolution of the Central and Western Alps. *Geol. Soc. Amer. Bull.*, 71, 843-908.
- TRÜMPY, R. (1980): Geology of Switzerland. A guide-book. Part A : An outline of the geology of Switzerland. Wepf and Co. Basel, 104 p.
- TRÜMPY, R. (1997a): Alpine orogeny. In: MOORES, E.M. and FAIRBRIDGE, R.W., eds., *Encyclopedia of European and Asian regional geology*, p. 16-26, Chapman & Hall, London.
- TRÜMPY, R. (1997b): Switzerland. In: MOORES, E.M. and FAIRBRIDGE, R.W., eds., *Encyclopedia of European and Asian regional geology*, p. 704-710, Chapman & Hall, London.
- VANOSI, M., ed. (1991): *Alpi Liguri. Guide geologiche regionali*. Soc. Geol. Ital., BE-MA editrice, 295 p.
- VOSHAGE, H., HOFMANN, A.W., MAZZUCHELLI, M., RIVALENTI, G., SINIGOI, S., RACZEK, I. and DEMARCHI, G. (1990): Isotopic evidence from the Ivrea zone for a hybrid lower crust formed by magmatic underplating. *Nature*, 347, 731-736.
- WAGREICH, M. (1995): Subduction tectonic erosion and Late Cretaceous subsidence along the northern Austroalpine margin (Eastern Alps, Austria). *Tectonophysics*, 242, 63-78.
- WANG, X. and NEUBAUER, F. (1998): The deformation and kinematics of the Salzachtal fault zone, the northern margin of the Tauern Window, eastern Alps, Austria. - *J. Struct. Geol.*, 20, 799-818.
- ZIMMERMANN, R., HAMMERSCHMIDT, K. and FRANZ, G. (1994): Eocene high pressure metamorphism in the Penninic units of the Tauern Window (Eastern Alps): evidence from  $^{40}\text{Ar}/^{39}\text{Ar}$  dating and petrological investigations. *Contrib. Mineral. Petrol.*, 117, 175-186.



Carpathian-Balkan Geological Association, XVI Congress	Field Guide "Transsect through central Eastern Alps"	pp. 25 - 32	Salzburg - Wien, 1998
--	--	-------------	-----------------------

## STRATIGRAPHY AND HYDROCARBONS IN THE MOLASSE FOREDEEP OF UPPER AUSTRIA AND SALZBURG

H. Polesny

A-1015 Vienna, Schwarzenbergplatz 16, RAG

### STRATIGRAPHY

The Molasse Basin of Upper Austria and Salzburg is part of the Alpine-Carpathian foredeep. It represents an asymmetric basin with an outcropping passive northern margin where the sediments are overlying the crystalline basement of the Bohemian Massif. From there the beds dip to the south. The southern part has been affected by the alpine orogeny and is overthrust (Encl. 3 and 4). A significant area of the Molasse lies below the nappes of the Helvetic, the Flysch and the Northern Limestone Alps.

Total thickness of the Molasse sediments can reach more than 3000 m. The **Pretertiary basement** consists (from base to top) of Precambrian to Palaeozoic rocks (**Crystalline of the Bohemian Massif**). Above this crystalline rocks there are remnants of **Mesozoic sediments** (Encl. 1). In one well fluvial sandstones and clays with coal seams of probably **Permo Carboniferous** age were penetrated.

A dominant structural high (**Central Swell Zone**) passes from Bavaria in a NW-SE direction through the Molasse Basin of Upper Austria. Numerous faults are cutting the pretertiary basement and separate it into different blocks. All these blocks are tilted to the E. The vertical displacement can amount to more than 1000 m.

The **Mesozoic sediments** indicate **two main cycles** of marine transgression and regression (Encl. 1). During the **first cycle** (Mid-Jurassic – Lower Cretaceous) the Molasse basement was part of the Middle European Carbonate platform. Sedimentation started with fluvial braided stream sandstones with coal layers, followed by shallow marine sandstones and carbonates. The salt lagoon and tidal flat deposits of the Purbeck form the upper part. Opening of the Atlantic (during Lower Cretaceous) caused uplifting of the Bohemian Massif and interrupted the sedimentation. This led to erosion and karstification of the Jurassic carbonates.

During the **second cycle** (in Aptian) the area S of the Central Swell was flooded by the sea. In Upper Cretaceous (Cenomanian) the whole Molasse basement was transgressed. Sedimentation continued to Upper Campanian. The lowest **Cenomanian** sediments are fluvial sandstones (Schutzfels beds) which infill the Jurassic karsts. They are overlain by marine sandstones and shales. The sandstones were deposited by storms in an inner shelf setting. The sedimentation turns then to outer shelf facies. Late Campanian shallow marine coarse clastics are reported from the NW part of Upper Austria. Restricted to the easternmost part, from Late Turonian onwards, fluvio – deltaic fans were deposited.

The Cenomanian is the second most important oil reservoir of Upper Austria. Uplifting of the European plate stopped the marine sedimentation. Extensive erosion flattened the tilted fault blocks.

The **Molasse Basin** is a result of the Alpine orogeny. Sedimentation started in **Late Eocene** when the Tethys Sea progressively encroached from the south. It's marine record terminated in Upper Oligocene (Encl. 1). In Late Eocene the Central Swell Zone acted as a shallow barrier which separated the lagoon in the N from the slope to the open sea in the S. The different facies zones started in the N with fluvial floodplains cut by channel sandstones of meandering rivers. The subsiding floodplain is capped by a coal

bed (swamp) which is overlain by dark paralic Cerithian beds with tidal channels, followed by shallow marine sands. All these sediments are sourced from the Crystalline of the Bohemian Massif in the north. The red algae and coral reefs (Lithothamnium limestone) are approximately centered on the Central Swell and shed its debris to the north (lagoon) and to the south (high energy, open marine shelf edge). On the slope, sediments of successively deeper environments are developed (Nummulitic Sandstone, Discocyclina Marl, Globigerina Limestone, ...).

Oil and thermal gas are produced from the different Eocene sandstones and partly from the Lithothamnium limestone. The Eocene is the main oil producer of Upper Austria.

Rapid subsidence during the earliest Oligocene provided deep – water conditions. The Molasse basin became the pelagic Alpine foredeep. The first post-eocene sediment is the **Schoeneck fish shale** (Lower Kiscellian) which was deposited under low oxygen conditions. It contains a high content of organic material and is the correlated source rock of the Upper Austrian Oil. Generation took place below the Alpine nappes starting in Miocene.

The **Dynow Marlstone** consists of nanno-ooze. In the following shales, coarse clastics of turbiditic origin are intercalated. The subsidence was accompanied by a dense network of W-E trending extensional antithetic and synthetic faults. It was caused by the subduction of the European plate under the Periadriatic plate and by the weight of the advancing Alpine nappes.

This fault pattern controls most of the Upper Austrian oil fields (Encl. 2-4). The trough axis of the basin moved northward with the shift of the Alpine units and the Molasse imbricates. The deep marine bottom currents were forced to deviate in this direction and massively eroded into older sediments. The erosional surface was rapidly filled by coarse clastics (gravity deposits and turbidites). Often the sediments were reworked (contourites). The sandstones and conglomerates of the **Upper and Lower Puchkirchen Formation** contain many gas fields (bacterial gas – Encl.2). The gravel of the Oligocene and Lower Miocene conglomerates (crystalline, darkgrey dolomites, ...) were derived from the Central Alps in the south. Equivalents are the "Augenstein" gravels found on the surface of the Northern Limestone Alps.

By the beginning of **Hall Formation**, the Flysch nappes and Molasse imbricates had reached their present day position. The front of the Flysch and Helveticum nappes (plus the imbricates) formed the south rim of the deep marine environment. The base of Hall Formation follows a prominent submarine erosion across the Molasse basin (new fauna immigrated). Compressional tectonics including strike-slip movements occurred and the erosional events continued. Typical Hall Formation sediments are gray, silty shales with sandstones of turbiditic origin. There are many gas fields in Hall Formation sands.

At the end of Hall Formation time and during the Innviertler Formation the basin became shallower. After a short brackish event in Late Ottnianian the sea regressed towards the east. The Molasse sediments became tilted and intensive erosion took place.

The braided river gravels of the Coal-bearing freshwater beds (Badenian-Pannonian) contain coal seams which have been mined. Since the Quaternary large areas of the Molasse basin have been covered by moraines and fluvial gravels.

## **OIL AND GAS FIELDS IN THE FOREDEEP OF UPPER AUSTRIA AND SALZBURG (Encl. 2)**

The first gas and oil in present Austria was found in the Upper Austrian Molasse Basin (1892 gas in Wels and 1906 heavy oil in Leoprechting). Both discoveries were accidentally encountered by water wells in the shallow northern part of the Molasse Foredeep.

Many years passed by without any other hydrocarbon finds. In 1956 RAG (Rohöl-Aufsuchungs Aktiengesellschaft), Austria's oldest oil company (founded 1935), encountered oil by drilling its first exploration well in Upper Austria. The well Puchkirchen 1 hit oil in Eocene sandstones (Cerithian beds).

Meanwhile, many oil and gas fields have been discovered. The largest oil field so far is Voitsdorf (1962/63), located a few kilometers NE of the core storage Pettenbach. Some 40 wells have been drilled in this field which is an E-W trending monocline with a major fault in the N. Erosional processes made a joint reservoir with Eocene sandstones (fluvial and marine) overlaying the Cenomanian sandstones (tempestites) which rest on Jurassic sandstones. This field is crowned by a gas cap. 3.1 MM tonnes (23 MM BBL) of oil have been produced in Voitsdorf up to the end of 1997.

The last important oil discovery was Kemating (1979) where the oil is trapped in shallow marine Eocene sandstones of a fault block. The oil fields are controlled by faults and the south dipping beds. Sometimes in addition the shale-out of the reservoir plays an important role.

RAG's first commercial gasfind happened 1962 (Schwanenstadt 2, in Miocene Hall Formation). Most of the gas (bacterial gas) is found in Oligocene and Miocene coarse clastics (turbiditic sandstones and sandy conglomerates). The gas is trapped in compaction anticlines, stratigraphic traps or in a combination.

In the last few years prospects in the area of the rather complex imbricated molasse have been drilled. So far only few gas fields have been discovered in these imbricates. Last year the well Haidach 1 found a remarkable gas field. The areal extent of this gas is small but the net pay of the massflow sediments amounts to more than 60 m.

Several gas fields were found by drilling deeper oil prospects. In most of the deeper horizons there is condensate associated with the biogenic gas. The largest gas field is Atzbach – Schwanenstadt – Zell am Pettenfirst with gas in the deep marine coarse clastics of Puchkirchen Formation and Hall Formation (cumulative production to end of 1997 4.23 BNcbm (158 BSCF)). Thermal gas is found in the eastern part of Upper Austria in Upper Cretaceous and Eocene sandstones. Some reservoirs contain a mixture of thermal and biogenic gas.

Since 1965 OMV has been successfully exploring in parts of Upper Austria. Deep prospects S of the Alpine thrustfront encountered only marginal oil and gas accumulations. One well in the imbricated zone had a good oil influx but due to a later high water cut the well was uncommercial.

The low oil price has compelled RAG to concentrate on gas prospects during the last 12 years. This caused a decline in the oil production. The gas sales have been supplied by new discoveries and development drilling. Though the big compaction structures have been drilled for many years more complex, but smaller, gas accumulations are being found.

The fault pattern is important for the occurrence of the reservoirs and the traps. The Molasse Foredeep of Upper Austria and Salzburg is the second most important hydrocarbon province of Austria. At the end of 1997, RAG had produced 7.5 MM tonnes (55 MM BBL) of oil and 16.3 BNcbm (606 BSCF) of gas. RAG installed an underground gas storage in the Puchkirchen gas field (Upper Puchkirchen Fm.). Six horizontal wells (horizontal length in the reservoir > 1000 m) have been drilled. Another gas storage project is handled by OMV. RAG has drilled more than 600 wells in the Molasse Foredeep. The basin is covered by a dense grid of 2 D-seismic lines and a relative large area by 3 D-seismic.

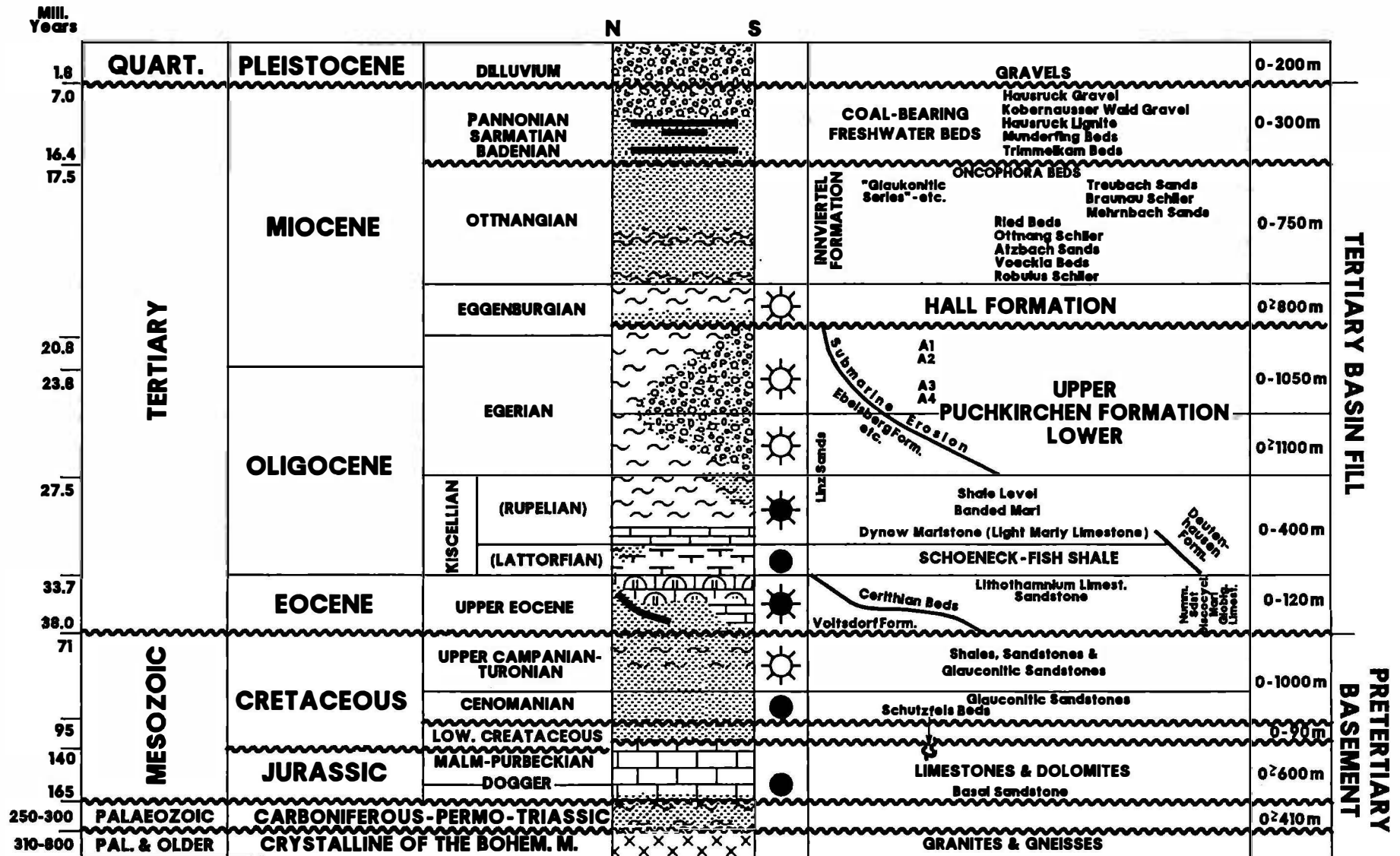
High temperatures (> 100°C) and appropriate reservoir rocks (karsted Jurassic carbonates) offer good geothermal potential. Some geothermal projects are already operating partially using old RAG wells. Next year, even electric power will be generated (Altheim).

## REFERENCES:

- ABERER, F. 1958: Die Molassezone im westlichen Oberösterreich und in Salzburg. *Mitteilungen der Geologischen Gesellschaft in Wien*, 50 (for 1957), 23-94.
- BRAUMÜLLER, E. 1961: Die paläogeographische Entwicklung des Molassebeckens in Oberösterreich und Salzburg. *Erdöl-Zeitschrift*, 77/11, 509-521.
- KOLLMANN, K. 1977: Die Öl- und Gasexploration der Molassezone Oberösterreichs und Salzburgs aus regional-geologischer Sicht. *Erdöl-Erdgas Zeitschrift*, 93, 36-49

- MALZER, O., RÖGL, F., SEIFERT, P., WAGNER, L., WESSELY, G., BRIX, F., 1993: Die Molassezone und deren Untergrund: in BRIX, F. & SCHULTZ, O. (Hrsg): Erdöl und Erdgas in Österreich. Naturhist. Mus. Wien und F. Berger, Horn, 281-358.
- WAGNER, L. 1980: Geologische Charakteristik der wichtigsten Erdöl- und Erdgasträger der oberösterreichischen Molasse. Teil I: Die Sandsteine des Obereozän. Erdöl-Erdgas Zeitschrift 96/9, 338-346.
- WAGNER, L., KUCKELKORN, K. & HILTMANN, W. 1986: Neue Ergebnisse zur alpinen Gebirgsbildung Oberösterreichs aus der Bohrung Oberhofen 1 – Stratigraphie, Fazies, Maturität und Tektonik. Erdöl-Erdgas Zeitschrift 102, 12-19.
- WAGNER, L. 1996: Stratigraphy and Hydrocarbons in the Upper Austrian Molasse Foredeep (active margin). In WESSELY, G. & LIEBL, W. (Eds.) Oil and Gas in the Alpidic Thrustbelts and Basins of Central and Eastern Europe. EAGE Special Publication, 5.

# STRATIGRAPHIC CHART OF THE MOLASSE BASIN UPPER AUSTRIA AND SALZBURG



GAS-BEARING



GAS- & OIL-BEARING



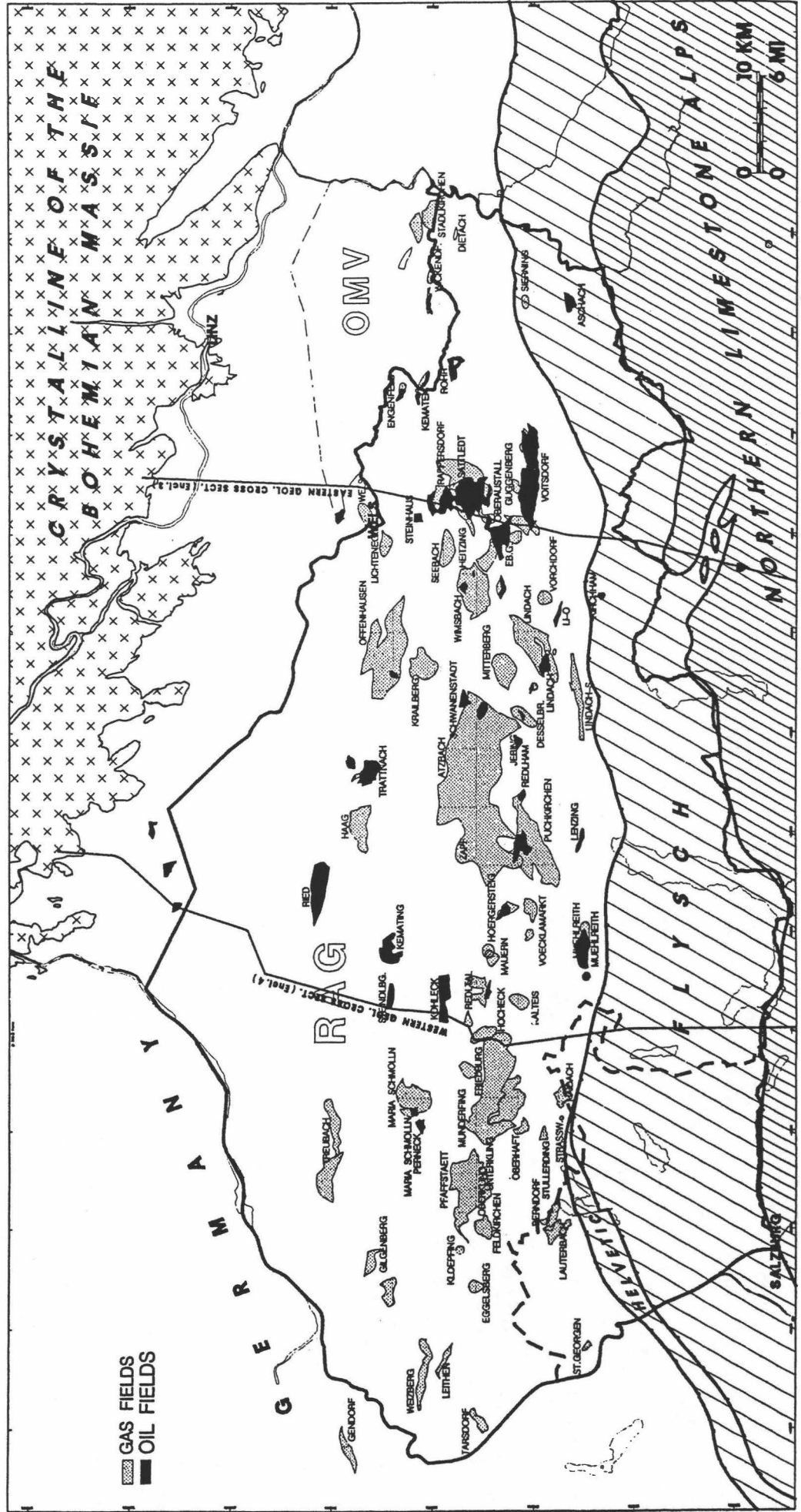
OIL-BEARING

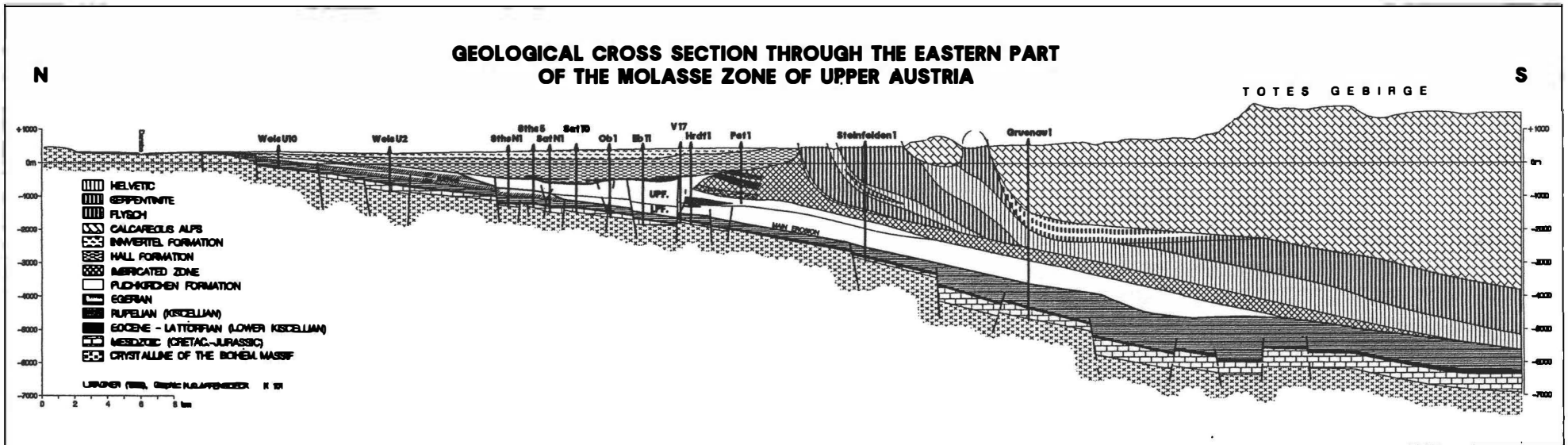


# UPPER AUSTRIA AND SALZBURG GAS and OIL FIELDS

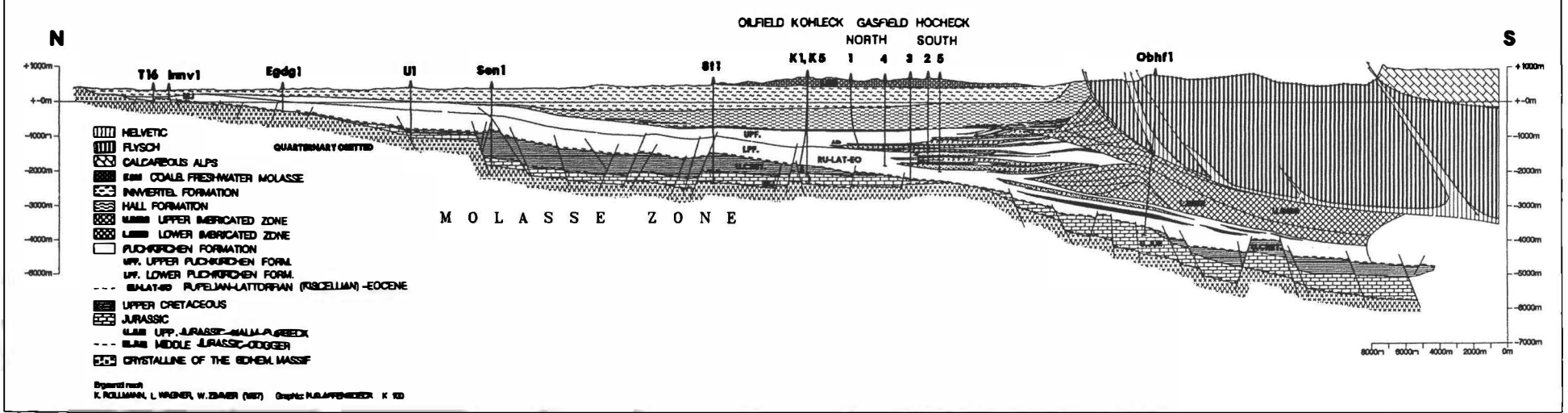
JULY 1998  
Graphic: H. KLAFFENBOECK

Encl. 2





### GEOLOGICAL CROSS SECTION THROUGH THE WESTERN PART OF THE MOLASSE ZONE OF UPPER AUSTRIA





Carpathian-Balkan Geological Association, XVI Congress	Field Guide "Transect through central Eastern Alps"	pp. 33 - 43	Salzburg - Wien, 1998
--	---	-------------	-----------------------

## **Late orogenic rebound and oblique Alpine convergence: new constraints from subsidence analysis of the Austrian Molasse basin**

**J. Genser <sup>1</sup>, S. Cloetingh <sup>2</sup>, and F. Neubauer <sup>1</sup>**

<sup>1</sup> Dept. of Geology and Paleontology, University, Hellbrunner Str. 34, 5020 Salzburg, Austria

<sup>2</sup> Dept. of Earth Sciences, Vrije Universiteit, De Boelelaan 1085, 1081 HV Amsterdam, The Netherlands

### **ABSTRACT**

Subsidence analysis of 16 wells in the Austrian Molasse basin documents major spatial and temporal changes in tectonic subsidence. The timing of main tectonic subsidence phase shifted from early Oligocene in the western part of the peripheral foreland to the early Miocene in the eastern part. These temporal and spatial changes in tectonic subsidence reflect a change from oblique dextral to sinistral convergence between the Alpine nappe stack and its foreland. The main phase of sediment accumulation was retarded to the early Miocene and led to the infill of the basin and a major second, sediment load driven phase of basement subsidence. Sediment accumulation rates in the basin reflect the build-up of topography in the Alpine mountain chain. Since approximately 6 Ma a pronounced regional uplift of the entire Molasse basin has taken place, marking the transition from lateral extrusion to orthogonal contraction within the Alpine-Carpathian system and deep-seated changes in geodynamic boundary conditions, likely delamination of previously thickened lithosphere.

### **INTRODUCTION**

Foreland basins develop in response to the bending of an elastic lithosphere due to loading by the advancing orogenic wedge and/or additional loads, as e.g. slab pull forces and thickened mantle lithosphere, operating on the lithosphere (Beaumont, 1981; Royden, 1993). Modeling of foreland basins so far has mostly only focused on the constructive stage of basin evolution, with relatively minor attention for their late-stage inversion of subsidence, as observed in the Austrian Molasse basin.

The Austrian Molasse basin provides a detailed stratigraphic response, from the late Eocene onwards, to the configuration of the Eastern Alpine orogenic wedge, allowing to place time constraints on the main young tectonic phases of the Alpine orogen. This is particularly important, as data on the timing of brittle deformation phases within the Alps are difficult to assess in the absence of related sediments. There are almost no other data on the uplift history of the Eastern Alps, apart from limited geodetic data on the present stage (e.g., Meurers, 1992) and exhumation histories from fission track data (Grundmann and Morteani, 1985; Staufenberg, 1987; Hejl, 1997). Below we will

demonstrate that the stratigraphic record of the Austrian Molasse basin provides important constraints on magnitudes and causes of vertical motions within and adjacent to the basin.

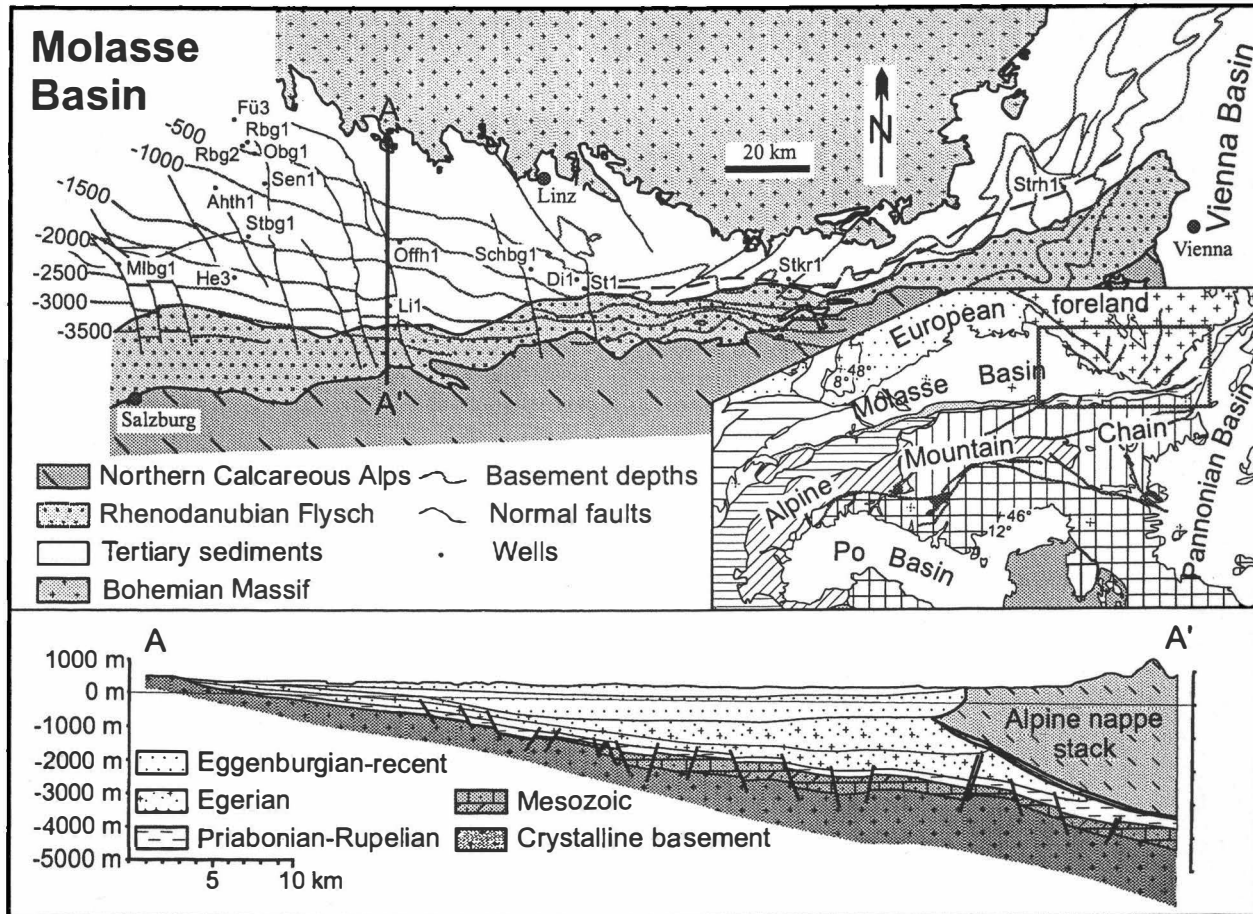


*Fig. 1: a) Tectonic map of the Molasse basin and its surroundings, showing basement depths and location of analyzed wells. Inset shows setting of the investigated basin in the Alpine arc. b) N-S section displays the basin geometry and main depositional units of the basin.*

## STRATIGRAPHIC FRAMEWORK

The Molasse basin of the Alps (Fig. 1) is a classical foreland basin developed in response to the loading of the southern margin of the European plate after the final continent-continent collision (Lemcke, 1984; Bachmann et al., 1987; Wessely, 1987; Malzer et al., 1993). The Austrian Molasse basin displays strong lateral changes in shape with a decrease in width from about 150 km in the German Molasse basin to less than 10 km at the spur of the Bohemian Massif (Fig. 1). To the east the basin widens again and changes its strike from E-W to NE-SW. Also the basement depths of the basin at its southern margin decrease from about 3500 m in the west to about 500 m in the east. In the same direction the ages of the oldest Molasse strata get

increasingly younger (Malzer et al., 1993). The overriding Alpine nappe complex comprises structurally upwards units derived from the outer shelf to slope of the European continental margin, followed by the Flysch nappes, and finally the Austro-Alpine complex in an upper plate position. The youngest sediments of these units are of lower Eocene ages. Reflection seismic profiles and well data support a post-Eocene shortening of more than 200 km (Wagner et al., 1986).

The Molasse sequence started in the Late Eocene with the subsidence of the European plate, with a deepening towards the south (Lemcke, 1984; Bachmann et al., 1987; Malzer et al., 1993). Sediments range from terrestrial to shallow marine clastics and limestones to marls of a deeper shelf. In the Latdorfian (early Oligocene), the basin subsided quickly to water depths of several hundreds of meters and dark shales to marls of a restricted basin were deposited. They are overlain by the Rupelian (32-28 Ma) sequence of light chalky marls, overlain by banded marls and then silty shales to marls. These marls pass into sandstones and conglomerates towards the south, that were derived from the rising Alps. Along the northern rim of the present basin and the spur of the Bohemian Massif terrestrial sediments prevailed. In the Egerian (28-20.5 Ma), the basin configuration remained essentially the same with terrestrial to shallow marine conditions along the northern margin. In the southern part of the basin thick turbiditic fans were shed into the basin. At the same time the southernmost part of the basin was overridden by the advancing nappe complex, incorporating also Molasse sediments (Malzer et al., 1993).

With the Egerian (20.5-18 Ma) the orogenic wedge reached essentially its present position and the basin axis shifted to the north. The basin also shows a transgression to the north and the spur of the Bohemian Massif shows a first major phase of subsidence. The main sediments were still sandy to silty shales and marls, only the turbiditic influence decreased. In the Ottnangian (18.0-17.2 Ma), the basin shallowed progressively and finally the sea regressed to the east of the Bohemian Massif at the end of this stage. From the Karpatian to the Pannonian terrestrial sediments were deposited in the basin west of the Bohemian Massif, which can be divided into several lithozones (Unger, 1989). These represent bodies of different sediment sources and transport directions and are also divided by erosional gaps. Only close to the Vienna basin marine incursions into the Molasse basin occurred up to the Sarmatian. In the Pannonian, a change from mainly W-directed to E-directed transport occurred. After the Pontian mainly erosion of the sediments took place, induced by the uplift of the Molasse basin. This uplift is documented in the present elevation of the shallow marine sediments of the late Ottnangian of about 550-600 m above sea-level.

## **SUBSIDENCE ANALYSIS**

Subsidence analysis of the Molasse basin was carried out for 16 wells together with an evaluation of seismic sections. We used the stages for the central Paratethys for the stratigraphic correlation and the absolute time scale of Steininger et al. (1996) for the Miocene to Pleistocene, and that of Cande and Kent (1992) for older stages. Most of the time markers used are sequence boundaries that are biostratigraphically tied to the stages of the central Paratethys (see also Jin et al., 1995). Sediments were decompacted accounting for lithology-dependent vertical fluid escape during decompaction with the program package PDI (IES, Jülich). We used program defined lithologies that match the observed lithologies. Missing stratigraphic sections were reconstructed from adjacent well data, seismic profiles, and geological maps. These eroded sections are less than about 200 m in most wells. For the

easternmost wells no reconstruction of missing sections was made due to the widespread erosion of the youngest strata in this area.

Along the northern margin of the basin shallow marine sediments allow us to obtain relatively well constrained water depths. Also to the west, during the Egerian, a deep marine basin (Puchkirchen basin) graded into shallow marine to terrestrial sediments (Lower Freshwater Molasse), pointing to an increase in water depths from the N to the S and from the W to the E. The subsequent terrestrial sediments range from the Karpatian to the late Pannonian/early Pontian (7.1 Ma). In the Vienna basin, close to the east, marine conditions prevailed up to the Sarmatian and changing transport directions in the Molasse basin point to very low east-west topographic gradients and low elevations up to this time span. We, therefore, conclude that major surface uplift of the basin commenced only in the Pontian.

Backstripping of the sediments to reconstruct the basement shape due to tectonic loading was carried out for a local isostatic model. The inferred general shape of the tectonic subsidence curve and the timing appear to be rather insensitive to assumptions on the flexural properties of the foreland plate. Subsidence curves corrected for eustasy (Haq et al., 1987) display only minor differences to uncorrected curves of both basement and tectonic subsidence and are largely well within uncertainties in water depths (Fig. 2).

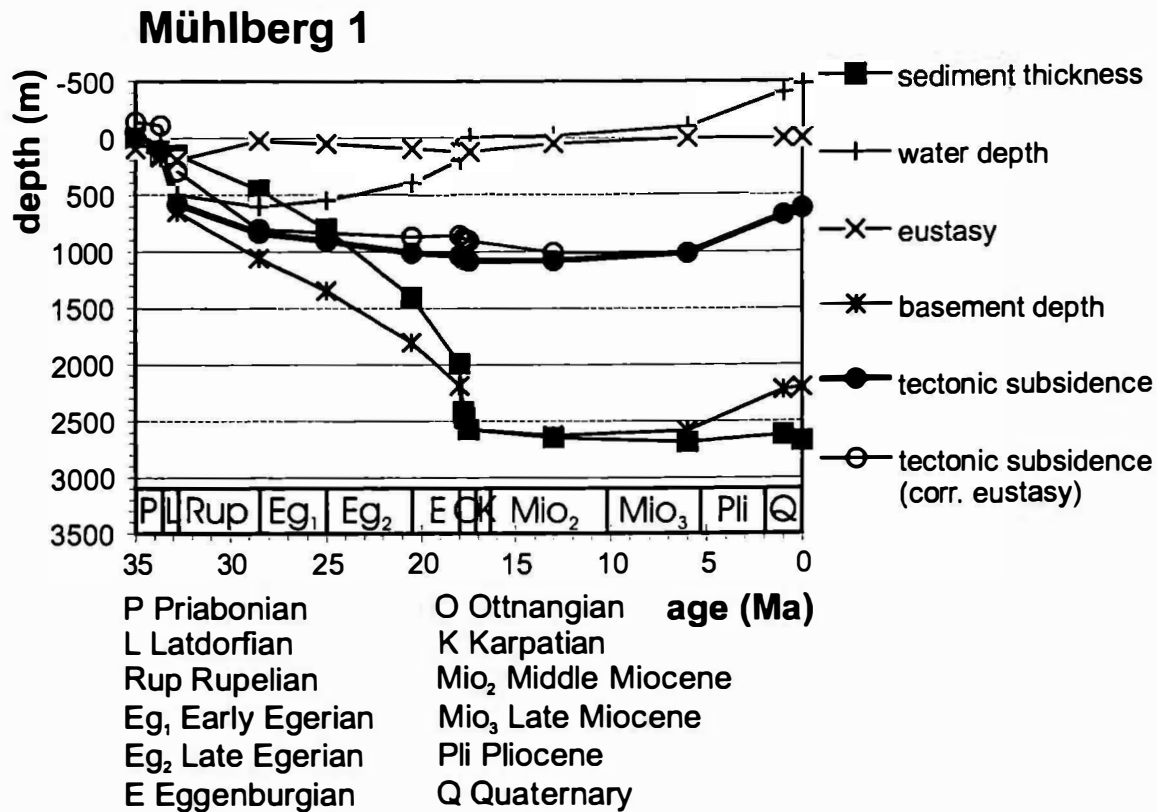


Fig. 2: Geohistory diagram displaying sediment thicknesses, basement subsidence, tectonic subsidence, water depths, and eustasy in time for well Mlbg 1 (Fig. 1a). Tectonic subsidence for local isostasy with a mantle density of  $3,300 \text{ kgm}^{-3}$ , sediment densities as calculated by the decompaction procedure.

## SUBSIDENCE PATTERNS

Along a N-S section in the western part of the Austrian Molasse basin all wells show similar temporal subsidence evolutions (Fig. 3). Subsidence started in the Late Eocene. In the early Oligocene, the basin strongly subsided to greater water depths and reached already large fractions of the maximum amounts of tectonic subsidence. The basement subsidence curves display for this time slice decreasing subsidence rates, followed by an increase in the Ottnangian. Basement subsidence is mainly driven by sediment loading and thus mainly reflects changing sediment accumulation rates. Only in the Ottnangian minor tectonic subsidence occurred. Basement depths and the amount of tectonic subsidence are well defined for the end of the Ottnangian, as paleowaterdepths are tightly constrained by the transition from marine to terrestrial conditions. After the Ottnangian subsidence rates decreased strongly. Subsequently, uplift to the present observed depths occurred with similar, only slightly decreasing amounts away from the orogen along the whole profile normal to the trend of the basin. The estimated tectonic uplift is in the order of 500 m, leading to a reduction of the present tectonic subsidence to about a half of its maximum values in the southern part of the basin and to net uplift in the peripheral part of the basin. The total amount of uplift since the Ottnangian/Karpatian is well constrained by the available data. The exact timing is more uncertain, with evidence for a major uplift beginning at the end of the concordant sedimentation in the Pontian.

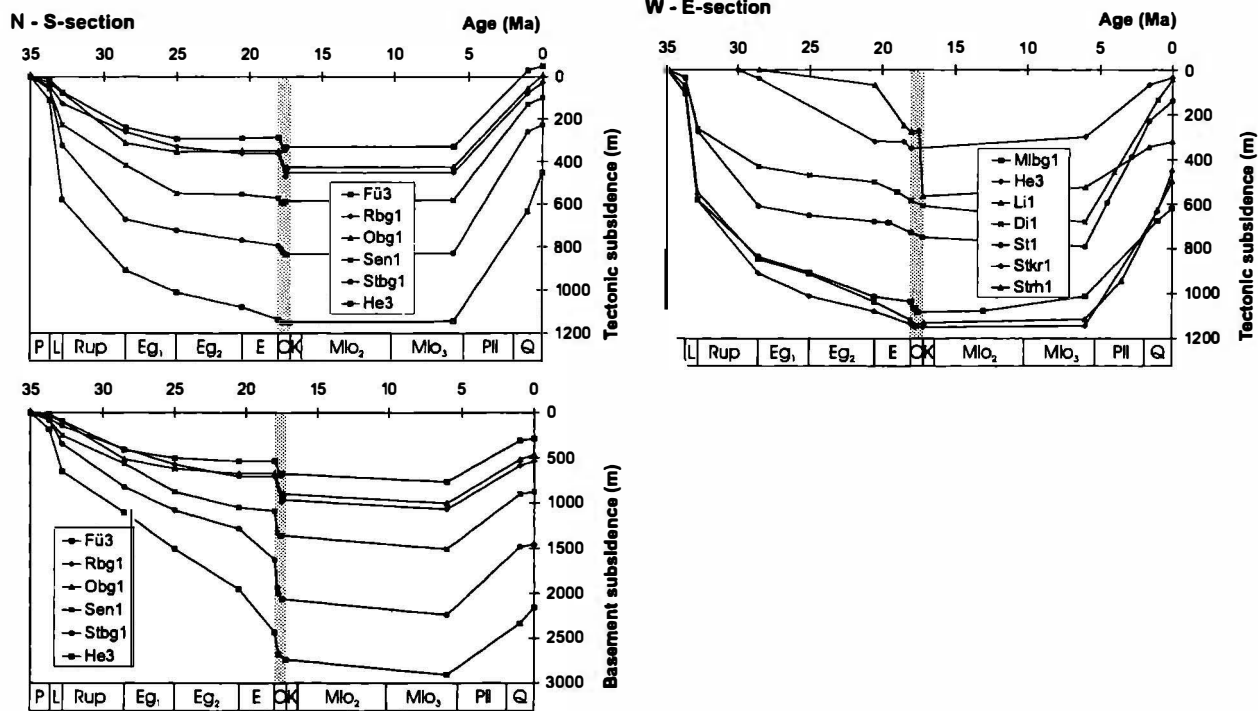


Fig. 3: Temporal evolution of subsidence in time. For stratigraphic stages, see Fig. 2. a) Tectonic and basement subsidence for N-S profile. b) Tectonic subsidence for E-W profile (for location of wells, see Fig. 1a).

Parallel to the Alpine front the basin displays marked differences in its subsidence history (Fig. 4). Towards the east, initial subsidence is retarded, occurring only in the late Egerian east of the spur of the Bohemian Massif. There, tectonic subsidence rates strongly increased in the Eggenburgian and Ottnangian, leading to the formation of the present eastern Austrian Molasse basin and the N-S trending spur of the Bohemian Massif. The subsequent tectonic uplift occurred along the whole strike of the basin, decreasing towards the east from about 600 m to 200 m. At the spur of the Bohemian Massif, tectonic subsidence was almost completely reversed.

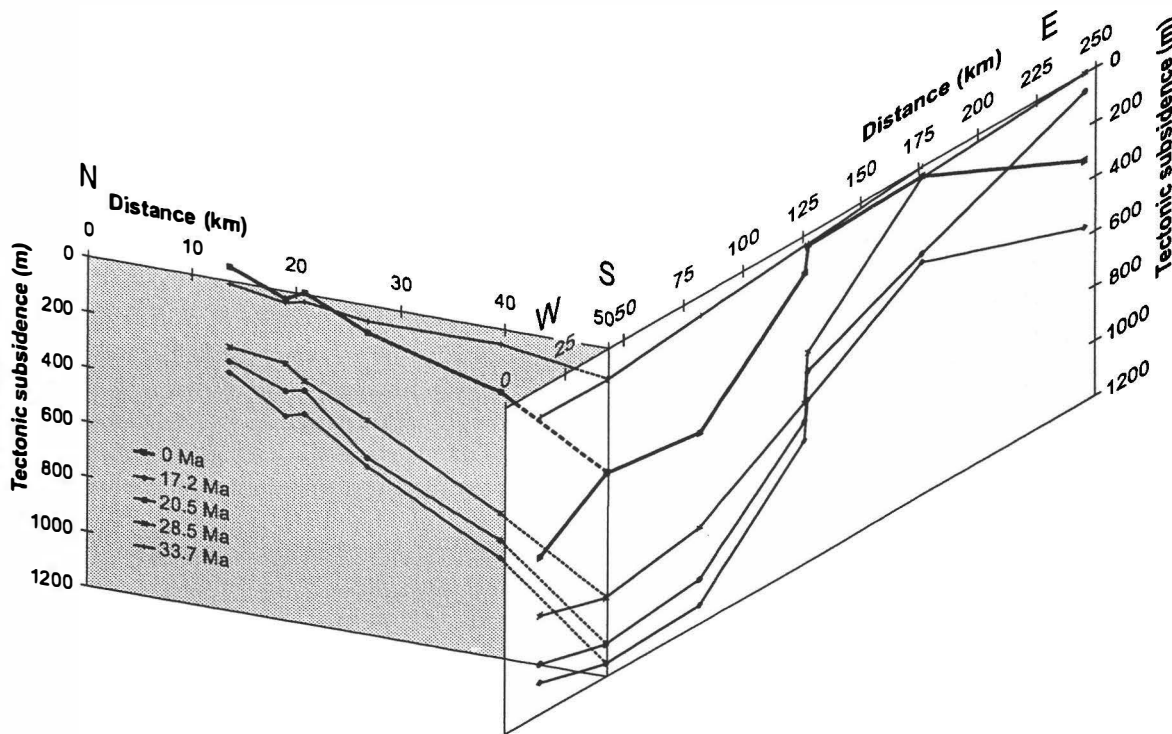


Fig. 4: Spatial view of tectonic subsidence for different time slices.

## CONSTRAINTS ON MECHANISMS FOR LATE CENOZOIC VERTICAL MOTIONS

The subsidence patterns record several sharp transitions that appear to reflect three major temporal changes in the geodynamic evolution of the orogenic belt.

### Stage 1. Onset of foreland subsidence and its linkage with the internal Alpine orogen.

The onset of subsidence during the Eocene may represent initial stages of flexural loading of the European continental crust by the advancing Alpine nappe complex and thickening of the Alpine nappe complex (Fig. 5a). Detailed work in the Eastern Alps revealed a kinematic path of dextral transpression during overthrusting of thinned continental outliers and the southern margin of the European continental lithosphere (Kurz et al., 1996; Genser et al., 1996). These basement rocks are presently exposed within the Penninic Tauern Window, and show a general WNW-directed transport direction up to the metamorphic peak, that has been dated at between about 30 and 20 Ma. Subsidence in the western part of the Austrian and the Swiss and German Molasse basin

appear to record, therefore, the collisional coupling of the European continental margin and the evolving Alpine nappe stack in the late Eocene to early Oligocene.

**Stage 2. Full coupling of internal orogen with Molasse basin.** In the late Early Miocene (Eggenburgian to Ottnangian) strong tectonic subsidence commenced in the eastern part of the Austrian Molasse basin. This stage coincides with the transition from WNW-directed contraction to eastwards directed lateral extrusion of central sectors within the Eastern Alps (Ratschbacher et al., 1991). The extruding wedge was bound by sinistral strike-slip faults that reach up to the foreland basin along its northern sector. Displacement along these faults led to progressive loading of more eastern parts of the foreland, whereas the preceding WNW-directed transport was subparallel to the strike of the Austrian Molasse basin. Lateral extrusion is associated with gravitational collapse of upper sectors within the Alpine nappe edifice and tectonic unroofing of metamorphic core complexes (Ratschbacher et al., 1991; Kurz and Neubauer, 1996). Sediment accumulation rates increased in the Early Miocene and peaked during the Ottnangian. As the basin configuration remained essentially the same, accumulation rates reflect sediment input rates and creation of topography in the adjacent mountain belt. The timing of extension and the formation of metamorphic core complexes in the internal zone are constrained by cooling ages of the uplifting metamorphic Tauern dome at between about 22 and 14 Ma. As this tectonic phase has led to the construction of strong topographic gradients, ongoing convergence between the European and Adriatic plates was likely largely compensated by orogenic thickening and lateral extrusion. The changes in displacement paths are also expressed in changing paleostress directions and regimes in frontal parts of the Alpine nappe edifice (Decker et al., 1993).

**Stage 3. Final uplift.** Several mechanisms, leading to either changes in the load configuration or the mechanical state of the flexed plate, may contribute to the late stage uplift of central and northern sectors of the Eastern Alps, comprising the Molasse basin. These include (for resulting subsidence/uplift patterns see Fig. 6): (1) Viscous relaxation of the flexed plate, reducing the flexural wavelength, would lead to uplift of peripheral parts of the basin, and subsidence of the internal parts (e.g., Beaumont, 1981). This is in contradiction to the observed uplift pattern with the highest amount of uplift at the orogenic front and only slightly decreasing amounts towards peripheral parts. Changes in loading can be either due to superficial processes, as (2) erosional or tectonic denudation of central sectors of the Alps, the former possibly enhanced due to climatic changes. The resulting uplift patterns resemble the observed ones, but especially for low effective elastic thicknesses (EET), as appropriate for the Molasse basin (compare observed and calculated basement profiles), uplift should vanish in peripheral parts of the basin and would also give stronger gradients. Additionally, judging from apatite fission track data (Grundmann and Morteani, 1985; Staufenberg, 1987; Hejl, 1997), denudation rates in this time span high enough to bring about the unloading required for the observed uplift, are only reached in a few places in the internal part of the Eastern Alps. Deep-seated processes leading to unloading can be either (3) slab break-off or (4) distributed delamination or convective removal of mantle lithosphere. Slab break-off, simulated by dropping previously applied end loads (vertical shear stresses and/or bending moments), leads to either negligible repercussions on the peripheral basin for low EETs or additional subsidence in the basin for large EETs due to shallowing of the peripheral bulge that is related to the end loads.

Therefore, we conclude that the late stage wide-spread uplift of the entire Alpine realm including the northern peripheral foreland basin is most likely explained by distributed delamination and/or convective removal of overthickened lithosphere and northward spreading of the mechanical decoupling between mantle and crust of the subducted lithosphere, enhanced by erosional unloading. This late-stage major change in the geodynamic boundary conditions of the Alpine system is also expressed in its present gravimetric state (Lyon-Caen and Molnar,

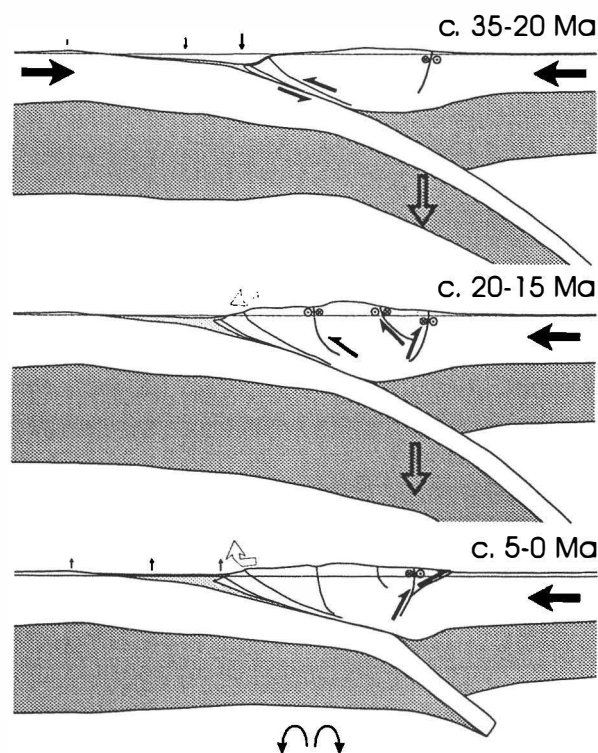


*Fig. 5: Proposed model for three-stage evolution of the eastern sector of the Alpine Molasse basin. a) Rapid initial foreland basin formation due to loading by the advancing Alpine nappe stack of the subducting southern margin of the European plate. b) Coupling of lower European plate and frontal orogenic wedge. Compensation of ongoing convergence by vertical thickening, leading to increasing sediment supplies to the foreland basin, and lateral extrusion (out of plane). c) Widespread uplift due to delamination and/or convective removal of thickened lithosphere and minor erosional unloading.*

1989). Recently, a number of studies have shown that the lithosphere in the cores of Alpine orogens is relatively weak (Okaya et al., 1996; Cloetingh and Burov, 1996), promoting the development of mechanical decoupling between upper crustal flexure and mantle lithosphere. Supporting evidence comes from modeling that resulted in unusual low effective thicknesses of the Northalpine Molasse basin. Values range between c. 25 km in the west and 10 km close to the investigated area (Andeweg and Cloetingh, 1998). Very low values were also reported from the mountain core (Okaya et al., 1996) and the western sectors of the Pannonian basin (Sachsenhofer et al., 1997). The timing of the mechanical decoupling appears to reflect major thermal relaxation following rapid exhumation of mechanically weak crust in the Early Miocene (Genser et al., 1996).

The onset of late Molasse basin uplift and similar uplift of the Styrian basin and western part of the Pannonian basin (Sachsenhofer et al., 1997) occurs at the time of a major reorganization of the external stress field at 6-5 Ma, recently recorded in the central European realm (e.g., Horvath and Cloetingh, 1996; Peresson and Decker, 1997). Such changes in stress acting on weak, decoupled lithosphere, caused by delamination, could provide an effective mechanism for regional rapid vertical motions of the crust. Lithospheric delamination is also inferred from



the 6-5 Ma onset of alkaline volcanism in the western part of the Pannonian basin, the Po basin, and the northern foreland of the Alps (e.g., Embey-Isztin et al., 1993).

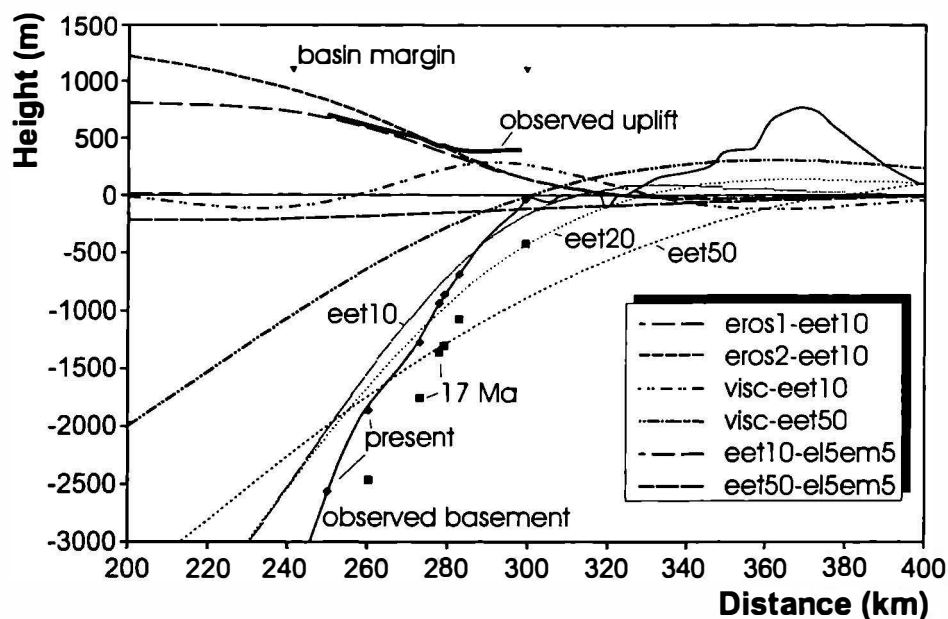


*Fig. 6: Observed uplift pattern and basement depths in comparison to modeled basement profiles (for effective elastic thicknesses (EET) of 10, 20, and 50 km, respectively) and uplift/subsidence patterns for different scenarios: (1) Erosional unloading in orogenic wedge by 1 km (eros1-eet10) and 2 km (eros2-eet10), respectively, for a flexed plate with an EET of 10 km; (2) viscous relaxation (visc) of plates with initial EETs of 10 and 50 km, respectively; (3) dropping of an initially applied vertical shear force of  $5 \cdot 10^{12}$  N/m and a bending moment of  $5 \cdot 10^{16}$  N at the end of the plate (0 km) for plates with EETs of 10 and 50 km, respectively.*

**Acknowledgments:** RAG and OMV companies provided industrial well data. Flexure modeling was carried out with the program tAo by Garcia-Castellanos. Work has been supported by a grant of the Jubiläumsfonds der Österreichischen Nationalbank (grant no. 4786).

## REFERENCES CITED

- Andeweg, B., and Cloetingh, S., 1997. Flexural modeling of the German and Austrian Molasse basin. Geological Society of London Special Publication (in press).
- Bachmann, G. H., Müller, M., and Weggen, K., 1987, Evolution of the Molasse Basin (Germany, Switzerland): Tectonophysics, v. 137, p. 77-92.
- Beaumont, C., 1981, Foreland basins: R. Astron. Soc. Geophys. J., v. 65, p. 291-329.
- Cande, S. C., and Kent, D. V., 1992, A new geomagnetic polarity time scale for the Late Cretaceous and Cenozoic: J. Geophys. Res., v. 97, p. 13917-13951.

- Cloetingh, S., and Burov, E. B., 1996, Thermomechanical structure of European continental lithosphere: constraints from rheological profiles and EET estimates: *Geophys. J. Int.*, v. 124, p. 695-723.
- Decker, K., Meschede, M., and Ring, U., 1993, Fault slip analysis along the northern margin of the Eastern Alps (Molasse, Helvetic nappes, North and South Penninic flysch, and the Northern Calcareous Alps): *Tectonophysics*, v. 223, p. 291-312.
- Embey-Isztin, A., Downes, H., James, D. E., Upton, B. G. J., Dobosi, G., Ingram, G. A., Harmon, R. S., and Scharbert, H. G., 1993, The petrogenesis of Pliocene alkaline volcanic rocks from the Pannonian Basin, Eastern Central Europe: *J. Petrol.*, v. 34, p. 317-343.
- Genser, J., van Wees, J. D., Cloetingh, S., and Neubauer, F., 1996, Eastern Alpine tectono-metamorphic evolution: constraints from two-dimensional P-T-t modelling: *Tectonics*, v. 13, p. 584-604.
- Grundmann, G., and Morteani, G., 1985, The young uplift and thermal history of the central Eastern Alps (Austria/Italy), evidence from apatite fission track ages: *Jb. Geol. B.-A.*, v. 128, p. 197-216.
- Haq, B. U., Hardenbol, J., and Vail, P. R., 1987, Chronology of fluctuating sea levels since the Triassic: *Science*, v. 235, p. 1156-1167.
- Hejl, E., 1997, "Cold spots" during the Cenozoic evolution of the Eastern Alps: *Tectonophysics*, v. 272, p. 159-173.
- Horvath, F., and Cloetingh, S., 1996, Stress-induced late-stage subsidence anomalies in the Pannonian basin: *Tectonophysics*, v. 266, p. 287-300.
- Jin, J., Aigner, T., Luterbacher, H. P., Bachmann, G. H., and Müller, M., 1995, Sequence stratigraphy and depositional history in the south-eastern German Molasse Basin: *Marine Petrol. Geol.*, v. 12, p. 929-940.
- Kurz, W., and Neubauer, F., 1996, Strain partitioning during updoming of the Sonnblick area in the Tauern Window (Eastern Alps, Austria): *J. Struct. Geol.*, v. 18, p. 1327-1343.
- Kurz, W., Neubauer, F., and Genser, J., 1996, Kinematics of Penninic nappes (Glockner Nappe and basement-cover nappes) in the Tauern Window (Eastern Alps, Austria) during subduction and Penninic-Austroalpine collision: *Eclogae geol. Helv.*, v. 89, p. 573-605.
- Lemcke, K., 1984, Geologische Vorgänge in den Alpen ab Obereozän im Spiegel vor allem der deutschen Molasse: *Geol. Rdsch.*, v. 73, p. 371-397.
- Lyon-Caen, H., and Molnar, P., 1989, Constraints on the deep structure and dynamic processes beneath the Alps and adjacent regions from an analysis of gravity anomalies: *Geophys. J. Int.*, v. 99, p. 19-32.
- Malzer, O., Rögl, F., Seifert, P., Wagner, L., Wessely, G., and Brix, F., 1993, Die Molassezone und deren Untergrund, in Brix, F. and Schultz, O., eds., *Erdöl und Erdgas in Österreich*: Wien, Naturhistorisches Museum Wien und F. Berger, p. 281-358.
- Meurers, B., 1992, Untersuchungen zur Bestimmung und Analyse des Schwerefeldes im Hochgebirge am Beispiel der Ostalpen: *Österr. Beiträge zu Meteorologie und Geophysik*, v. 6, p. 1-146.
- Okaya, N., Cloetingh, S., and Mueller, S., 1996, A lithospheric cross-section through the Swiss Alps (part II): constraints on the mechanical structure of a continent-continent collision zone: *Geophys. J. Int.*, v. 127, p. 399-414.
- Peresson, H., and Decker, K., 1997, Far-field effects of Late Miocene subduction in the Eastern Carpathians: E-W compression and inversion of structures in the Alpine-Carpathian-Pannonian region: *Tectonics*, v. 16, p. 38-56.
- Ratschbacher, L., Frisch, W., Linzer, H. G., and Merle, O., 1991, Lateral extrusion in the Eastern Alps, part 2: Structural analysis: *Tectonics*, v. 10, p. 257-271.
- Royden, L. H., 1993, The tectonic expression slab pull at continental convergent boundaries: *Tectonics*, v. 12, p. 303-325.
- Sachsenhofer, R. F., Lankreijer, A., Cloetingh, S., and Ebner, F., 1997, Subsidence analysis and quantitative basin modelling in the Styrian basin (Pannonian Basin system, Austria): *Tectonophysics*, 272: 175-196.

- Staufenberg, H., 1987, Apatite fission-track evidence for postmetamorphic uplift and cooling history of the eastern Tauern Window and the surrounding Austroalpine (Central Eastern Alps, Austria): *Jb. Geol. B.-A.*, v. 130, p. 571-586.
- Steininger, F. F., Berggren, W. A., Kent, D. V., Bernor, R. L., Sen, S., and Agusti, J., 1996, Circum Mediterranean Neogene (Miocene and Pliocene) marine-continental chronologic correlations of European mammal units: *in* Bernor, R. L., Fahlbusch, V., and Rietschel, S., eds., *The evolution of Western Eurasian Neogene mammal faunas*: New York, Columbia University Press, p. 7-46.
- Unger, H. J., 1989, Die Lithozonen der Oberen Süßwassermolasse Südostbayerns und ihre vermutlichen zeitlichen Äquivalente gegen Westen und Osten: *Geologica Bavarica*, v. 94, p. 195-237.
- Wagner, L., Kuckelkorn, K., and Hiltmann, W., 1986, Neue Ergebnisse zur alpinen Gebirgsbildung Oberösterreichs aus der Bohrung Oberhofen 1 - Stratigraphie, Fazies, Maturität und Tektonik: *Erdöl, Erdgas, Kohle*, v. 102, p. 12-19.
- Wessely, G., 1987, Mesozoic and Tertiary evolution of the Alpine-Carpathian foreland area in eastern Austria: *Tectonophysics*, v. 137, p. 45-59.



Carpathian-Balkan Geological Association, XVI Congress	Field Guide "Transsect through central Eastern Alps"	pp. 45 - 48	Salzburg - Wien, 1998
--	--	-------------	-----------------------

## New $^{40}\text{Ar}/^{39}\text{Ar}$ ages and geochemical data from the Molasse zone north of Salzburg (Upper Austria)

**Detlef Schneider, Franz Neubauer, Johann Genser, Robert Handler and Dan Topa**  
 Univ. Salzburg, Dept. of Geology and Paläontology, Hellbrunner Str. 34, A-5020 Salzburg  
[Detlef.Schneider@sbg.ac.at](mailto:Detlef.Schneider@sbg.ac.at)

The Alpine foreland basin north of the Alpine front is a Tertiary molasse basin which is separated from detached flysch sequences which were incorporated in the Alpine nappe stack (e.g. Nachtmann & Wagner 1987). Volcanic influence is modest or absent in detrital mode both in molasse and flysch sequences. Sandstones are relative high mature. Rare earth element patterns of sandstones from the Molasse zone are shown in Fig. 1.  $^{40}\text{Ar}/^{39}\text{Ar}$  ages of detrital white mica measured from 6-8 grains indicate two different sources (Fig. 2): a) Variscan (320-280 Ma) and b) Cretaceous ages (140-100 Ma). Mixed ages are common due to the variable proportions of grains from these two sources (Schneider et al. 1998).

The sediment input into the Molasse zone originated from two main source areas: In the Upper Eocene (Priabonian) sediments derived from the Variscan Bohemian Massif in the north (Wagner 1980). Ar/Ar-dating of detrital white mica shows plateau-like ages ( $319.5 \pm 1.2$  Ma), which fit well with Ar/Ar-ages from inside the Bohemian Massif. Chemical compositions of mica indicate metamorphism at rather low pressure conditions (Fig. 3). Rare earth element pattern display a high diversity within this stage. The terrestrial limnic beds show highest REE concentration, which are clue to wash-like, high mature sediments with high contents of heavy minerals. Opposite to this, marine sediments of the hanging wall (limestone-sandstone stage) are depleted in REE (Fig. 1).

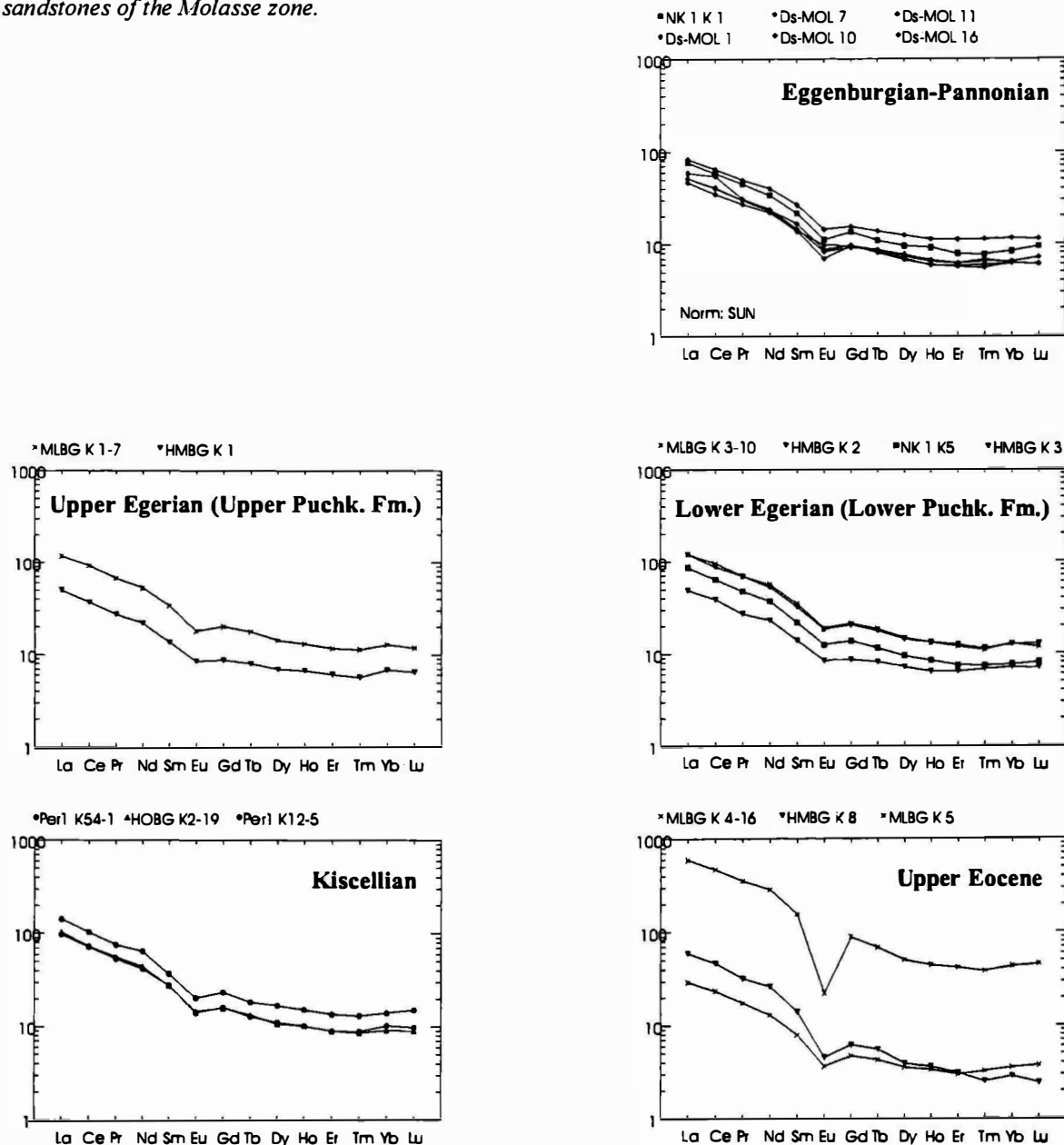
Post-Eocene sediments were mainly washed from the rising Alpine mountain belt. These rocks are uniform in REE pattern. Ar/Ar-ages of multi grain-specimens vary in a broad range between 285 Ma and 145 Ma due to mixing of Variscan and Alpine ages.

In Eocene samples no phengitic white mica or phenite occur due to the **regional metamorphic** granites and granodiorites on the southern margin of the Variscan Bohemian Massif where the Eocene sediments derived from. In Oligocene and Miocene sandstones phengite-rich white mica appear. Phengite-rich white mica and phengite indicate exhumation and erosion of high-pressure metamorphic source rocks. Moderate to high phengite values are recorded in Oligocene to lower Miocene. Source rocks should be Cretaceous deformed Austroalpine units of the rising Alpine mountain belt. Highest phengite values in white mica are present in Middle to Upper Miocene sandstones. At this time the deepest tectonic and high-pressure metamorphic unit of the eastern Alps - the Tauern Window - was uplifted and exhumed (Schneider et al. 1997). Further investigations in Ar/Ar single-grain dating, whole-rock geochemistry, and provenance analysis are in progress.

## References

- Nachtmann, W. & Wagner, L. (1987): Mesozoic and Early Tertiary evolution of the Alpine foreland in Upper Austria and Salzburg, Austria. – *Tectonophysics*, 137, 61-76
- Schneider, D. et al. (1997): Chemische Diversität detritischer Hellglimmer in Molassesedimenten des westlichen Innviertels (Salzburg und Oberösterreich, Österreich). – *Terra Nostra*, 97/2, 216-217
- Schneider, D. et al. (1998): A comparison between sandstones of two peripheral foreland basins: the Alpine Molasse basin versus the Variscan Moravo-Silesian basin. – Abstract
- Wagner, L. (1980): Geologische Charakteristik der wichtigsten Erdöl- und Erdgasträger der oberösterreichischen Molasse; Teil I: Die Sandsteine des Obereozän. – *Erdoel-Erdgas-Zeitschrift*, 96, 338-346.

Fig. 1: Chondrite-normalized rare earth element patterns from sandstones of the Molasse zone.



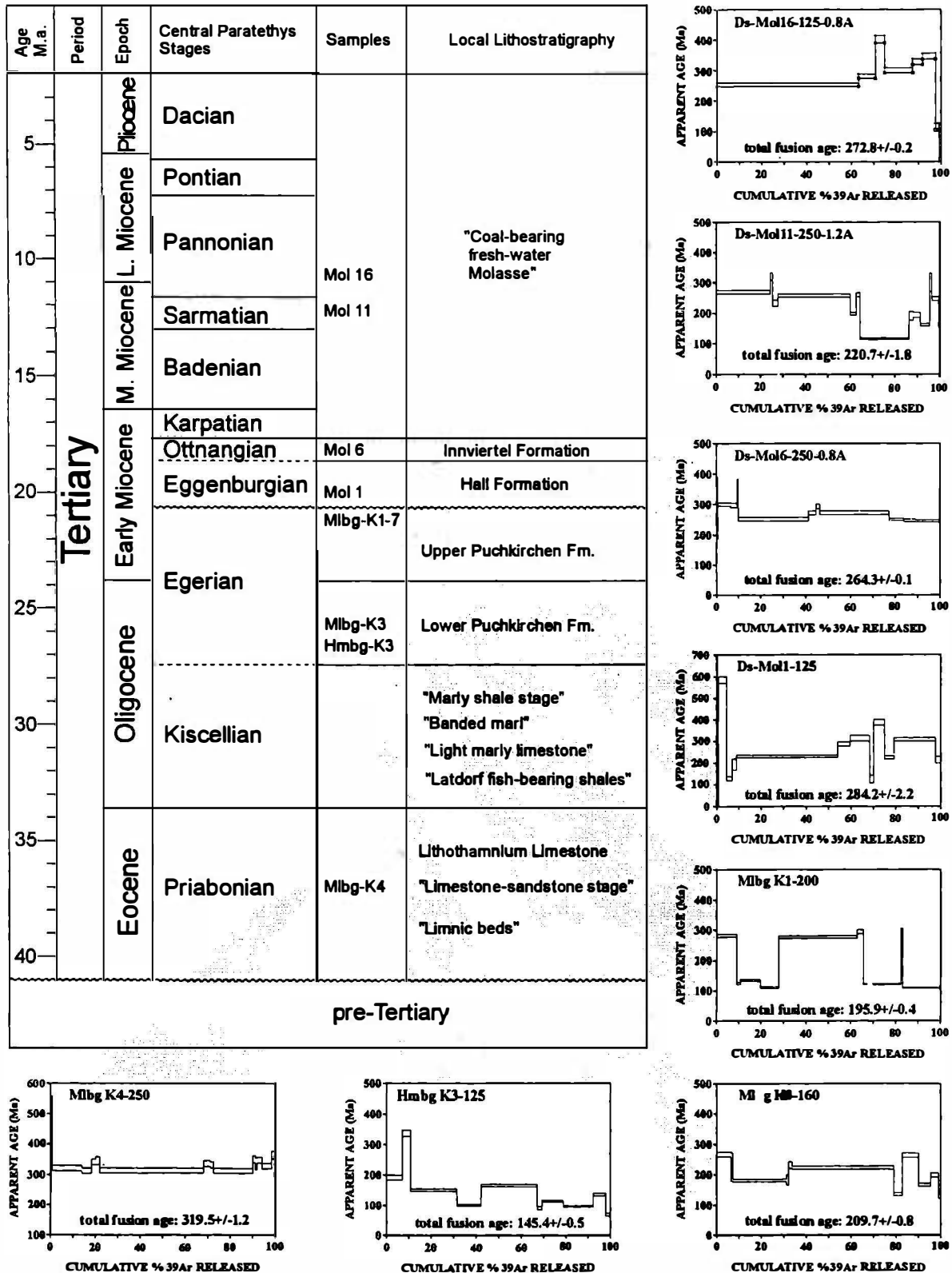
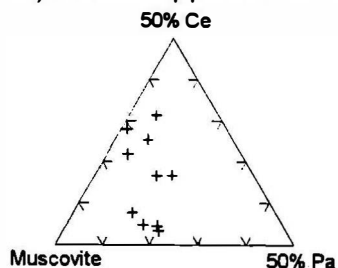
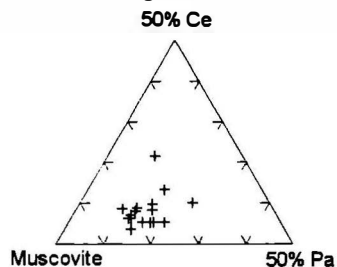
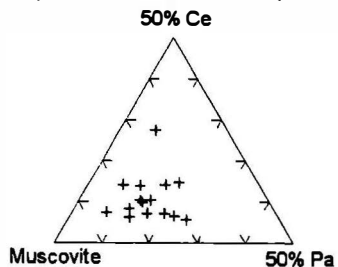


Fig. 2.  $^{40}\text{Ar}/^{39}\text{Ar}$  ages of detrital white from various stratigraphic levels within the Molasse zone.

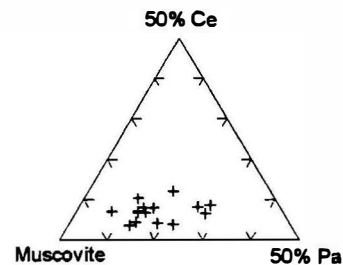
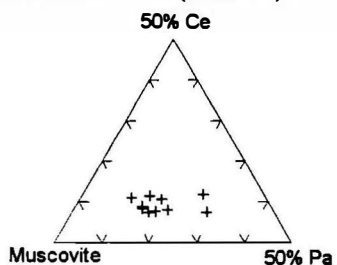
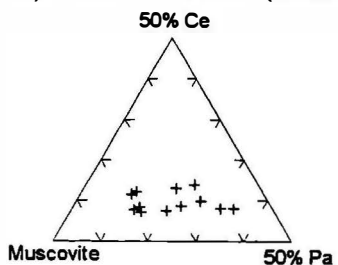
a) Middle-Upper Miocene (Pannonian): Kobernaußerwald-Gravel (Mol 16)



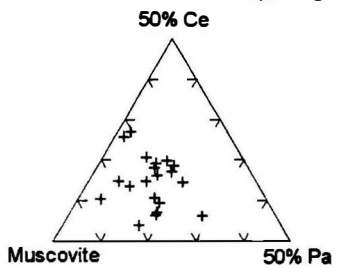
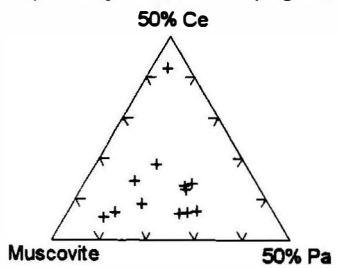
b) Middle Miocene (Sarmatian): Coal-bearing fresh-water Molasse (Mol 11)



c) Lower Miocene (Ottangian): Innviertel Fm. (Mol 07)



d) Early Miocene (Egerian): Upper Puchkirchen Fm. (Mlbg K1)



e) Upper Eocene (Priabonian): Limnic beds (Mlbg K5)

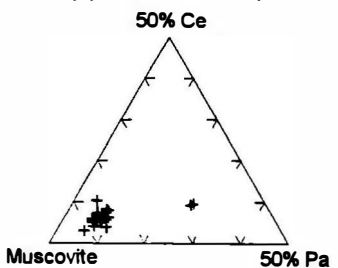


**Fig. 3:** Chemical diversity of detrital white mica. Plotted in a triplot-graph Muscovite - 50% Paragonite - 50 % Celadonite (=Phengite)



Carpathian-Balkan Geological Association, XVI Congress	Field Guide "Transect through central Eastern Alps"	pp. 49 - 52	Salzburg - Wien, 1998
--	---	-------------	-----------------------

## **Petrography of sandstones from the Rhenodanubian Flysch Zone of the Salzburg region**

**Franz Neubauer and Robert Handler**

Institute of Geology and Paleontology, Paris-Lodron-University of Salzburg, Hellbrunner Str. 34,  
A-5020 Salzburg, Austria

### **Introduction**

The Rhenodanubian flysch zone comprises a Neocomian to Eocene succession of turbidites intercalated by marls, shales and very subordinate tuffs. The Rhenodanubian flysch zone is interpreted to represent the infilling of a deep sea trough located between the Helvetic/Ulltrahelvetic slope and the Penninic ocean (Fig. 1). On detailed discussion of the paleogeographic origin of this zone, see Egger (1992), Faupl and Wagreich (1992), Schnabel (1992) and Oberhauser (1994).

The Rhenodanubian flysch unit comprises several formations with variable thickness (Fig. 2). These formations include stratigraphically upward Tristel, Reiselsberg, the Seisenburg, Zementmergel, Perneck and Altlenzbach Formations. The Seisenburg, Zementmergel and Perneck Formations are dominated by variegated or grey marls. The Altlenzbach Fm. includes several subformations. Tristel, Reiselsberg and Altlenzbach Formations are dominated by graywackes intercalated within marl and shale. No measured sections exist to these formations.

The goal of the present study is to reveal the respective source regions of these siliciclastic sediments and possible changes during the ca. 80 Ma long history of sediment deposition. Main goals are the study of sandstone composition according to the Dickinson-Gazzi method, chemical composition of some detrital minerals and dating of detrital white mica with the  $^{40}\text{Ar}/^{39}\text{Ar}$  technique.

### **Sandstone petrography**

We investigated the modal composition of ca. 50 sandstone samples from all turbiditic formations, from Tristel to Altlenzbach Formations, between the Mondsee and Salzach, mainly from outcrops where stratigraphy is proofed by biostratigraphy (mainly following Egger, 1989, 1992, 1995). We applied the Dickinson-Gazzi method where framework constituents between 0.063 and 2 mm are counted. Main results are (Fig. 3):

- All investigated sandstones have a calcite matrix and are largely interbedded by marls. This constrains deposition above calcite compensation depth.

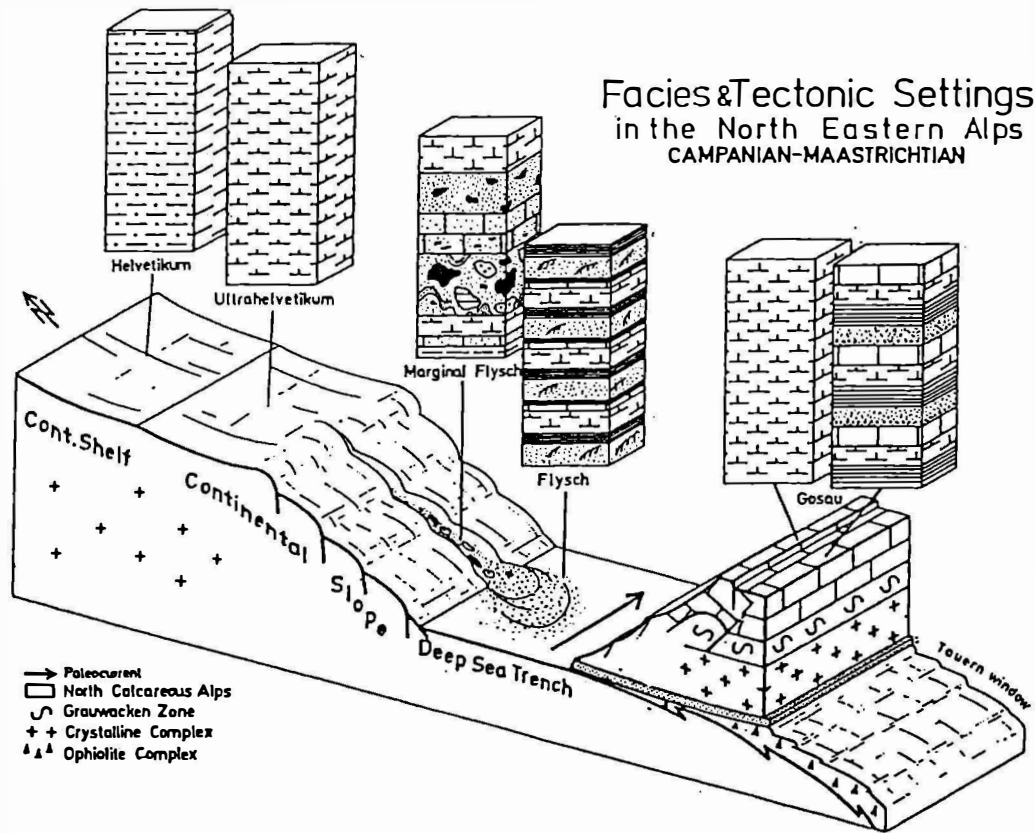


Fig. 1. Block diagram showing the Late Cretaceous arrangement of facies zones in Alps (from Egger et al., 1997).

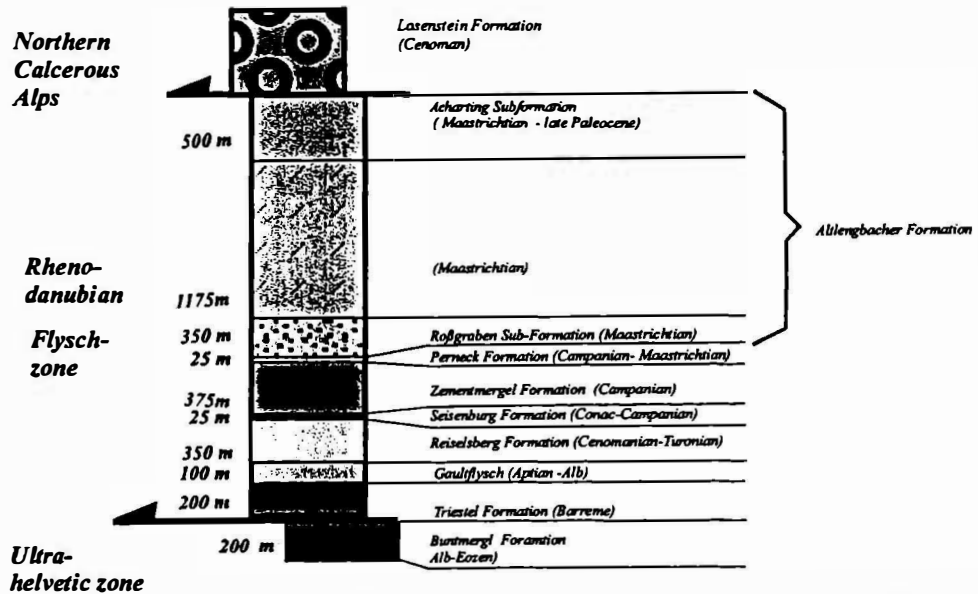
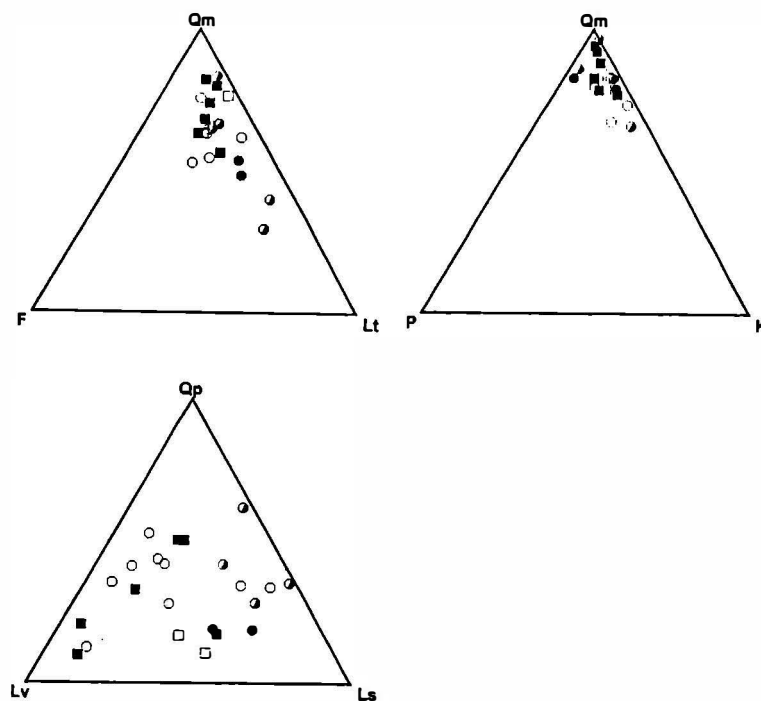


Fig. 2. Succession of formations of the Rhenodanubian Flysch Zone in the Salzburg-Upper Austria region (from Freimüller, 1998, based on Egger, 1992, 1995).

- Most sandstones have abundant carbonate clasts (until ca. 40 percent of framework constituents) including bioclasts like bryozoa, foraminifera and lamellibranchiata which in part constrain shallow water origin of clasts.
- The siliclastic detritus is dominated by monocrystalline quartz. Components from highly metamorphic rocks like sillimanite-bearing gneisses dominate. Volcanic clasts are dominated by acidic, phenocryst-bearing components.
- There is no significant difference in composition between sandstones of different ages. This argues for similar source regions from Early Cretaceous to Eocene.
- The composition of sandstones argues for an origin close to collisional orogenic belt applying discriminations, of e.g., Dickinson (1985).

The composition of detrital white mica suggest the predominance of muscovite. Only very minor phengitic micas were found. Garnet is generally unzoned and of almandine-rich compositions. Feldspars are pure K-feldspar and oligoclase. The composition of these minerals indicates the predominance of temperature-dominated, highly metamorphic rocks in the source region.



*Fig.3. Diagrams from sandstones of Rhenodanubian Flysch Zone displaying the compositional variation and geodynamic significance. In these diagrams, only those samples are plotted where the modal carbonate clast and carbonate cement abundance is below 50 percent. Legend: Qm - monocrystalline quartz; Qp - polycrystalline quartz; Qt - Quartz total (Qm + Qp); K - K-feldspar, P - plagioclase; F - feldspar (K + P); Lv -lithic volcanic clast; Ls - lithic sedimentary clast; Lt - total lithic clasts (Qp + Lv + Ls). Filled square: Tristel Fm.; Reiselsberg Sandstone; Zementmergel Fm; open and half-filled circles: Altengbach Fm.*

## References

- Dickinson, W.R., 1985: Interpreting provenance relations from detrital modes of sandstones. In: Zuffa, G.G., Provenance of arenites. Reidel Publ. Co., Dordrecht, p. 333-362.
- Egger, H., 1989: Zur Geologie der Flyschzone im Bundesland Salzburg. Jb. Geol. Bundesanst., 132: 375-395.
- Egger, H., 1992: Zur Geodynamik und Paläogeographie des Rhenodanubischen Flysches (Neokom - Eozän) der Ostalpen. Z. dt. geol. Ges., 143: 51-65.
- Egger, H., 1995: Die Lithostratigraphie der Altenglach-Formation und der Anthering Formation im Rhenodanubischen Flsch (Ostalpen, Penninikum). N. Jb. Geol. Paläont. Mh., 196: 69-91.
- Egger, H., Lobitzer, H., Polesny, H. and Wagner, L.R., 1997: Cross section through the oil and gas-bearing Molasse Basin into the Alpine units in the area of Salzburg, Austria. AAPG Vienna '97, Field Trip Notes, Trip no. 1, 104 p., Vienna.
- Faupl, P. and Wagreich, M., 1992: Cretaceous flysch and pelagic sequences of the Eastern Alps: correlations, heavy minerals, and palaeogeographic implications. Cretaceous Research, 1992; 13: 387-403.
- Freimüller, St., 1998. Die strukturelle Entwicklung der Rhenodanubischen Flschzone zwischen Attersee und Traunsee, Oberösterreich. MSc thesis, University of Salzburg.
- Oberhauser, R., 1994: Zur Kenntnis der Tektonik und der Paläogeographie des Ostalpenraums zur Kreide-, Paläozän- und Eozänzeit. Jb. Geol. Bundesanst., 138, 369-432.
- Schnabel, G.W., 1992: New data on the Flsch Zone of the Eastern Alps in the Austrian sector and new aspects concerning the transition to the Flysch Zone of the Carpathians. Cretaceous Research, 13: 405-419.

Carpathian-Balkan Geological Association. XVI Congress	Field Guide "Transsect through central Eastern Alps"	pp. 53 - 63	Salzburg - Wien, 1998
--	--	-------------	-----------------------

## **The structural evolution of the Rhenodanubian/Ultrahelvetic thrust wedge in the Attersee to Traunsee region**

**Stefan Freimüller, Franz Neubauer and Johann Genser**

Institute of Geology and Paleontology, Paris-Lodron-University of Salzburg, Hellbrunner Str.  
34, A-5020 Salzburg, Austria

### **Abstract**

The structure and the structural development of the Rhenodanubian/Ultrahelvetic Wedge (RUW) in the Attersee to Traunsee region (Upper Austria) have been examined by structural analysis and 2D and 3D structural modelling. The structure is dominated by thin-skinned tectonics mode of deformation of the infilling of the flysch basin, which took place within a wedge at the northern, buttress-type front of the Northern Calcareous Alps. Ultrahelvetic successions that were laid down on a northern continental slope were incorporated into a combined RUW. The structure is dominated by ca. E trending, kilometre-scale kink fold anticlines and synclines, blind thrust faults and splay thrusts. Several major deformation stages can be distinguished. These include: (i) overthrusting of the Ultrahelvetic continental margin sequences by the Rhenodanubian Flysch Zone during Late Eocene (mainly D<sub>2</sub> stage, out-of-sequence thrusts), (ii) subsequent shortening of the combined Ultrahelvetic/Rhenodanubian thrust wedge, likely associated with the emplacement onto the southern margin of the Molasse Zone during Oligocene to Early Neogene, and (iii) disruption of the combined Ultrahelvetic/Rhenodanubian thrust wedge by strike-slip faults during the Neogene.

### **Introduction**

The Rhenodanubian Flysch Zone is exposed along northern margins of the Eastern Alps. It comprises the infilling of a deep-sea basin likely located onto oceanic crust (Decker, 1990). On ideas of the paleogeographic evolution inform Prey (1980), Hesse (1982), Egger (1992), Faupl and Wagreich (1992) and Schnabel (1992). The Rhenodanubian Flysch represents a classical thrust-fold belt. We studied central sectors of the combined Rhenodanubian Flysch/Ultrahelvetic wedge, Eastern Alps, which has been emplaced onto the Molasse zone, the classical peripheral foreland/molasse basin (e.g., Malzer et al., 1994). From the flysch zone detailed modern structural studies are largely lacking although, except scarce structural data (Mattern, 1988), some paleostress data based on evaluation of fault and slickenside data were reported (Meschede and Decker, 1992; Decker et al., 1993). We did choose for our structural study the region between Attersee and Traunsee because of the availability of modern geological maps (Egger, 1996; van Husen, 1989) and because of relatively good exposure compared to western and eastern adjacent regions.

## Geological framework

In the study area, southern deformed sectors of the Molasse basin with late Eocene to Miocene clastic successions form the structural base of the combined Rhenodanubian/Ultrahelvetic wedge (RUW). Seismic reflection profiles and some boreholes demonstrate that the molasse sediments and European basement rocks can be traced with a gently south-dipping surface beneath the RUW and the southerly adjacent Northern Calcareous Alps which is part of the Austroalpine nappe complex. The northern boundary of the NCA unit is a steeply south-dipping thrust which result in a wedge shape of RUW in between. Sedimentary sequences of the Molasse basin were deposited on the flexured European lithosphere.

In the study area, the RUW mainly consists of (1) the Rhenodanubian flysch zone with Neocomian to Middle Eocene turbidites intercalated in marls and shales and (2) of the Ultrahelvetic unit with the Cretaceous to Early Late Eocene Buntmergel Formation, which uniformly comprises variegated marls of not more than ca. 100 - 200 metres (structural) thickness. The Ultrahelvetic unit comprises less than five percent of surface exposure and is largely overridden by the Rhenodanubian Flysch unit, and is mainly exposed along northern footwall sectors and within some windows within the Rhenodanubian flysch unit.

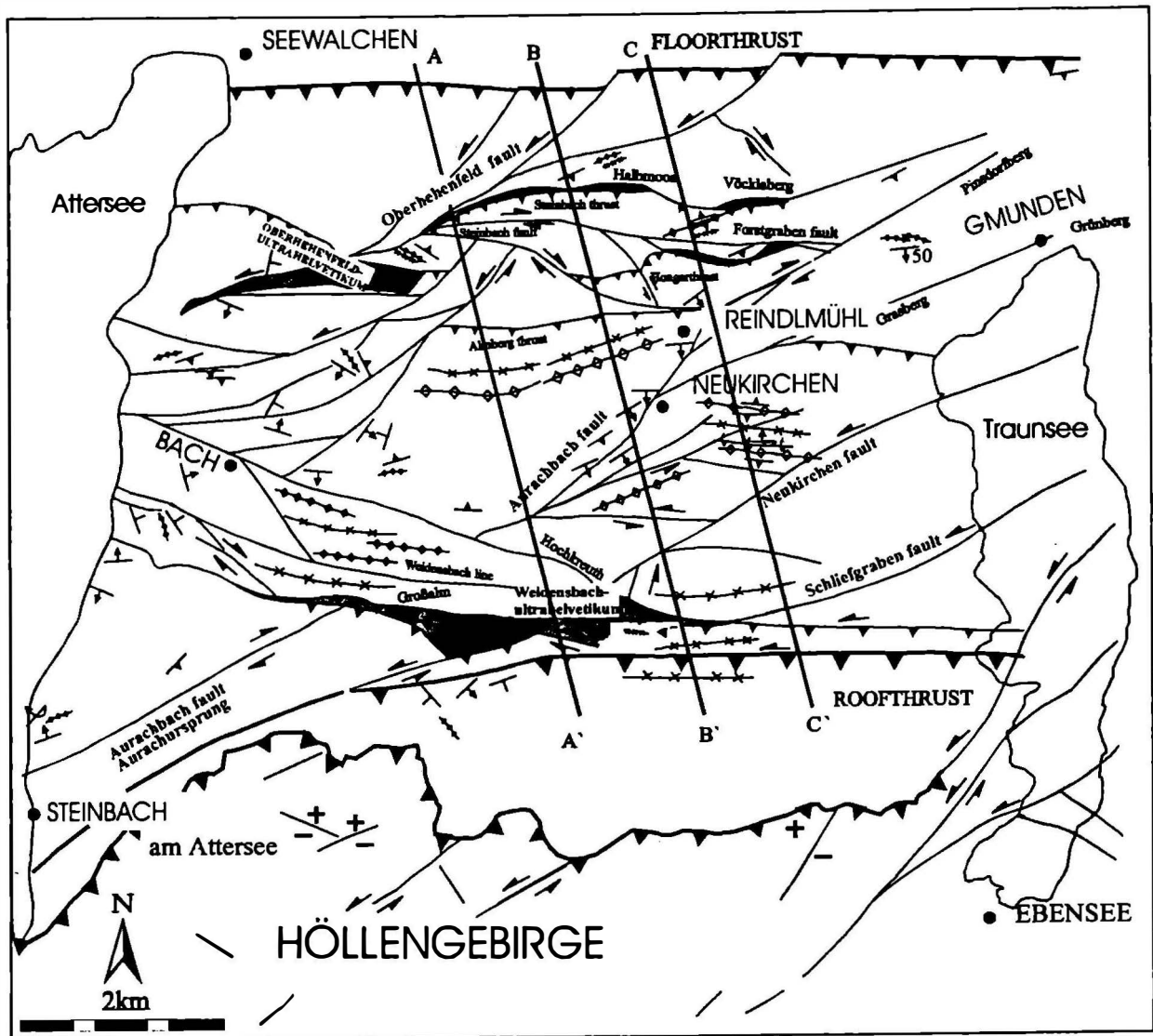
The Rhenodanubian flysch unit comprises several formations with variable thickness (Fig. 2). These formations include, stratigraphically upward, the Tristel Formation, Reiselberg Formation, Seisenburg, Zementmergel and Perneck Formations, which all three are dominated by variegated or grey marls, and the Altlengbach Formation (Egger, 1995, 1996). The latter includes several subformations. No measured sections exist to these formations. Consequently, we estimated the structural thickness for all these formations from available geological maps during the course of our study (Fig. 1). The basement of the Rhenodanubian Flysch Zone is not known in the study area. Decker (1990) described uppermost portions of a Jurassic ophiolite sequence as the stratigraphic base of the Rhenodanubian Flysch Zone. Similarly, the basement of the Ultrahelvetic unit is also unknown.

## Structure

The structure of the region was evaluated from available maps and from own field work along sections. Fault and striation data were collected in ca. 60 stations between Traunsee and Attersee in order to evaluate fault kinematics. In many outcrops superimposed, partly complicated sets of faults and striations were found which indicate a polyphase reactivation of faults. Note that along fault traces itself outcrop conditions are poor, and only a few large exposures can be found on individual faults, e.g., the Gmunden quarry (see, e.g., Meschede and Decker, 1993; Decker et al., 1992). We used the GEOSEC 3D<sup>®</sup> software package for construction, assessment and balancing of the three-dimensional structure.

The structure of the RUW is dominated by a shallow frontal, floor thrust which brought the RUW over the molasse zone and a medium angle to steep roof thrust at the backfront towards the Northern Calcareous (Fig. 1). The gentle dip to the south of the frontal thrust is also documented by well data within the RUW and southerly adjacent NCA, and by seismic reflection profiles. These relationships suggest a wedge-shape form of the RUW which was deformed along the northern front of the NCA.

The internal structure of the RUW between Traunsee and Attersee is complicated. It generally includes E-trending kink-type anticlines and subordinate synclines which are well documented by stratigraphy. These folds are in part overturned towards N. Furthermore, S-dipping thrust surfaces are exposed. Ultrahelvetic Buntmergel Fm. is exposed along thrust



- |      |            |      |                    |
|------|------------|------|--------------------|
| ◇◇◇◇ | anticline  | ↗↘   | main thrust        |
| ⊕⊕⊕  | overturned | ↗↘↗↘ | splay thrust       |
| ×××× | syncline   | ↔↔↔  | strike-slip fault  |
| ⊥    | 6° - 30°   | +    | displacement along |
| ⊥    | 31° - 60°  | -    | normal faults      |
| ⊥    | 61° - 85°  |      |                    |
| ⊥    | 85° - 90°  |      |                    |

Fig. 1. Simplified structural map of the study area (based on Egger, 1996).

surfaces and partly overrides Rhénodanubian flysch formation in the Oberhehenfeld and Weidensbach windows.

Folds and thrust faults are transected by numerous ENE trending, sinistral strike-slip faults including the Oberhehenfeld, Aurachbach, Neukirchen and Schließgraben faults (Brandlmayr, 1995; Egger, 1996). These are interpreted to be part of eastern sectors of the supposed ISAM fault system (Egger, 1997). The displacement along these faults varies between several hundred metres to several kilometres. These sinistral faults are transected by the dextral Hochkreuth fault which also cuts the Weidensbach Ultrahelvetic window.

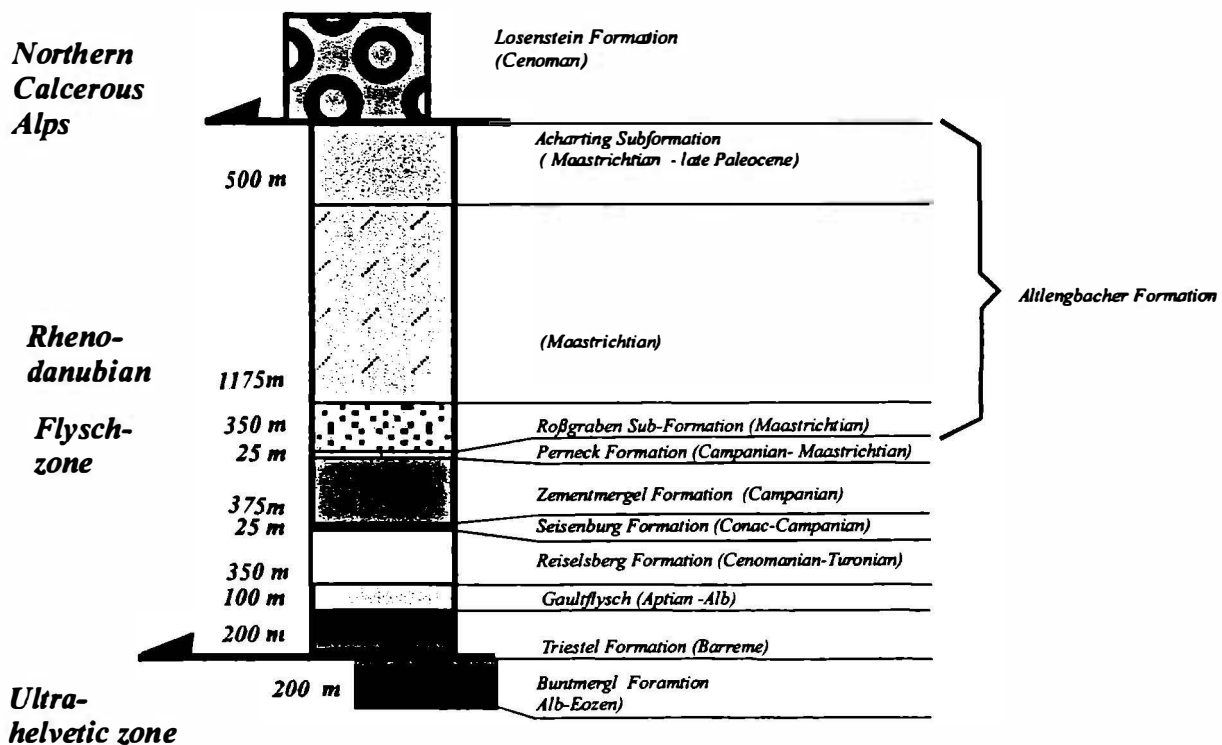


Fig. 2. Lithostratigraphy of individual tectonic units within the study area.

At outcrop scale, a number of detailed structures are observed which include: Ramp anticline and blind thrusts, layer parallel buckling and layer-parallel faults and slickensides. These structures document northward thrusting and shortening of the RUW. Furthermore, faults of all scales are common features documenting together with slickensides complex development and a relative succession of eight deformation stages (see below).

### Succession of deformation stages

Several major deformation stages can be distinguished. These include: (i) overthrusting of the Ultrahelvetice continental margin sequences by the Rheno-danubian Flysch Zone during Late Eocene, (ii) subsequent shortening of the combined Ultrahelvetice/Rheno-danubian thrust wedge, likely associated with the emplacement onto the southern margin of the Molasse Zone during Oligocene to Early Neogene, and (iii) disruption of the combined Ultrahelvetice/Rheno-danubian thrust wedge by strike-slip faults during the Neogene which also cut into Neogene successions of the Molasse Zone. Exposure of Ultrahelvetice units is along D<sub>2</sub> stage, out-of-sequence thrusts. Palaeostress tensors were deduced using fault-slip data (for methods, see Angelier, 1989) from more than fifty stations (Fig. 3-6). A succession of superimposed palaeostress tensors by means of superimposed fault and striae can be deduced as follows: Top-to-NNE nappe stacking led to the compound of RFZ units above the Ultrahelvetice Buntmergelserie. Mainly bedding plane striae yield reduced palaeostress tensors, which have been calculated from separated, homogeneous data sets with the orientations of the principal kinematic axes of D<sub>1</sub> with  $\sigma_1 = 217/24$ ,  $\sigma_2 = 122/24$ ,  $\sigma_3 = 9/63$ . Subsequent top-to-N



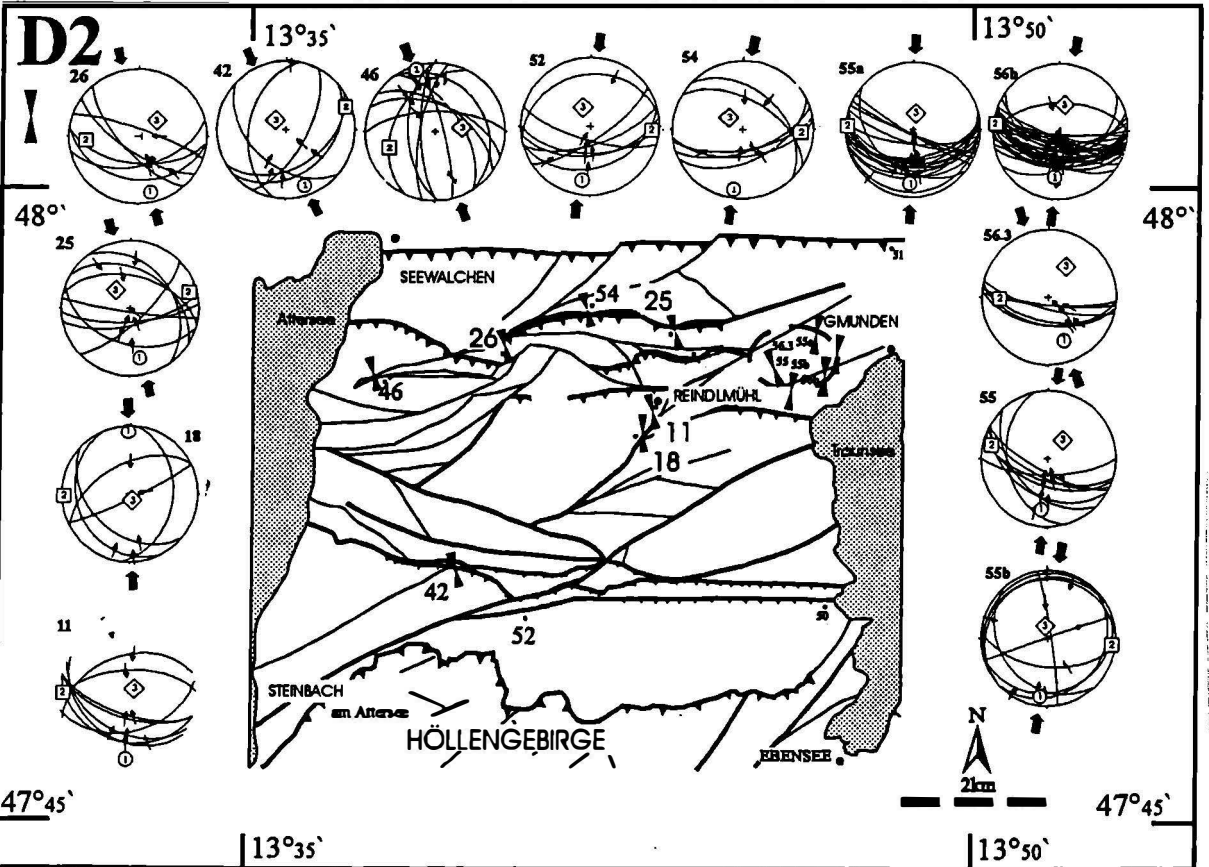
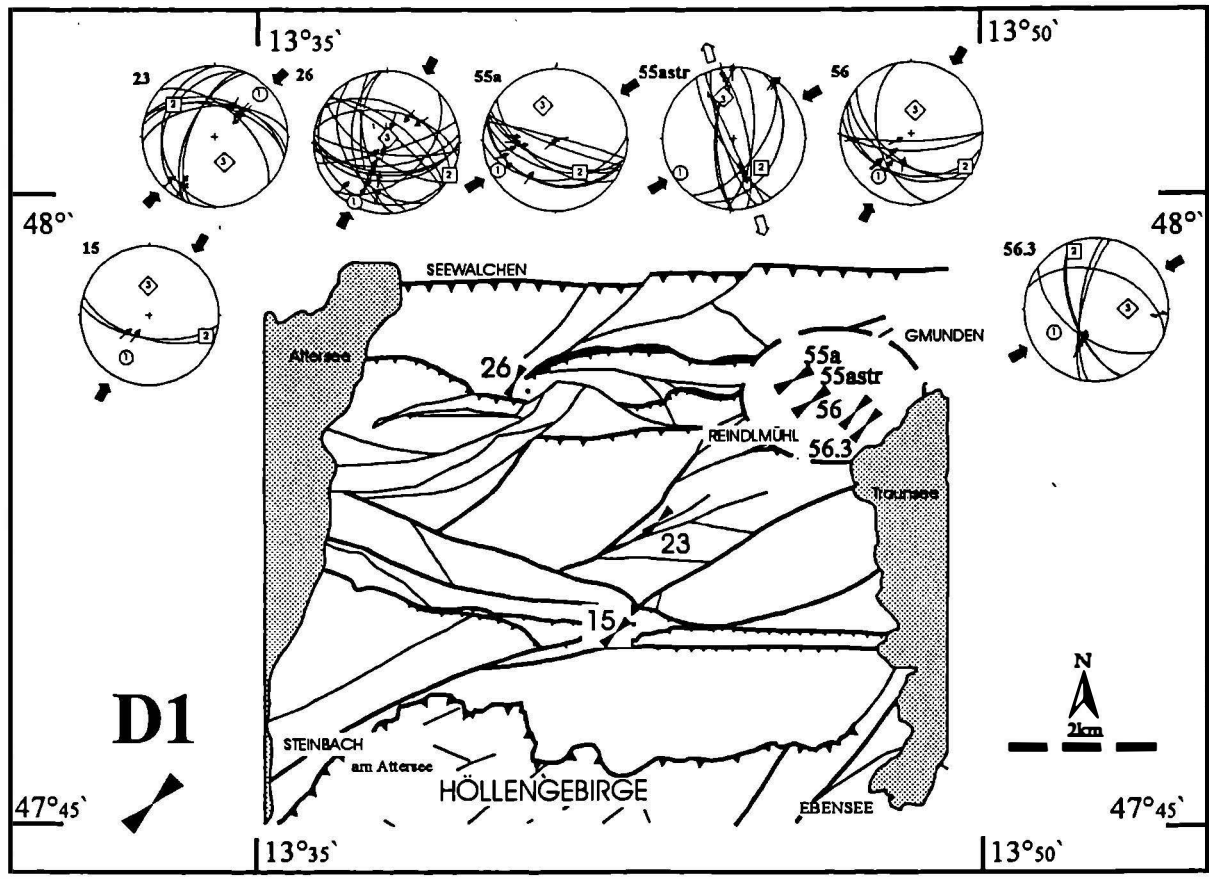


Fig. 3. Paleostress patterns of deformation stages D<sub>1</sub> (above) and D<sub>2</sub>(below).

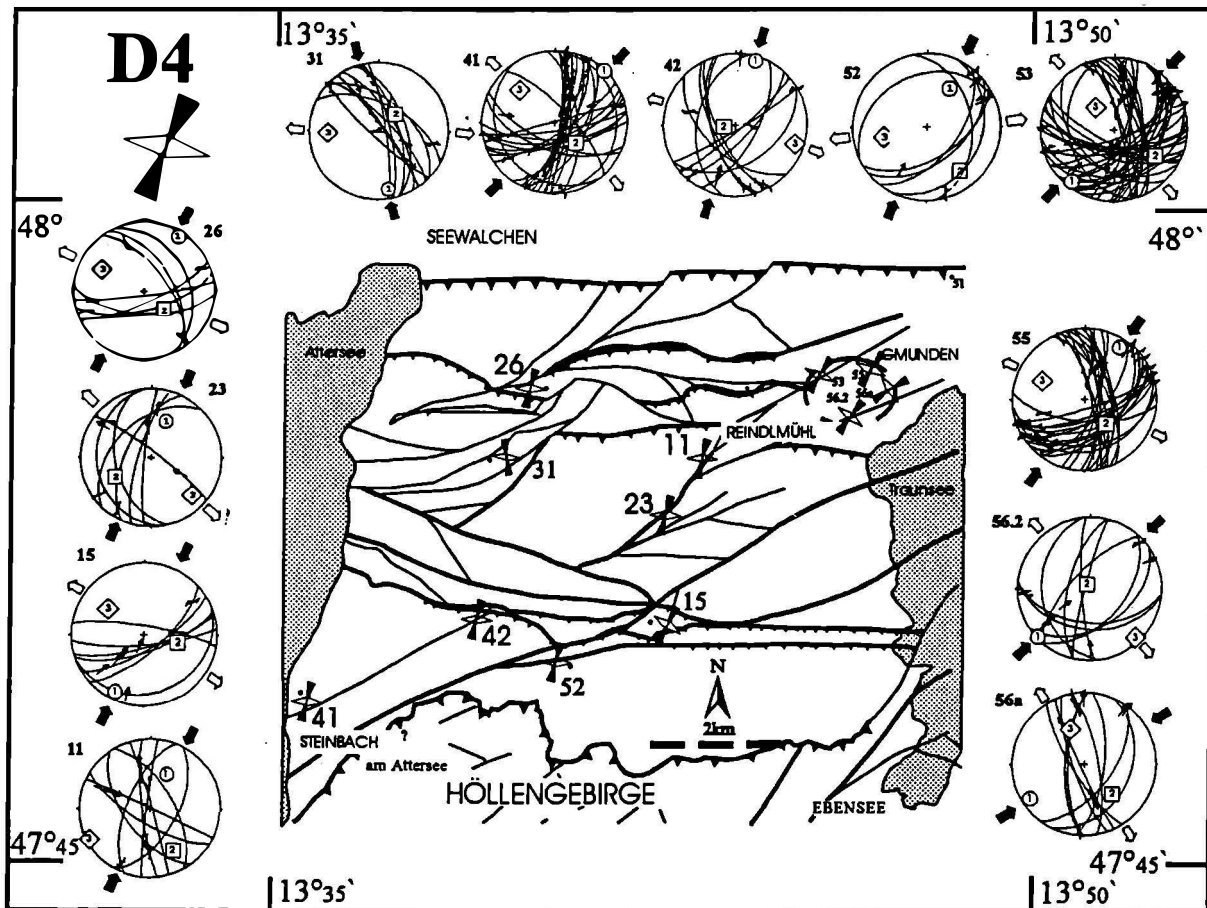
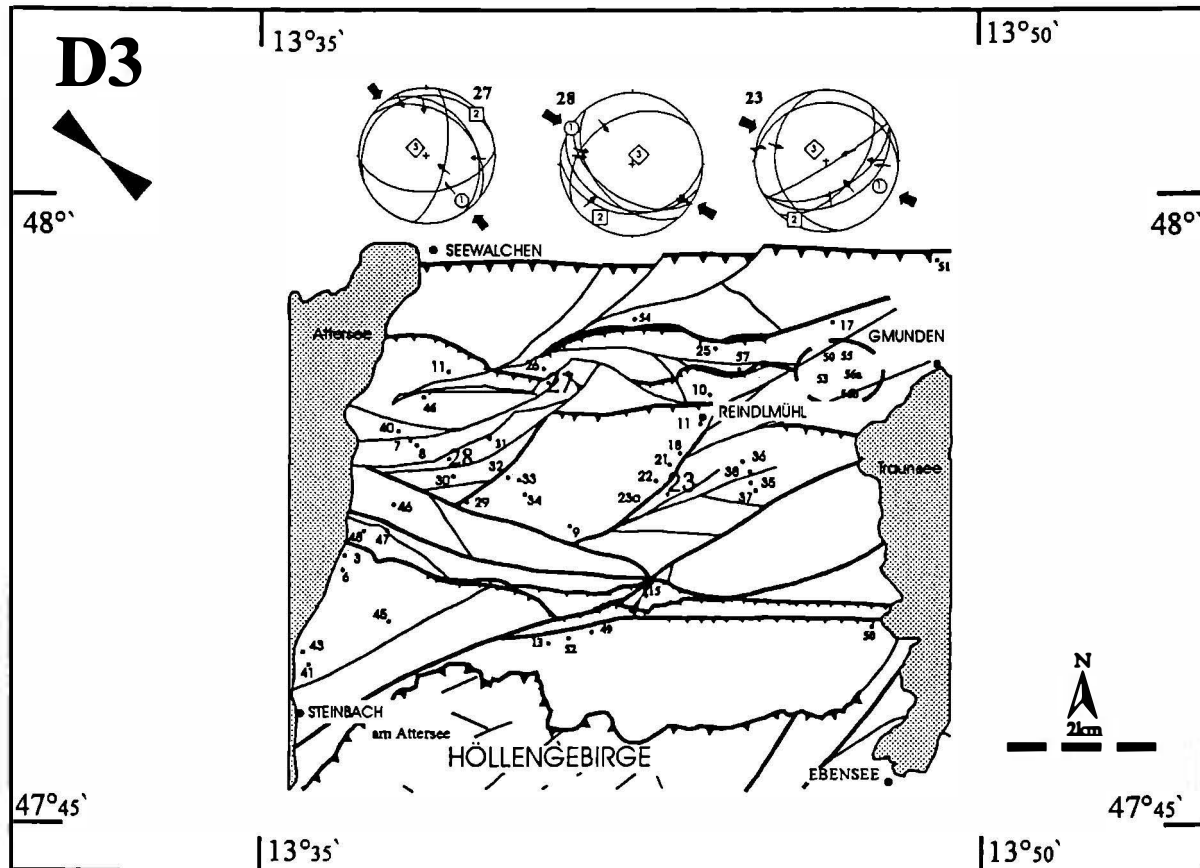


Fig. 4. Paleostress patterns of deformation stage  $D_3$  (above) and  $D_4$  (below).

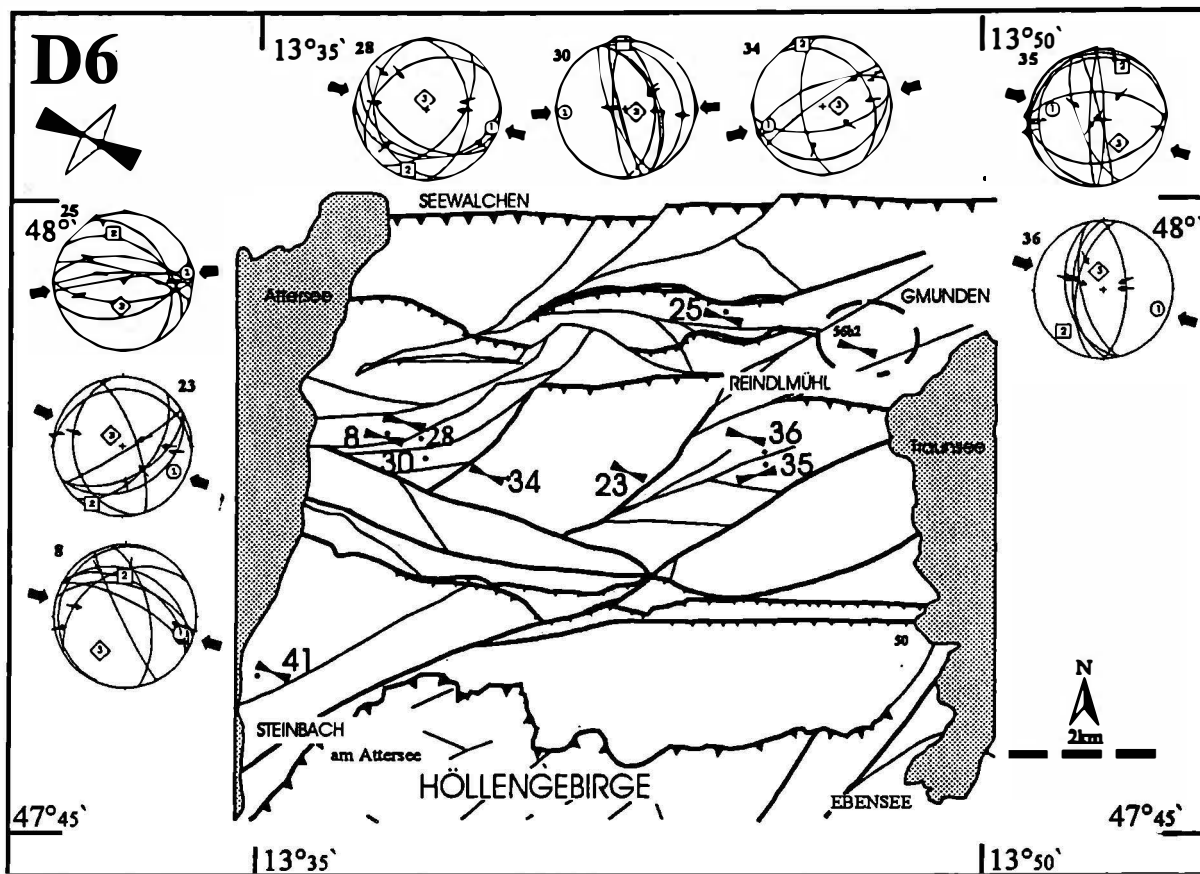
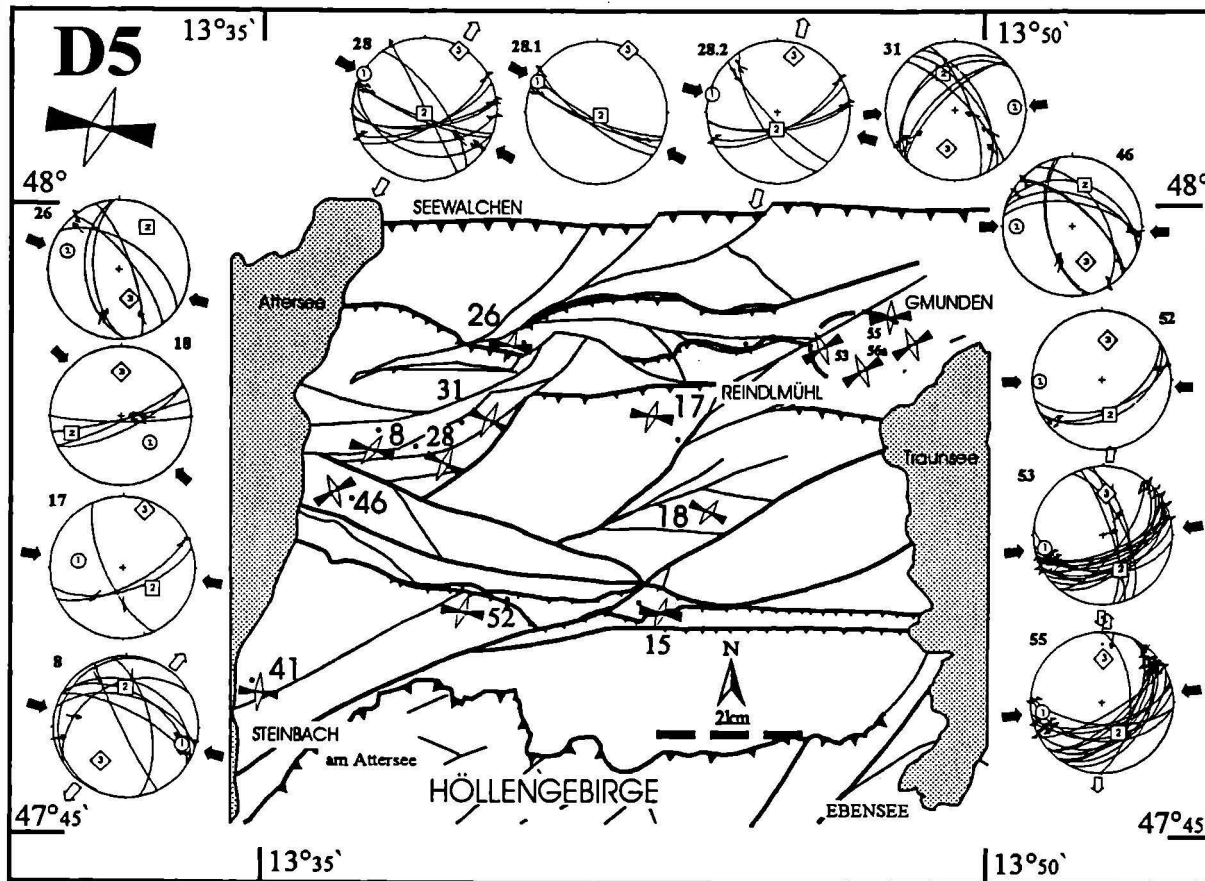


Fig. 5. Paleostress patterns of deformation stage  $D_5$  (above) and  $D_6$  (below).

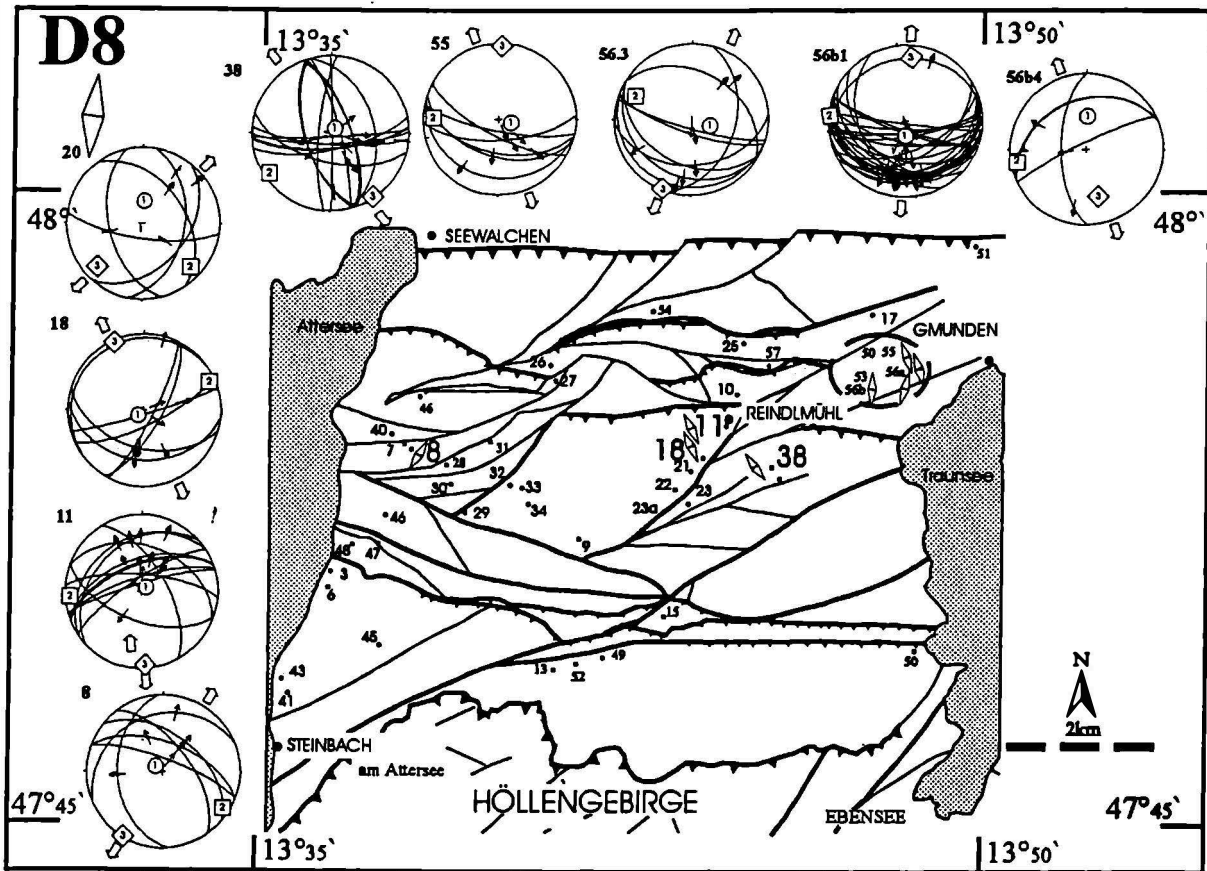
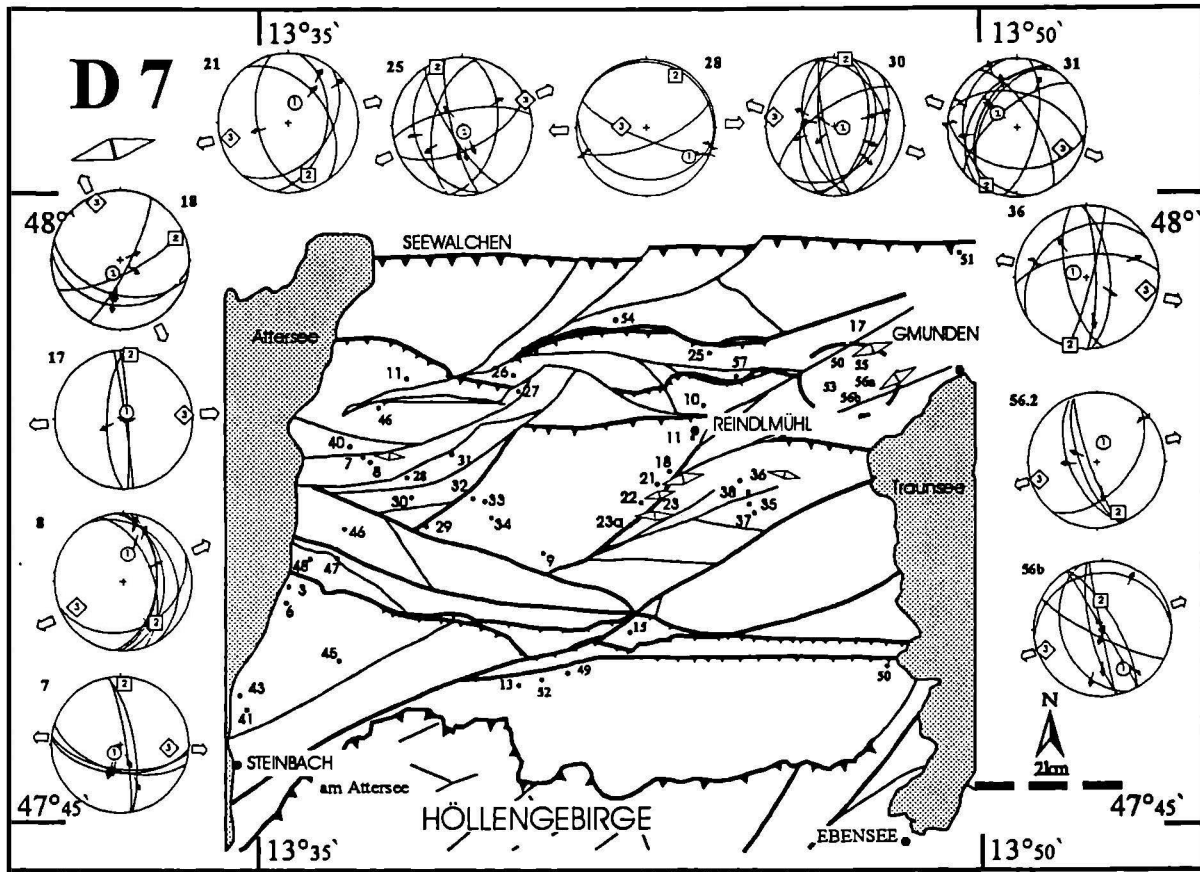


Fig. 6. Paleostress patterns of deformation stages  $D_7$  (above) and  $D_8$  (below).

thrusting is documented tectonically by different styles of splay thrusts, kink folds, and blind thrusts - all detectable on both outcrop- and map-scales. Data separation of bedding plane parallel slickensides and of E-trending faults led to a tensor group  $D_2$  with the orientations of principal stress axes  $\sigma_1 = 185/23$ ,  $\sigma_2 = 277/32$ , and  $\sigma_3 = 12/57$ . An anticlockwise rotation of the palaeostress field from N-S shortening  $D_2$  to a final top-to-NW thrusting tensor group finished the architecture of the Rhenodanubian fold and thrust belt. The calculation of bedding plane parallel E-W trending fault results in a palaeostress tensor group  $D_3$  with orientations of the main stress axes  $\sigma_1 = 160/31$ ,  $\sigma_2 = 268/27$ , and  $\sigma_3 = 30/47$ .

Conjugate steep strike-slip, NNW- and ENE-trending faults formed due to further, ca. N-S contraction respectively left-lateral wrenching. The orientations of the kinematic axes for this event have been calculated with  $\sigma_1 = 153/33$ ,  $\sigma_2 = 357/55$ , and  $\sigma_3 = 255/12$ . Dextral reactivation of  $D_4$  strike-slip fault patterns under transtensional E-W wrenching conditions ( $D_5$ :  $\sigma_1 = 237/11$ ,  $\sigma_2 = 137/42$ ,  $\sigma_3 = 338/46$ ). East and westward directed normal faults ( $D_6$ ), and reactivated  $D_4/D_5$  fault patterns depict E-W stretching of northern sectors of the Alps even in this northern RFZ zone ( $\sigma_1 = 241/34$ ,  $\sigma_3 = 89/53$ ). Subsequent E-W compression ( $D_7$ ) due to the geomorphic shape of the basement in this area of the RFZ led to a tensor group with E-W compressional and subvertical extensional directions ( $\sigma_1 = 116/18$ ,  $\sigma_3 = 314/71$ ). Finally, N-S extension ( $D_8$ ) is related to final collapse of the RFZ during uplift ( $\sigma_1 = 109/69$ ,  $\sigma_2 = 293/21$ , and  $\sigma_3 = 202/1$ ).

These data shows a similar but more complicated sequence of deformation stages as reported from regions further to the south (e.g., Ratschbacher et al., 1991; Meschede and Decker, 1992; Decker et al., 1993; Linzer et al., 1997). An important new result is that NNE-SSW motion oblique to the foreland is responsible for the formation of the Rhenodanubian/Ultrahelvetic wedge similar as in central sectors of the Eastern Alps (e.g., Ratschbacher et al., 1991; Neubauer, 1994).

## 2D- and 3D-modelling

A 2D and 3D structural model of the Rhenodanubian/Ultrahelvetic thrust wedge exposed within the Attersee and Traunsee has been performed by Freimüller (1998). The main idea was to model, based on structural field data and kinematics, the development of the thrust wedge. A restorable 2D model is shown in Fig. 7a. Principal complications for balancing are the presence of major sinistral and dextral strike-slip faults which cut oblique through the thrust-fold wedge. The balancing of these yield the fold-thrust wedge (Fig. 7b, c).

*Fig. 7 (color copy after references). Structural model of the Rhenodanubian thrust wedge between Traunsee and Attersee (from Freimüller, 1998). a (upper figure) - 2D structural model (section C-C' in Figure 1); b (middle figure) - 3D model balanced for late-stage strike-slip faults displaying thrusts (yellow) and balanced strike-slip faults. c (lower figure) - 3D model balanced for late-stage strike-slip faults displaying thrusts (yellow) and various formations but no strike-slip faults.*

## Conclusions

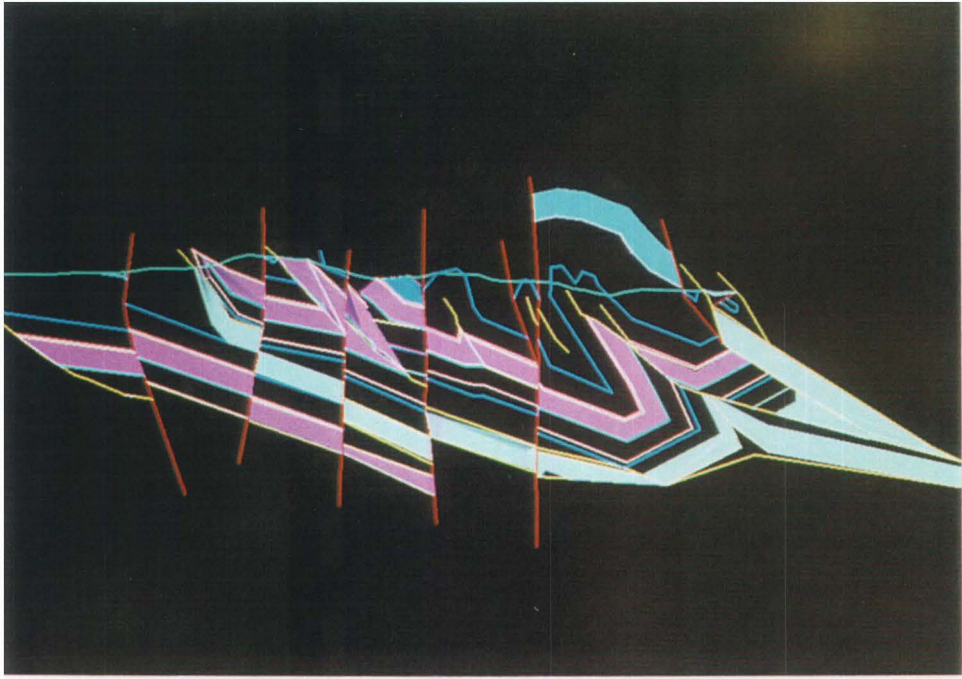
The following essential conclusions can be reached from the new data of the combined Rhenodanubian/Ultrahelvetic thrust wedge:

- (1) The RUW forms a wedge which was deformed during emplacement of these units onto the Molasse zone.
- (2) The RUW is dominated by folds and thrust faults which formed during shortening of the RUW thrust wedge.
- (3) The Ultrahelvetic windows within the RUW are explained as out-of-sequence thrusts.
- (4) A polyphase thrusting formed within complicated external paleostress conditions which shifted from initial NE-SW principal stress orientation to later NW-SE maximum principal stress orientations.
- (5) The RUW thrust wedge was subsequently dissected by E-W shortening and extension, and major strike-slip fault systems.

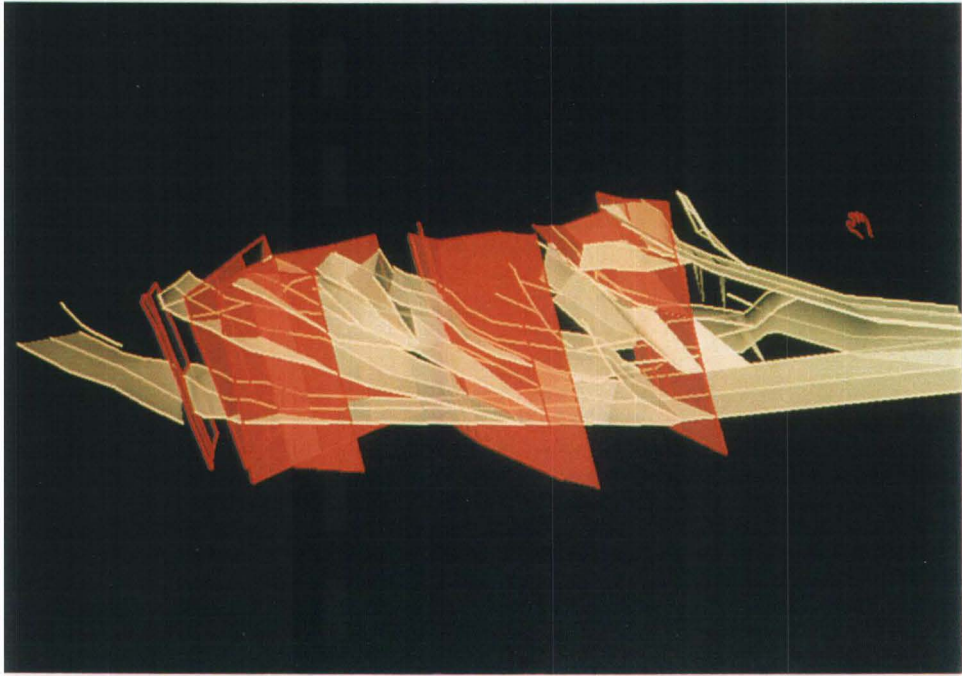
## References

- Angelier, J., 1989. From orientation to magnitudes in paleostress determination using fault slip data. *J. Struct. Geol.*, 11, 37-50.
- Brandlmayr, P., 1995. Die Geologie des Aurachtals (OÖ). *Jb. Geol. Bundesanst.*, 138: 583-602.
- Dahlen, F. A., 1990. Critical taper model of fold-and-thrust belts and accretionary wedges. *Ann. Rev. Earth Planet. Sci.*, 18, 55-99.
- Dahlen, F.A. and Barr, T. D., 1989. Brittle frictional mountain building 1: Deformation and mechanical energy budget. *J. Geophys. Res.*, 94 (B4): 3906-3922.
- Decker, K., 1990: Plate tectonics and pelagic facies: Late Jurassic to Early Cretaceous deep-sea sediments of the Ybbsitz ophiolite unit (Eastern Alps). *Sed. Geol.*, 67: 85-99.
- Decker, K., Meschede, M. and Ring, U., 1993. Fault slip analysis along the northern margin of the Eastern Alps (Molasse, Helvetic nappes, North and South Penninic flysch, and the Northern Calcareous Alps). *Tectonophysics*. 223, 291-312.
- Egger, H. Zur paläogeographischen Stellung des Rhenodanubischen Flysches (Neokom-Eozän) der Ostalpen. *Jb. Geol.B.-A.* 1990; 133(2): 147-155.
- Egger, H., 1992: Zur Geodynamik und Paläogeographie des Rhenodanubischen Flysches (Neokom - Eozän) der Ostalpen. *Z. dt. geol. Ges.*, 143: 51-65.
- Egger, H., 1995: Die Lithostratigraphie der Altengbach-Formation und der Anthering Formation im Rhenodanubischen Flysch (Ostalpen, Penninikum). *N. Jb. Geol. Paläont. Mh.*, 196: 69-91.
- Egger, H., 1996: Geologische Karte der Republik Österreich 1 : 50.000, 66 Gmunden. Geologische Bundesanstalt, Wien.
- Egger, 1997. Das sinstrale Innsbruck-Salzburg-Amstetten-Blattverschiebungssystem: ein weiterer Beleg für die miozäne laterale Extrusion der Ostalpen. *Jb. Geol. Bundesanst.*, 140: 47-50.
- Egger, H., Lobitzer, H., Polesny, H. and Wagner, L.R., 1997: Cross section through the oil and gas-bearing Molasse Basin into the Alpine units in the area of Salzburg, Austria. *AAPG Vienna '97, Field Trip Notes, Trip no. 1, 104 p., Vienna.*
- Faupl, P. and Wagreich, M., 1992. Cretaceous flysch and pelagic sequences of the Eastern Alps: correlations, heavy minerals, and palaeogeographic implications. *Cretaceous Research*, 13, 387-403.
- Faupl, P. and Wagreich, M., 1992: Cretaceous flysch and pelagic sequences of the Eastern Alps: correlations, heavy minerals, and palaeogeographic implications. *Cretaceous Research*, 13: 387-403.
- Freimüller, St., 1998. Die strukturelle Entwicklung der Rhenodanubischen Flischzone zwischen Attersee und Traunsee, Oberösterreich. MSc thesis, University of Salzburg.

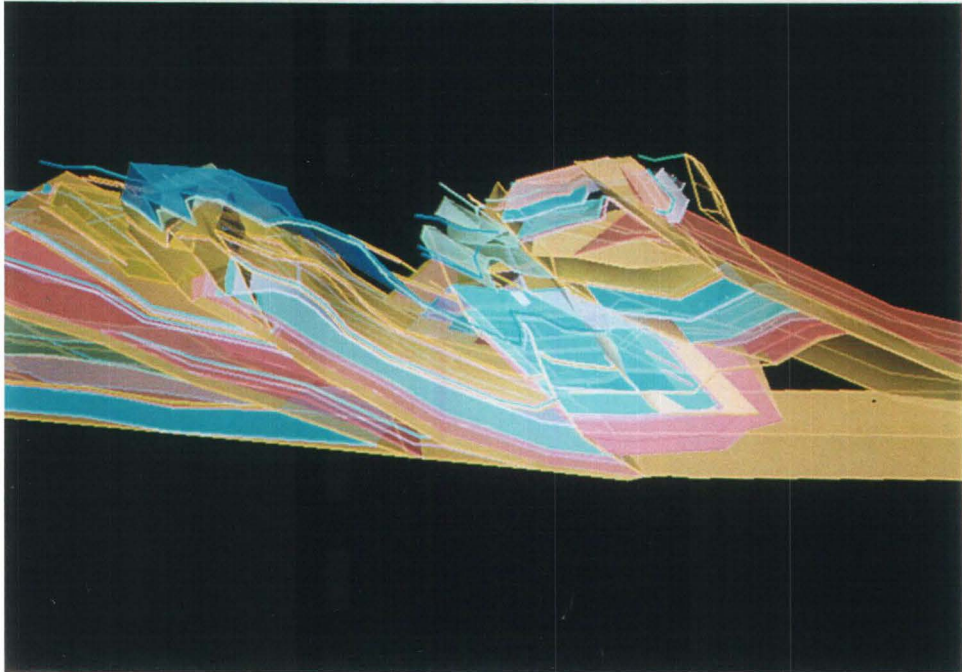
- Herb, R., 1989. Eocene Paläogeographie und Paläotektonik des Helvetikums. *Eclogae geol. Helv.*, 81(3), 611-657.
- Hesse, R., 1982. Cretaceous - Paleogene flysch zone of the East Alps and Carpathians: identification and plate tectonic significance of "dormant" and "active" deep-sea trenches in the Alpine-Carpathian Arc. In: Leggett, J. K., Ed. *Trench-Forearc Geology: Sedimentation and tectonics of modern and ancient active plate margins*. Oxford: Geol. Soc. Spec. Publ., 10, 471-494.
- Husen, D. van, 1989: Geologische Karte der Republik Österreich 1 : 50.000, 65 Mondsee. Geologische Bundesanstalt, Wien.
- Kollmann, K., 1977. Die Öl- und Gasexploration der Molassezone Oberösterreichs und Salzburgs aus regional-geologischer Sicht. *Erdoel-Erdgas-Zeitschrift*, 93, 36-49.
- Linzer, H.G., Moser, F., Nemes, F., Ratschbacher, L. and Sperner, B., 1997: Build-up and dismembering of the eastern Northern Calcareous Alps. *Tectonophysics*, 272: 97-124.
- Malzer, O., Rögl, F., Seifert, P., Wagner, L., Wessely, G. and Brix, F., 1994. Die Molassezone und deren Untergrund. in: *Erdöl und Erdgas in Österreich*. 1994, 281-358.
- Matern, F., 1988. Die interne Überschiebungstektonik im Flysch (Kreide) der westlichen Bayerischen Alpen. *Berliner geowiss. Abh.* 101, 1-94.
- Meschede, M. and Decker, K., 1992: Störungsflächenanalyse entlang des Nordrandes der Ostalpen - ein methodischer Vergleich. *Z. dt. Geol. Ges.*, 144: 419-433.
- Neubauer, F., *Kontinentkollision in den Ostalpen*, *Geowissenschaften*, 12, 136-140.
- Oberhauser, R., 1994: Zur Kenntnis der Tektonik und der Paläogeographie des Ostalpenraumes zur Kreide-, Paläozän- und Eozänzeit. *Jb. Geol. Bundesanst.*, 138, 369-432.
- Peresson, H. and Decker, K., 1997. The Tertiary dynamics of the northern Eastern Alps (Austria): changing palaeostress in a collisional plate boundary. *Tectonophysics*, 272: 125-157.
- Peresson, H. and Decker, K., 1997: The Tertiary dynamics of the northern Eastern Alps (Austria): changing palaeostress in a collisional plate boundary. *Tectonophysics*, 272: 125-157.
- Prey, S. Helvetikum, Flysche und Klippenzonen von Salzburg bis Wien. In: Oberhauser, R., Ed. *Der geologische Aufbau Österreichs*. Wien: Springer, 1980: 189-217.
- Ratschbacher, L., Frisch, W., Linzer, G., and Merle, O., 1991. Lateral Extrusion in the Eastern Alps, part 2: Structural Analysis, *Tectonics*, 10, 257-271.
- Schnabel, G.W., 1992. New data on the Flysch Zone of the Eastern Alps in the Austrian sector and new aspects concerning the transition to the Flysch Zone of the Carpathians. *Cretaceous Research*. 13, 405-419.



a



b



c



Carpathian-Balkan Geological Association, XVI Congress	Field Guide "Transect through central Eastern Alps"	pp. 65 - 83	Salzburg - Wien, 1998
--	---	-------------	-----------------------

## **Deformation phases and age data of the Austro-Alpine – Penninic plate boundary, Eastern Tauern Window**

**Johann Genser**

Institute of Geology and Palaeontology, Paris-Lodron-University of Salzburg, Hellbrunner  
Str. 34, A-5020 Salzburg, Austria

### Introduction

One of the main questions regarding the tectonic evolution of the Eastern Alps is the relation between nappe stacking and metamorphism in the Austro-Alpine unit to the subduction of the Penninic units beneath, as new data challenge important assumptions of present (plate) tectonic models (Hawkesworth et al. 1975, Frisch 1979, Tollmann, 1987, Frank 1987, Behrmann 1990). These models relate the early to middle Cretaceous nappe stacking and Barrovian type metamorphism in the Austro-Alpine unit to the subduction of the South Penninic ocean beneath or to the final collision with the Middle Penninic basement complex, exposed in the Tauern Window. Recognition of a Cretaceous high-P metamorphism (Thöni and Jagoutz 1992) in the Austro-Alpine unit in the last years points to a Cretaceous subduction of the AA and hence a lower plate position for this unit during that time span, rather. The two mega-units also show very different timings of the metamorphic evolution, but very similar metamorphic paths (eclogite facies followed by amphibolite facies). In the Austro-Alpine, the temperature peak occurred in the early Late Cretaceous, cooling below *c.* 300°C was completed in the late Cretaceous, already (Fig. 1). In the Penninic units, the thermal peak falls into the late Palaeogene, cooling into the Miocene (Frank et al 1987) (Fig. 2).

The following is a presentation and discussion of mainly structural and thermochronological data from the Eastern Tauern window, where in the area of the Malta and Lieser valleys, a continuous profile from the deepest tectonic units of the eastern Tauern window up to the Middle Austro-Alpine units is exposed (Fig. 3). It is situated ideally, therefore, to study the relationships between the two mega-units. The area of the eastern TW includes three tectonic mega-units, the Austro-Alpine upper plate, the Glockner Nappe and the basement units of the Venediger Nappe (Fig. 3). The Austro-Alpine unit consists of three individual nappes in the area, that were stacked during the Cretaceous and subsequently thrust onto the Penninic unit. The Penninic unit comprises the remnants of the South Penninic oceanic crust, the Glockner Nappe, and Middle Penninic units comprising a basement complex and an overlying Permo-Mesozoic cover unit. Between the Glockner Nappe and the parautochthonous basement are several nappes that were derived from the Middle Penninic continental complex (Kurz et al. 1998).

## Cretaceous metamorphism Austro-Alpine units

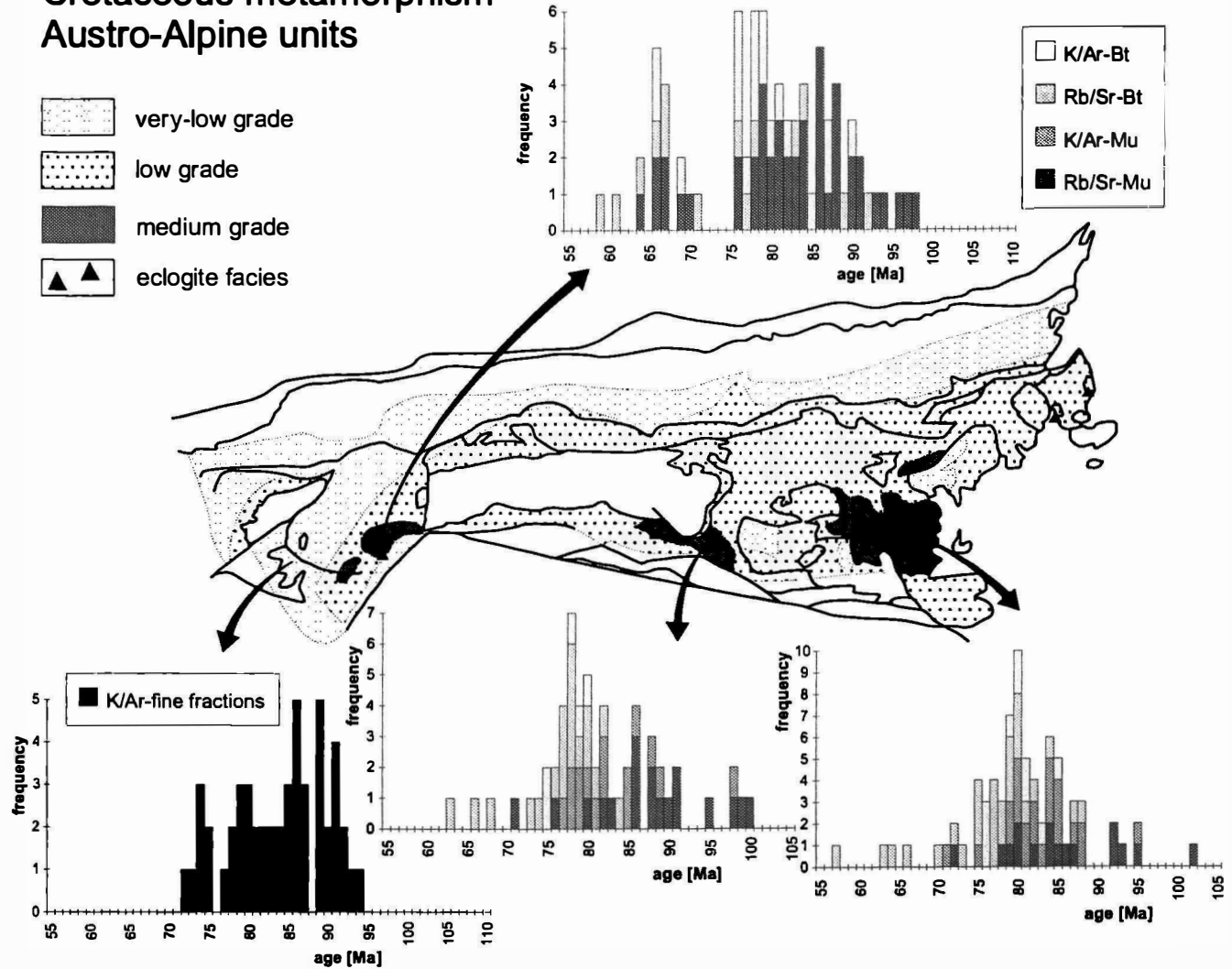
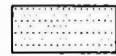
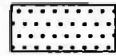




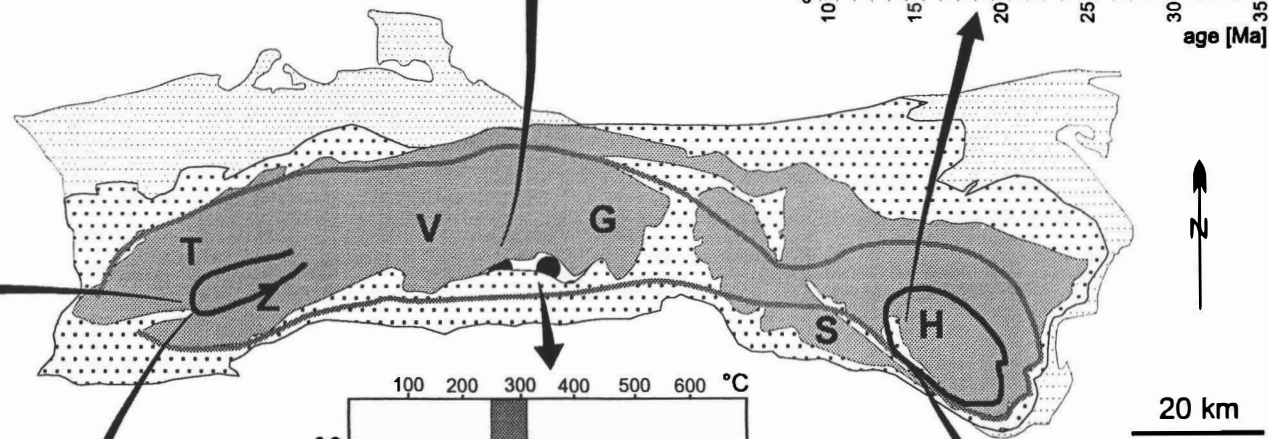
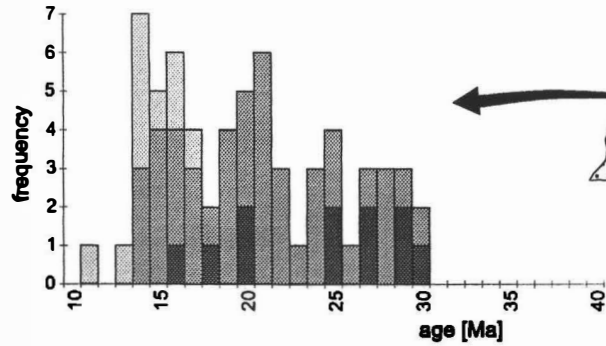
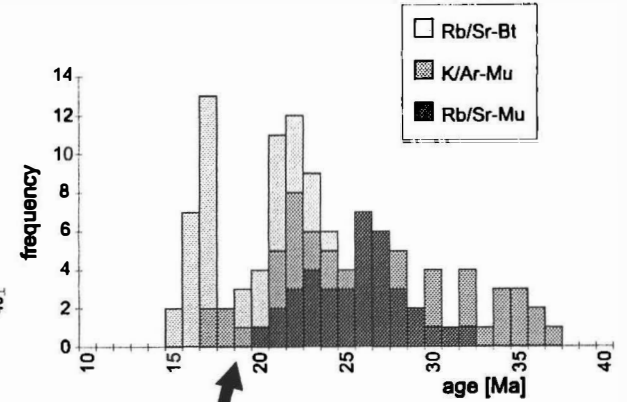
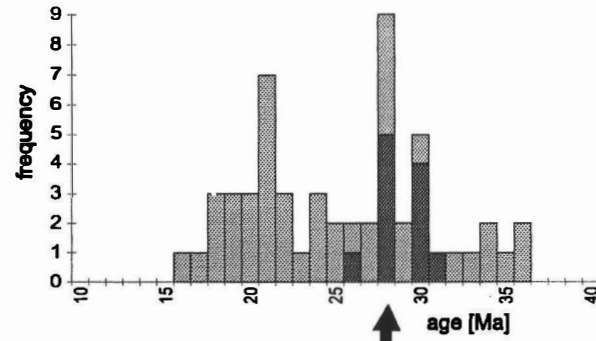


Fig. 1: Map of the Cretaceous metamorphism in the Austro-Alpine unit with radiometric age data from various systems (from Genser et al. 1996; see references therein).

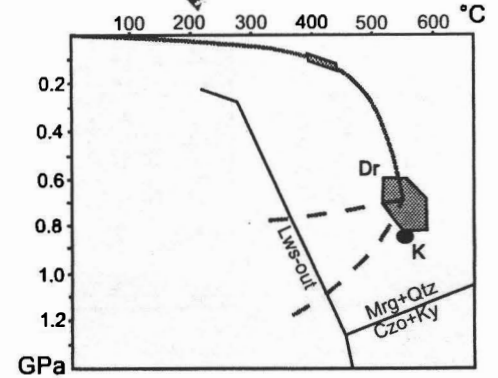
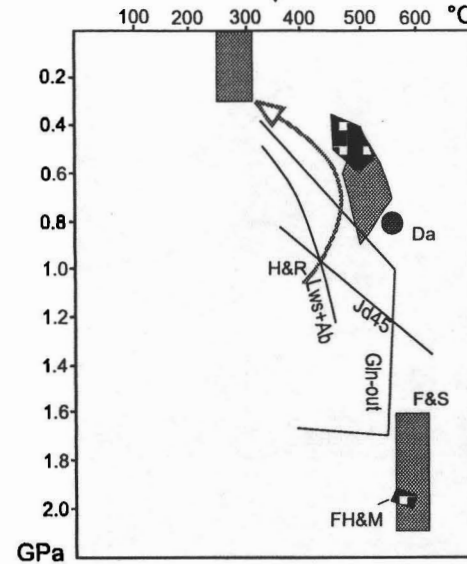
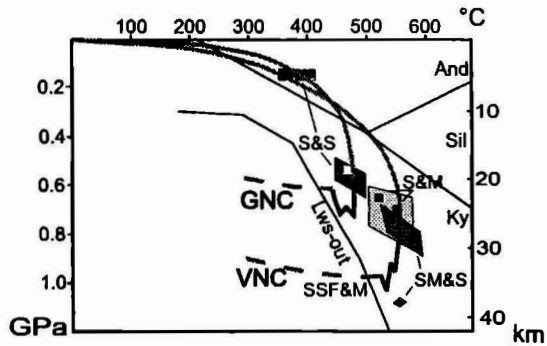
Fig. 2: Alpine metamorphism in the Tauern window with  $p$ - $T$  paths and radiometric age data (from Genser et al. 1996; see references therein).

# Alpine metamorphism Tauern Window

-  Lower Austro-Alpine
-  Glockner nappe complex
-  Eclogite unit
-  Venediger nappe complex
-  Ab/Olig isograde
-  St+Bt in



67



## Tectonic setting and structural evolution

### Penninic unit

From bottom to top we can distinguish the following tectonic units (Fig. 3), which can be correlated over the entire Tauern window (Kurz et al. 1998):

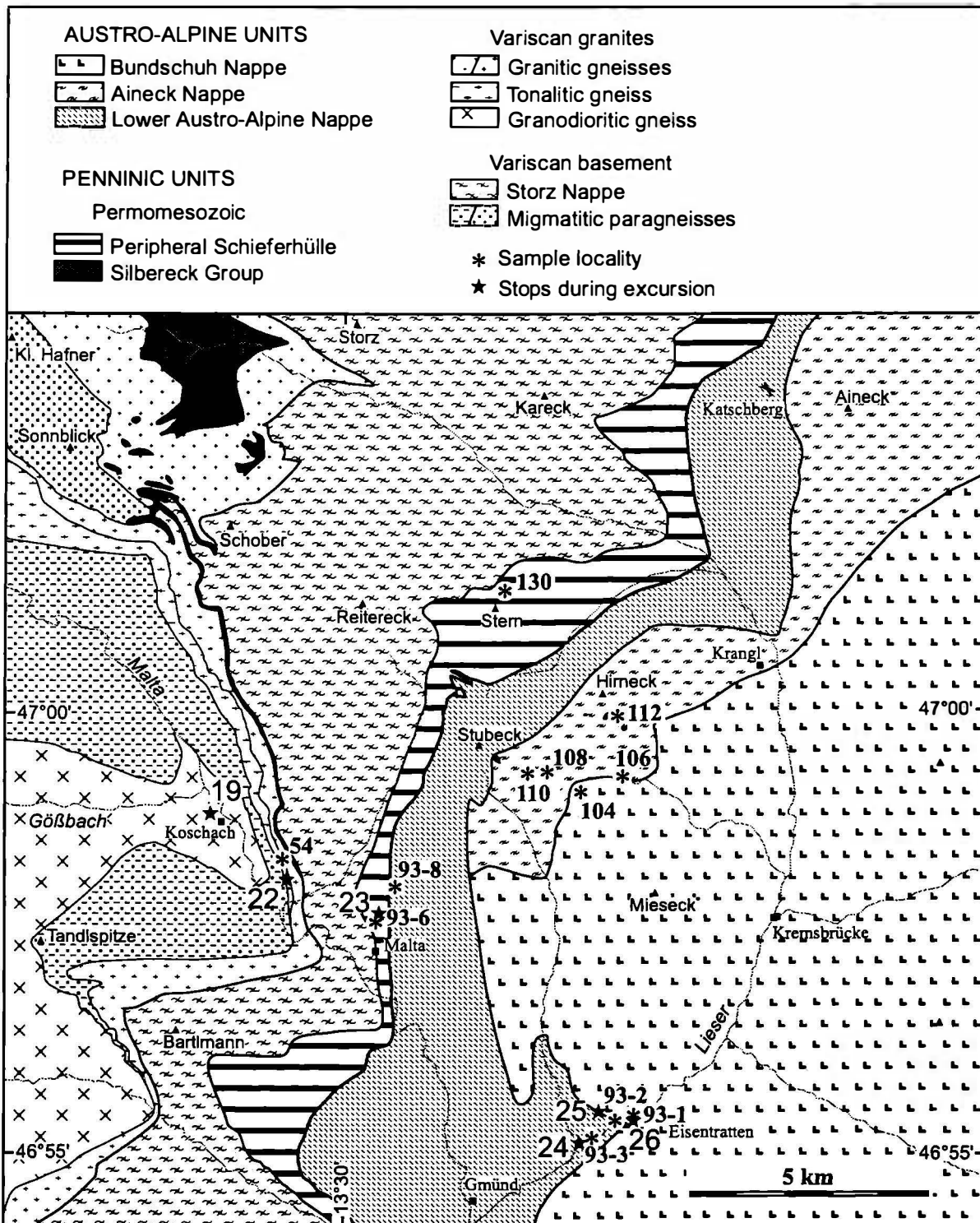


Fig. 3: Geological map of the area of the eastern Tauern window, Lieser and Malta valleys.

1. Parautochthonous basement consisting of a pre-Permian basement complex intruded by Variscan granitoids, the Zentralgneis (Central gneisses). On top is a primary Permo-Mesozoic cover sequence, the Silbereck Group in this area.
2. The Eclogite zone, that occurs only in the middle part of the Tauern window.
3. Nappes that consist of basement and cover parts that were derived from continental margin sequences of the Middle Penninic terrane.
4. The Glockner nappe, comprising ophiolites and mainly volcano-sedimentary sequences of the South Penninic oceanic basin.
5. The Matri and the Nordrahmen units, melange units deposited during the active margin stage.

In detail, the basement essentially consists of migmatitic paragneisses and minor micaschists and amphibolites (e.g., Frisch et al. 1993). The Variscan granitoids represent intrusions ranging from tonalites to granites, with the main members (Holub and Marschallinger 1989, Marschallinger and Holub 1991, Finger et al. 1993): a high-K, calc-alkaline I-type series with syenite, Malta tonalite, Hochalm porphyrygranite, Kölnbrein leucogranite, and two-mica granite and the Na-rich Göß granodiorites to granites. These Variscan granites occur in several cores, divided by metasedimentary basement units. In the eastern Tauern Window (TW), these are the Göß, Hochalm, Hölltor, Sieglitz and Sonnblick cores.

These basement units are overlain by the post-Variscan, Permo-Mesozoic sedimentary sequence of the Silbereck Group. It comprises basal quartzites, overlain by marbles, calc-schists, dolomites and finally calcschists, phyllites to micaschists and minor greenschists.

Thrusted onto this parautochthonous unit are the Mureck and the Storz Nappe that comprises mainly Variscan metamorphic paragneisses, amphibolites and micaschists (Vavra 1989, Vavra and Frisch 1989, Frisch et al. 1993) and minor granites that intruded during the Variscan (Vavra and Hansen 1991).

The overlying Murtörl unit consists of black albite-phyllites, chloritoid-bearing chlorite-micaschists and graphitic quartzites that are probably of post-Variscan age (because of missing intrusions) and the primary cover of the Storz Group (Kurz et al 1998).

The Schrovín Nappe comprises orthogneisses and mainly Permo-Mesozoic sediments, quartzites, calcite and dolomite marbles and calcschists. It must be derived from a continental shelf sequence, too.

The Glockner Nappe is delineated by some ophiolitic remnants (serpentinites, MOR-basalts) at its base (Höck and Miller 1987). It mainly consists of the so called Bündner schists, calcschists, grading into marbles and phyllites, and greenschists, deposits of a deep oceanic basin. In this area, the relationship of the basement rocks of the Storz Nappe to the overlying sequence of black phyllites, a Permian shelf sequence and the deep-sea sediments of the Glockner facies is obscured by the strong tectonic overprint, expressed in the parallelism of all the lithological boundaries and also in the strong thinning of the units. All the post-Variscan series are therefore often subsumed in the Peripheral Schieferhülle.

Detailed descriptions of the rock successions and lithologies can be found in the papers by Exner (1971, 1980b, 1982, 1983, 1984, 1989).

The oldest brittle to semiductile deformation structures in the Penninic units are overprinted by the main, ductile deformation. Indications of earlier deformations under cooler conditions are imbrications of different rock units and parallel trails of graphitic material, preserved in porphyroblasts (mainly albite), pointing to pressure solution as an early deformation mechanism.

The earliest kinematically interpretable deformation structures are a mylonitic foliation parallel to the lithological boundaries with only few intrafolial isoclinal folds (transposition)

and a related N-S trending stretching lineation (Fig. 4). Kinematic indicators, as asymmetric porphyroclasts in granitoids and asymmetric quartz textures, the latter preserved in Triassic quartzites of the Peripheral Schieferhülle, indicate tectonic transport top to the N (Figs. 4, 5).

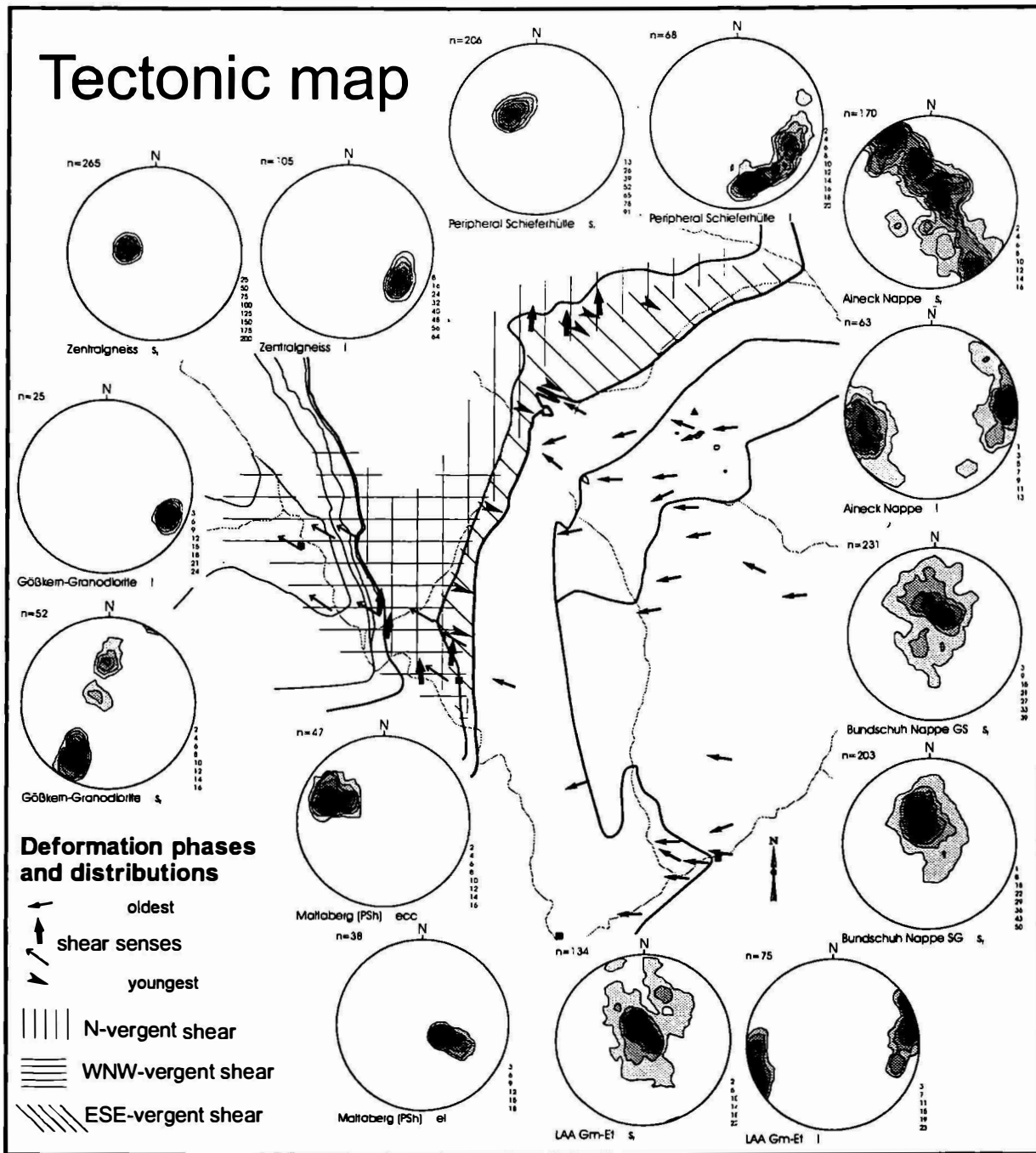


Fig. 4: Tectonic map showing the spread of deformation structures, shear senses, and plots (equal area, lower hemisphere) of foliations and lineations. s<sub>1</sub> and l<sub>1</sub> are the penetrative foliations and stretching lineations, ecc and el extensional crementation cleavage and related extensional lineation, respectively.

This N-S trending stretching lineation can be traced from the Peripheral Schieferhülle down to the base of the Silbereck-Fm., affecting the uppermost part of the basement, sometimes (Fig. 4). A mylonitic foliation with N-S trending stretching lineations can be found throughout the Storz nappe, especially well developed in granitic rocks and amphibolites. In paragneisses and micaschists an older (pre-Alpine?) foliation is folded isoclinally and transposed by this foliation. The structures related to this deformation are best preserved in Triassic rocks of the Peripheral Schieferhülle in northern parts of the investigated area (around Stern). Quartzites, dolomites and intercalated calcite marbles display a strong mylonitic foliation with a pronounced N-S trending stretching lineation. Earlier planar structures, as graphitic trails, are folded isoclinally, but also the mylonitic foliation can show a progressive isoclinal refolding with fold axes parallel to the stretching lineation. During this deformation quartz, calcite, and dolomite recrystallised dynamically. In the Peripheral Schieferhülle this deformation occurred until peak metamorphic conditions were reached, as dolomite was deformed by crystal-plastic mechanisms. Dolomite marbles and quartzites kept their synkinematic deformation features, only calcite shows evidence for a subsequent static recrystallization.

In deeper Penninic units, this deformation preceded the temperature peak, but occurred at higher pressure conditions than those of the metamorphic peak. This deformation started within the stability field of albite, even at tectonic levels that later on reached the oligoclase field during metamorphic peak conditions. Granitic gneisses affected by this deformation display the growth of white mica, with celadonite-rich cores and celadonite-poor rims, pointing to a pressure decrease during this deformation.

The next deformation phase affects almost all of the Penninic units in the investigated area and represents the main deformation phase in the mass of the Variscan granitoids. Only parts of the deeper Peripheral Schieferhülle and also parts of the deeper basement complex remain spared. It develops a mylonitic foliation with a very consistent WNW-ESE trending stretching lineation (Fig. 4). Numerous sense-of-shear criteria, as asymmetric porphyroclasts ( $\delta$ - and  $\sigma$ -clasts), shear bands, C/S structures and quartz textures (Fig. 5) unequivocally prove shear of top-to-the WNW.

In the higher Penninic parts, especially in the Storz-Nappe, this deformation is expressed in discrete, W-dipping shear bands with WNW-ESE trending striations, without obliterating the penetrative N-S trending stretching lineation. But quartz textures, mainly oblique cross to single girdle c-axes distributions, indicating WNW-directed shearing, prove a penetrative deformation during this phase in these parts, too. In deeper parts, this deformation phase is the first penetrative event, except in country rocks of the Variscan granitoids that display pre-Alpine deformation structures (sometimes even several phases of superposed folding sealed by Variscan intrusions). Along the northern side of the Malta valley the foliation dips to the E to SE, the stretching lineations to the ESE, in the deepest exposed levels the stretching lineation keeps this very consistent plunge to the ESE, but the foliations display a great circle distribution around this lineation (Fig. 4). Across the Malta valley the foliations in the granodiorites of the Göß core dip gently to the ESE on the northern side of the valley, steeply to the NNE in the middle (Koschach) and moderately to the S on the southern side. In the central part no foliation can be defined, the rocks display apparently uniaxial extension. In the area of steep foliations pronounced stretching lineations also point to deformation in the constrictional field, but some shear criteria, as asymmetric porphyroclasts, asymmetric quartz textures (Fig. 5), and asymmetric distributions of extensional and compressional quadrants of aplitic veins point to general non-coaxial deformation with a right-lateral sense of shear. In the granitoids of the Göß core, discordant aplitic and pegmatitic veins show a strong deformation too, although not very obvious macroscopically. It is expressed in a strong recrystallization of feldspars and quartz, mostly occurring in elongated aggregates, and strong lattice preferred orientations of quartz (Fig. 5).

During this deformation all major rock forming minerals recrystallised dynamically. It continued until peak metamorphic conditions were reached in deeper tectonic levels. Feldspars recrystallised dynamically, with inversely zoned recrystallised grains of oligoclase, pointing to deformation at at least uppermost greenschist facies conditions.

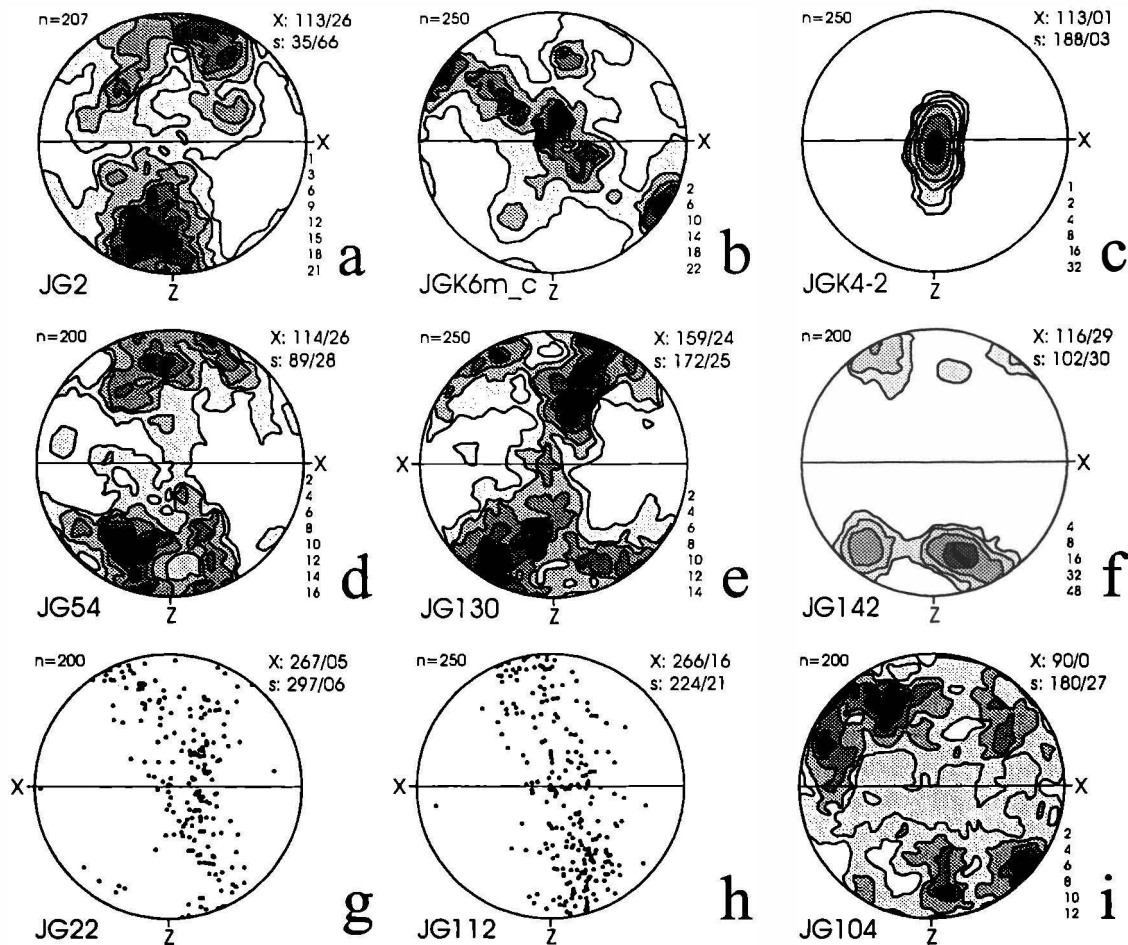


Fig. 5: Quartz-c-axes textures. Equal area, lower hemisphere diagrams, gradation of isolines are given at the right. For location see Fig. 3.

(a) Granodiorite of the Göß core, Koschach quarry; (b) discordant aplite in granodiorite of Göß core, Koschach quarry; (c) late-stage, discordant shear zone in granodiorite of Göß core, Koschach quarry; (d) tonalite gneiss from the Hochalm core, Rödern; (e) Triassic quartzite from the Schrovín nappe, Stern area; (f) quartzite from Peripheral Schieferhülle, Maltaberg; (g) quartzite from the Lower Austro-Alpine unit, Lieser valley between Gmünd and Eisentratten; (h) Triassic (?) quartzite from the Aineck Nappe, Hirneck; (i) quartzite from the base of the Bundschuh Nappe, Krangl Alm.

The last main deformation event led to the exhumation of the Penninic unit. The main shearing was concentrated within a low-angle fault zone in the top of the Glockner Nappe, displacing the AA nappe stack to the ESE (Genser and Neubauer 1989, Elsner 1991). Structures range from mylonitic shear zones with penetrative deformation, especially in calcschists, to the development of a discrete extensional crenulation cleavage (Fig. 4), often as multiple sets. Other structures are extension veins and boudinage of competent rock layers. Numerous shear criteria prove shearing top-to-the-ESE. This deformation started at elevated temperatures (crystal-plastic deformation of quartz), but continued until cool, brittle conditions under



the same kinematic frame (Kurz et al. 1994). In deeper parts, flat-lying, conjugate shear zones are related to this event. Prominent examples are fine grained, cm-thick shear zones in granitoids of the Göß core, that cross-cut the main foliation. In these shear zones, feldspars, quartz, and biotite recrystallised dynamically, quartz-c-axes textures show a maximum parallel to the Y-axis (Fig. 5). Deformation here also started near peak metamorphic conditions, but can then be followed to cool, brittle conditions within the same kinematic frame.

### Austro-Alpine unit

In the area of investigation (Fig. 3), the Austro-Alpine (AA) unit can be divided into three nappes: from the top to the bottom, the (1) Bundschuh Nappe, the (2) Aineck Nappe, and (3) the LAA Nappe (Theiner 1987). These nappes are distinguished by distinct pre-Alpine and Alpine metamorphic conditions (Fig. 7).

The Bundschuh Nappe comprises mainly paragneisses, micaschists and granitic gneisses and shows a two-stage metamorphic evolution. The Bundschuh Nappe shows widespread Variscan amphibolite facies metamorphism, with garnet and staurolite (Exner 1980a). The Alpine metamorphism reached lower amphibolite facies conditions, leading to the growth of a second, Alpine garnet generation, often as rims around pre-Alpine garnet cores (Schimana 1986, Theiner 1987) (Fig. 6). Thermobarometry on the Alpine paragenesis yielded *c.* 600°C and 10 kbar for the Alpine metamorphic peak.

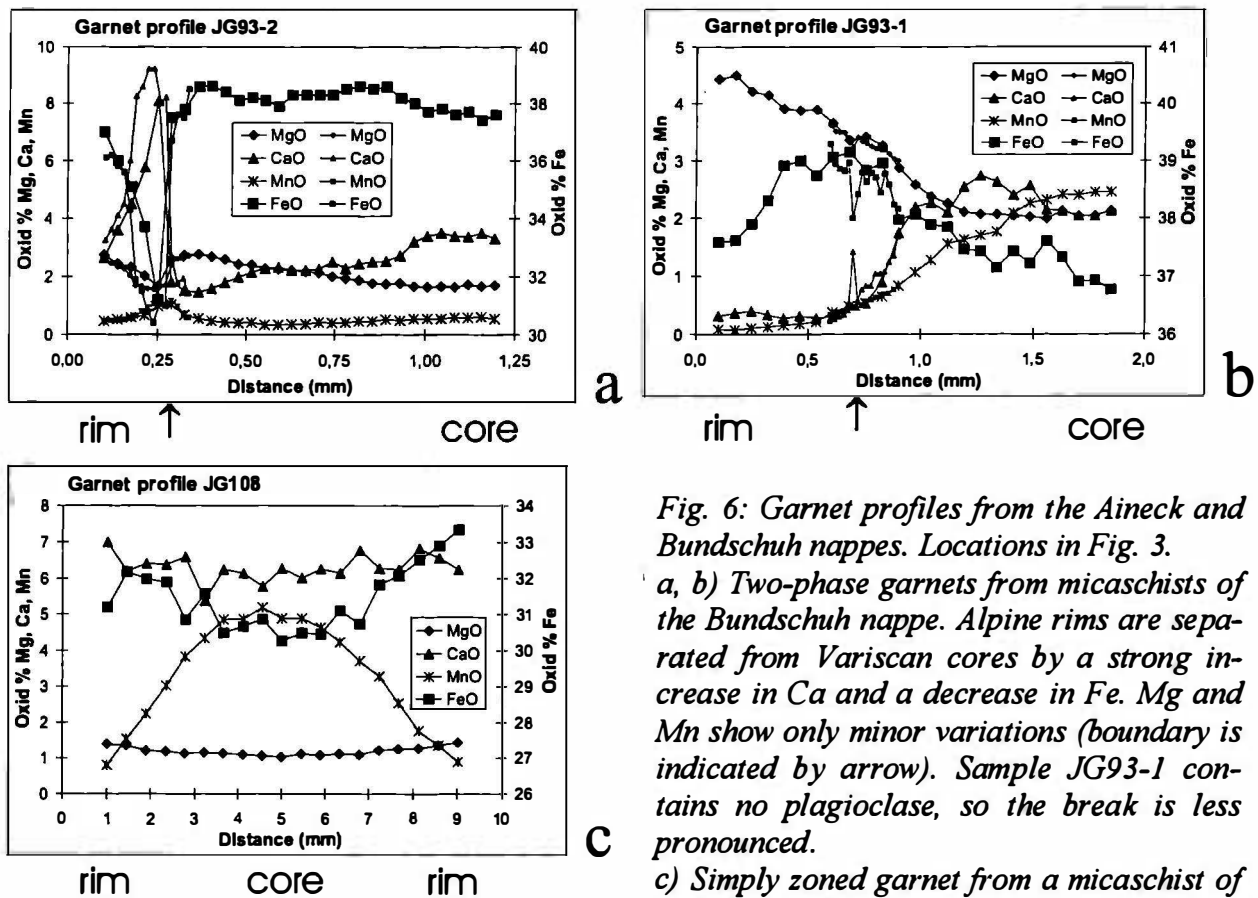


Fig. 6: Garnet profiles from the Aineck and Bundschuh nappes. Locations in Fig. 3.

a, b) Two-phase garnets from micaschists of the Bundschuh nappe. Alpine rims are separated from Variscan cores by a strong increase in Ca and a decrease in Fe. Mg and Mn show only minor variations (boundary is indicated by arrow). Sample JG93-1 contains no plagioclase, so the break is less pronounced.

c) Simply zoned garnet from a micaschist of the Aineck Nappe.

The underlying Aineck Nappe includes garnet-micaschists, paragneisses, and amphibolites and shows only one peak metamorphic assemblage of upper greenschist facies conditions. Garnets typically show continuous zonations and the same suite of inclusion minerals from the core to the rim (Theiner 1987) (Fig. 6). Thermobarometry gave conditions for the metamorphic peak of approximately 540°C and 9 kbar. The Radenthein unit that underlies the Bundschuh Nappe in the south, displays also only a single stage metamorphism, but shows somewhat higher temperatures (amphibolite facies conditions) (Schimana 1986).

The LAA Nappe along the eastern margin of the Tauern window is only a remnant of the prominent development at the north-eastern corner in the Radstädter Tauern. There, the Lower Austro-Alpine unit consists of several nappes, build up of pre-Alpine basement slices (para- and orthogneisses, often retrogressed) and thick Permo-Mesozoic cover units of a terrestrial to shallow marine evolution (e.g., Tollmann 1977, Becker 1993). In this area, the only remaining nappe displays an inverted tectonic and metamorphic position with pre-Alpine relics of upper greenschist facies minerals, as e.g. garnet, in tectonic higher parts, and only lower greenschist facies conditions in deeper parts. This setting is also evidenced by a remnant Permo-Mesozoic cover sequence at the base of the unit, that is inverted too (Exner 1971, 1982).

The main deformation event in the Bundschuh Nappe, related to thrusting, occurred prior to the metamorphic peak. This deformation is characterised by an E–W-trending stretching lineation and the transposition of a pre-Alpine planar fabric (Fig. 4). Pre-Alpine garnets are broken and pulled apart, the individual pieces overgrown by a rim of Alpine garnet. Micas show only weak alignments in the Alpine foliation, quartz has recrystallised statically as well (random lattice preferred orientations, Fig. 5). The main deformation must have taken place in the ductile domain, however, i.e. at least within greenschist facies conditions. The thermal peak must have outlasted the thrust-related deformation, however, and annealed earlier deformation fabrics.

In the Aineck Nappe, the main deformation, again with an E–W-trending stretching lineation (Fig. 4), is pre- to syn-metamorphic. Micas are aligned in the foliation, garnets show helicitic inclusion trails and quartz various degrees of lattice preferred orientations (Fig. 5). The main foliation is folded into upright folds around NE–SW-trending axes, with white mica of the first generation folded around fold hinges. This fabric is overprinted by a static recrystallization under lower greenschist facies conditions, with the growth of white mica, chlorite, albite, and rare stilpnomelane randomly across the older fabric. The main deformation must thus have occurred under upper greenschist facies conditions, followed by a phase of cooling and folding of the main foliation. The static overprint happened under lower greenschist facies conditions, most likely driven by fluid infiltration.

The nappe contact between the Bundschuh Nappe and the Aineck Nappe is cut by the basal thrust that carried the two units on top of the LAA Nappe (Fig. 3). Thrusting must thus post-date the internal imbrication within the MAA units.

The LAA Nappe shows the same E–W-trending stretching lineation as the Bundschuh Nappe and the Aineck Nappe (Fig. 4), but the main deformation occurred under lower greenschist facies conditions. Quartz was deformed by low-temperature plasticity and shows lattice preferred orientations typical for cool deformation conditions (Fig. 5). Pre-Alpine garnets are mostly chloritised and deformed into elongated ellipsoids. White micas are frequently rotated into the main Alpine foliation, but also occur in microlithons, tracing an older foliation.

## Ar/Ar data

Single grain  $^{40}\text{Ar}/^{39}\text{Ar}$  laser probe (step-wise heating) dating was carried out on white mica, biotite, and amphibole across the Penninic–Austro-Alpine suture at the eastern margin of the Tauern Window in order to constrain the timing of the main Alpine deformation events that led to the juxtaposition of the regarded units. Selected age data for white mica are presented in Fig. 7.

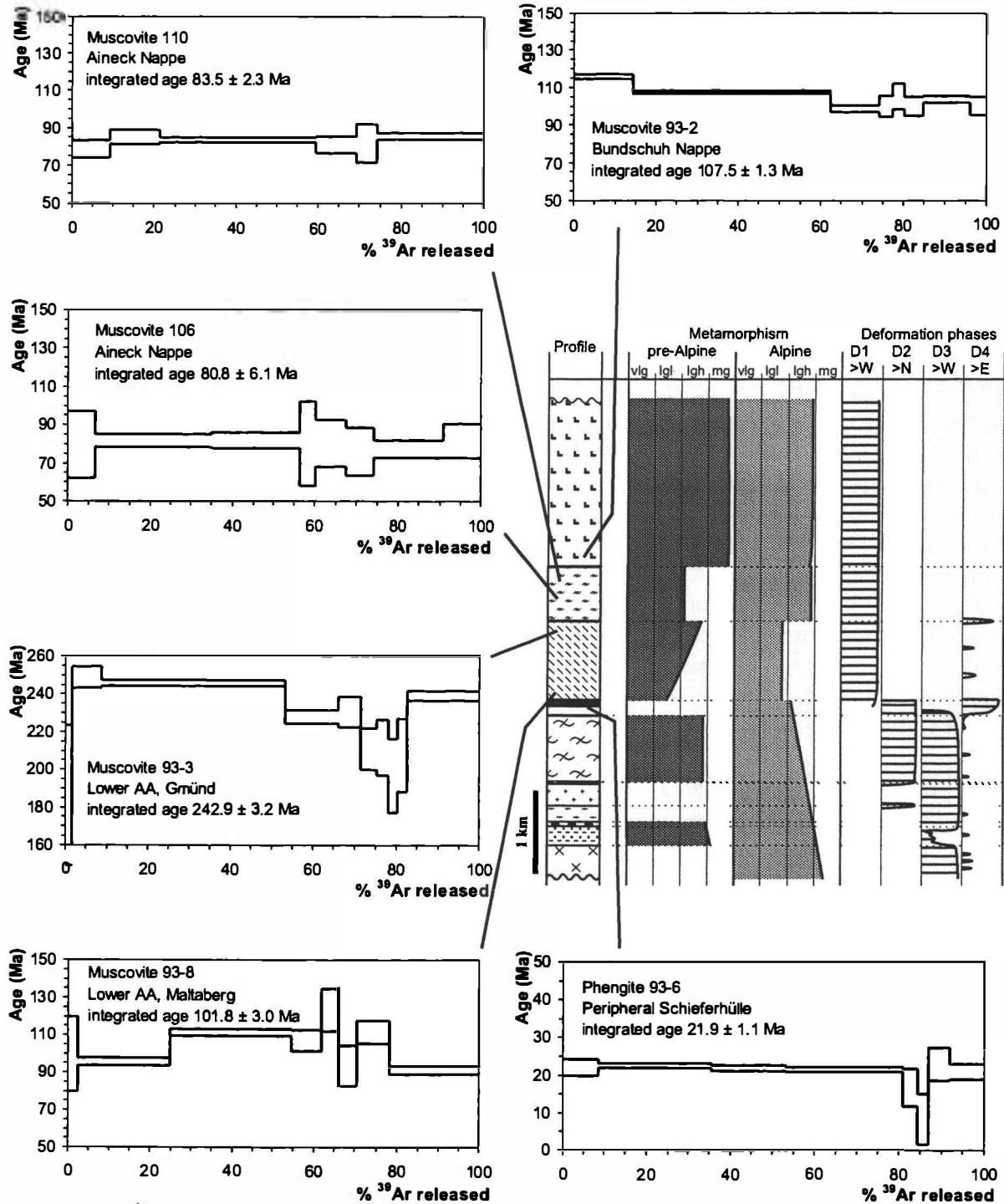


Fig. 7:  $^{40}\text{Ar}/^{39}\text{Ar}$  age diagrams of single grains of white mica and profile of the tectonic units at the eastern margin of the Tauern window. Distributions of pre-Alpine and Alpine metamorphic conditions (vlg: very low grade, lgl, lgh: low grade, mg: medium grade) and parts affected by the main deformation phases are given. For location of samples see also Fig. 3.

The Bundschuh Nappe, mainly deformed prior to the metamorphic peak of lower amphibolite facies conditions, yielded an integrated age of  $107.5 \pm 1.3$  Ma for muscovite, giving a minimum age for the main deformation. The next deeper unit (Aineck Nappe), deformed close to the metamorphic peak of slightly lower temperatures, gave an integrated age of  $83.5 \pm 2.3$  Ma for white mica of the peak metamorphic assemblage. White mica of a second generation, grown due to a static, fluid-driven metamorphic overprint, gave ages of  $80.8 \pm 6.1$  Ma. The static metamorphic overprint of lower greenschist facies conditions in the Aineck Nappe should be constrained in time by the age of the second generation of muscovite, as the temperature of this event is below or at about the closure temperature of muscovite. The cooling age of Mu I (110) of *c.* 85 Ma gives a lower age limit for the penetrative deformation in the Aineck Nappe, related to the W-directed nappe stacking process. From these data a short time interval between cooling from the metamorphic peak (Mu I, sample 110) and the static metamorphic overprint (Mu II, sample 106) can be deduced, as the ages are the same within the  $2\sigma$ -error limits. A common cause for cooling from the peak metamorphic conditions, for shortening, expressed in the folding of the penetrative foliation at already cooler conditions, and for the subsequent static metamorphic overprint by fluid infiltration can be the thrusting of the Aineck Nappe onto a cool, fluid-rich unit. This could be the LAA unit, derived from the continental margin, on the one hand and the oceanic South Penninic unit on the other hand. The LAA contains mainly low-grade metamorphic pre-Alpine basement rocks and a Mesozoic, carbonate shelf cover sequence that should be rather depleted in fluids in comparison with the shaly-marly deep sea sequence of the South Penninic unit. Also the retrogressive overprint of the LAA with chloritization of garnet needs external fluid sources. These fluids, infiltrating the base of the MAA, are therefore most likely derived from the South Penninic unit, and give a possible age constraint on the subduction of the South Penninic ocean beneath the AA continental margin.

The deepest, Lower AA Nappe, yielded Variscan white mica ages ( $242.9 \pm 2.2$  and  $239.6 \pm 1.1$  Ma) from tectonically high levels and strongly disturbed ages of *c.* 100 Ma from the base. Alpine metamorphic conditions were obviously too low to reset the Ar-system of white mica completely, consistent with the observed deformation conditions and metamorphic assemblages. From the presented data no direct time constraint on the deformation of this unit can be given, but if no marked inverted thermal gradient existed during deformation, the Alpine deformation must be younger than the 85 Ma of Mu I of the overlying Aineck Nappe (sample 110). Thermal models indicate that in shallow to medium crustal levels, that are appropriate for the burial of the LAA in this area, no inverted thermal gradients occur at reasonable thrusting rates (Genser et al. 1996). Additionally, the age sequence with cooling of the higher nappe well before cooling of deeper levels indicates that no inverted geothermal gradient existed during nappe stacking within the exposed crustal levels. The observed inverted metamorphic gradient in the AA edifice must therefore be attributed to the late to post-metamorphic transport of those nappes over deeper ones.

For the LAA Nappe in this area, no pressure data are available that could constrain its burial depths. Its position at the base of the AA nappe complex, however, points to burial depths that are in the same order as for the overlying units. This would imply reduced geothermal gradients during underthrusting of the LAA, a scenario that could be met in an oceanic subduction zone environment. Beginning subduction of the SP oceanic lithosphere, together with the leading edge of the AA continental margin that is deformed into the LAA nappe complex, and fluid infiltration of the base of the MAA, fit into this scenario (Peacock 1993). Tectonic inversion of the continental margin, as presently exposed, at the beginning of oceanic subduction conforms, too. We thus correlate the underthrusting of the LAA with the beginning of subduction of the SP ocean rather than with the end, as proposed by Slapansky and Frank (1987), who connected it with the collision of the AA and the MP units. It is

constrained in time by the second generation of muscovite in the Aineck Nappe at about 80-85 Ma.

A white mica from tectonically high parts of the Penninic unit, showing a normal metamorphic gradient of greenschist facies conditions, yielded an age of  $21.9 \pm 1.1$  Ma. The flat age spectra record the cooling of the Peripheral Schieferhülle through *c.* 375° C. The second penetrative deformation event in the Penninic units, the WNW-directed shearing that occurred on the heating path and at thermal peak conditions, that were higher than the closure temperature of phengite, must thus precede these ages. This deformation event should thus be Late Oligocene (Harland et al. 1990) in age. The cooling age of 22 Ma gives the onset or an upper age constraint for the ESE-directed shearing, as structural features (e.g. low-temperature plasticity of quartz, calcite twinning) indicate that this deformation started at lower greenschist facies conditions at these tectonic levels, hence at or below the closure temperature of this system. The resulting differential uplift of the Penninic unit should continue to *c.* 16.5 Ma, the cooling ages of biotite (Rb/Sr) across the centre of the Hochalm Dome (Cliff et al. 1985).

## Discussion

Structural, metamorphic and age data demonstrate distinct Alpine evolutions for the Austro-Alpine and Penninic units. Thrusting in the Austro-Alpine units is generally towards the W, following by folding around E-W to NE-SW trending axes. This thrusting occurred over an extended time-span. The Alpine thrusting in the highest unit (pre-metamorphic) and the subsequent cooling from the highest greenschist to lower amphibolite facies to about 350-400 °C predates 100 Ma. In the next lower unit, thrusting could have persisted until *ca.* 85 Ma. Nappe stacking must have propagated from the hangingwall to the footwall, therefore, incorporating successively more external and deeper units.

The attainment of higher peak temperatures in higher nappes of the Austro-Alpine unit and the subsequent thrusting onto progressively cooler units of the same mega-unit points to a continuous accretion of parts of the footwall to the hangingwall in the stacking process. Thus thrusting could be explained by an intra-Austro-Alpine subduction. This progressive accretion can also explain the observed inverted metamorphic gradient, without need to invoke inverted temperature gradients.

The beginning of subduction of the oceanic Penninic lithosphere could be dated by the second generation of white mica at the base of the Austro-Alpine unit, that grew due to fluid infiltration. The ages of 80 – 85 Ma indicate a possible interference between intra-Austro-Alpine thrusting and commencing subduction of the Penninic ocean beneath.

In the Penninic units, three distinct deformation stages can be distinguished, that can be found in a very consistent manner over the entire Tauern window (Kurz et al. 1997). The oldest deformation is a shearing top-to-the N to NE, and is found especially the South Penninic Glockner nappe and the underlying gneiss nappes. This event is followed by a shearing top-to-the WNW, that affected most of the units, particularly the deeper parautochthonous Zentralgneis unit. The main deformation in the higher Penninic parts, related to their subduction and intra-Penninic stacking is pre- to syn-metamorphic. Hence the oldest ages from that unit of about 30 – 32 Ma, already cooling ages, give a minimum age for N-directed shearing, the oldest, ductile deformation. The ages of about 22 Ma place a lower age limit on the WNW-directed shearing, occurring at about peak metamorphic conditions, and an upper age constraint on the subsequent ESE-directed, extensional shearing. K/Ar ages from 22 to 17 Ma for white mica are common along the central dome of the eastern Tauern window, biotite

Rb/Sr ages are very uniform at about 15.5 - 17 Ma (Cliff et al. 1985). This ages point to rapid exhumation of the Penninic units from depths of 25 to 20 km to near to the surface in this time span (Cliff et al. 1985). This rapid exhumation was enabled by the tectonic unroofing of the Tauern window along the low-angle normal faults along the Penninic–Austro-Alpine interface. Laterally, the window is bound by sinistral strike-slip faults, indicating that extension subparallel to the orogen took place in a wrench regime (Genser and Neubauer 1989, Kurz and Neubauer 1996).

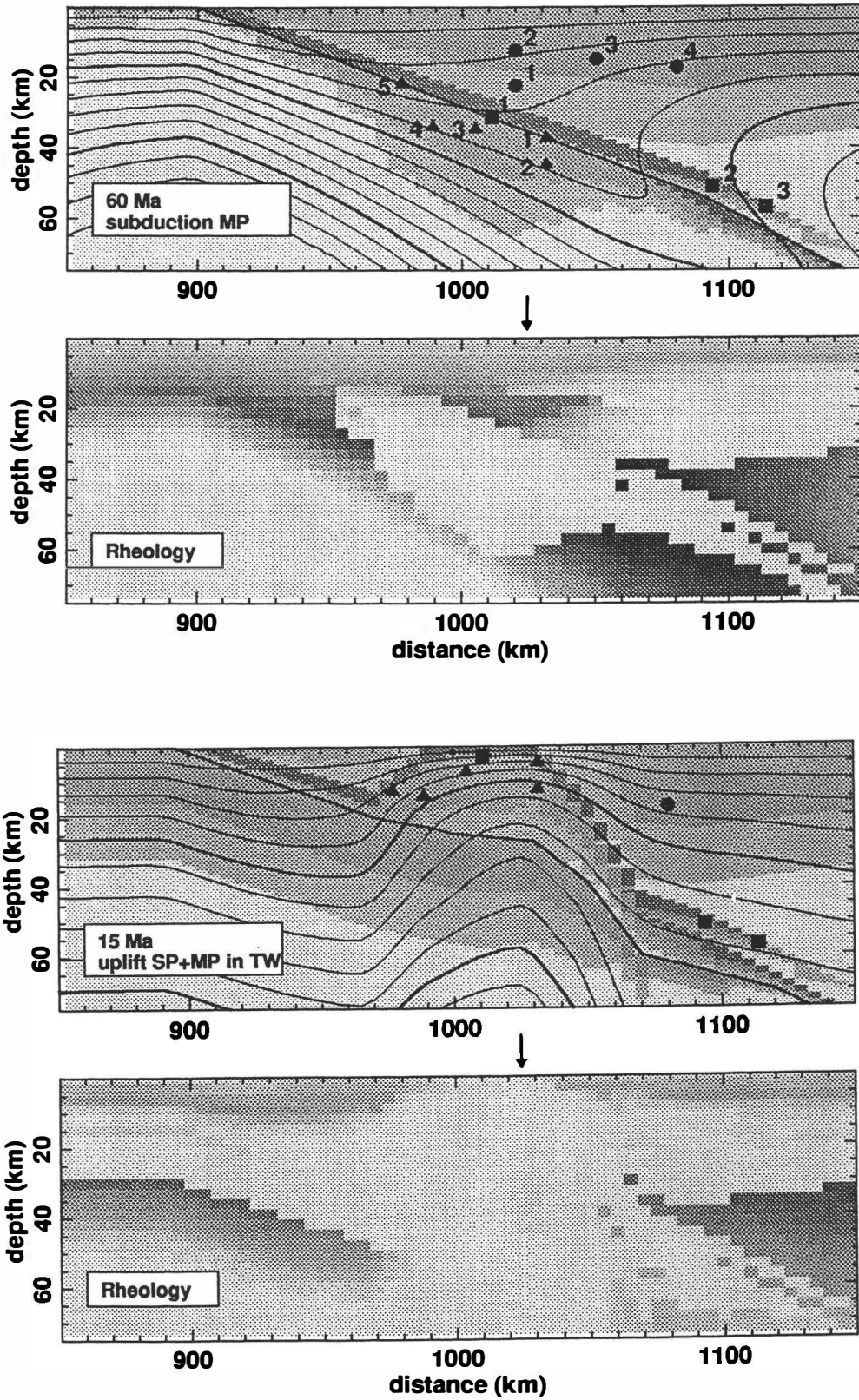


*Fig. 8: Thermo-rheological models for subduction of Penninic and subsequent Helvetic-European units beneath the Austro-Alpine upper plate. Thermal modelling was carried out with a 2-D finite difference scheme. From Genser et al. (1996).*

*(a) Situation after subduction of the South Penninic (90-70 Ma) and subsequent Middle Penninic (70-60 Ma) beneath the Austro-Alpine unit.*

*(b) Situation after consecutive subduction of North Penninic basin and the southern margin of the European foreland (Helvetic) from 50 to 20 Ma and the rapid uplift of the Penninic units in the Tauern window by extensional unroofing from 20 to 15 Ma.*

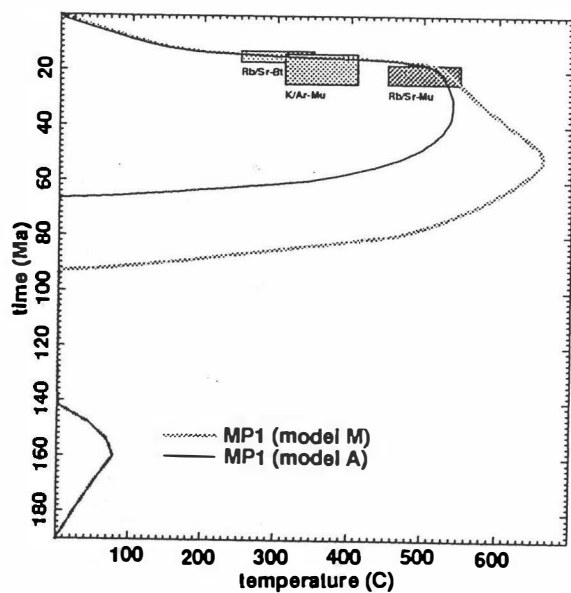
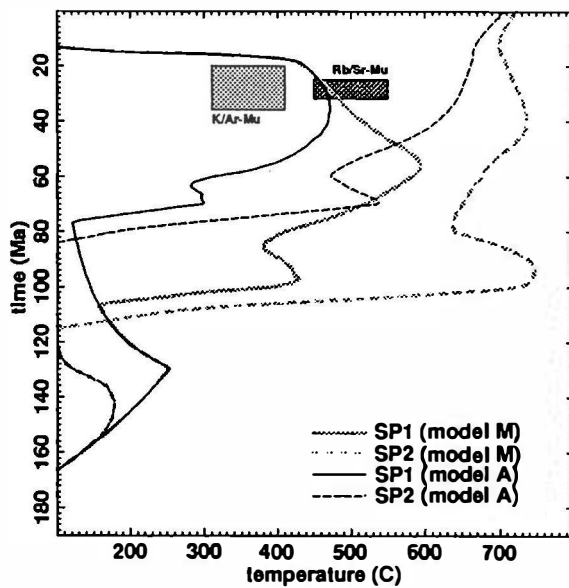
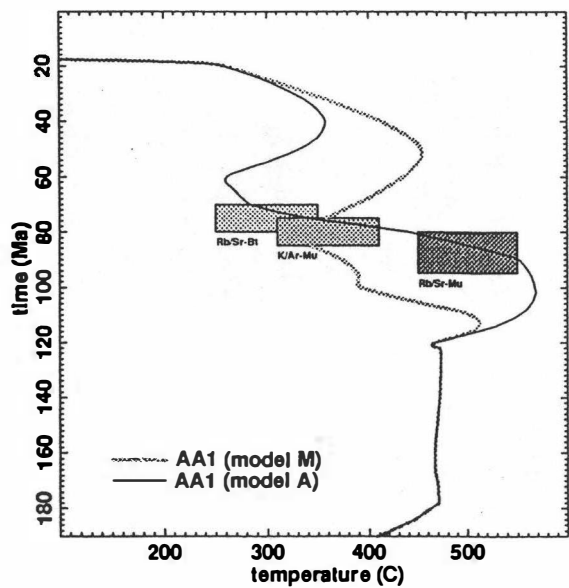
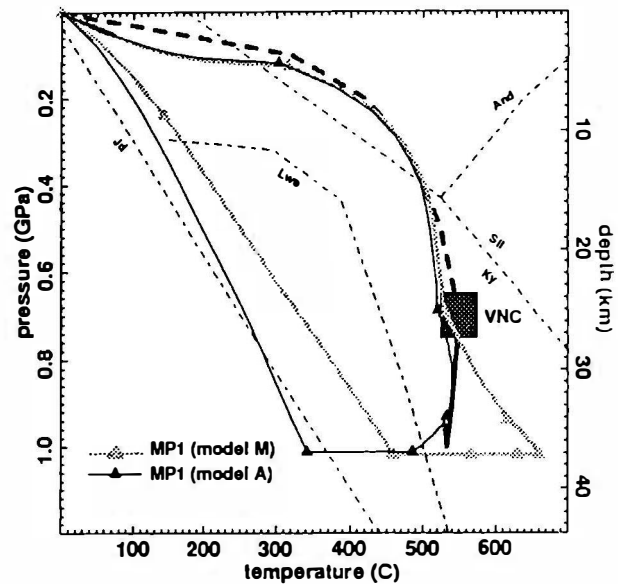
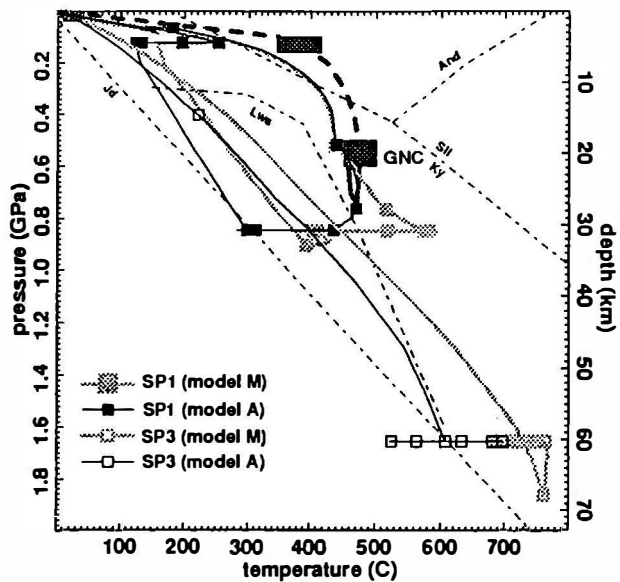
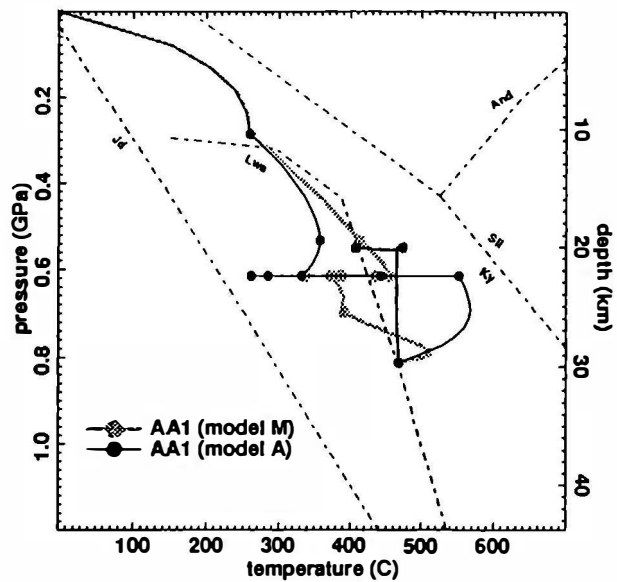
---

Thermal modelling of the metamorphism in and around the Tauern window by Genser et al. (1996) also substantiate an independent Alpine evolution of the Penninic and Austro-Alpine units, respectively. A model, where subduction of the South Penninic ocean commenced after the main nappe stacking in the Austro-Alpine unit (Fig. 8), give P-T-t paths, that are in accordance with petrological and thermochronological data (Fig. 9). Models that relate compression and metamorphism in the Austro-Alpine to subduction of the South Penninic ocean and its subsequent collision with the Middle Penninic continental block (model M of Fig. 9) are grossly inconsistent with these constraining data. A sketch of our preferred model of the relative and absolute timing of the major events is given in Fig. 10.

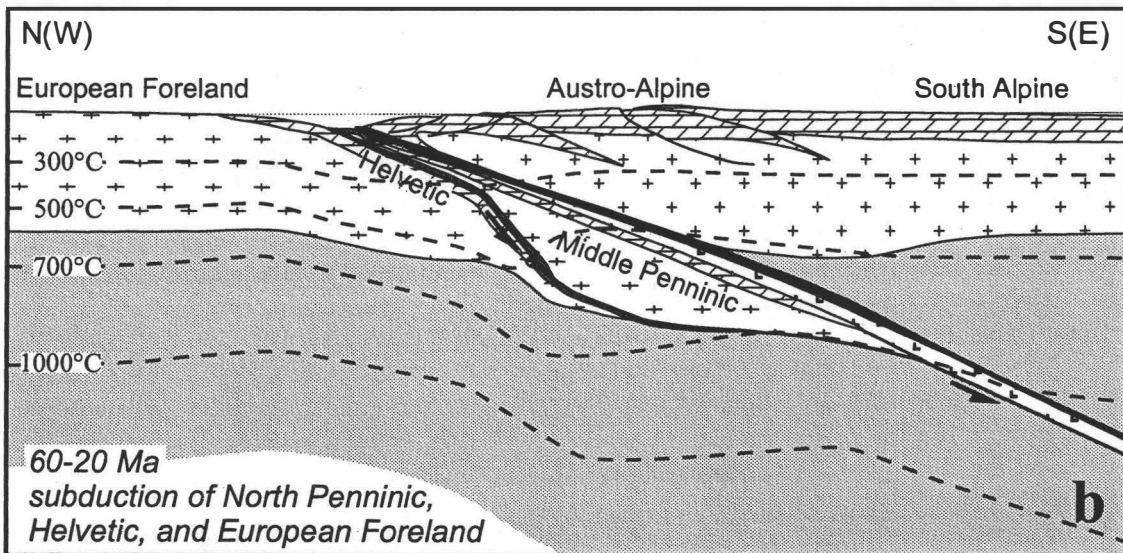
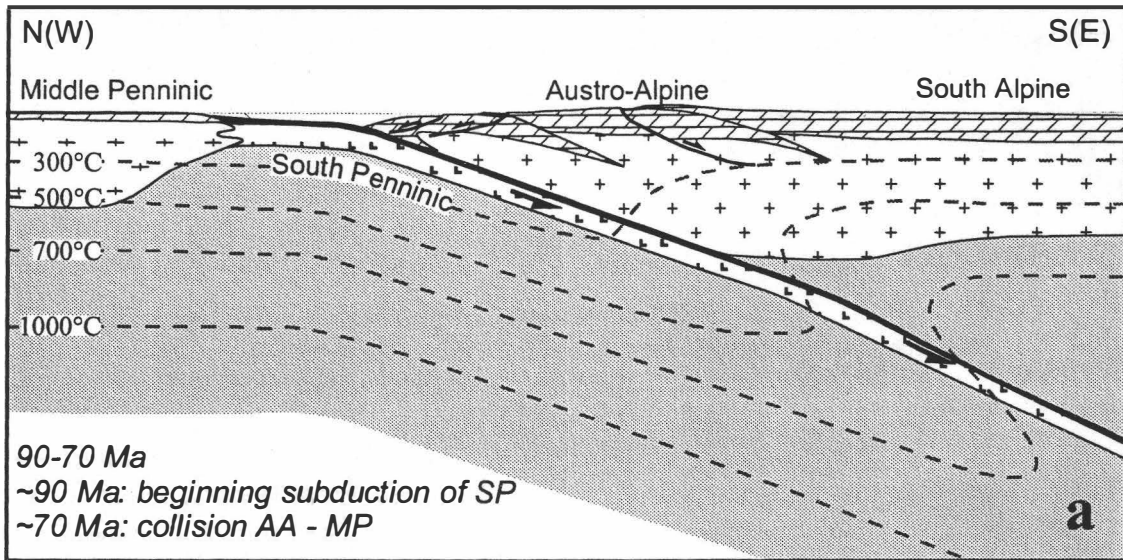
---

*Fig. 9: Modelled P-T and T-t paths for points (for location see Fig. 8) within the AA, South and Middle Penninic units. The preferred model (model A, shown in Fig. 8) gives paths, that closely correspond to observed metamorphic paths and cooling ages. Model M, with early subduction of Penninic units during nappe stacking in the AA unit, is grossly inconsistent.*

*Fig. 10: Thermo-tectonic model for the subduction of the Penninic and Helvetic units beneath the Austro-Alpine hangingwall plate (from Genser et al. 1996).*







## References

- Becker, B., The Structural Evolution of the Radstadt Thrust System, Eastern Alps, Austria - Kinematics, Thrust Geometries, Strain Analysis, *Diss., Univ. Tübingen*, 76, 1993.
- Behrmann, J.H., Zur Kinematik der Kontinentkollision in den Ostalpen, *Geotekt.Forsch.*, 76, 1-180, 1990.
- Cliff, R. A., Droop, G.T.R., and Rex, D.C., Alpine metamorphism in the south-east Tauern Window, Austria: II. heating, cooling and uplift rates, *J. metamorphic Geol.*, 3, 403-415, 1985.
- Elsner, R., Geologie des Tauern-Südostrandes und geotektonische Konsequenzen, *Jahrb. Geol. B.-A.*, 134, 561-645, 1991.
- Exner, Ch., Der Südrand des Tauernfensters bei Spittal an der Drau, *Jb. Geol. B.-A.*, 127, 349-367, 1984.
- Exner, Ch., Geologie der peripheren Hafnergruppe (Hohe Tauern), *Jb. Geol. B.-A.*, 114, 1-119, 1971.
- Exner, Ch., Das Kristallin östlich der Katschbergzone, *Mitt. Österr. Geol. Ges.*, 71/72, 167-189, 1980a.
- Exner, Ch., Geologie der Hohen Tauern bei Gmünd in Kärnten, *Jb. Geol. B.-A.*, 123, 343-410, 1980b.
- Exner, Ch., Geologie der zentralen Hafnergruppe (Hohe Tauern), *Jb. Geol. B.-A.*, 125, 51-154, 1982.
- Exner, Ch., Geologische Karte der Hafnergruppe 1 : 25.000, mit Erläuterungen, *Mitt. Ges. Geol. Bergbaustud. Österr.*, 29, 41-74, 1983.
- Exner, Ch., Geologie des mittleren Lungaus, *Jahrb. Geol. B.-A.*, 132, 7-103, 1989.
- Exner, Ch., Erläuterungen zur Geologischen Karte des mittleren Lungaus, *Mitt. Ges. Geol. Bergbaustud. Österr.*, 36, 1-38, 1990.
- Finger, F., G. Frasl, B. Haunschmid, H. Lettner, A. von Quadt, A. Schermaier, A. O. Schindlmayr, and H. P. Steyrer, The Zentralgneise of the Tauern Window (Eastern Alps): Insight into an intra-Alpine Variscan batholith, in *Pre-Mesozoic geology in the Alps*, edited by J. F. von Raumer, and F. Neubauer, pp. 375-391, Springer-Verlag, Berlin Heidelberg New York, 1993.
- Frank, W., Evolution of the Austroalpine elements in the Cretaceous, in *Geodynamics of the Eastern Alps*, edited by H. W. Flügel, and P. Faupl, pp. 379-406, Deuticke, Vienna, 1987.
- Frank, W., V. Höck, and Ch. Miller, Metamorphic and tectonic history of the central Tauern Window, in *Geodynamics of the Eastern Alps*, edited by H. W. Flügel, and P. Faupl, pp. 34-54, Deuticke, Vienna, 1987.
- Frank, W., M. Kralik, S. Scharbert, and M. Thöni, Geochronological data from the Eastern Alps, in *Geodynamics of the Eastern Alps*, edited by H. W. Flügel, and P. Faupl, pp. 272-281, Deuticke, Vienna, 1987.
- Frisch, W., Tectonic progradation and plate tectonic evolution of the Alps, *Tectonophysics*, 60, 121-139, 1979.
- Frisch, W., K. Gommeringer, U. Kelm, and F. Popp, The upper Bündner Schiefer of the Tauern Window - a key to understanding eoalpine orogenic processes in the Eastern Alps, in *Geodynamics of the Eastern Alps*, edited by H. W. Flügel, and P. Faupl, pp. 55-69, Deuticke, Vienna, 1987.
- Frisch, W., G. Vavra, and M. Winkler, Evolution of the Penninic basement of the Eastern Alps, in *Pre-Mesozoic geology in the Alps*, edited by J. F. von Raumer, and F. Neubauer, pp. 349-360, Springer-Verlag, Berlin Heidelberg New York, 1993.
- Genser, J., Struktur-, Gefüge- und Metamorphoseentwicklung einer kollisionalen Plattengrenze: Das Beispiel des Tauernostrandes (Kärnten/Österreich). Unpubl. Diss. Univ. Graz, Graz, 1992.
- Genser, J., and F. Neubauer, Low angle normal faults at the eastern margin of the Tauern Window (Eastern Alps), *Mitt. österr. geol. Ges.*, 81, 233-243, 1989.
- Genser, J., J.D. van Wees, S. Cloetingh, and F. Neubauer, Eastern Alpine tectono-metamorphic evolution: constraints from two-dimensional P-T-t modelling, *Tectonics*, 13, 584-604, 1996.
- Harland, W. B., R. L. Armstrong, A. V. Cox, L. E. Craig, A. G. Smith, and D. G. Smith, A geologic time scale 1989, Cambridge University Press, Cambridge, 1990.
- Hawkesworth, C.J., Rb/Sr geochronology in the Eastern Alps, *Contrib. Mineral. Petrol.*, 54, 225-244, 1976.
- Hawkesworth, C.J., D.J. Waters, and M.J. Bickle, Plate tectonics in the Eastern Alps, *Earth Planet. Sci. Lett.*, 24, 405-413, 1975.

- Holub, B., and R. Marschallinger, Die Zentralgneise im Hochalm-Ankogel-Massiv (östliches Tauernfenster). Teil I: Petrographische Gliederung und Intrusionsabfolge, *Mitt. Österr. Geol. Ges.*, 81, 5-31, 1989.
- Höck, V., and Ch. Miller, Mesozoic ophiolitic sequences and non-ophiolitic metabasites in the Hohe Tauern, in *Geodynamics of the Eastern Alps*, edited by H. W. Flügel, and P. Faupl, pp. 16-33, Deuticke, Vienna, 1987.
- Kruhl, J.H., The P-T-d development at the basement-cover boundary in the north-east Tauern Window (Eastern Alps): Alpine continental collision, *J. metamorphic Geol.*, 11, 31-47, 1993.
- Kurz, W., F. Neubauer, H. Genser, and H. Horner, Sequence of Tertiary brittle deformations in the eastern Tauern Window (Eastern Alps), *Mitt. Österr. Geol. Ges.*, 86 (1993), 153-164, 1994.
- Kurz, W., and F. Neubauer, Deformation partitioning and shear localization during the updoming of the Sonnblick area in the Tauern Window (Eastern Alps, Austria), *J. Struct. Geol.*, 18, 1327-1343, 1996.
- Kurz, W., F. Neubauer, and J. Genser, Kinematics of Penninic nappes (Glockner Nappe and basement-cover nappes) in the Tauern Window (Eastern Alps, Austria) during subduction and Penninic-Austroalpine collision, *Eclogae geol. Helv.*, 89, 573-605, 1996.
- Kurz, W., F. Neubauer, J. Genser, and E. Dachs, Alpine geodynamic evolution of passive and active continental margin sequences in the Tauern Window (eastern Alps, Austria, Italy): a review, *Geol. Rdsch.*, 87, 225-242, 1998.
- Marschallinger, R., and B. Holub, Die Zentralgneise im Hochalm-Ankogel-Massiv (Östliches Tauernfenster, Österreich). Teil II: Zirkontypologische und geochemische Charakteristik, *Mitt. Österr. Geol. Ges.*, 82, 19-48, 1990.
- Oberhauser, R. (ed.), *Der geologische Aufbau Österreichs*. Springer, Wien, 1980.
- Reddy, S.M., R.A. Cliff, and R. East, Thermal history of the Sonnblick Dome, south-east Tauern Window, Austria: Implications for Heterogeneous Uplift within the Pennine basement, *Geol. Rdsch.*, 82, 667-675, 1993.
- Schimana, R., Neue Ergebnisse zur Entwicklungsgeschichte des Kristallins um Radenthein (Kärnten, Österreich), *Mitt. Ges. Geol. Bergbaustud. Österr.*, 33, 221-232, 1986.
- Theiner, U., Das Kristallin der NW-Nockberge - Eine kristallingeologische Neuuntersuchung, *Unveröff. Diss. formal-naturw. Fak. Univ. Wien*, 154 S, 1987.
- Tollmann, A., Das östliche Tauernfenster, *Mitt. Österr. Geol. Ges.*, 71/72, 73-79, 1980.
- Tollmann, A., Die Geologie von Österreich (Band I): Die Zentralalpen. Deuticke, Wien, 1977.
- Vavra, G., Die Entwicklung des penninischen Grundgebirges im östlichen und zentralen Tauernfenster der Ostalpen - Geochemie, Zirkontypologie, U/Pb-Radiometrie, *Tüb. Geowiss. Abh. Reihe A*, 6, 1-150, 1989.
- Vavra, G., and W. Frisch, Pre-Variscan back-arc and island arc magmatism in the Tauern Window (Eastern Alps), *Tectonophysics*, 169, 271-280, 1989.
- Vavra, G., and B.T. Hansen, Cathodoluminescence studies and U/Pb dating of zircons in pre-Mesozoic gneisses of the Tauern Window: implications for the Penninic basement evolution, *Geol. Rundschau*, 80, 703-715, 1991.



Carpathian-Balkan Geological Association, XVI Congress	Field Guide "Transect through central Eastern Alps"	pp. 85 - 101	Salzburg - Wien, 1998
--	---	--------------	-----------------------

## **Middle and Upper Austroalpine units of Gurktal Mountains/Nock region**

**Franz Neubauer <sup>1</sup>, Balázs Koroknai <sup>2</sup>, Johann Genser <sup>1</sup>, Robert Handler <sup>1</sup>, Dan Topa <sup>1</sup>**

<sup>1</sup> Institut für Geologie und Paläontologie der Paris-Lodron-Universität Salzburg,  
Hellbrunner Str. 34, A-5020 Salzburg, Austria

<sup>2</sup> Academic Research Group, Eötvös Lóránd University, Múzeum krt. 4/A,  
H-1088 Budapest, Hungary

### **Abstract**

Petrological and structural investigations were carried out on samples of Middle and Upper Austroalpine units at the western edge of the Gurktal nappe complex, Eastern Alps (Nock mountains). Based on thermobarometric calculations applying to garnet-plagioclase-muscovite-biotite paragenesis the Alpine metamorphic conditions in the Middle Austroalpine crystalline basement (Radenthein and Bundschuh nappes) can be estimated at c. 600°C and 10-11 kbar within upper epidote-amphibolite facies conditions. Moreover, the presence of an earlier stage with even higher pressure conditions is likely. Pre-Alpine (probably Variscan) relict mineral parageneses are not preserved in all investigated Middle Austroalpine rocks. Calcite-dolomite thermometry in the Upper Austroalpine (Murau nappe) yielded temperatures of c. 460-500°C which are interpreted to represent Alpine metamorphic conditions in contrast to temperatures of 550-600°C from garnet-biotite thermometry which are assumed to indicate pre-Alpine metamorphic conditions. Garnet-biotite parageneses were later strongly overprinted by retrogression within greenschist facies conditions. The break in metamorphic P-T conditions between Middle Austroalpine units and the Murau nappe is considered to result from Late Cretaceous low-angle normal faulting that juxtaposed these two units along a ductile shear zone with top-to-the-ESE displacement.

### **Introduction**

Crustal-scale nappe assembly within collisional orogens regularly leads to burial and metamorphic overprint of crustal pieces (e.g., England and Thompson, 1984). Subsequent extensional processes result in exhumation of previously buried crustal pieces. Vertical motion in relation to the Earth's surface can be, therefore, monitored by changing metamorphic pressure conditions. Furthermore, varying metamorphic pressure-temperature conditions can be used to discriminate tectonic bodies, e.g. nappes and extensional allochthons.

This paper is dealing with the structural and metamorphic relationships between the Middle and Upper Austroalpine nappe units along the western margin of the Gurktal nappe complex (Upper Austroalpine units) in the Eastern Alps (Fig. 1) with strongly contrasting metamorphic pressure-temperature conditions of the penetrative Cretaceous overprint (e.g., Frank, 1987;

Schimana, 1986). New structural, textural and petrological data are used to constrain the Cretaceous tectonic processes of that region where previous data suggest Late Cretaceous extension (e.g., Ratschbacher et al., 1990).

### **Geological setting**

The Austroalpine units within the Eastern Alps form a coherent plate composed of a number of nappes that were assembled during Late Cretaceous nappe stacking under ductile strain and a wide spectrum of metamorphic pressure-temperature conditions (e.g., Frank, 1987; Tollmann, 1987, Ratschbacher and Neubauer, 1989). Available data show that penetrative internal deformation occurred during the Cretaceous (e.g., Frank et al., 1987; Dallmeyer et al., 1996), partly associated with high pressure metamorphic conditions up to eclogite facies (e.g., c. 18 kbar; Miller, 1990; Ehlers et al., 1994). Major portions of these units are interpreted to represent lower plate sequences emplaced during Cretaceous subduction of Austroalpine continental crust beneath Meliata-like oceanic tectonic elements (Neubauer, 1994; Dallmeyer et al., 1996, 1998). Late Cretaceous exhumation led to crustal thinning and cooling of previously overthickened crust (Ratschbacher et al., 1989; Neubauer et al., 1995; Dallmeyer et al., 1998). Subsequent Tertiary piggy-back emplacement of these units onto Penninic units did not lead to major internal deformation of Austroalpine units.

East of the Penninic Tauern window all major Austroalpine units are exposed in the classical Bundschuh area where Holdhaus (1921), based on fossil discoveries, argued for an intra-Austroalpine nappe structure (Fig. 1b). Here, the Austroalpine units comprise from footwall to hangingwall (Tollmann, 1975; 1977; Schimana, 1986; Neubauer, 1987; Neubauer and Pistotnik, 1984; von Gosen, 1989): (1) the Radenthein micaschist complex (RMC), a basement complex constituting the Radenthein nappe; (2) the Bundschuh nappe including the Bundschuh complex (BC), a gneissic, pre-Permian basement unit, and a Permian to Mesozoic cover sequence (Stangalm group); Radenthein and Bundschuh nappes are classically interpreted to represent the Middle Austroalpine units; (3) the Murau nappe with a phyllitic Paleozoic basement; and (4) the Stolzalpe nappe also with a phyllitic Paleozoic basement, and Late Carboniferous to Triassic cover sequences. Murau and Stolzalpe nappes are part of the Gurktal nappe complex (Upper Austroalpine nappe complex).

The superposition of the Gurktal nappe complex over Middle Austroalpine units is interpreted to result from Cretaceous nappe stacking within ductile deformational conditions (Tollmann, 1977; Neubauer, 1980, 1987; Ratschbacher and Neubauer, 1989; von Gosen, 1989) although there is a wide disagreement on the nature and extent of displacement (e.g., Clar, 1965; Tollmann, 1975; Frank, 1987; Frimmel, 1986a, b; 1988). Based on scarce shear sense criteria a top to the W (WNW) displacement of hangingwall units was proposed (Neubauer, 1987; Ratschbacher and Neubauer, 1989; Ratschbacher et al., 1989; von Gosen, 1989). Furthermore, many structural data favour an overprint by a second ductile phase with a general top to the ESE displacement (Neubauer, 1987) that was interpreted to represent subsequent Late Cretaceous east-directed motion due to extension (Ratschbacher et al., 1989, 1990; Stock, 1992; Antonitsch and Neubauer, 1992). The second event was also interpreted to be responsible for a break in Cretaceous peak metamorphic conditions between the Middle Austroalpine units/Murau nappe and the overlying Stolzalpe nappe (Neubauer, 1980; Ratschbacher et al., 1990).

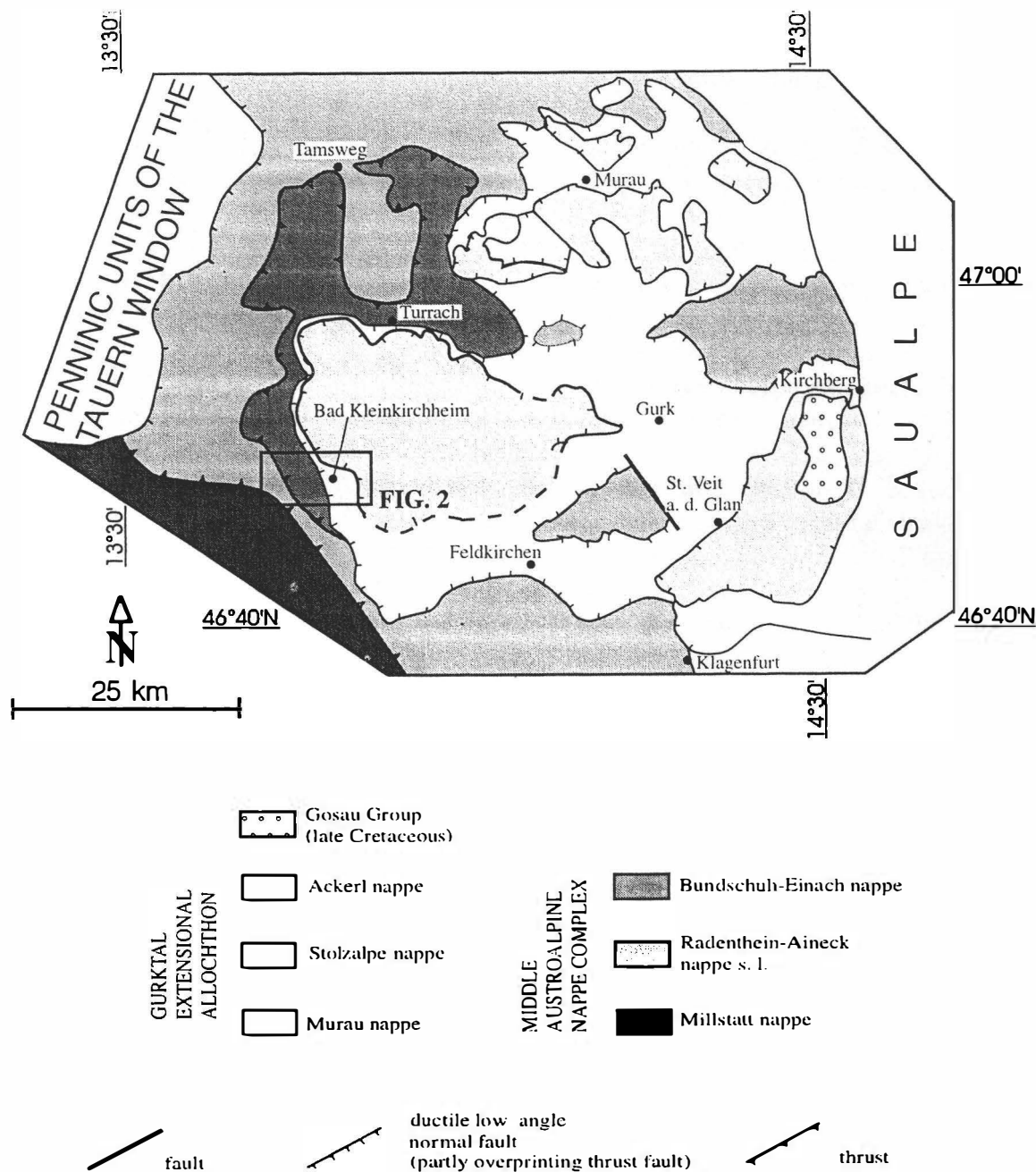


Fig. 1. Simplified geological map showing general geological relationships of the Gurktal nappe complex/Gurktal extensional allochthon to underlying units.

### Stolzalpe nappe

The Stolzalpe nappe comprises a low-grade metamorphic, Variscan basement and a very low-grade metamorphic Late Carboniferous to Triassic cover succession (for detailed reviews, see Krainer 1989a, b) Neubauer, 1992; Neubauer and Sassi, 1993). The stratigraphy of the basement is nearly exclusively based on conodonts which were found in thin dolomite interlayers within the otherwise clastic and volcanic sequences. Models to the paleogeographic evolution are shown in Figures 2 and 3. As a rule, thick mafic volcanic sequences occur at the base. This are divided into a late Middle to Late Ordovician Magdalensberg Formation, Nock

Formation, and the likely Late Ordovician Kaserer Formation, and into the Silurian Eisenhutschiefer Formation. The Nock Fm. exhibits calc-alkaline geochemical affinities, other mafic volcanic formations display mildly alkaline geochemical characteristics (Giese, 1988; Loeschke, 1989).

A slaty facies with cherts and allodapic limestones persists through the Wenlockian to the boundary of Lochkovian/Pragian (Magdalensberg facies). This facies is contrasted by thick sandstones, quartzwackes and quartzarenites (Pranker facies) covering the same time span. A  $^{40}\text{Ar}/^{39}\text{Ar}$  age of detrital white mica yielded a Cadomian age (ca. 560 Ma). The Auen facies with dolomite and pelagic limestone of Late Wenlockian to Pragian form a third facies realm. Similar carbonates spread from the Pragian/Zlichovian onwards over all other facies realms and persist up to the Early Carboniferous. Locally, cherts were found at the Tournaisian/Visean boundary. These are overlain by synorogenic grawwackes.

The cover sequence of the Stolzalpe nappe occurs along western and eastern margins of the Gurktal nappe complex. At the western margins, the succession starts with the Late Carboniferous Stangnock Formation with conglomerate, sandstone and anthracite. The sequence was deposited by a river system under a humid climate. The overlying Permian Werchzirm Formation with redbeds and some acidic tuffs in basal portions monitors a gradual transition into semi-arid climatic conditions.

The Pfannock sequence at the westernmost sectors of the Gurktal nappe complex is partly overturned and is interpreted to represent a detached portion of the Stolzalpe nappe. There, the cover sequence is deposited on the Pfannock gneiss, a Silurian or Devonian acidic orthogneiss. The cover sequence on top of it range from Permian to Late Triassic. It includes the Permian Bock Breccia, the Skythian Werfen Fm., the Anisian Pfannock Fm., the Anisian-Ladinian Wetterstein Dolomite, and the Late Triassic Hauptdolomite and Kössen Formations. A detrital white mica age of ( $317.6 \pm 0.6$  Ma) from the Pfannock Fm. constrain a Variscan source region of this succession.

The Krappfeld Gosau is laid down on tilted and partly eroded Triassic cover sequences along eastern margins of the Gurktal nappe complex. It comprises a Late Santonian to lower Late Maastrichtian sequence (Neumann, 1989) with basal reef limestone and later marls and olistolitic beds (Thiedig, 1975). The Gosau is interpreted to represent a collapse basin on top of exhuming overthickened continental crust.

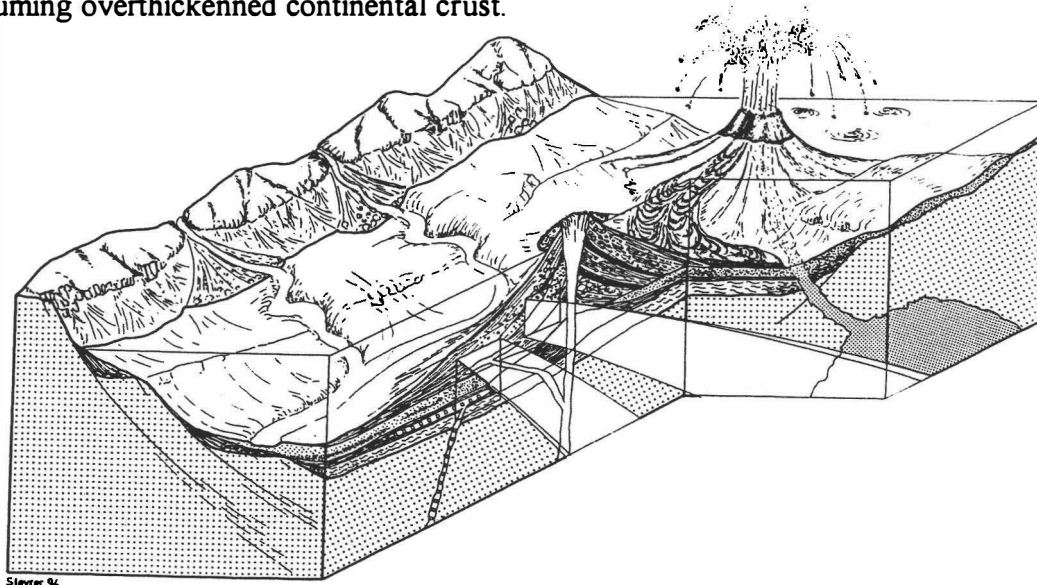


Fig. 2. Sketch showing Silurian paleogeography of the Stolzalpe nappe (from Antonitsch-Genser et al., in prep.).



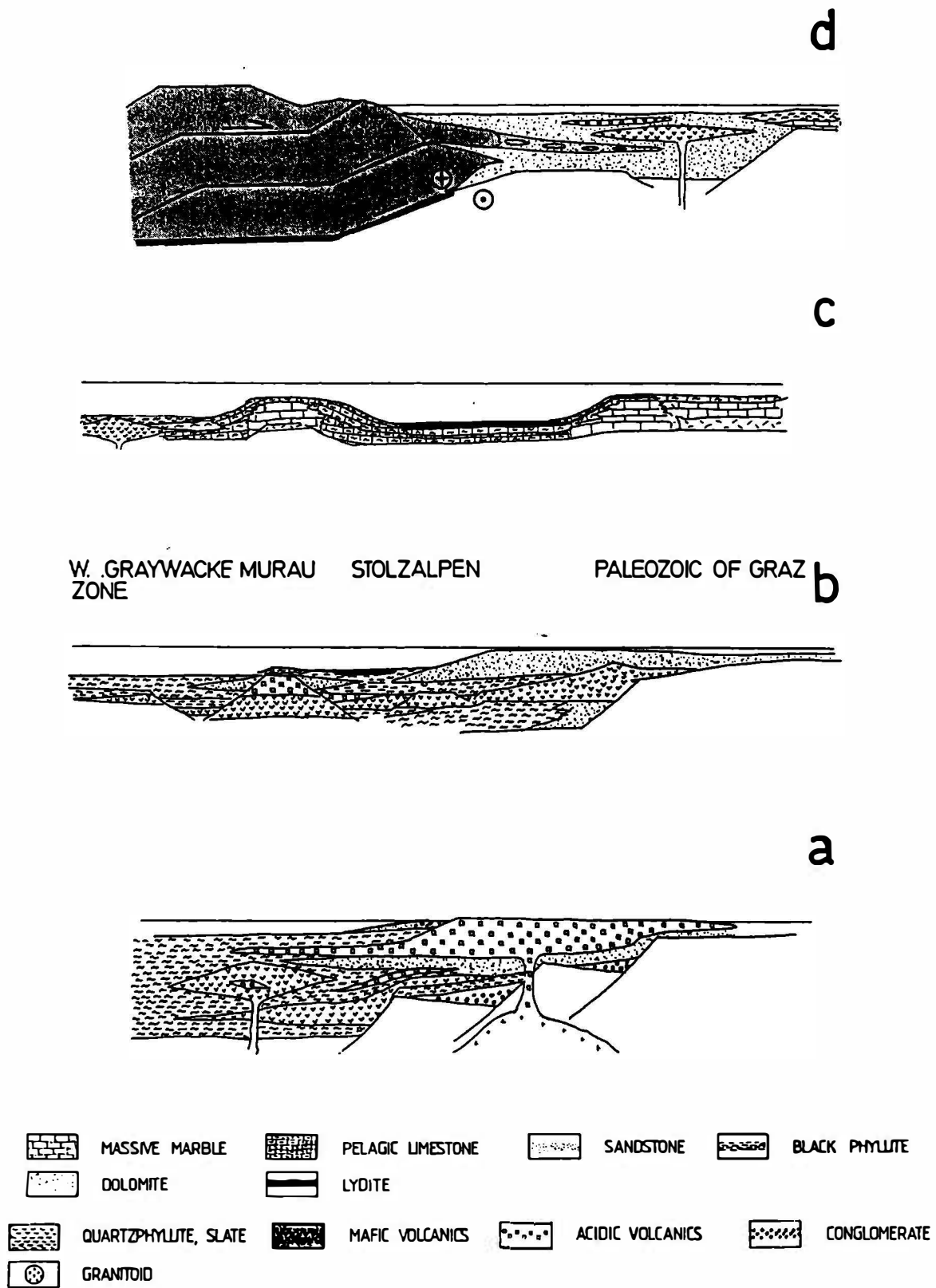


Fig. 3. Evolution of Upper Austroalpine units including sequences exposed within the Stolzalpe nappe during the Paleozoic. a - Late Ordovician; b - Late Silurian to Lower Devonian; c - Late Devonian to Early Carboniferous; d - late Early Carboniferous.

## New Ar-Ar ages

New  $^{40}\text{Ar}/^{39}\text{Ar}$  ages measured from 2-5 white mica grains have been prepared at the Salzburg Ar-Ar Laboratory. These new ages include (Fig. 4): 1) A plateau age of  $89.0 \pm 0.6$  Ma from metamorphic sericite (sample FN-G-3) from a Skythian quartzite at the stratigraphic base of the Stangalm Mesozoic sequence. It is interpreted to represent the age of cooling through appropriate Ar retention temperatures (ca.  $350\text{-}400^\circ\text{C}$ ) during exhumation of this sequence. 2) A disturbed Cretaceous-age pattern from a further sample (FN-G-1) from hangingwall portions from the Skythian Quartzite. 3) Detrital white mica from the Pfannock Formation (FN-G-14) at the northern slope of Pfannock yielded a plateau-type Variscan age ( $317.6 \pm 0.6$  Ma). This age is interpreted to constrain the cooling through ca.  $350\text{-}400^\circ\text{C}$  in the source region in the hinterland.

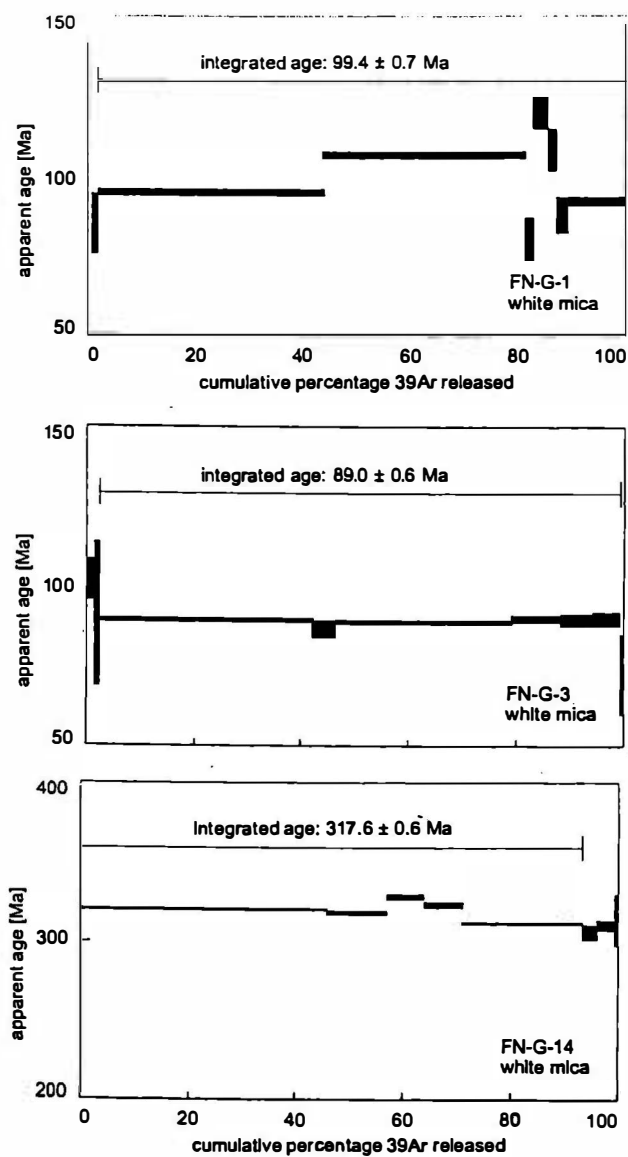


Fig. 5:  $^{40}\text{Ar}/^{39}\text{Ar}$  ages from the basal, Skythian Quartzite (samples FN-G-1, FN-G-3) and detrital white mica from the Pfannock Formation (sample FN-G-14).

## Structural investigations

Two sets of structures have been observed in all tectonic units (along the Radenthein - Patergassen section; Fig. 5): (1) penetrative ductile structures that formed within peak and/or retrogressive metamorphic conditions; and (2) late-stage brittle structures that overprinted the earlier ones.

Lithologies of the upper portions of the Radenthein Micaschist Complex show a flat-lying, NE-dipping, penetrative foliation and an associated ESE-plunging stretching lineation (Fig. 2). These rocks generally are well-recrystallized and do not show retrogression.

Paragneisses and micaschists of the Bundschuh nappe as well as marbles of the Stangalm group also include a gently NE-dipping penetrative foliation and an associated E- to ESE-plunging stretching lineation. The foliation of the Murau and Stolzalpe nappes gently dips N to NE, while the associated stretching lineation trends mostly E (Fig. 6). The foliation of phyllitic rocks within the Murau nappe is penetrative, closely spaced, and comprises fine ribbon quartz and sericitic layers. Shear bands are common within phyllitic lithologies and indicate E- to ESE-directed shear. The penetrative foliation is refolded into open, upright NNE-plunging folds that also contain a widely spaced axial surface foliation. Subvertical N-trending tension gashes are common within the Murau nappe. They indicate approximately E-W oriented, (sub)horizontal extension. Both, open upright folds and steep tension gashes also occur within the Bundschuh nappe.

Mesoscale faults and striae are common both in upper portions of the Bundschuh nappe and in the Murau nappe (Fig. 7). In general, these are dominated by a conjugate set of ENE respectively NW-dipping normal faults. Resulting paleostress orientation patterns indicate a subvertical orientation of  $\sigma_1$  and a subhorizontal WNW trending  $\sigma_3$  direction due to WNW-ESE stretching of rocks (Fig. 7).

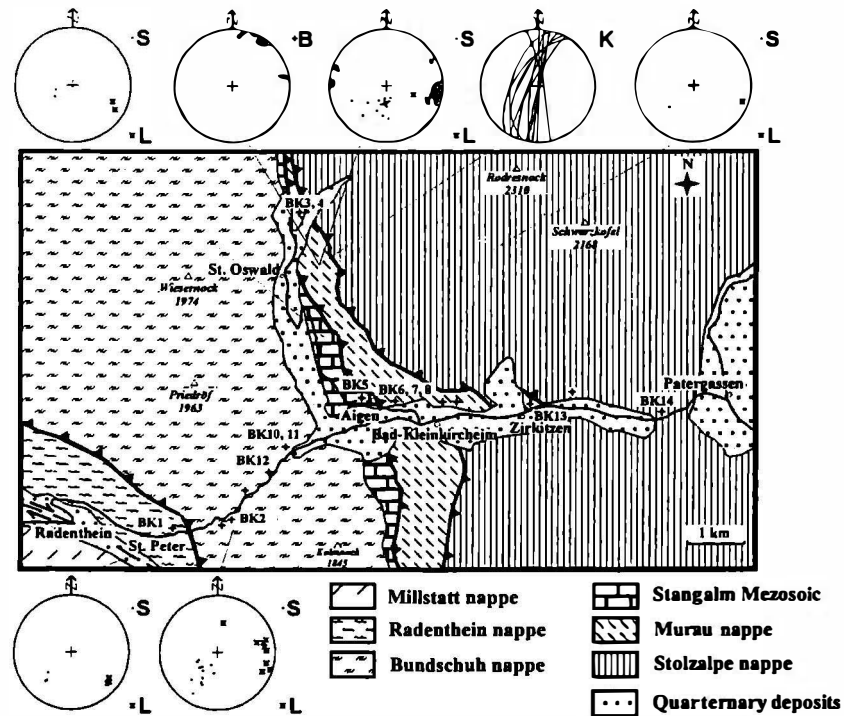


Fig. 6. Simplified structural map of the investigated area with outcrop localities and showing the main structural elements. Location is shown on Fig. 1b. Legend: S - foliation, L - stretching lineation, B - fold axis, K- tension gash. Lambert projection, lower hemisphere.

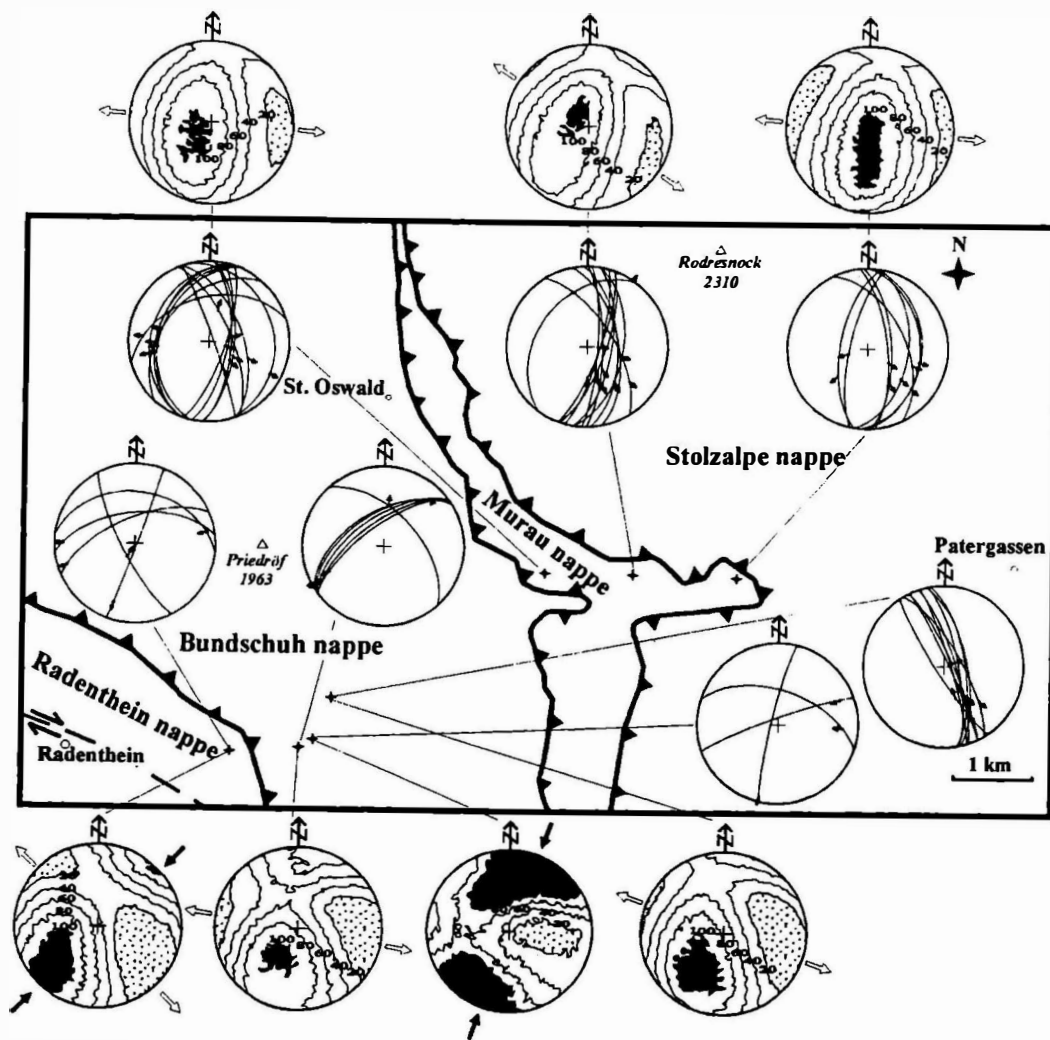


Fig. 7. Orientations of faults and striae and deduced paleostress orientations. Lambert projection, lower hemisphere. Legend of paleostress projections: Black - possible maximum principal stress orientation; stippled - possible minimum principal stress orientation.

## Microfabrics and textures

Quartz c-axis patterns of some lithologies from the Radenthein micaschist complex usually display a small circle distribution around the Y direction (Fig. 8). Rotated  $\sigma$ -porphyroclasts of garnet and intrafolial folds show top-to-the W transport. The orientation of tensional fractures between garnet fragments indicates ca. ESE-WNW orientated stretching. Crenulation of the foliation can be observed, too.

Rocks of the Bundschuh Complex are well-recrystallized and annealed, and do not contain a preferred orientation of quartz c-axes (Fig. 8). Well-developed shear indicators are missing here.

In the Murau nappe, sample BK3 a very well-developed quartz mylonite, shows a prominent preferred quartz c-axis orientation. Shear bands and S-C fabrics, indicating top to the ESE shear, are common within this type of mylonite. For other studied rocks (samples BK6, 8, and 14 from Murau and Stolzalpe nappes) no preferred quartz c-axis orientation could be observed (Fig. 8). Shear bands and asymmetrical pressure shadows around garnets are also characteristic for the Murau nappe. Occasionally, normal slip crenulation and asymmetrical foliation boudinage occur as well. These indicate mostly top-to-the E to ESE transport. Boudinaged white mica indicates E-W stretching, too.

Grain boundaries of quartz layers and lenses of rocks exposed within the Murau nappe are dentate to lobate in most cases, recording that deformation occurred after the thermal peak of the metamorphism. Elongated grains, undulose extinction, deformation lamellae and mortar texture also record strong deformation after peak metamorphic conditions. However, well-equilibrated grain boundaries are also present in some samples. These are interpreted to represent remnants of an earlier stage and suggest strain partitioning within the Murau nappe during the last deformation stage. Feldspar and garnets often appear as rigid porphyroclast (0.2-0.7 mm) with pressure shadows in rocks of the Murau nappe, but also small (0.01-0.1 mm) well-recrystallized grains, often with strain-free optical properties can be observed.

These relationships suggest that rocks of Bundschuh nappe are mostly annealed. In contrast, quartz of rocks from the Murau nappe is heavily deformed under low temperature

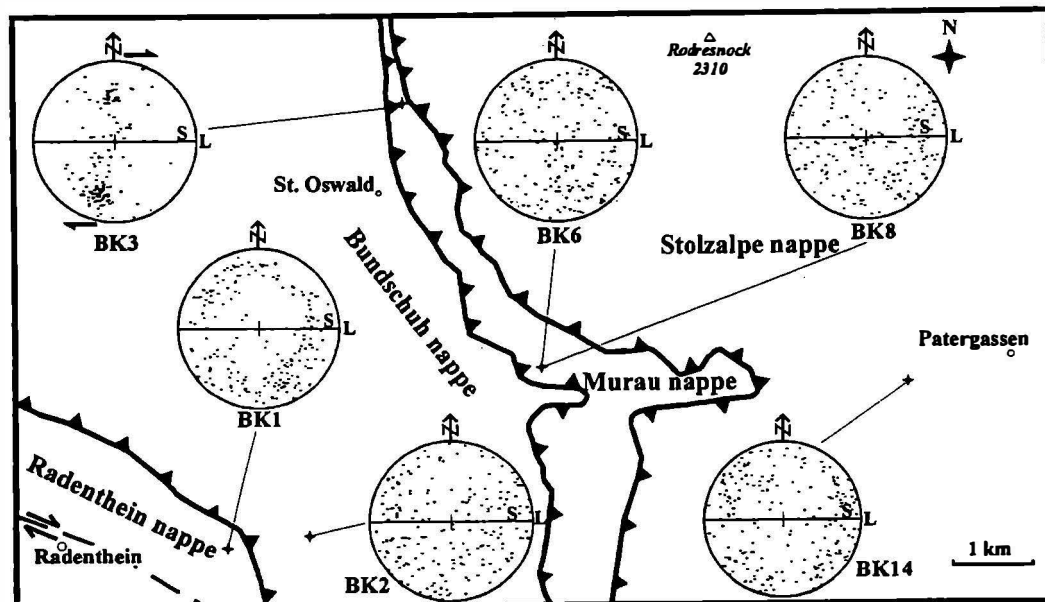


Fig. 8: Quartz c-axis patterns from the Radenthein - Pattergassen section.

## Petrological investigations

Metamorphic conditions were determined on the basis of equilibrium mineral parageneses in each tectonostratigraphic unit, concentrating - first of all - on the Middle Austroalpine crystalline basement (Radenthein and Bundschuh nappes). Garnet is a characteristic metamorphic mineral in these rocks and therefore numerous profiles were measured from several locations and tectonic units. Representative garnet profiles are shown in Fig. 10. We applied Tweek (Berman, 1991) (Fig. 9) and Thermocalc programs (Powell and Holland, 1988) for the calculation of P-T conditions, using also the calibrations of KLEEMANN and REINHARDT (1994), HOISCH (1991) and HODGES and CROWLEY (1985), respectively, on mineral assemblages which are in textural equilibrium. The solid solution models used for Tweek where from Berman (1990) for garnet, from Furmann and Lindsley (1988) for feldspar, from Chatterjee and Froese (1975) for mica, and from McMullin et al. (1991) for biotite. As examples, results of P-T estimates using the calibrations of KLEEMANN and REINHARDT (1994), HOISCH (1991) and HODGES and CROWLEY (1985) for chemical compositions presented in Table 1.

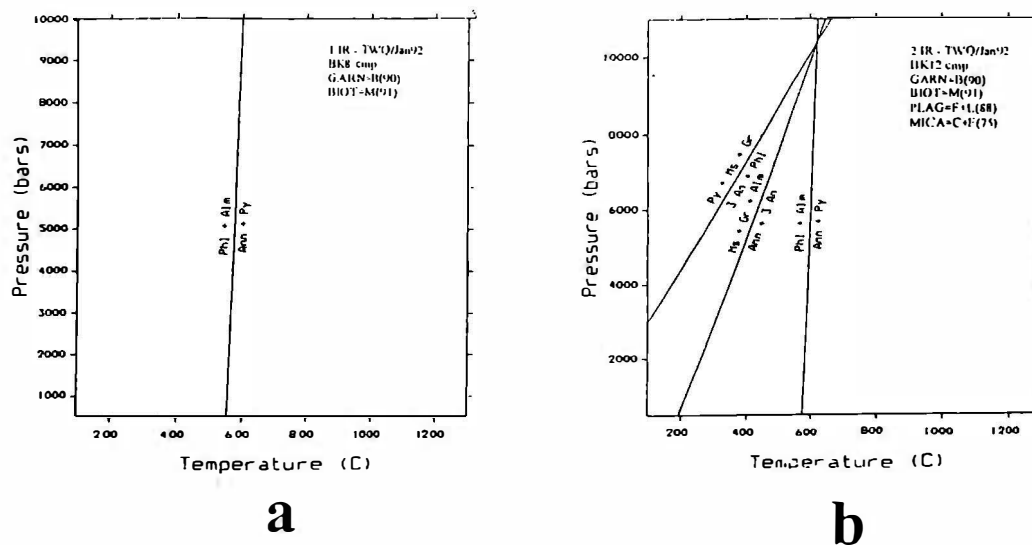


Fig. 9. Representative examples of thermobarometric results with the Tweek program. a - BK8: Garnet-biotite thermometry, b - BK12: garnet-biotite-muscovite-plagioclase thermobarometry.

Tab. 1. Overview on P-T estimates of samples collected from Radenthein and Bundschuh nappes. The P-T estimates using geothermometers and geobarometers of KLEEMANN and REINHARDT (1994), HOISCH (1990) and HODGES and CROWLEY are listed for representative mineral compositions.

Sample	BK1	BK2	BK10	BK11	BK12
Tweeku	600 °C, 11 kbar	600 °C, 9.8 kbar	600 °C, 10.3 kbar	580 °C, 9.7 kbar	630 °C, 10.3 kbar
Thermocalc	627 ± 117 °C 11.2 ± 2.6 kbar	632 ± 27 °C 10.2 ± 1.1 kbar	675 ± 43 °C 12.1 ± 1.6 kbar	631 ± 28 °C 12.7 ± 1.0	642 ± 27 °C 10.6 ± 1.1 kbar
garnet-biotite Kleemann and Reinhardt, 1994	604 °C	597 °C	593 °C	578 °C	607 °C
Hoisch, 1990		10.6-10.7 kbar	11.1 kbar	10.3 kbar	11.5 kbar
Hodges & Crowley, 1985		10.3 kbar	10.5 kbar	9.8 kbar	10.7 kbar

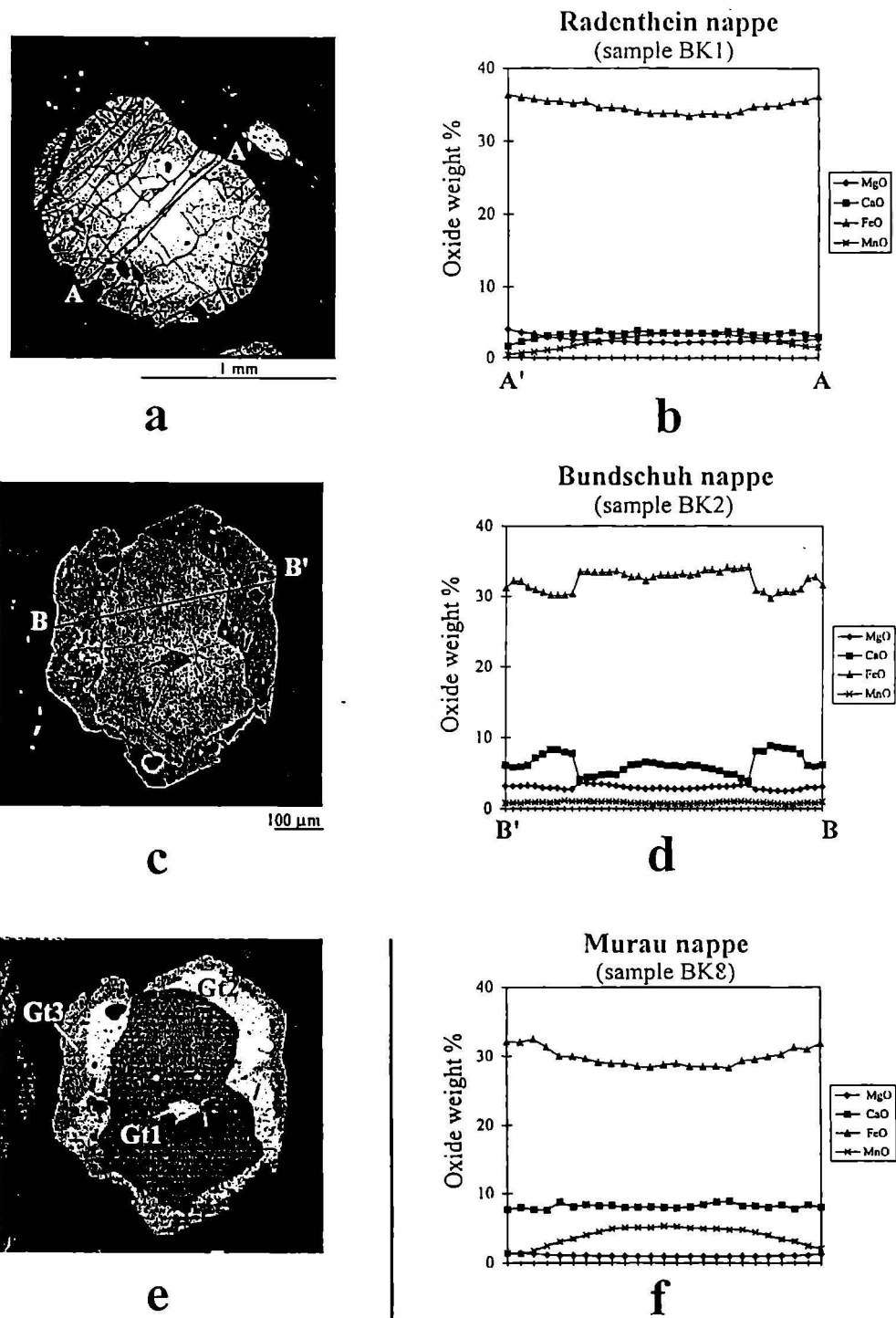


Fig. 7. Representative chemical composition of garnet from the Radenthein, Bundschuh and Murau nappes. a - Back-scattered electron image of garnet in BK1 (Radenthein nappe). No core-rim structure is developed. b - Element distribution in BK1. Length of section line is shown in Fig. 7a. c - Back-scattered electron image of garnet in BK2 (Bundschuh nappe). Note the characteristic core-rim structure. d - Element distribution in BK2. Section line is shown in Fig. 7c. e - relative intensity distribution for Ca- $K_{\alpha}$  X-ray line in the same grain. Note the three garnet generations. f - Element distribution in BK8. Length of section line is ca. 4.5 mm, analyzed grain is not shown. Murau nappe.

## Discussion of the Cretaceous tectonic evolution

Geochronological data constraining the age of the metamorphic event(s) of investigated tectonic units were published by Frimmel, 1986a, Schimana, 1986, and Hawkesworth, 1976. The minimum age of metamorphism in the Radenthein nappe is about 88-84 Ma according to Rb/Sr small scale whole rock and mineral isochrons. K/Ar data record an Alpine age in the Radenthein and Bundschuh (Priedröf) nappes mostly in the range of 70-110 Ma. The muscovite K/Ar age from Stangalm Mesozoic cover rocks is about 70 Ma (Schimana, 1986). Bundschuh gneiss samples from sites W of Turrach (Fig. 1b) Nappe have given ages of 363 to 403 Ma (Rb/Sr whole rock isochrons) which were interpreted as mixed Caledonian-Variscan protolith ages (Frimmel, 1986a, b). Rb/Sr muscovite ages also indicate an early Variscan event (350-354 Ma) within these rocks. In orthogneisses deformed intensively during the Cretaceous metamorphism Rb/Sr mineral ages (muscovite, feldspar) are variably reset to 119 to 91 Ma (Frimmel, 1986a, b). According to these data, the Radenthein and Bundschuh tectonic units were strongly affected by Cretaceous metamorphism, while pre-Alpine metamorphism is restricted to the Bundschuh basement.

The results of the thermobarometric calculations with the two different programs (Tweeq and Thermocalc) are roughly in agreement. Based on these data, the Alpine metamorphic conditions are estimated in the Middle Austroalpine crystalline basement (Radenthein and Bundschuh nappes) to be around 600°C and 10-11 kbar. These values mean upper epidote-amphibolite facies conditions within the stability field of kyanite, although it was not observed in the investigated rocks (because of the Al-poor bulk composition). However, kyanite and staurolite are found in the surrounding area in the Radenthein nappe (kyanite-garnet micaschist with the local name "Radentheinit"; e.g., Schimana, 1986). The estimated pressure suggests that these rocks were at a depth of ca. 35 km during the Cretaceous metamorphic event. This depth nearly corresponds to the base of continental crust with a normal thickness.

Among the Middle Austroalpine units two types can be identified (see also Schimana, 1986): The Radenthein nappe was affected by one (Alpine) metamorphism only, while in the Bundschuh nappe two regional (Alpine and a pre-Alpine, probably Variscan) metamorphic events are recorded. Moreover, chemical zonation (with an inner and outer garnet-rim) suggests two stages within the Alpine metamorphism. The very CaO-rich inner zone of the Alpine rim in the garnets may indicate earlier, higher pressure metamorphic conditions than the outer, Ca-poorer, zone. The albite-rich core of the zoned plagioclases may be correlated with the above mentioned inner zone; because of the absence of minerals in equilibrium, P-T conditions could not be calculated, however.

The Variscan metamorphic conditions are less clear in the investigated rocks, because pre-Alpine relict minerals apart from the Fe-rich cores of the garnets were not preserved. The element distribution in the almandine-rich cores indicates a progressive metamorphism at least in the case of sample BK2. The homogeneous element distribution in garnet-cores of sample BK10 may indicate a complete rehomogenization during the pre-Alpine metamorphic event. This would mean that garnets grew before the thermal peak of the pre-Alpine metamorphism which had to reach temperatures of at least 650°C. The pseudomorphs containing paragonite are probably after staurolite, which is also wide-spread and well-preserved in surrounding and northwestern areas in the Bundschuh nappe (e.g., Schimana, 1986). This suggests at least upper epidote-amphibolite facies conditions for the pre-Alpine metamorphism.

Common mineral assemblages (quartz, muscovite, chlorite, albite ± garnet, biotite, epidote, clinozoisite, calcite, dolomite) in the Gurktaler phyllite (Murau nappe, samples BK3, 4, 6, 7, 8 and 13) and in the meta-arkose (Stolzalpe nappe, BK14) suggest greenschist facies metamorphic conditions within the Upper Austroalpine units. Von Gosen et al. (1987) found,



based on illite crystallinity studies, very low grade to low grade metamorphic conditions within the Stolzalpe nappe exposed immediately to the north of the study area. Conodont color alteration and conodont surface recrystallization studies indicate similar conditions (Neubauer and Friedl, 1997), in agreement with the presence of anthracite in Late Carboniferous cover sequences (Rantitsch and Russegger, in prep.). A reasonable estimate for temperature conditions within the Stolzalpe nappe is, therefore, ca.  $325 \pm 50^\circ\text{C}$  (Frey, 1987; Kisch, 1987).

Metamorphic conditions within the Murau nappe were calculated with the calcite-dolomite thermometer (Anovitz and Essene, 1987; Dachs, 1990) which gives ca.  $460\text{-}500^\circ\text{C}$  (BK13) and with garnet-biotite equilibria (BK8) yielding ca.  $550\text{-}600^\circ\text{C}$ . Calcite-dolomite microfabrics are obviously associated with extensional deformation, indicating re-equilibration of calcite-dolomite mineral assemblages. The age of the metamorphism in the Murau nappe is rather uncertain, no geochronological data are available in the investigated area yet. We consider a pre-Alpine age of peak conditions of metamorphism recorded by garnet-biotite equilibria because these are constrained within garnet porphyroclast (first stage of textural evolution) which are overprinted by a second-stage tectonothermal event within greenschist facies conditions. The second stage including the calcite-dolomite equilibria is considered to represent the Alpine metamorphic overprint. Similar polyphase fabrics were also reported from other regions of the Murau nappe (von Gosen, 1989, and references cited therein).

A break in metamorphic isogrades obviously coincides with the lower low angle normal fault boundary of the Gurktal nappe complex. It appears, furthermore, that the entire Murau nappe along the western margins of the Gurktal nappe complex is thinned out extremely (to minimum several tens of metres) along the east-directed ductile low angle normal fault. Further local evidence of east-directed motion has already been provided by Neubauer (1987), Ratschbacher and Neubauer (1989), Stock (1989; 1992), and Ratschbacher et al. (1990) always recorded from basal sectors of the Gurktal nappe complex. Therefore, the entire Gurktal nappe complex represents an extensional allochthon. Middle Austroalpine footwall units are entirely annealed and recrystallized within a distance of several hundreds of metres in the footwall of the basal tectonic contact of the Gurktal nappe complex.

In summary, the data presented above suggest the following Cretaceous tectonic history of Austroalpine units along western margins of the Gurktal nappe complex: Middle Austroalpine continental units were buried during Cretaceous contraction to depths close to the base of continental crust (35 km). In contrast, the Murau and Stolzalpe nappes remained at middle to upper crustal levels (Fig. 10a). The direction of nappe stacking is not evidenced from our data except some weak indications of westward rotation recorded in garnets of the Radenthein nappe. Later on, a crustal-scale, east-directed, ductile low angle normal fault developed at the upper margin of the Bundschuh nappe probably reactivating older thrust surfaces. A late stage brittle normal fault has already been described by Clar (1965) along this contact. Mineral cooling ages of 84-80 Ma from Bundschuh and Radenthein nappes (Hawkesworth, 1976; Schimana, 1986; Frimmel, 1986a, b) are contemporaneous with sediment deposition within the Late Cretaceous (Krappfeld) Gosau basin (van Hinte, 1963; Thiedig, 1975) on top of the Stolzalpe nappe along the eastern margin of the present exposure of the Gurktal nappe complex (Fig. 1b).

The tectonic scenario derived from these investigations in the Gurktal nappe complex is similar to that described from other regions of the Austroalpine nappe complex exposed east and west of the Tauern window, where east-directed Late Cretaceous syn-Gosau normal faulting is recorded (e.g., Neubauer and Genser, 1990; Ratschbacher et al., 1991; Froitzheim et al., 1994, 1997; Neubauer et al., 1995; Handy, 1996).

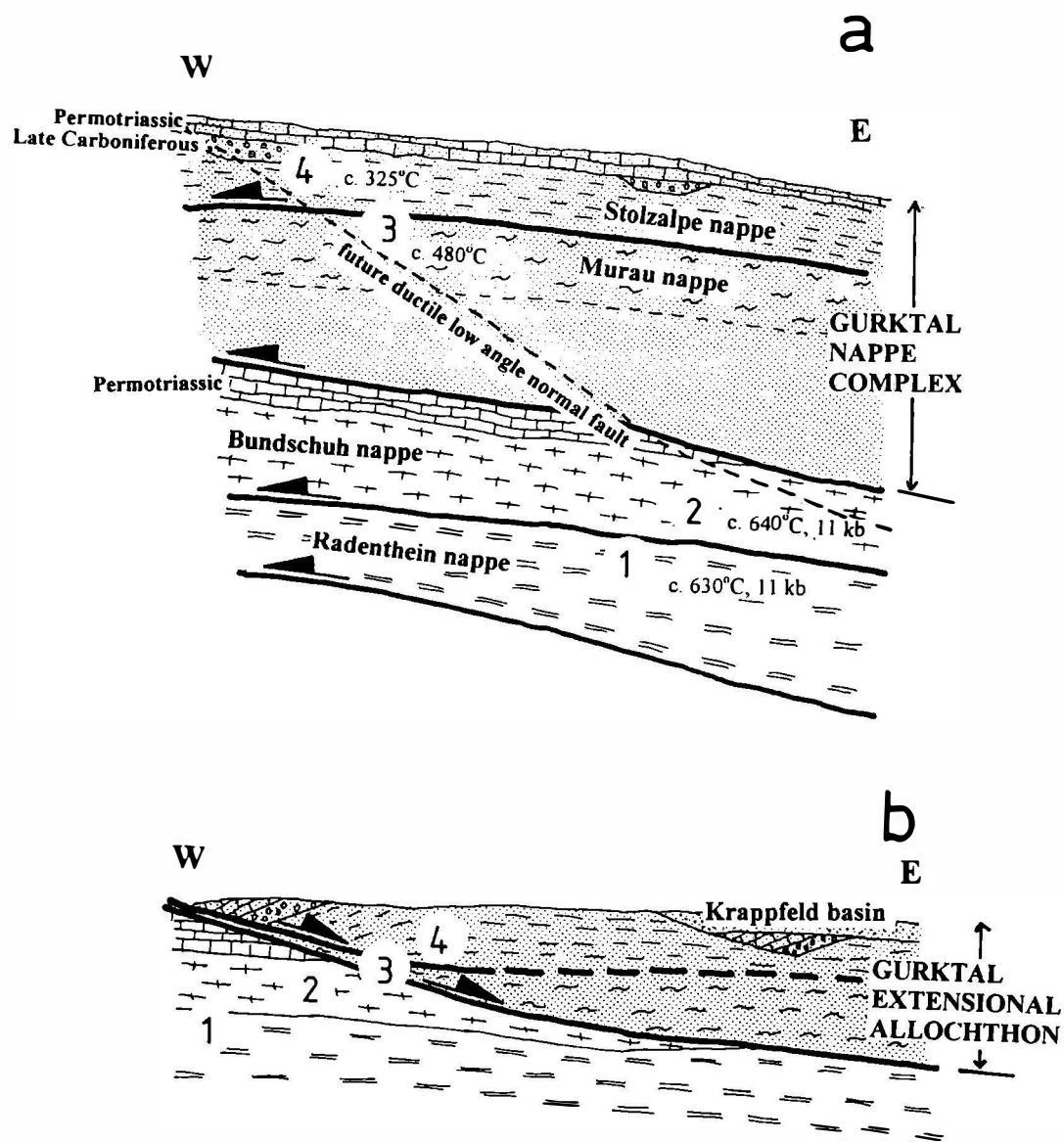


Fig. 5. Models of the tectonic evolution along the western margin of the Gurktal nappe complex. A - Nappe stacking at the stage of maximum peak metamorphic conditions in the Bundschuh and Radenthein nappes. B - Stage after extension by east-directed, ductile, low-angle normal faulting. 1 - 4 represent suggested locations with Cretaceous peak metamorphic conditions (A) and post-extensional locations (B) within all four investigated structural units.

#### References

- Angelier, J. and Mechler, P. (1977): Sur une méthode graphique de recherche des contraintes principales également utilisable en tectonique et en séismologie: la méthode des dièdres droits. Bull. Soc. Géol. France, VII, 19, 1309-1318; Paris.
- Anovitz, L.M. and Essene, E.J. (1987): Phase equilibria in the system  $\text{CaCO}_3\text{-MgCO}_3\text{-FeCO}_3$ . J. Petr., 28, 389-414.

- Antonitsch, W. and Neubauer, F. (1992): Altpaläozoischer alkalischer Riftvulkanismus und kretazische Imbrikation in der westlichen Gurktaler Decke, Ostalpen. *Frankf. Geowiss. Abh.*, A11, 15-18.
- Berman, R.G. (1990): Mixing properties of Ca-Mg-Fe-Mn garnets. *Am. Miner.* 75, 328-344.
- Berman, R.G. (1991): Thermobarometry using multi-equilibrium calculations: A new technique with petrological applications. *Can. Mineral.*, 29, 833-855.
- Chatterjee, N.D. and Froese, E. (1975): A thermodynamic study of the pseudo-binary join muscovite-paragonite in the system  $KAlSi_3O_8$ - $NaAlSi_3O_8$ - $Al_2O_3$ - $SiO_2$ - $H_2O$ : new phase equilibria data, some calculated phase relations, and their petrological applications. *Contrib. Mineral. Petrol.*, 88, 1-13.
- Choukroune, P., Gapais, D. and Merle, O. (1987): Shear criteria and structural symmetry. *J. Struct. Geol.*, 9: 525-530.
- Clar, E. (1965): Zum Bewegungsbild des Gebirgsbaues der Ostalpen. *Z. Deutsch. Geol. Ges.* 116, 267-291.
- Dachs, E. (1990): Geothermobarometry in metasediments of the southern Grossvenediger area (Tauern Window, Austria). *J. Met. Geol.*, 8, 217-230.
- Dallmeyer, R. D., Neubauer, F., Handler, R., Fritz, H., Müller, W., Pana, D. and Putis, M. (1996): Tectonothermal evolution of the internal Alps and Carpathians: Evidence from  $^{40}Ar/^{39}Ar$  mineral and whole-rock data. *Eclogae geol. Helv.* 89, 203-227.
- Dallmeyer, R.D., Handler, R., Neubauer, F. and Fritz, H. (1998): Sequence of thrusting within a thick-skinned tectonic wedge: evidence from  $^{40}Ar/^{39}Ar$  and Rb-Sr ages from the Austroalpine nappe complex of the Eastern Alps. *J. Geol.*, 106, 71-86.
- Ehlers, K., Stüwe, K., Powell, R., Sandiford, M. and Frank, W. (1994): Thermometrically inferred cooling rates from the Plattengneis, Koralm region, Eastern Alps. *Earth Planet. Sci. Lett.*, 125, 307-321.
- England, P.C. and Thompson, A.B. (1984): Pressure-temperature-time paths of regional metamorphism. Part I: Heat transfer during the evolution of regions of thickened continental crust. *J. Petrol.*, 25, 894-928.
- Frank, W. (1987): Evolution of the Austroalpine elements in the Cretaceous. In: Flügel, H.W., and Faupl, P., eds., *Geodynamics of the Eastern Alps*. Deuticke, Wien, p. 379-406.
- Frey, M. (1987): Very low-grade metamorphism of clastic sedimentary rocks. In: Frey, M., ed., *Low temperature metamorphism*. Chapman and Hall, New York, pp. 9-58.
- Frimmel, H. (1986a): Petrographie, Gefügemerkmale und geochronologische Daten von Kristallingeröllen aus dem Oberkarbon der Gurktaler Decke im Vergleich zum benachbarten Altkristallin. *Mitt. Ges. Geol. Bergbaustud. Österr.*, 32, 39-65.
- Frimmel, H. (1986b): Isotopengeologische Hinweise für die paläogeographische Nachbarschaft von Gurktaler Decke (Oberostalpin) und dem Altkristallin östlich der Hohen Tauern (Österreich). *Schweiz. Mineral. Petrogr. Mitt.*, 66, 193-208.
- Frimmel, H. (1988): Metagranitoide am Westrand der Gurktaler Decke (Oberostalpin) - Genese und paläotektonische Interpretation. *Jb. Geol. Bundesanst.*, 131, 575-592.
- Froitzheim, N., Schmid, S.M. and Conti, P. (1994): Repeated change from crustal shortening to orogen-parallel extension in the Austroalpine units of Graubünden. *Eclogae Geol. Helv.*, 87, 559-612.
- Froitzheim, N., Schmid, S.M. and Frey, M. (1996): Mesozoic paleogeography and the timing of eclogite-facies metamorphism in the Alps: A working hypothesis. *Ecl. Geol. Helv.*, 89, 81-110.
- Froitzheim, N., Conti, P. and van Daalen, M. (1997): Late Cretaceous, synorogenic, low-angle normal faulting along the Schlinig fault (Switzerland, Italy, Austria) and its significance for the tectonics of the Eastern Alps. *Tectonophysics*, 280, 267-293.
- Fuhrman, M.L. and Lindsley, D.H. (1988): Ternary feldspar modeling and thermometry. *Am. Mineral.*, 73, 201-215.
- Giese, U., 1987. Altpaläozoischer Vulkanismus am NW-Rand der Gurktaler Decke. – Geologie, Petrologie, Geochemie - Unpubl. PHD-thesis, University of Tübingen, p.227.
- Giese, U., 1988. Lower Paleozoic volcanic evolution at the northwestern border of the Gurktal nappe Upper Austroalpine eastern Alps. *Schweiz. Mineral. Petrogr. Mitt.* 68: 381-396.
- Gosen, W. von (1982): Geologie und Tektonik am Nordostrand der Gurktaler Decke (Steiermark/Kärnten - Österreich). *Mitt. Geol.-Paläont. Inst. Univ. Hamburg*, 53, 33-149.

- Gosen, W. von (1989): Gefügeentwicklungen, Metamorphosen und Bewegungen der ostalpinen Baueinheiten zwischen Nockgebiet und Karawanken (Österreich). *Geotekt. Forsch.*, 72, 1-247
- Gosen, W. von, Pistotnik, J. and Schramm, J.M. (1987): Schwache Metamorphose in Gesteinsserien des Nockgebietes und im Postvariszikum des Karawankenvorlandes (Ostalpen, Kärnten). *Jb. Geol. Bundesanst.*, 130, 31-36.
- Handy, M.R. (1996): The transition from passive to active margin tectonics: a case study from the zone of Samedan (Eastern Switzerland). *Geol. Rundsch.*, 85, 832-851.
- Hawkesworth, C.J. (1976): Rb/Sr Geochronology in the Eastern Alps. *Contrib. Min. Petr.*, 54, 225-244.
- Hodges, K.V. and Crowley, P.D. (1985): Error estimates and empirical geobarometry for pelitic systems. *Am. Mineral.*, 72, 671-680.
- Hoisch, T.D. (1991): Equilibria within the mineral assemblage quartz-muscovite-biotite-garnet-plagioclase and implications for the mixing properties of octohedrally coordinated cations in muscovite and biotite. *Contrib. Mineral. Petrol.*, 108, 43-54.
- Holdhaus, K. (1921): Über die Auffindung von Trias im Königstuhlgebietes in Kärnten. *Anz. Akad. Wiss. Wien, math.-naturwiss. Kl.*, 58, 19-21.
- Kisch, H.J. (1987): Correlation between indicators of very low-grade metamorphism. In: Frey, M., ed., *Low temperature metamorphism*. Chapman and Hall, New York, p. 227-300.
- Kleemann, U. and Reinhardt, J. (1994): Garnet-biotite thermometry revisited: the effect of Al<sup>VI</sup> and Ti in biotite. *Eur. J. Mineral.*, 6, 925-941.
- Krainer, K., 1984. Sedimentologische Untersuchungen an permischen und untertiradischen Sedimenten des Stangalm-Mesozoikums (Kärnten/Österreich). *Jahrb. Geol. Bundesanst.*, 127: 159.179.
- Krainer, K., 1989a. Molassesedimentation im Oberkarbon der Ostalpen am Beispiel der Stangnock Formation am NW-Rand der Gurktaler Decke (Österreich). *Zentralbl. Geol. Paläont. Teil 1*, 1988, H. 7/8: 807-820.
- Krainer, K., 1989b. Die fazielle Entwicklung der Oberkarbonsedimente (Stangnock Formation) am NW-Rand der Gurktaler Decke. *Carinthia II*, 179/99:563-601.
- Loeschke, J., 1989. Lower Paleozoic volcanism of the Eastern Alps and its geodynamic implications. *Geol. Rdsch.*, 78: 599-616.
- McMullin, D.W.A., Berman, R.G. and Greenwood, H.J. (1991): Calibration of the SGAM thermobarometer for pelitic rocks using data from phase-equilibrium experiments and natural assemblages. *Can. Miner.*, 29, 889-908.
- Miller, C. (1990): Petrology of the type locality eclogites from the Koralpe and Saualpe (Eastern Alps), Austria. *Schweiz. Mineral. Petrogr. Mitt.*, 70, 287-300.
- Neubauer, F. (1980): Zur tektonischen Stellung des Ackerlkristallins (Nordrand der Gurktaler Decke). *Mitt. Österr. Geol. Ges.*, 73, 39-53.
- Neubauer, F. (1987): The Gurktal Thrust System within the Austroalpine region - some structural and geometrical aspects. In: Flügel, H.W. and Faupl, P., eds., *Geodynamics of the Eastern Alps*. Deuticke, Wien, p. 226-236.
- Neubauer, F., ed., (1992): *ALCAPA Field Guide - The eastern Central Alps of Austria*. 245 p., IGP/KFU Graz.
- Neubauer, F. (1994): Kontinentalkollision in den Ostalpen. *Geowissenschaften*, 12, 136-140.
- Neubauer, F. and Friedl, G. (1997): Conodont preservation within the Gurktal nappe complex, Eastern Alps. *Zentralbl. Geol. Paläont. Teil II*, 1997, 277-289.
- Neubauer, F. and Pistotnik, J. (1984): Das Altpaläozoikum und Unterkarbon des Gurktaler Deckensystems (Ostalpen) und ihre paläogeographischen Beziehungen. *Geol. Rundsch.*, 73, 149-174.
- Neubauer, F. and Sassi, F.P., 1993: The quartzphyllite and related units of the Austro-Alpine domain. - In: Raumer, J.von and Neubauer, F., eds., *Pre-Mesozoic Geology in the Alps*. Berlin (Springer), 423-439.
- Neubauer, F., Dallmeyer, R.D., Dunkl, I. and Schirnik, D. (1995): Late Cretaceous exhumation of the metamorphic Gleinalm dome, Eastern Alps: kinematics, cooling history and sedimentary response in a sinistral wrench corridor. *Tectonophysics*, 242, 79-98.

- Neumann, H.H., 1989. Die Oberkreide des Krappfeldes. In: T. Appold and F. Thiedig (Editors), Arbeitstagung der Geol. Bundesanst., 1989. Geol. Bundesanst., Wien, pp. 70-79.
- Powell, R. and Holland, T.J.B. (1988): An internally consistent thermodynamic dataset with uncertainties and correlations. III. Application methods, worked examples and a computer program. *J. metamorphic Geol.*, 6, 173-204.
- Rantitsch, G. and Russegger, B. (1998): Thrust-related very low grade metamorphism within the Gurktal nappe complex (Eastern Alps). (submitted).
- Ratschbacher, L. and Neubauer, F. (1989): West-directed decollement of Austro-Alpine cover nappes in the eastern Alps: geometrical and rheological considerations. *Geol. Soc. Spec. Publ.*, 45, 243-262.
- Ratschbacher, L., Frisch, W., Neubauer, F., Schmid, S. M. and Neugebauer, J. (1989): Extension in compressional orogenic belts: The eastern Alps. *Geology*, 17, 404-407.
- Ratschbacher, L., Schmid, S.M., Frisch, W. and Neubauer, F. (1990): Reply on the Comment of S.R. Wallis to "Extension in compressional orogenic belts: the eastern Alps. *Geology*, 18, 675-676.
- Schimana, R. (1986): Neue Ergebnisse zur Entwicklungsgeschichte des Kristallins um Radenthein (Kärnten, Österreich). *Mitt. Ges. Geol. Bergbaustud. Österr.*, 33, 221-232.
- Simpson, C. and Schmid, S.M. (1983): An evaluation of criteria to deduce the sense of movement in sheared rocks. *Geol. Soc. Amer. Bull.*, 94, 1281-1288.
- Stock, P. (1989): Zur antithetischen Rotation der Schieferung in Scherbandgefügen - ein kinematisches Deformationsmodell mit Beispielen aus der südlichen Gurktaler Decke (Ostalpen): *Frankfurter Geowiss. Arb.*, A7, 1-155.
- Stock, P. (1992): A strain model for antithetic fabric rotation in shear band structures. *J. Struct. Geol.*, 14, 1267-1275.
- Thiedig, F. (1975): Submarine Brekzien als Folge von Felsstürzen in der Turbidit-Fazies der Oberkreide des Krappfeldes in Kärnten (Österreich). *Mitt. Geol.-Paläont. Inst. Univ. Hamburg*, 44, 495-516.
- Tollmann, A. (1975): Die Bedeutung des Stangalm-Mesozoikums in Kärnten für die Neugliederung des Oberostalpins in den Ostalpen. *N. Jb. Geol. Paläont. Mh.*, 150, 19-43.
- Tollmann, A. (1977): *Geologie von Österreich. Band 1. Die Zentralalpen.* XVI + 710 p., Vienna (Deuticke).
- Tollmann, A. (1987): The Alpidic Evolution of the Eastern Alps. In: Flügel, H.W. and Faupl, P., eds., *Geodynamics of the Eastern Alps.* Deuticke, Wien, p. 361-378.
- Van Hinte, J.E. (1963): Zur Stratigraphie und Mikropaläontologie der Oberkreide und des Eozäns des Krappfeldes (Kärnten). *Jb. Geol. Bundesanst. Sdbd.*, 8, 1-147.



Carpathian-Balkan Geological Association, XVI Congress	Field Guide "Transect through central Eastern Alps"	pp. 103 - 137	Salzburg - Wien, 1998
--	---	---------------	-----------------------

## Transect through the central Eastern Alps: Description of stops

Johann Genser<sup>1</sup>, Franz Neubauer<sup>1</sup>, Stefan Freimüller<sup>1</sup>, Robert Handler<sup>1</sup>, F. Nemes<sup>1</sup>, H. Polesny<sup>2</sup>, J. Schweigl<sup>1</sup>, Hans-Peter Steyrer<sup>1</sup> and Xianda Wang<sup>1</sup>

<sup>1</sup> Institute of Geology and Paleontology, Paris-Lodron-University of Salzburg, Hellbrunner Str. 34, A-5020 Salzburg, Austria.

<sup>2</sup> RAG AG, Schwarzenbergplatz 16, A-1015 Wien, Austria.

### Introduction

The locations of stops refer to official Austrian maps OEK 50 (scale 1:50,000). A set of copied maps with detailed locations can get received from authors on request.

#### Stop no. 1. Pettenbach, Upper Austria..

**Location:** OEK 50 Grünau. Core storage of the Rag AG at Pettenbach.

For introduction, see H. POLESNY (this volume).

#### Stop no. 2. Rehkogelgraben section S of Hagenmühle. Middle to upper Cretaceous marls of the "Buntmergelserie" (Ultrahelvetic unit)

*Location: ÖK 50, sheet 67 Grünau im Almtal, 13°55' E/ 47°56' N. Creek south of Hagenmühle, situated in the valley of the Dürre Laudach (S of Vorchdorf).*

Description is from follows Egger et al. (1997).

Prey (1952; see Tollmann, 1976; and Plöching, 1983) introduced the term "Buntmergelserie" (variegated coloured marls) for the pelitic rocks of the Ultrahelvetic continental slope. These rocks were deposited from the Albian to the Eocene. Due to increasing water depths to the south the marls were replaced by claystones and might interfinger with thinbedded turbidites and variegated shales of the Rhenodanubian flysch (Egger, 1995). Within the Rhenodanubian flysch a number of tectonic windows with Ultrahelvetic rocks exist. Some of these structures are bound to internal overthrusts within the flysch nappes, others cut the flysch units diagonally. The Rehkogelgraben window belongs to the latter type of structures which were formed by huge, dextral strike-slip faults. The age of these faults is estimated as Oligocene. In the Miocene, ENE-striking sinistral strike-slip faults cut the older NW-striking dextral strike-slip faults. These younger faults terminate the Rehkogelgraben window to the west and to the east (Egger, 1996).

The narrow road and the creek expose steeply south-dipping reddish marls and grey marly limestones of Coniacian to Santonian age. Samples (180 and 181) from the outcrop at

the outer bend of the creek contained well preserved planktonic foraminifers of Santonian age (*Marginotruncana coronata* (BOLLI), *Marginotruncana sinuosa* PORTHAULT, *Marginotruncana marginata* (REUSS), *Marginotruncana paraconcovata* PORTHAULT and *Globotruncana lapparenti* BROTZEN). The Santonian rocks border tectonically to grey marls and highly bioturbated spotted marly limestones of Cenomanian age. Sample 182 contained only badly preserved and small foraminifers: *Hedbergella cf. planispira* (TAPPAN), *Hedbergella cf. delrioensis* (CARSEY), and *Globigerinelloides sp.* In sample 185, *Biticinella breggensis* (GANDOLFI), *Hedbergella planispira* (TAPPAN), *Clavihedbergella subcretacea* (TAPPAN) and *Globigerinelloides sp.* prove the late Albian.

Just beside the small road bridge red marls are exposed along the creek. They are of early Campanian age (*Marginotruncana coronata* (BOLLI), *Marginotruncana marginata* (REUSS), *Globotruncana lapparenti* BROTZEN, *Globotruncana bulloides* VOGLER, *Globotruncana elevata* (BROTZEN)).

### Stop no. 3. Hatscheck quarry near Gmunden. Altlenbach Formation of the Rhenodanubian flysch zone

*Location: OEK 66 Gmunden. Upper levels of the quarry S Pinsdorfberg.*

St. FREIMÜLLER, F. NEUBAUER

The quarry exposes the Ahornleiten member (Maastrichtian) of the Altlenbach Formation of the Rhenodanubian flysch zone (Egger et al., 1997). Grey calcareous marls representing Bouma T<sub>4</sub> are typical for the Ahornleiten member. These marl layers can reach thicknesses up to 8 metres. Together with sandy to silty hardbeds at their base isolated complete turbidites are up to 10 meters thick. The sand/shale ratio is generally low. The southern, stratigraphically higher part of the quarry exposes some altered, greenish ash tuffs, the northern, deeper level altered whitish tuffs intercalated within marls and greywackes.

From a structural point of view, the outcrop exposes a superposed sequence of structures. These structures include: (1) blind thrusts and buckling structures due to bedding-parallel slip; (2) structures related to faults postdating folding and thrusting, e.g. E-W extension (Figs. 1, 2). A complicate sequence of superposed fault patterns can be found in the outcrop (see Fig. 3).

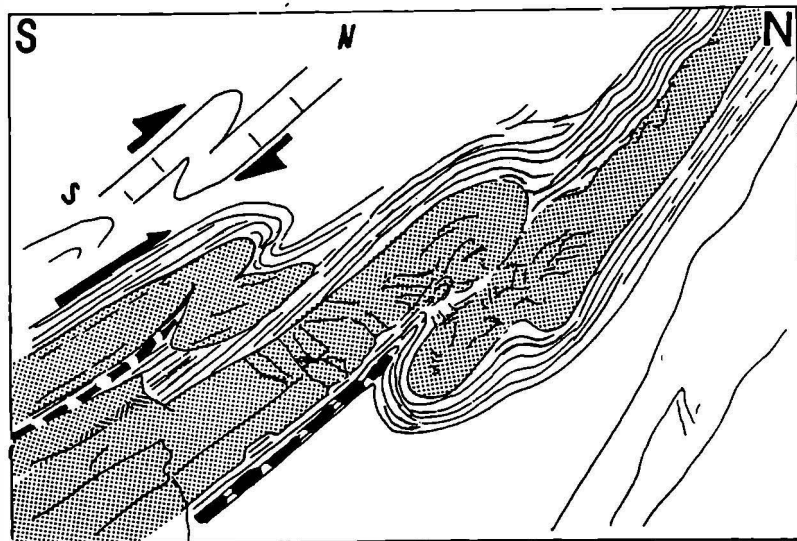


*Fig. 1. Structures related to bedding-parallel slip within the Hatscheck quarry (from Freimüller, 1998).*



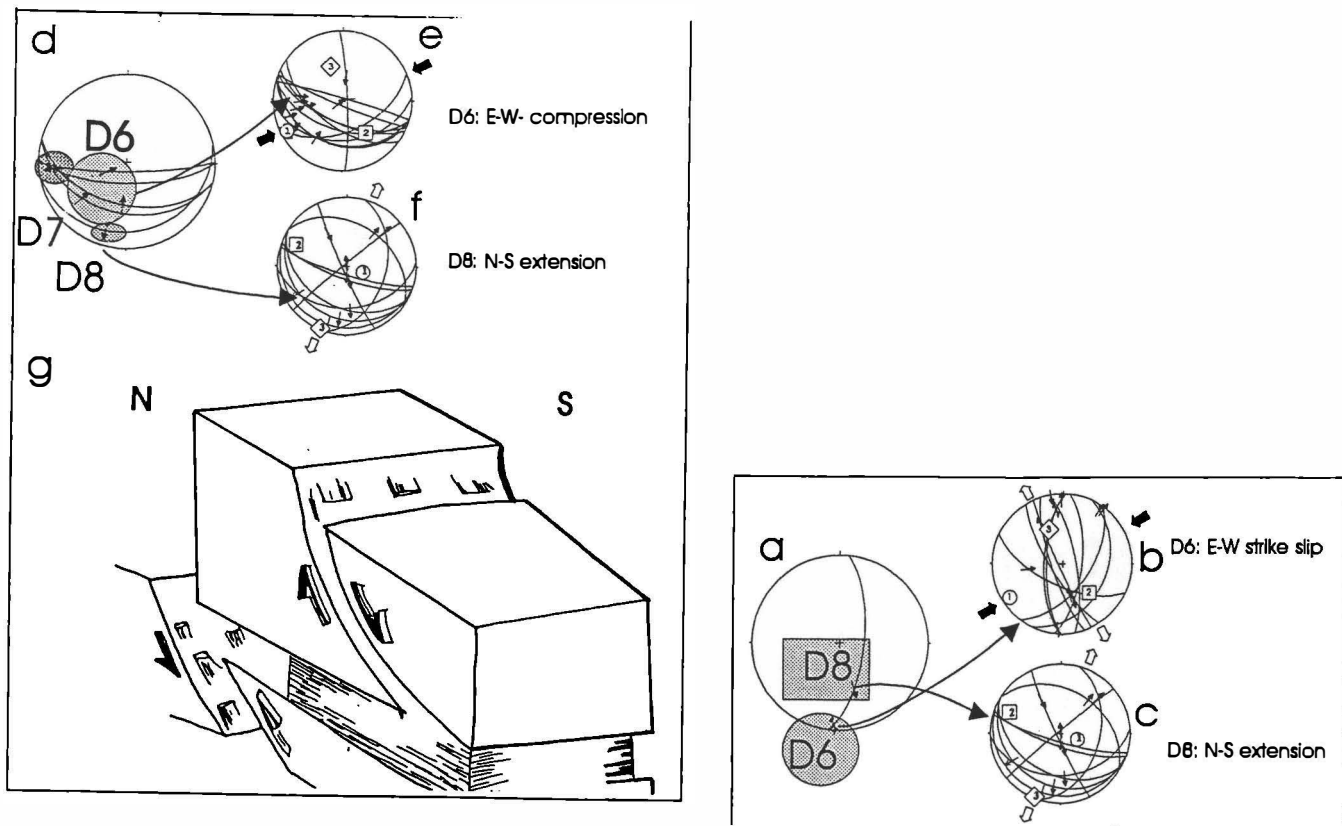


Fig. 2. Faults postdating thrusting in the Hatscheck quarry (from Freimüller, 1998).

**Further reading:** Egger et al. (1997); Freimüller (1998); Meschede and Decker (1994).

**Stop no. 4. Lukasedt-Dreimühlen. Hall Group – Lukasedt Formation, Lower Miocene, Eggenburgian to Ottnangian; Fan-delta sediments of the Palaeo-Salzach.**

**Location:** ÖK 50, sheet 63 Salzburg, Oichtental, ca. 1.3 km E of Oberndorf, ca. 300 m N of Lukasedt, ca. 100 m N Dreimühlen. Ca. 35 m long and 6-8 m high road cut to the N of Lukasedt, between two mills, at the right side of the Oichten creek.

The outcrop is situated immediately N of the basal thrust of the Helvetic unit and shows a dipping of the beds with 45°-70° towards the NW.

The basal strata consist of c. 8 m thick silty sands to silts with clasts of quartz, quartzite, and dolomite. The silty matrix contains up to c. 80 cm large clasts of fine grained sandstone. Fossil fragments (gastropods, bivalves, scaphopods, corals, balanides, and foraminifers) are rather abundant. They are followed by 3.7 m of laminated and ripple bedded, brown and grey silts-fine sands, rich in plant material, and then fine sands. The brown and grey, micaceous sandstones are cemented with calcite.

These sediments belong to the Eggenburgian, deposited in distal parts of a fan-delta complex. The Lukasedt Formation is restricted to the SW in Salzburg and was deposited on top of the Perwang imbricates in a relative narrow erosional channel. This fan-delta is the main sediment source for the Ottnangian sediments (Innviertel group) of the Upper Austrian Molasse basin.

**Further reading:** Egger et al. (1997).

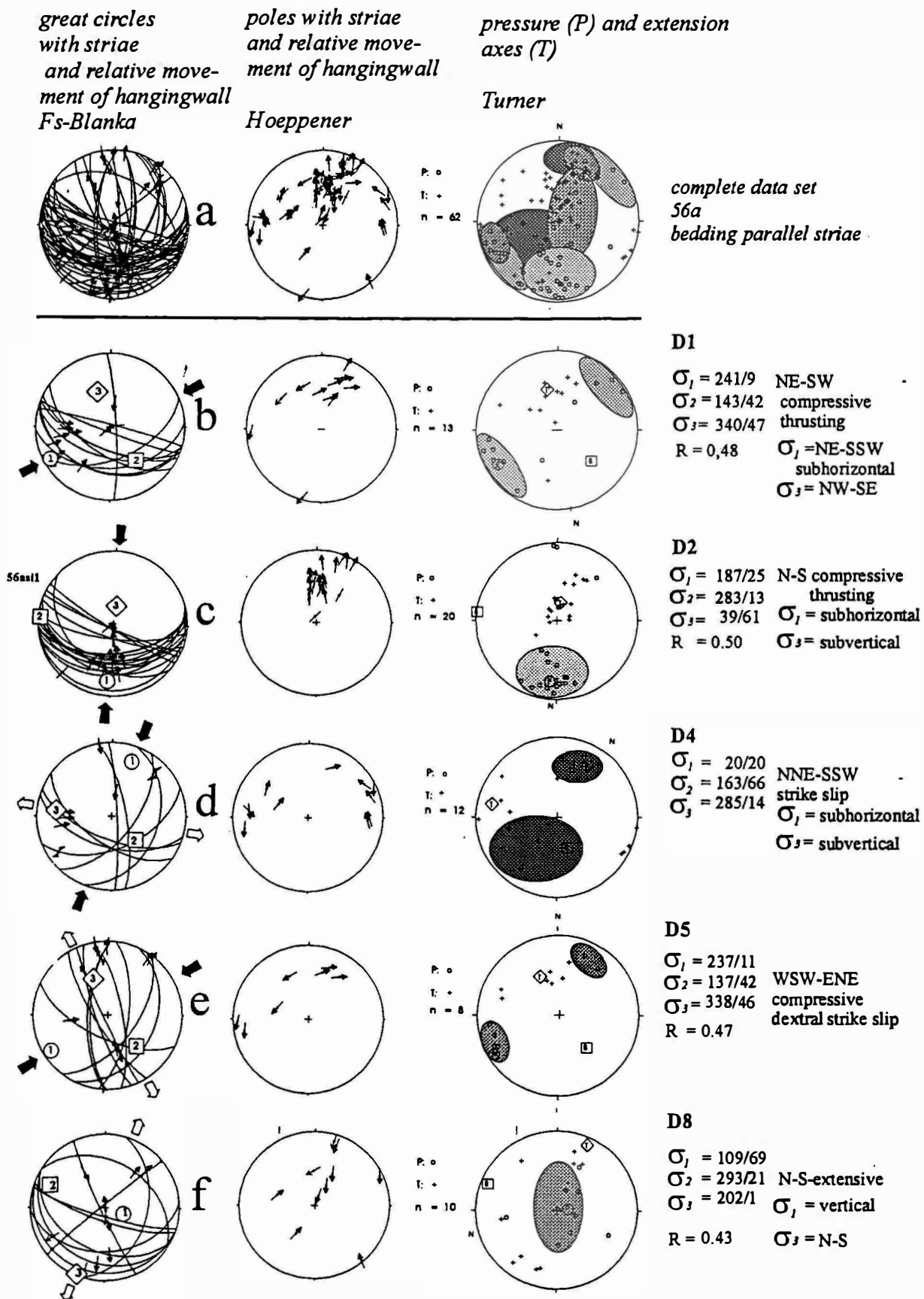


Fig. 3. Paleostress patterns from the Hatscheck quarry (from Freimüller, 1998).

**Stop no. 5: Haunsberg-St. Pankraz. Roterzschichten and Mittelschichten (Ypresian), Schwarzerzschichten (Lutetian), Fossilschicht (Lutetian) of the Helvetic zone.**

*Location: ÖK 63 Salzburg, Quarry (Schlößlbruch) ca. 3.7 km ESE of Oberndorf, ca. 1.8 km NNW point 835 (Haunsberg), ca. 700 m S of Kroisbach.*

General description: The Roterzschichten are red-brown, quartz-bearing calcarenites rich in nummulites. They are overlain by yellowish-white fine- to medium-grained quartzarenites (Mittelschichten), and then again quartz-bearing, brown-grey calcarenites. The Fossilschicht is a marly sand very rich in macrofossils. These sediments represent the deposits of a subtropical, oxygen-rich, shallow sea with different amounts of terrigenous influx.

The quarry also shows various sets of subvertical brittle faults. The dominating set trends NNE parallel to the Saalach fault further to the west. This set was activated first as a sinistral strike-slip fault by N-S contraction, later as a dextral fault due to ENE-WSW contraction. Furthermore, some sinistral strike-slip faults parallel to subvertical bedding planes can be observed. Relationships between the earlier two fault sets remain unclear.

**Further reading:** Egger et al. (1997).

**Stop no. 6: Nockstein. Basal thrust of the Tirolic nappe complex.**

*Location: OEK 64 Strasswalchen. Quarry at the toe of Nockstein.*

F. NEUBAUER

The quarry exposes Cenomanian marls of the "Cenomanian Randschuppe" which are overridden by Triassic Hauptdolomite of the Tirolic nappe complex within the Northern Calcareous Alps. The thrust surfaces shows brittle, bedding-parallel slickensides and stylolites and NNE-directed striations due to NNE transport of the Tirolic nappe. The overlying Hauptdolomite is heavily faulted.

**Stop no. 7: Gaisberg: Panorama**

*Location: OEK 64 Strasswalchen. Plateau of Gaisberg (1287 m).*

H.P. STEYRER, F. NEUBAUER

The Gaisberg panorama (Fig. 4) is one of most impressive overview of the structural units exposed at the transition to the foreland along northern margins of the Alps. The northern part exposes the Molasse peripheral foreland basin as plain and the hilly area with the Rhenodanubian/Helvetic thrust wedge. The basal thrust surface of the Northern Calcareous Alps is at the northern toe of the Gaisberg and extends towards W through Salzburg city where it is located at the northern toe of the Kapuzinerberg and Hohensalzburg castle.

The Gaisberg and the southern adjacent Osterhorn mountains belong to the Tirolic nappe within the Northern Calcareous Alps. The view towards SW exposes the overlying Lower Juvavic nappe with Hallstatt limestones. These are overridden by the Upper Juvavic nappe exposed within the Untersberg mountains.

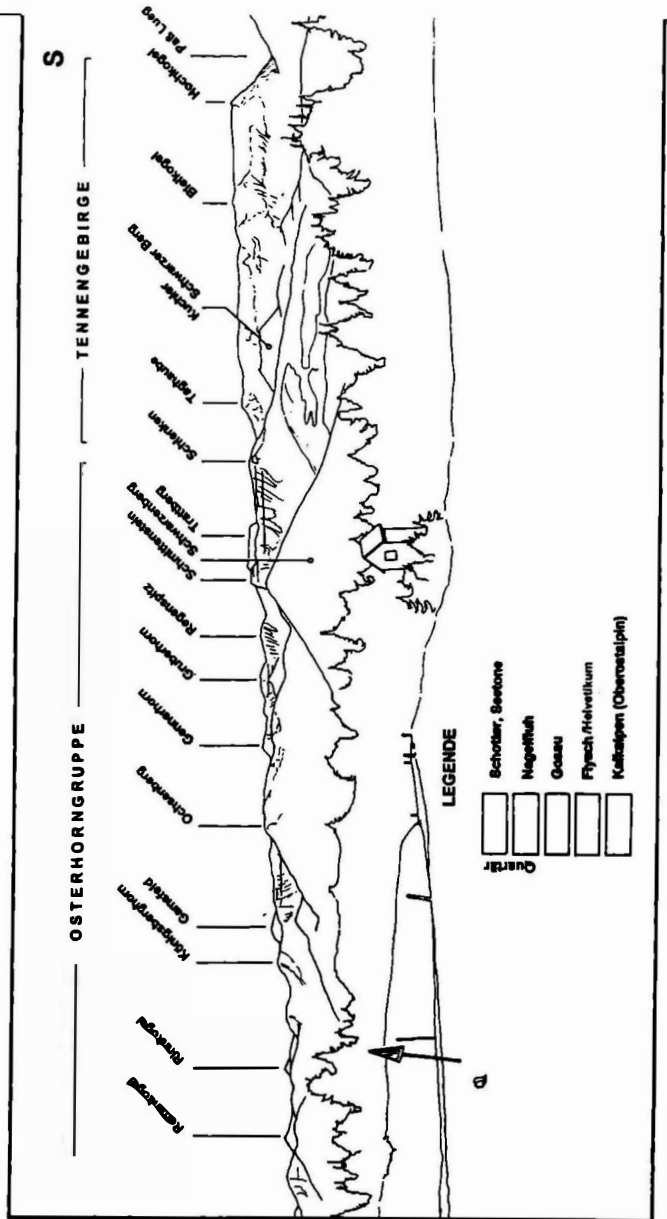
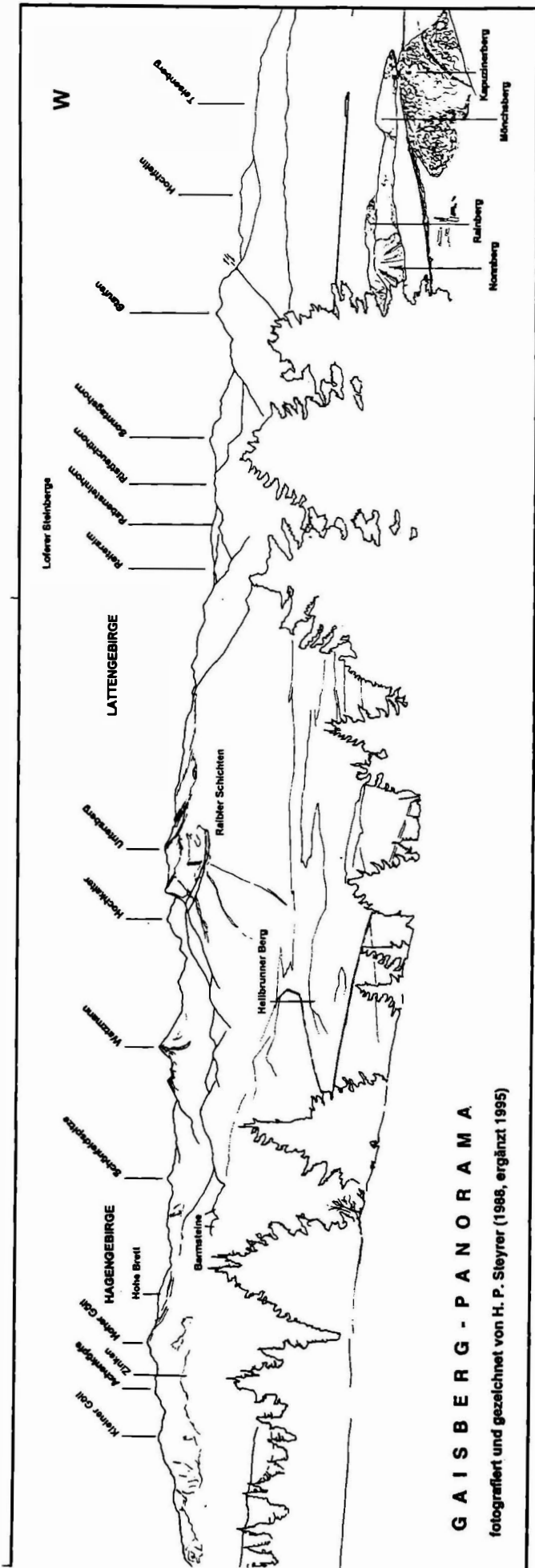


Fig. 4: The Gaisberg panorama.

**Stop no. 8: Adnet quarries (Scheck and Lienbacher quarries). Liassic Adnet limestone.**

*Location: OEK 94 Hallein. The quarries are located to the NE of the village Adnet.*

The Adnet Limestone is exposed in many quarries towards east of Adnet village. Illite-crystallinity data of this region and pre-depositional apatite fission track ages indicate that formation temperatures never exceeded diagenetic conditions (Kralik et al. 1987; Schweigl, 1997).

The Adnet Formation is 30 metres thick at the type-locality Adnet and ranges chronologically from the Hettangian to the Aalenian (e.g., Tollmann 1976). Where breccias are intercalated, the whole sequence attain thicknesses up to 100 metres (Tollmann 1976, Böhm et al. 1995). The Adnet Formation overlies Upper Triassic basin and reef limestones which were exposed during the lowermost Hettangian time. Doggerian limestones rich in cherts form the hanging wall.

The Adnet Knollenkalk facies (Fig. 5) is found in both the lower and upper parts of the Adnet Formation, where it averages approximately 15 m in thickness. The transition from the Adnet Knollenkalk to overlying Upper Liassic marls and to the paleogeographically adjacent Hierlatz limestone are continuous. Crinoidal Hierlatz Limestones also occur as fillings of Neptunian dikes cutting through the Adnet limestone. Thick (up to 60 m) nodular breccias, known locally as Adnet Scheck, occur within the Adnet Formation in the Pliensbachian. The Adnet Scheck and its equivalents in the Osterhorn mountains are interpreted as products of redeposition of a nodular limestone in a swell or seamount area (Hallam 1967, Hudson & Jenkyns 1969, Jurgan 1969, Bernoulli & Jenkyns 1970, Böhm et al. 1995).

The Adnet Knollenkalk facies is a red, cephalopod-rich, nodular, phacoidal limestone (Figs. 5, 6). It consists of limestone-marl interbeds and/or limestone nodules within a marly matrix. The red color is caused by hematite coatings. Occasionally the Adnet Knollenkalk has a pale green to grey color as a result of secondary alteration. The facies frequently contains ferromanganiferous crusts and nodules, which often contain sessile foraminifera and serpulæ that are sometimes associated with boring algae. These facts have been used to interpret the Adnet Knollenkalk and all red limestones of the Tethyan Jurassic as having been deposited in relatively shallow water environments. However, other investigations indicate that these Jurassic nodular limestones appear to have formed in pelagic, deep water environments.

In exposures of the Adnet facies, red nodular limestone containing abundant cephalopods, manganiferous nodules, and crusts are the predominant rock types. The more calcareous parts of red nodular limestones contain calcite-replaced sponge spicules, crinoid fragments, and foraminifera in a marly or micritic matrix. Marl-rich layers have higher fossil contents and are especially rich in crinoid fragments. The micritic nodules are generally pink to light red and make up the bulk of the rock, while the marly, micritic matrix is dark red. Where manganese has been replaced by iron, the matrix becomes black. The matrix sometimes includes abundant white or red crinoidal or other skeletal fragments. A complete spectrum of microfacies, from extremely nodular beds to homogeneous beds of red limestone with different amounts of ferruginous or manganiferous crusts and nodules, is present.

Ammonites occur on nearly every bedding plane, but are most often preserved as molds. Nautiloids, belemnites, gastropods, bivalves, calpionella, coccolithophorida, radiolaria, and trace fossils are rare. Shells and skeletal fragments of benthonic crinoids, echinoids, ostracods, pelecypods, gastropods, sponge spicules and benthonic foraminifera make up 20 to 40 percent of the rock and are embedded in a fine grained, micritic matrix. There are deep sea stromatolites (Böhm & Brachert, 1993). Solution effects are evident in the preservation state of fossils, especially ammonite moulds and corroded crinoid stems.

Unlike typical concretions primary laminations do not pass across matrix and nodules of the nodular limestone; rather the whole rock is strongly deformed. The boundaries of the

Adnet nodules are generally sharp, stylolitic, often with truncated fossils and enriched with ferruginous or manganese minerals (Garrison & Fischer 1969). In contrast, Jenkyns (1974, his Fig. 3) reported a belemnite that crosses the matrix-nodule boundary. The nodules may laterally grade into more continuous centimetre-thick beds with irregular surfaces.

Depending on their clay content nodular limestones are comprised of nodule-rich layers. Most nodules are rounded while others are distinctly angular. Some have a ferruginous or manganiferous rim or their boundary to the matrix is stylolitised.

The Adnet Scheck generally occurs as a breccia of red Adnet limestone nodules within a red marly Adnet matrix. In the Adnet quarries the Scheck is a breccia with a matrix of white, sparry calcite

The Adnet Knollenkalk includes many structures, including stylolites, that are characteristic of protomylonites (standard structural terminology in e.g., Wise et al. 1982, Heizmann 1985). These include stylolitic bed-parallel foliation, S-C-fabrics, shear bands, and  $\sigma$ -clasts resulting from deformation in a semiductile regime. The semiductile structures cut synsedimentary Neptunian dikes filled by Hierlatz or Adnet sediments and postdate both sediment deposition and early submarine lithification. The roughly E-trending Neptunian dikes are centimeters to decimeters wide and are mainly oriented perpendicular to bedding. Brittle deformation structures, thrust faults, dip-slip faults with en-echelon extension vein arrays cut the semiductile structures. At Adnet, the limestones of the Adnet Formation lie subhorizontally or dip gently towards the S (maximum angle of dip: 15°).

Most bedding planes in the Knollenkalk were formed by anastomosing stylolitic foliation. The stylolites have their stylolite teeth oriented parallel to the maximum compressive stress. In the Adnet Knollenkalk, only a small proportion of the stylolites are oriented subvertically, indicative that they were produced by sedimentary or tectonic load. Many stylolites are obliquely oriented to bedding, which suggests principal stress  $\sigma_1$  oblique to the bedding plane, e.g., by contraction due to transport of a thrust sheet over the Adnet Formation. Subvertically oriented stylolites are older than the obliquely oriented ones. Bedding-parallel fibrous slickensides and lineations within the Knollenkalk are associated with the stylolites. Thus most of the stylolites of the Adnet Knollenkalk are tectonic in origin.

Two types of extension gashes occur in the Adnet quarries: the first type is filled with white calcite and are millimetres to several centimetres in width. They are cut by stylolitic seams and shear planes. They are subvertical to the bedding planes and trend predominantly E-W. The second type are veins filled with white calcite and have a width of several centimetres. They are often overprinted by dip-slip faults and cut the solution seams and shear zones. There are two sets of these veins, oriented N-S and roughly E-W, respectively. Riedl shears and S-C-fabrics give the shear sense of movement of the hanging wall to the NNE.

Shear bands that cut nodule margins are up to several centimetres thick. Many nodules appear to represent  $\sigma$ -clasts with pressure shadow tails. During advanced stages of deformation, mesoscale out-of-sequence shear planes caused decomposition of competent limestone layers into boudin-like clasts and nodules, often containing remnants of fossils (e.g., ammonoidea). These clasts acted as rigid particles within a more deformable, argillaceous matrix. Sometimes these nodules rotated, producing asymmetric pressure shadows until  $\sigma$ -clasts developed. Porphyroclasts of  $\sigma_a$  and  $\sigma_b$ - type (Passchier & Simpson, 1986) are present, but formation temperature was not high enough to produce recrystallisation within pressure shadows. Biogenic and other clasts were flattened and partially dissolved along clast edges (Figs. 5d, e). The transition between more or less nodular beds depends on the silt and clay contents. While limestones with very little clay contents were structurally resistant to strain, clay-rich limestones tended to be structurally responsive.

Offsets of crinoidal Neptunian dikes (along cm-wide, internally finely foliated, shear zones that subparallel bedding planes) clearly demonstrate the occurrence of ductile shear

zones in otherwise nearly undeformed limestone. Lineation along stylolitic foliation surfaces are weakly developed, but trend NNE to NE. Strata-parallel slickensides indicate top to the NNE displacement (Fig. 7).

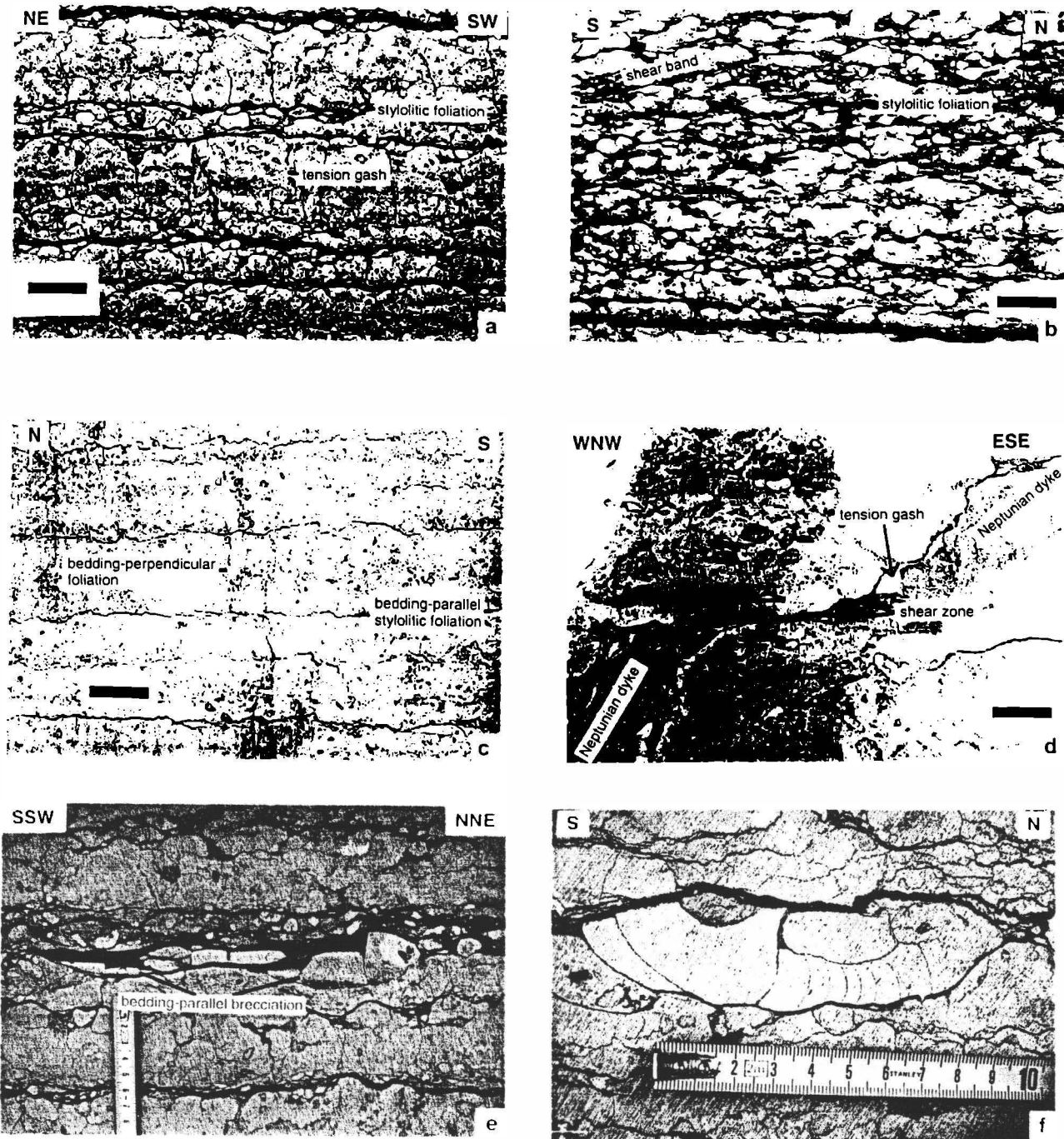


**Fig. 5. Field photographs:** a) Representative nodular limestone with mainly competent layers; stylolites parallel and perpendicular to bedding planes; scale bar = 10 cm. b) Nodular limestone with shear planes; rich in nodules; scale bar = 5 cm. c) Sets of oblique and subvertical stylolites; scale bar = 10 cm. d) Neptunian dike offset by a subhorizontal semiductile shear zone; note S-C fabric; scale bar = 5 cm. e) Protomylonitic character of the nodular limestone: ammonite dissected and elongated by a shear zone; scale in centimetres. f) Ammonite mold deformed by pressure solution along seams oriented oblique to bedding; scale in centimetres.

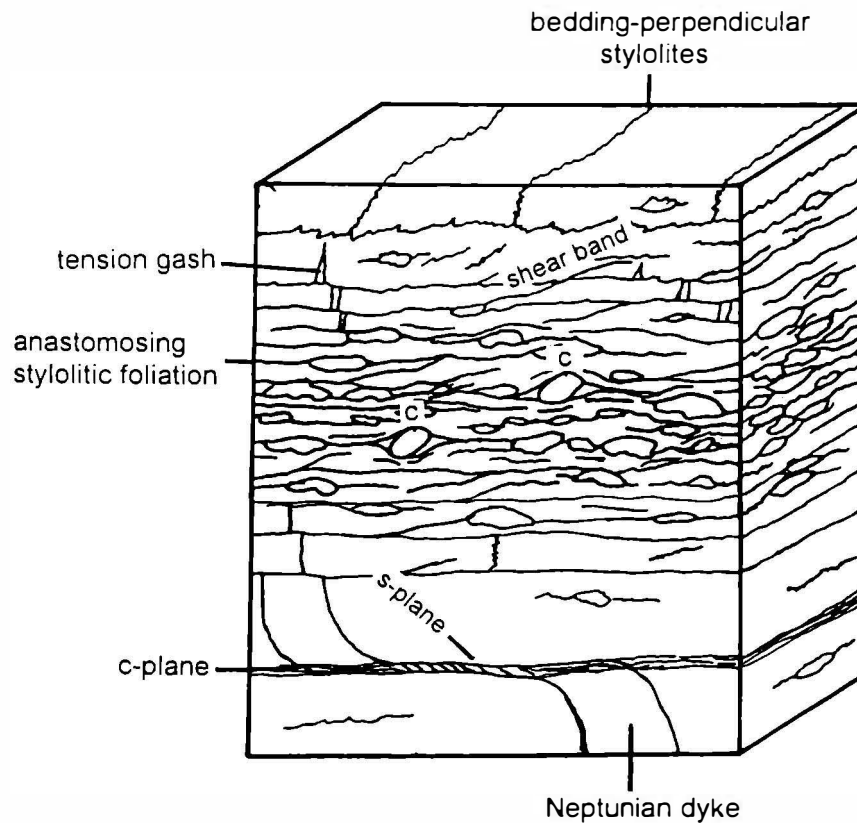


Fig. 6: Sketch of deformation features observed in the Adnet Knollenkalk, shear bands, stylolites,  $\sigma$ -clasts, and semiductile shear zone offsetting a Neptunian dike. c = tectonic clast with strain shadows.

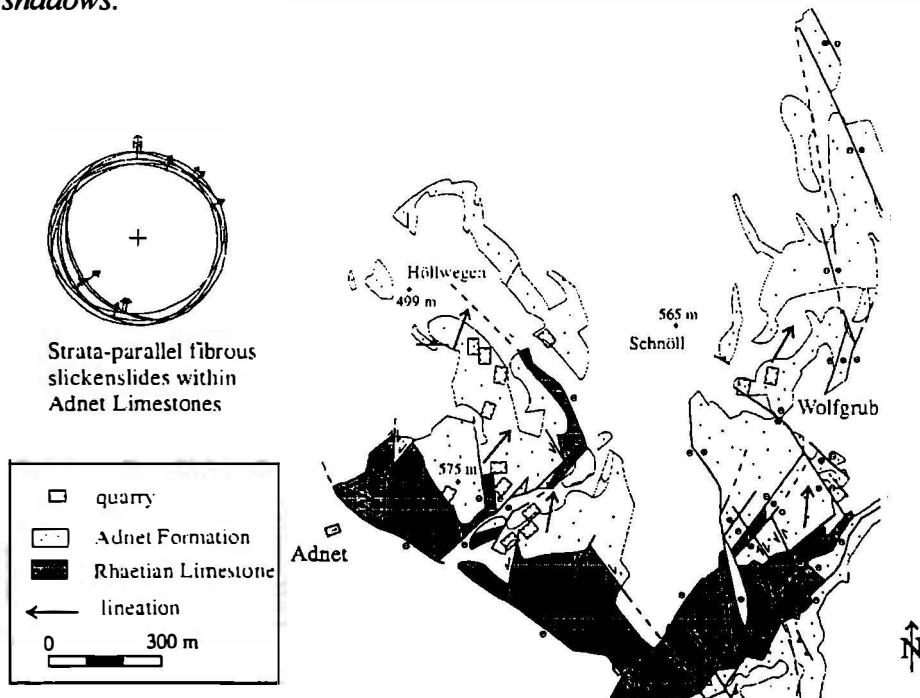


Fig. 7: Orientations of three deformation stages recorded in the Adnet quarries from oldest to youngest: a) Extension gashes filled with calcite, mainly oriented E-W. b) Strata-parallel fibrous slickensides and twins 1a and 2a indicating NNE-SSW contraction. c) Extension veins, oriented N-S and E-W and twins 1b and 2b showing extension with  $\sigma_1$  subvertical. Schmidt plots, lower hemisphere.



**Further Reading:** Böhm et al. in Egger et al. (1997); Schweigl (1997); Schweigl and Neubauer (1997); Schweigl and Neubauer (submitted).

**Stop no. 9: Quarry Leube, Oberalm and Roßfeld Fm.**

**Location:** OEK 63 Salzburg. The quarry of the Leube Cement Co. is located on Guthratsberg near Gartenau.

The quarry of Leube Company exposes a section from Oberalm Limestone (Tithonian to Early Berriasian), Schrambach Marl Fm. (Berriasian-Early Valangian) to the Rossfeld Formation (Hauterivian-?Barremian). The Oberalm Limestone is a grey, cherty, decimetre-bedded deep-water limestone with allodapic limestone interlayers (Barmstein Limestone). The uppermost level of the quarry exposes impressive very coarse-grained Barmstein Breccia. The source of these allodapic limestones is located to the west and represented by a carbonate platform which is similar to Plassen Limestone. Furthermore, Permian Haselgebirge clasts are common.

The Oberalm Limestone grade into the Schrambach Marl Fm. within which allodapic limestone layers are missing. Oberalm and Barmstein Limestones and Schrambach Marls are rich of nannofossils including calpionellids, radiolarians and foraminifera. The siliciclastic Roßfeld Formation starts with a spectacular "wildflysch" bed which is rich in carbonate clasts (e.g. Dachstein Limestone), which are typical for Upper Juvavic nappe, and some green basaltic components. The Roßfeld Formation is interpreted to represent the infilling of a deep sea trench in front of thrust sheets (Faupl and Tollmann, 1979).

In terms of structures, the succession is exposed on limb of an anticline (Schneiderwald anticline: Fig. 8). In the core of the anticline Haselgebirge is found.

**Further reading:** Wagneich et al., 1996; Böhm et al. in Egger et al. (1997); Plöchinger (1983).

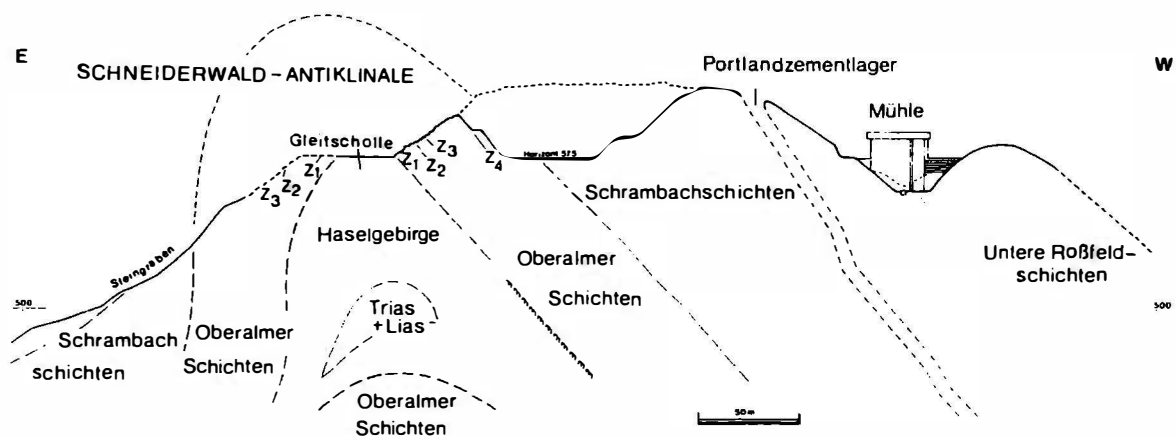


Fig. 8. N-S trending Schneiderwald anticline (from Plöchinger, 1983).

**Stop no. 10: Kiefer quarry. Untersberg Limestone of the Gosau Group.**

Location: OEK 63 Salzburg.

The Untersberg Limestone represents a detritic carbonate sediment deposited on a slope and derived from a carbonate platform. It also comprises clasts from the underlying Triassic Dachstein Limestone and from the Late Jurassic Plassen Limestone. Basal sectors of the section are stained by fine-dispersed bauxite-mud clasts. These grade into white, well-sorted detritic limestone and grey marls. Lower and middle portions of the section are interpreted to represent an inclined carbonate platform slope with erosional channels, scour and fill structures, slumping, olistolites, mass and debris flows with angular clasts. Beds with graded bedding and grain flows with reversed grading are interpreted to represent channel fillings.

The Untersberg "Marble" represents one of the most prominent building stones used for sculptures, fountains and decorations in Salzburg city.

**Further reading:** Leiss (1988); Wagreich et al., 1996; Böhm et al. in Egger et al. (1997).

**Stop no. 11: Dürrnberg: Salt mine**

Location: OEK 94 Hallein. Salt mine at Dürrnberg near Hallein.

The Salt mine is located within the Hallstatt unit (Lower Juvavic unit). It exposes the Permian Haselgebirge which comprises salt and grey shale. Various kinds of salts are exposed which are likely the result of deformation and recrystallization (modern structural investigations are missing). There is a controversy whether the emplacement of Haselgebirge results from tectonic transport or gravity sliding into the Upper Jurassic Oberalm basin. For detailed, see Fig. 9.

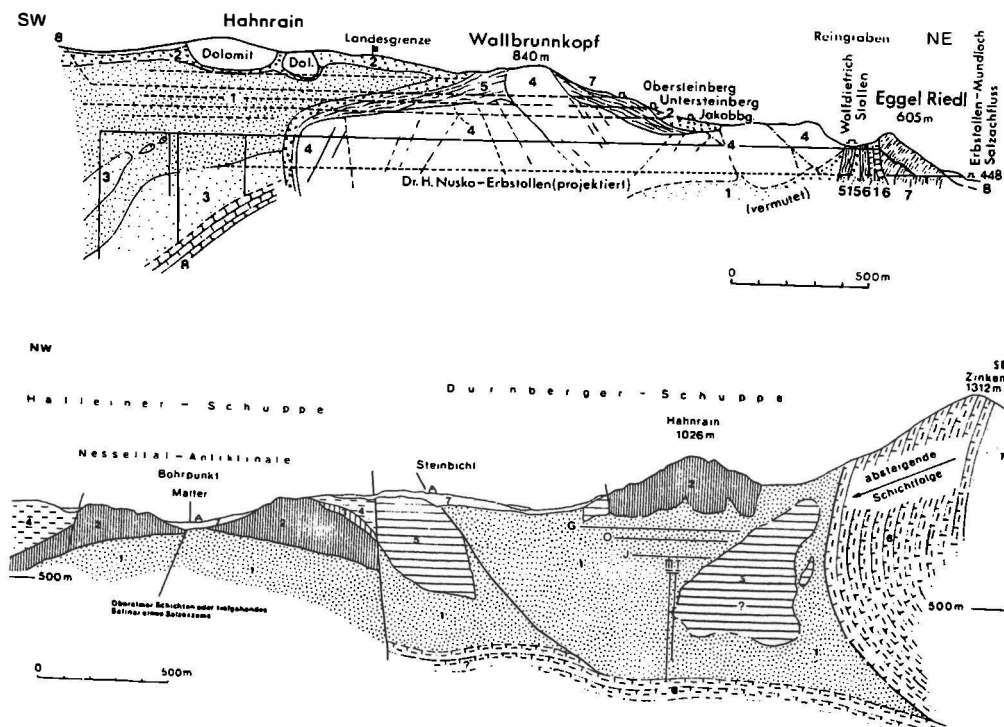


Fig. 9. Geology of the salt mine of Dürrnberg (from Plöchinger, 1983).

The salt mining started at ca. 2,500 B.C. and continued with intense mining during the Hallstatt period.

**Further reading:** Plöching (1983).

**Stop no. 12: Paß Lueg: Dachstein Limestone**

*Location: OEK 94 Hallein. Road cut to the S of Lueg saddle along the Federal Road.*

The road cut exposes bedded Dachstein Limestone with the famous loferite cycle. The exposure, an ice-polished surface, is rich megalodonts (*Conchodus infraliasicus* STOPPANI).

**Further reading:** Plöching (1983).

**Stop no. 13: Road cut between Alpendorf and Sulzau: Salzach-Enns fault**

*Location: OEK 125 Bischofshofen. Road cut along road to Sulzau (2 km SW of Alpendorf).*

X. WANG

From Sulzau to the north of Alpendorf, the Salzach-Enns fault extends ENE-WSW and represents the boundary between the Upper Austroalpine unit, namely Grauwacken zone, and the Lower Austroalpine cover of Radstädter Tauern to the south. The Grauwacken zone is here composed of black phyllite. The southern side of the Salzach-Enns fault exposes grey to dark calcitic phyllite of the Lower Austroalpine cover. The valley on the eastern side of the road follows the fault zone, indicating that formation of the valley is likely related with movement of the fault. Structures related with the fault occur mainly in calcite phyllite/calcitic schist of the southern side of the fault. Overall, the calcite phyllite steeply dips to NNE. Crenulation lineations occur universally in phyllite and calcite schist. Outcrop-scale, transected folds trend gently ESE. Crenulation lineations always cut transected folds in a counterclockwise sense. This indicates a sinistral strike-slip displacement. Predominant south-dipping slickensides and gently plunging striations indicate a sinistral strike-slip shear, toe. In many cases, striations are subparallel with lineations. In general, steeply plunging striations overprint gently plunging lineations, showing uplift of the southern side of the fault following sinistral strike-slip shear.

**Further reading:** Wang and Neubauer (1998).

**Stop no. 14: Peterlehen/Steinbach E of Wagrain: Neogene Wagrain basin**

*Location: OEK 126 Radstadt. Brook S Steinbach S of the road between Reitdorf and Wagrain.*

X. WANG

In Peterlehen, southeast of Mayerdörfel, Lower Miocene sedimentary rocks are exposed along a nearly S-N trending valley. This sedimentary sequence includes a conglomerate at the bottom, upwards follow alternations of conglomerate and micaceous sandstone, and fine-grained

sandstone, mudstone and shale at the top (Trauth, 1925). The middle sector of the succession occurs in Peterlehen. The rock association comprises mainly grey, middle- to fine-grained micaceous sandstone and conglomerate with intercalations of thin coal layer. The conglomerate shows a well-developed roundness. Diameter of components of the conglomerate is between 5 to 8 cm. The beds dip to SE ( $158^\circ$ ) at an angle  $52^\circ$ . Occasionally, step normal faults cut through the sequence. A lot of slickensides and striations occur in sandstone and only a few in conglomerate. Most of the slickensides dip to SE with striations indicating downsliding of the hangingwall, but a minority of them with low angle striations indicate dextral strike-slip shear. Tensor analysis yielded two stages of palaeostress. One maintains the principal stress axes:  $\sigma_1$ : 84/358,  $\sigma_2$ : 06/194,  $\sigma_3$ : 02/104, the other shows the principal axes  $\sigma_1$ : 03/157,  $\sigma_2$ : 86/287,  $\sigma_3$ : 04/066, which represent by dextral strike-slip shear.

**Further reading:** Wang and Neubauer (1998).

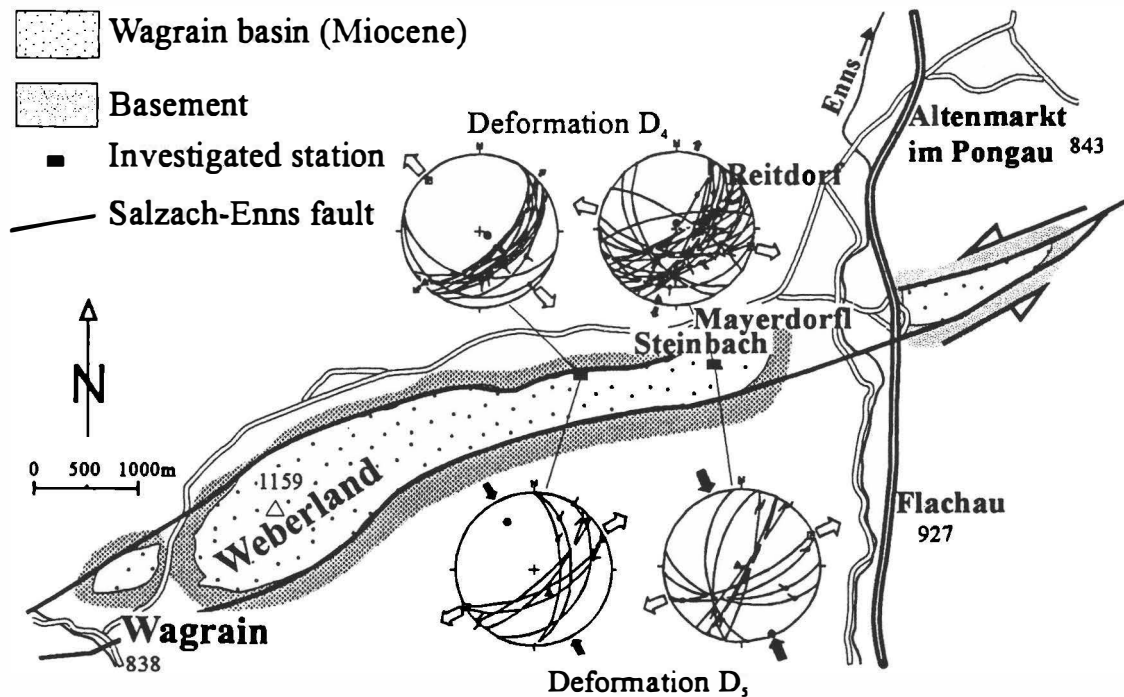


*Fig. 10: Paleostress patterns of the Wagrain basin (from Wang and Neubauer, 1998).*

#### **North-eastern Tauern window, Zederhaus valley**

The Zederhaus valley exposes a section through the Permomesozoic sequence of the Penninic Tauern window, that can be divided into several nappes, here. On top of the Storz nappe follow the Schrovín nappe, the Glockner nappe, and the so called Nordrahmenzone (north frame zone), finally overthrust by the nappes of the Lower Austro-Alpine unit.

The Storz nappe comprises mainly basement rocks, migmatites and amphibolites intruded by Variscan granites and on top black phyllites. The Schrovín unit includes quartzites, dolomite and calcite marbles, interpreted as Triassic, and some slivers of orthogneisses. They likely represent the sheared-off cover of a continental basement. The Glockner nappe comprises some ultrabasic rocks (serpentinites), greenschists and calcschists, grading into phyllites and marbles, respectively. It represents rocks of an oceanic lithosphere. The overlying Nordrahmenzone is essentially a melange, consisting of a phyllitic matrix with clasts of mainly basement and Triassic cover rocks, that range in size from mm to mountain (e.g., the Weißbeck) scale.

Structurally, the oldest foliation in the Storz nappe strikes E-W to NW-SE, the stretching lineation plunges gently to the WSW to SW. Shear sense indicators point to NE-vergent transport during this deformation phase (Kruhl, 1993, Kurz et al., 1996). In the Schrovín unit this stretching lineation plunges to the N to NNE. This penetrative foliation is overgrown by kyanite, chloritoid, hornblende and white mica. In the Glockner nappe and the Nordrahmenzone, these structures are overprinted by a N-dipping penetrative foliation and a related ESE-trending stretching lineation. The foliation is subparallel to lithologic contacts, also sheath folds develop during this deformation. N-plunging stretching of the older deformation phase are only preserved in some quartzites. Asymmetric quartzite boudins in thick calcschists indicate shear senses top-to-the-WNW, but mostly coaxial structures dominate.

Subsequently, the penetrative foliation was isoclinally folded around subhorizontal axes subparallel to the older ESE-trending stretching lineation. The axial plane foliation  $s_3$  is subparallel to the penetrative foliation. A further deformation led to the formation of tight to closed, N-vergent folds, which axes are subhorizontal or plunge gently to the W. Younger structures, belonging to the doming of the Tauern window, indicate orogen-parallel, ESE-WNW-directed extension.

**Stop no. 15. Quartzites and whiteschists at the base of the Schrovín unit.**

*Location: ÖK 50, sheet 157 Tamsweg. National road from St. Michael to Zederhaus, ca. 500 m SE of Fell.*

J. GENSER

Strongly foliated, fine grained yellow quartzite to mica quartzite and whiteschists consisting of albite, white mica, and minor garnet and stilpnomelane.

**Stop no. 16. Greenschists and calcschists of the Glockner nappe.**

*Location: ÖK 50, sheet 156 Muhr. National road at highway bridge at Kraglau, c. 1.2 km SE of Zederhaus village.*

J. GENSER

**Stop no. 17. Graphitic phyllites with dolomite clasts of the Nordrahmenzone.**

*Location: ÖK 50, sheet 156 Muhr. National road at highway bridge c. 1 km SE of highway tunnel.*

J. GENSER

Biotite phyllites with cm thick layers of graphitic quartzites and massive clasts of unfoliated dolomite, several metres to deca-metres thick.

**Stop no. 18. Chlorite-muscovite schist of the Nordrahmenzone.**

*Location: ÖK 50, sheet 156 Muhr. Rieding valley, road on top of the entrance of the highway tunnel (Tauerntunnel).*

J. GENSER

Well-foliated, fine grained, phyllitic chlorite-muscovite schists with quartz lenses up to dm in size.

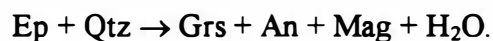
**Stop no. 19. Granodiorite of the Göß core**

*Location: ÖK50, sheet 182 Spittal an der Drau. Quarry Koschach. 13°27'45''E/46°58'15''N. Gmünd-Malta-Koschach (bridge across the Malta river)*

J. GENSER

In the Göß valley the structurally lowest units of the eastern Tauern Window (and also the Eastern Alps) are exposed (Göß core). It consists mainly of different orthogneisses, ranging from granites to tonalites, that represent deformed Variscan granites (intrusion ages of ca. 320 Ma according to Cliff and Cohen, 1980). These orthogneisses are separated from the orthogneisses of the Hochalm core by a paragenetic series. In the Koschach quarry, a strongly lineated, light grey granodioritic augengneiss that is crosscut by several generations of pegmatites to aplites, is exposed.

The magmatic paragenesis of the granodiorite comprises plagioclase, K-feldspar (Karlsbad twinning), quartz, biotite, titanite, allanite, epidote, zircon, and apatite. Geochemically, the rocks resemble Na-rich, high K calcalkaline I-type granitoids, in part featuring almost trondhjemitic affinity (Marschallinger and Holub, 1991). Trace elements show volcanic arc granite characteristics with selective enrichment of LIL elements and low Rb/Zr. The Alpine metamorphic paragenesis includes oligoclase, K-feldspar, quartz, biotite, clinozoisite(epidote), garnet, magnetite and sphene. Oligoclase displays inverse zoning (c. An<sub>15</sub> → An<sub>25</sub>), K-feldspar is marginally replaced by myrmekite. Garnet formed due to the general reaction



In this outcrop one can distinguish 3 main deformational events:

1) The main deformation is responsible for the formation of the penetrative foliation and the pronounced lineation of the orthogneisses. Pegmatite veins are sometimes folded due to this deformation, older aplitic veins mostly not, pointing to low viscosity contrasts during deformation. The strain distribution is generally very homogenous. The dominant stretching lineation indicates a constrictional deformation geometry, corroborated by quartz-c-axes distributions (type I crossed girdles). In the Koschach quarry, the foliation dips steeply to the NNE (30/70), on the southern side of the Malta valley to the S (180/40), on the northern side to the ESE. The poles to the foliation hence display a great circle distribution around the stretching lineation (120/20), which is very consistent over the whole area. This distribution we interpret also to have formed in the constrictional deformation field, and not due to later

folding. Shear criteria that are mostly only weakly expressed and quartz-c-axes distributions indicate a non-coaxial deformation path with a dextral shear component. This deformation occurred at elevated temperatures up to the Alpine metamorphic peak, with dynamic recrystallization of plagioclase, K-feldspar and quartz. This deformation event must be placed in Oligocene times, based on radiometric dating of the metamorphic peak at about 20 Ma in deep tectonic levels of the eastern Tauern Window by Cliff et al., 1985.

2) Conjugate, ductile shear zones that are a few mm to cm wide, cut discordantly across the penetrative foliation. These shear zones dip to the ESE and WNW, and show a normal sense of shear to the ESE and WNW, respectively. This deformation led to a subvertical shortening and ESE-WNW-directed extension, therefore. In the shear zones, plagioclase, quartz, and biotite recrystallised, green amphiboles and calcite, respectively, formed. This indicates an activity of these structures at still elevated temperatures (upper greenschist to lower amphibolite facies conditions). This ESE-WNW extension is related to the uplift of the Penninic units.

3) Steeply dipping, ESE-WNW-trending faults (parallel to the main foliation) that show a normal sense of shear of the northern hangingwall indicate an extension in NNE-SSW direction, too. They were active from near peak metamorphic conditions (asymmetric folding of biotite schists and aplites, with static recrystallization of biotite after this deformation) to cool conditions (slickensides, calcirites, fault gouges).

#### **Stop no. 20. Intrusive contact of the Malta tonalite with country rocks.**

*Location: ÖK50, sheet 156 Muhr. Bed of the Malta creek.*

J. GENSER

The Malta tonalite is the oldest member of the intrusion sequence of the Hochalm core (Holub & Marschallinger, 1989) with an age of ca. 320 Ma (Cliff & Cohen, 1980). In the inner parts of the Hochalm core it is mostly a massive, medium grained rock. In places, swarms of elliptical diorite inclusions occur. The magmatic paragenesis of the tonalite comprises plagioclase, quartz, K-feldspar, biotite, allanite, titanite, and epidote. Geochemically it represents a high-K, calcalkaline, I-type granitoid, that is strongly enriched in Na. The trace element spectrum is typical of VAG intrusions, enriched in Ce (Marschallinger & Holub, 1991).

In this outcrop, the intrusive contact to their country is perfectly preserved. These are migmatitic two mica gneisses, that are thought to be derived from shales. They contain oligoclase, quartz, biotite, white mica, K-feldspar, epidote and sphene. Locally, boudins of calcisilicate rocks occur. Other extensional structures, that interfere with the intrusion of the tonalite, can be found as well.

#### **Stop no. 21. Leucocratic granitoid gneisses (Kölnbrein leucogranite).**

*Location: ÖK50, sheet 156 Muhr. Kölnbrein quarry NW Kölnbrein dam.*

J. GENSER

The huge quarry near the Kölnbrein dam exposes the latest large area Variscan intrusion, the so called Kölnbrein leucogranite (Holub, 1988). This granite intruded in several phases that may be distinguished mainly on the basis of mafic mineral amounts. The fine to medium grained leucocratic rocks incorporate a consistent population of country rocks, ranging from migmatitic paragneisses to older intrusives like the Malta tonalite or the Hochalm porphyric

granite. Places of incomplete resorption of country rocks are characterised by schlieren textures.

The rock composition ranges from leucocratic granodiorites to granites, containing oligoclase, K-feldspar, quartz, muscovite, biotite, epidote and in places garnet. Geochemically, it is a high-K calc-alkaline I-type, Na-enriched plutonite; trace elements show a strong enrichment in LIL and Ce, with patterns typical of VAG types according to Pearce et al. (1984).

**Stop no. 22. WNW-directed shear deformation in tonalitic gneisses of the Hochalm core.**

*Location: ÖK50, sheet 182 Spittal an der Drau. 13°29'02''E/46°58'05''N. Rock wall on the NW side of the Malta valley (Rödern). From Malta village to the bridge over the Feistriz brook (first brook NW of village Malta), then 500 m along a path to a ledge.*

J. GENSER

In this outcrop, the same Malta tonalite as in stop no. 20 occurs., only strongly deformed. The magmatic paragenesis comprises plagioclase, quartz, K-feldspar, biotite, allanite, titanite, and epidote. The Alpine metamorphic paragenesis consists of oligoclase, quartz, biotite, K-feldspar, clinozoisite, titanite, and muscovite (phengite). Oligoclase displays inverse zoning (An<sub>15</sub> → An<sub>25</sub>), white mica is present in minor amounts only, mostly restricted to strongly deformed domains.

The tonalitic gneiss reaches the Malta valley as a strongly thinned lamella (ca. 200 m thick), which is due to high ductile deformation. The tonalite shows a pronounced, homogeneous, penetrative foliation and a well developed stretching lineation. Aplites are folded due to this deformation, the foliation is parallel to the axial planes of the folds. The foliation dips gently to the E (90/30), the stretching lineation to the ESE (120/25). An abundance of shear criteria, as shear bands,  $\sigma$ -porphyroclasts, and also quartz textures indicate shearing top-to-the WNW.

This deformation occurred up to the metamorphic peak, with dynamic recrystallization of plagioclase, quartz, and biotite. It must be placed in Miocene times, too.

**Stop no. 23. Ductile to brittle low-angle normal faulting to the ESE in the Peripheral Schieferhülle.**

*Location: ÖK50, sheet 182 Spittal an der Drau. 13°30'25-30''E/46°57'35''N. Road cut on the road Malta - Maltaberg. From Malta village by car (difficult to access by big buses) or on foot (ca. 25 minutes to walk) on the road to Maltaberg up to the second corner closing to the W (1010 m NN).*

J. GENSER

This roadcut exposes a succession from the uppermost Storz Group (Vavra & Frisch, 1989), a pre-Variscan basement unit, here mainly amphibolites and plagioclase gneisses, overlain by the post-Variscan sequence of the Peripheral Schieferhülle. The latter sequence starts, approximately 70 m after the crossing path, with black albite porphyroblast schists. Then follow whiteschists, strongly retrogressed orthogneisses, and quartzites of probably Permian-Triassic age, and finally calcschists with intercalated greenschists and metapelites, the so called Bündner Schiefer, Jurassic-Cretaceous deep-sea metasediments and -volcanics. A detailed description of this section can be found in Exner (1980).



Alpine metamorphic parageneses comprise:

*Quartz-albite-phengite-phlogopite-calcite-ilmenite (quartzites)*

*Albite-quartz-phengite-biotite-chlorite-calcite-ilmenite (semipelites)*

*Calcite-quartz-albite-muscovite-rutile-chlorite (calcschists)*

*Amphiboles-chlorite-albite-epidote-quartz-titanite-biotite-calcite (greenschists)*

Two structural events can be distinguished in these outcrops:

1) A penetrative foliation with an only weakly developed stretching lineation. The foliation dips moderately to the ESE, the lineation trends NNE-SSW. These structures can best be seen in the rocks of the Storz Group, in higher units they are strongly overprinted by the second deformation. In deeper parts of the Storz unit and in more northerly parts of the Peripheral Schieferhülle, where these structures are often well preserved, a tectonic transport of top-to-the N can be derived. This deformation occurred close to metamorphic peak conditions.

2) The second deformation led to a further flattening of the older foliation and an extension in an ESE-WNW-direction. The deformation is noncoaxial, expressed in ESE-dipping shear bands, which often occur in multiple sets with different dip angles. A conjugated, WNW-dipping set of shear bands is only weakly developed and restricted to strongly deformed domains. Lineations on the shear bands plunge to the ESE and WNW, respectively. In calcschists zones with a new mylonitic foliation, angular to the older foliation, develop. This structures, as well as asymmetric calcite-c-axes textures, prove a dominant normal shear of the hanging-wall to the ESE. Other structures related to this extension are extension veins and boudins, mainly in competent quartzites. Small-scale, asymmetric folds that are overturned to the ESE are related to this shearing, too.

This deformation commenced after metamorphic peak conditions, as evidenced by greenschist facies minerals (chlorite, epidote) in shear zones in amphibolites and continued to cool conditions up to the formation of brittle normal faults. The main part of this deformation is ductile, however.

This deformational event, a low-angle normal faulting, led to the unroofing of the metamorphic dome of the Tauern Window by displacement of the Austro-Alpine upper crust to the ESE.  $^{40}\text{Ar}/^{39}\text{Ar}$  dating of a single phengite grain from the quartzites yielded a plateau age of  $21.9 \pm 1.1$  Ma. This age should give the age of cooling below ca. 375 °C and hence an upper limit for the low-angle normal faulting. This event must be place in the lower Miocene, hence. This is also corroborated by data from Cliff et al. (1985), which indicate nearly isothermal decompression and a following rapid cooling of the Penninic units in the time span between 20 and 16 Ma.

#### **Stop no. 24. Metamorphism and deformation in the Lower Austro-Alpine unit.**

*Location: ÖK50, sheet 182 Spittal an der Drau. 13°30'25-30''E/46°57'35''N. Road cut on the national road between Gmünd and Eisentratten, at the mouth of the Drehtal creek (point 789 in ÖK, parking place).*

J. GENSER

The outcropping diaphthoritic quartz-phyllites comprise a pre-Alpine mineral paragenesis of garnet, biotite, and large white mica. The retrograde Alpine paragenesis comprises chlorite, sericite, quartz and pyrite. Pre-Alpine garnets are often completely retrogressed to chlorite and white mica, biotites are bleached.

The rocks show a penetrative foliation, often with relics of a pre-Alpine foliation. Pre-Alpine quartz veins are folded isoclinally, during the Alpine foliation a second, discordant

generation of quartz veins developed. The stretching lineation strikes c. E – W. Pre-Alpine mica are rotated into the new foliation. Pseudomorphs after garnet are often stretched parallel to the lineation. Quartz-c-axes textures (oblique, simple girdles with marginal maxima) indicate shearing top-to-the-W. These textures and low-temperature plasticity of quartz point to cool, ductile deformation conditions. The foliation is subsequently folded around NE-SW striking axes into upright folds. Late-stage structures are slickensides and kink bands.

$^{40}\text{Ar}/^{39}\text{Ar}$  dating of single muscovite grains from this outcrop gave late Variscan cooling ages (integrated ages of  $242.9 \pm 3.2$  Ma and  $239.6 \pm 1.1$  Ma).

#### **Stop no. 25. Boundary between the Lower and Middle Austro-Alpine units**

*Location: ÖK50, sheet 182 Spittal an der Drau.  $13^{\circ}34'13''\text{E}/46^{\circ}55'22''$ . Road cut on a minor road that leads to a farm from the road from Eisentratten to Heitzelsberg.*

J. GENSER

Here, the same diaphthoritic quartz-phyllites with pre-Alpine garnet, biotite and white mica and the same ductile deformation structures as in the last stop crop out. Towards the base of the Middle Austro-Alpine unit, however, you can see an increase of late, brittle deformation structures. Cataclastic shear zones with calcites that comprise fault breccias with clasts of several dm to fault gouges, develop. Motion on this late brittle shears is normal faulting towards the E. Therefore, it should be contemporaneous to the ductile low-angle normal faulting in the Penninic unit, representing the same orogen-parallel extension, but at a higher, and therefore cooler tectonic level.

Going towards the MAA, note the morphologic depression and the lack of outcrops, which must be due to an increase in brittle faulting towards the tectonic boundary. The boundary between the two units is a thrust that was reactivated as normal fault, therefore.

#### **Stop no. 26. Base of the Middle Austro-Alpine unit (Bundschuh nappe)**

*Location: ÖK50, sheet 182 Spittal an der Drau.  $13^{\circ}34'13''\text{E}/46^{\circ}55'22''$ . Outcrop at the branch-off of the road Eisentratten – Heitzelsberg from the main road, immediately E of the new church.*

J. GENSER

The Bundschuh nappe of the MAA is here represented by typical garnet-micaschists. These mica-schists display two stages of metamorphism, a Variscan and an Alpine event. The Variscan paragenesis comprises staurolite and garnet, the Alpine one garnet (mostly as rims around Variscan cores), biotite, muscovite, plagioclase, chlorite, and quartz. Mostly, staurolite occurs as pseudomorphs only that are often deformed.

The micaschists display a well developed Alpine foliation with isoclinally folded quartz veins and boudinage garnets (Variscan cores). The main deformation occurred before the metamorphic peak, as mica and quartz recrystallised statically. Quartz-c-axes textures show random distributions. Late-stage structures are slickensides that indicate E–W extension. Geothermobarometry of the Alpine paragenesis indicate conditions of c.  $600^{\circ}\text{C}$  and 10 kbar for the Alpine peak.  $^{40}\text{Ar}/^{39}\text{Ar}$  dating of single muscovite grains from this outcrop gave a weakly disturbed plateau with an integrated age  $107.5 \pm 1.3$  Ma. This age must be interpreted as cooling age after the Alpine metamorphism. The main deformation of the Bundschuh nappe must hence be older than this date.

**Stop no. 27. Middle Austro-Alpine basement with Priedröf micaschist/paragneiss and Bundschuh orthogneiss; Alpine metamorphic overprint.**

*Location: OEK 50, sheet 183, Radenthein. Road exposure along the Nockalm road in the Heiligenbach valley, ca. 400 metres South to the custom-house at Innerkrams.*

F. NEUBAUER

Both the Priedröf micaschist/quartzitic paragneisses (footwall) and the Bundschuh orthogneisses (hangingwall) are exposed along the Nockalm road and along the opposite wall of the valley. The Priedröf micaschist/paragneiss essentially contains quartz, feldspar, biotite, muscovite, garnet and rare pseudomorphs after staurolite. The Bundschuh orthogneiss is composed of K-feldspar porphyroclasts, quartz, plagioclase and light-greenish white mica.

Theiner (1987) found a polymetamorphic evolution with a Variscan metamorphic overprint in nearby localities with ca. 600 – 640°C and Alpine temperatures ranging from 500 to 520°C based on garnet-biotite geothermometry. The age of the Bundschuh orthogneiss is uncertain. Rb-Sr whole rock investigations resulted in sets of subparallel isochrons with model ages between 371 and 397 Ma and high  $Sr_{87}/Sr_{86}$  ratios between 0.721 and 0.739 (Frimmel, 1988). White mica of the Bundschuh orthogneiss from the Innerkrams area range between  $305 \pm 12$  and  $119 \pm 1$  Ma (Theiner, 1987). Geochemical and petrography indicate a syn-collisional granites (Frimmel, 1988). The first age is interpreted to be close to the time of Variscan metamorphism, the second age as result of Cretaceous resetting of the Rb-Sr isotopic system.

Both lithologies contain a ESE plunging stretching lineation. Shear criteria suggest both a first top WNW shear and a later, semiductile ESE displacement.

**Further reading:** Frimmel, 1988; Pistotnik, 1974; Theiner, 1987.

**Stop no. 28. Bridge Postmeister Alm. Primary base of the Stangalm Mesozoic sequence.**

*Location: OEK 50, sheet 183, Radenthein. Road exposure along the Nockalm road in the Heiligenbach valley, E of bridge E PostmeisterAlm.*

F. NEUBAUER

The outcrop exposes the primary contact between the basement (micaschist) and the transgressively overlying Quartzite (Skythian). The basement micaschist displays open folds which are discordantly overlain by quartzites of suggested Skythian age. The quartzite represents the basal formation of the Stangalm Mesozoic sequence. Hangingwall sectors of the quartzite are well foliated and displays an E-dipping foliation. New sericite is grown on the foliation plane. A new  $^{40}\text{Ar}-^{39}\text{Ar}$  age of a concentrate of a few grains yielded a plateau age of ca.  $89.0 \pm 0.6$  Ma.

**Further reading:** Pistotnik (1976).

**Stop no. 29: Ductile low angle normal fault at the tectonic boundary between the Stangalm and Pfannock Permo-Mesozoic sequences and the Gurktal thrust system.**

*Location: OEK 50, sheet 183, Radenthein. Nockalm road. Park your car at the Eisentalhöhe parking place. Follow the path to the Eisentalhöhe (exposure of Hauptdolomite and Kössen*

*Formation of the Pfannock slice of the Gurktal Nappe Complex). Follow ridge from the Eisentalhöhe to the West which exposes the phyllonite zone and the underlying dolomite marble of the Stangalm unit.*

F. NEUBAUER

The dolomite marbles of the Stangalm Mesozoic sequence are in part strongly foliated and linedated. The lineation plunges E and ESE. The marbles are overlain by a several tens of metres thick phyllonite which exhibit a clearly visible extensional crenulation cleavage fabric. Sense of displacement is top to the E/ESE. The phyllonite was interpreted as Carnian Raibl Formation. But the inclusion of chlorite schists exclude this stratigraphic interpretation. This level is now interpreted as part of the Murau Nappe of the Gurktal Nappe Complex because lithological composition and continuous exposure to true Murau Nappe along the structural base of the Gurktal Nappe Complex. In the hangingwall, dark Late Triassic limestones which belong to the cover of the Pfannock Nappe of the Gurktal Nappe Complex are exposed. These limestones include in part rich faunas (*Thamnasteria rectilamellosa*, *Isoclinus bavaricus*, *Cardita austriaca*). Views from the parking place to the N (Fig. 11) and to the S show the structural contacts between various structural units (Fig. 12).

**Further reading:** Gosen, 1989; Pistotnik, 197 , Ratschbacher et al., 1990; Tollmann, 1975.

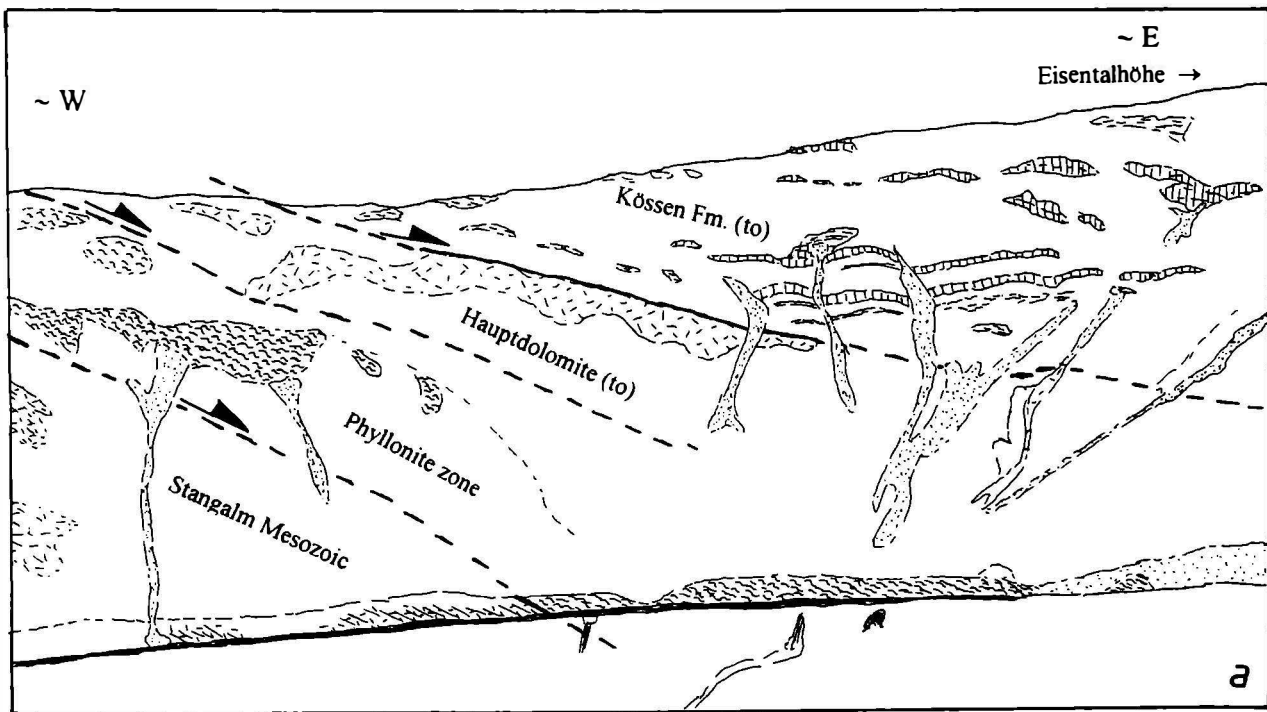


*Fig. 11: View from the parking place "Eisentalhöhe" towards N displaying the low-angle normal fault contact between Middle and Upper Austroalpine structural units.*

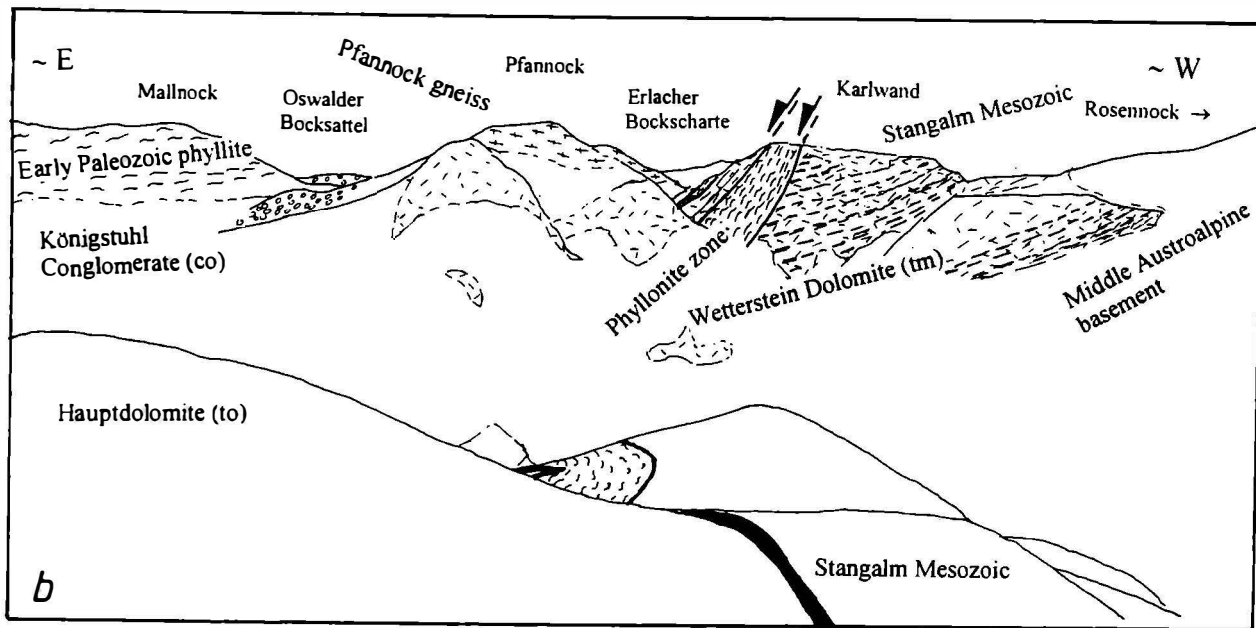


Fig. 12: View from the parking place "Eisentalhöhe" towards S displaying a high-angle normal fault contact between Middle and Upper Austroalpine structural units.

**Stop no. 30: Saddle E Eisentalhöhe. Late Carboniferous molasse sediments (Stangnock Formation) of the Gurktal Nappe Complex.**

*Location: OEK 50, sheet 183, Radenthein. Walking tour to the western flank of Königstuhl. From the parking place "Eisentalhöhe" (2,100m) of the Nockalmstraße (National Park "Nockberge") footpath to the Königstuhl (2,336m) (about 1 hour) and Stangnock (2,316m).*

The description is taken from K. KRAINER in Neubauer (ed., 1992).

The best outcrops of the Stangnock Formation are situated at the northern flanks of the Königstuhl and Stangnock mountains (Fig. 13).

The Stangnock Fm., exposed at the NW-margin of the Gurktal thrust system (Upper Austroalpine), represents a more than 400m thick sequence of intermontane molasse fillings, which accumulated under humid climatic conditions. The sequence starts with polymict conglomerates and intercalated immature, coarse-grained sandstones (poorly sorted, angular-subangular, feldspathic lithic arenites) at the base, deposited on the proximal part of a fluvial system (?alluvial fan). The main series is built up by a few, indistinctly developed megasequences, beginning at the base above a sharp, erosive boundary with sediments of a gravelly, braided river system, grading upward into a gravelsandstone facies, sometimes showing characteristic features of a meandering river system.

At the top of this sequences usually shales are developed, containing abundant plant fossils. At some places the shales, which are interpreted as overbank fines deposited on flood plains and in oxbow lakes, are overlain by thin anthracite seams. Conglomerates of the main series are very rich in quartz (>90%), sandstones are classified as moderately sorted, subangular lithic arenites - sublitharenites, in part lithic wackes, with high amounts of polycrystalline quartz (Fig. 14).

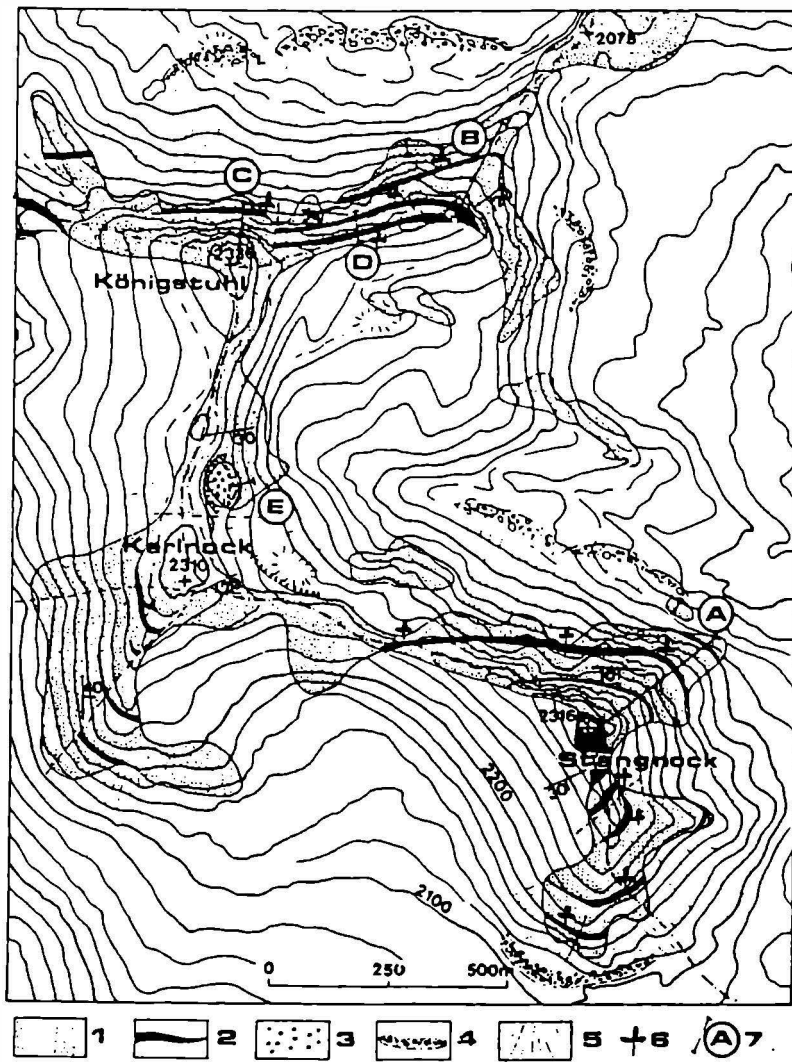


*Fig. 13: Geologic map of the Stangnock-Königstuhl area with position of investigated sections and some important plant fossil localities. 1 Conglomerates and sandstones of the Stangnock Fm., 2 shales of the Stangnock Fm., 3 sediments of the Lower Permian Werchzirm Fm., 4 boulder walls, 5 talus cones, 6 plantfossil localities, 7 investigated sections (from Krainer, 1989b).*

The top series does not show significant differences in facies compared to the main series, slight differences exist concerning the composition of the sediments. Volcanic rock fragments, especially volcanic quartz, are a characteristic feature of the sandstones, referring to first volcanic activity during the uppermost Carboniferous in the studied area.

The sharp, erosional appearance of the megasequences and the top series, starting with coarsegrained accretions, is referred to syndimentary fracture tectonics. From current directions which show a significant eastward trend, it is concluded that the intermontane basin developed in an approximately east-west-direction.

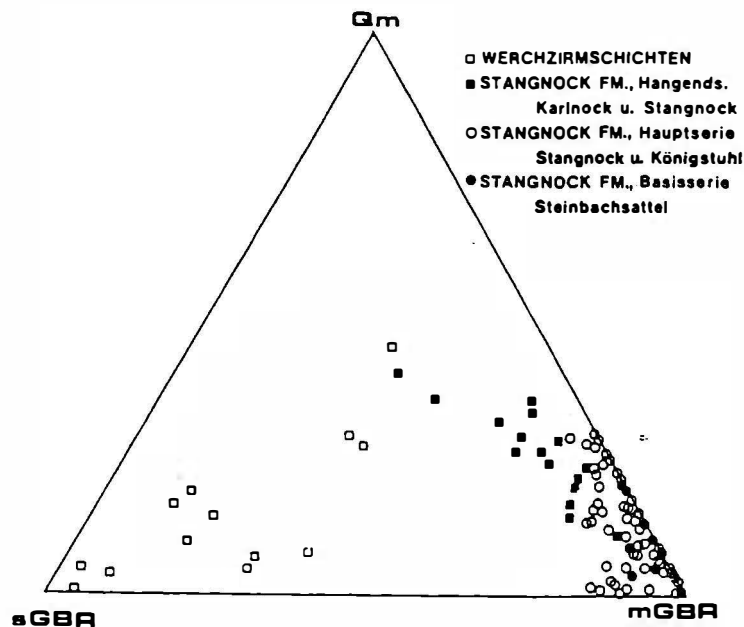


Fig. 14: Sandstones of the Stangnock Formation and overlying Lower Permian Werchzirm Formation plotted in the  $Q_m$  (total quartz) - sGBR (sedimentary rock fragments) - mGBR (metamorphic rock fragments) compositional diagram. Sandstones of the top series (Hangendserie) are characterized by higher amounts of monocrystalline quartz and sedimentary rock fragments, sandstones of the Werchzirm Formation are mainly composed of sedimentary rock fragments (from Krainer, 1989 b).

Well preserved plant fossils from dark shales of the Stangnock Fm. are known from several localities for more than 200 years. The complete fossil list contains 72 taxa (see Fritz, Boersma and Krainer, 1990). A flora rich in *Linopteris neuropteroides* and *Lycophyta*, containing *Neuropteris scheuchzeri* and *Sphenophyllum oblongifolium* but without *Pecopteris feminaeformis* in the lower part of the Stangnock Formation (localities Brunnachhöhe and Turrach 1) indicates Cantabrian age (*Odontopteris cantabrica* Zone). The flora from the horizon Königstuhl 31a (lower part of the Stangnock Formation) with *Sphenophyllum oblongifolium*, *Callipteridium pteridium*, *Odontopteris* and *Pecopteris feminaeformis* points to Barruelian age (*Lobatopteris lamuriana* Zone). The *Alethopteris zeilleri* Zone (Stephanian B) with the significant species *Sphenophyllum thonii* var. minor is represented by the flora Turrach 5 (lower part of the Stangnock Formation). The *Sphenophyllum angustifolium* Zone (Stephanian C) is indicated by the flora from the localities Königstuhl 25a and Reißbeck (middle part of the Stangnock Formation) containing the species *Sphenophyllum angustifolium*.

The uppermost part of the Stangnock Formation is characterized by the first appearance of *Callipteris* cf. *conferta* (locality Stangnock Südostgrat 1), indicating uppermost Stephanian C/Autunian age (*Callipteris conferta* Zone).

**Further Reading:** Frimmel, 1986, 1988. Fritz et al., 1990; Krainer, 1989a, b.

### Stop no. 31. Schiestlscharte, Nock Formation

*Location: OEK 50, sheet 183, Radenthein. Schiestlscharte at the Nockalm Road.*

F. NEUBAUER; descriptions follows partly Giese in Neubauer (1992).

The exposed rocks belong to the undated, basal part of the Nock sequence which is composed of mafic schists, quartz-feldspar-schists and phyllites. Quartzites, white marbles and Fe-dolomites are sometimes intercalated. Due to the lack of marker horizons and intense imbrication with overlying phyllites, a detailed lithostratigraphic section has not been established. The structural details of the section are shown in Fig. 15.

Mafic schists are often laminated. The layers are mm to cm thick and are composed of chlorite-epidote, chlorite-actinolite-epidote and quartz-albite-epidote. In these layers phenocrysts of plagioclase and brown basaltic hornblende occur which are regarded as primary volcanic constituents. The lamination refers to different tuff, ash-tuff, crystal tuff and tuffite layers. Therefore, most of the mafic schists are pyroclastic in origin. Massive, partly feldspar porphyritic rocks which represent effusives are rare.

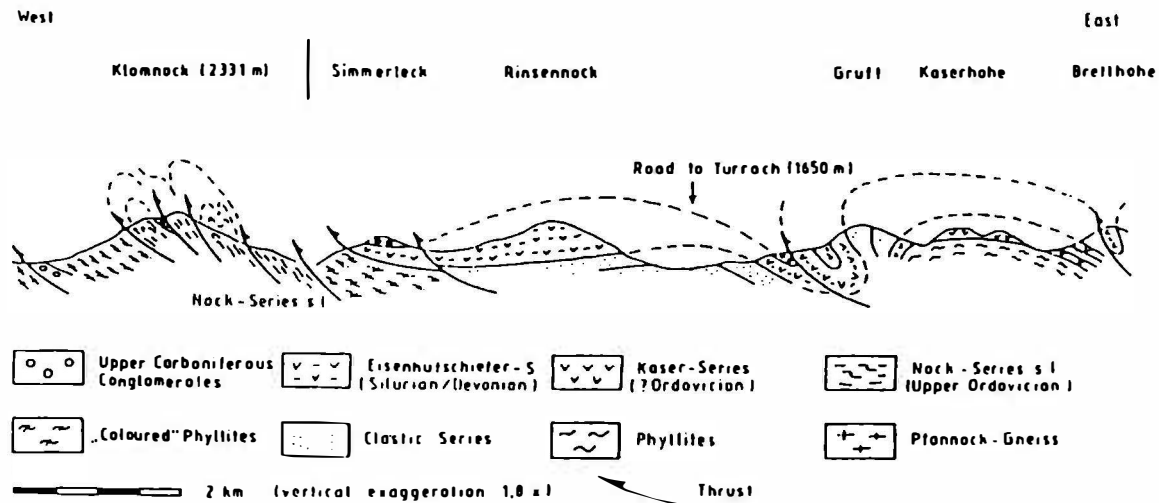


*Fig. 15: Schematic sketch of the Eisenhutschiefer series at the eastern and northeastern side of the Rinsennock (Loeschke, 1989; from Giese in Neubauer, ed., 1992).*

Pyroclastics are dominated by fine-grained ash tuffs and tuffites, in part reworked with turbiditic features. Coarse lapilli tuffs, volcanic breccias and agglomerates indicate proximal, shallow marine deposition close to a former eruption center. Basaltic conglomerates and 'tailed bombs' in volcanic breccias argue for temporarily subareal conditions of a volcanic island.

Pillow basalts have aphyric, vesicular and poiphyritic textures with phenocrysts of Ti-rich clinopyroxene and plagioclase. Intrusives show intersertal and intergranular textures and consist of Ti augite, plagioclase, kaersutite and red- to brown-colored biotite.

Chemical compositions clearly reveal an alkaline character. Pillow basalts classify mainly as alkali basalts and hawaiites. Intrusives are more evolved and have compositions of hawaiites and mugearites. Intermediate rocks show strong enrichment of incompatible



elements and are phonolytic trachytes. MORB normalised distribution patterns are in excellent accordance with alkali basalts of oceanic islands.

In conclusion, the Eisenhutschiefer series at the Rinsenock represents an alkali basalt hawaiite - mugearite - trachyte suite of an oceanic island volcano.

**Stop no. 32. Twengbach/Hohensaß. Paragneiss of the Bundschuh nappe.**

*Location: OEK 183 Radenthein. East of bridge over Twengbach (700 metres E bridge 880) on road between Bad Kleinkirchheim and Radenthein.*

F. NEUBAUER

The road cut exposes well recrystallized basement gneisses a few hundred metres beneath the ductile low angle normal fault beneath the Gurktal extensional allochthon. The gneisses contain The mineral assemblage plagioclase + quartz + muscovite + garnet + ilmenite ± pargonite. Geothermobarometry yielded ca. 600 and 10-11 kbar. These conditions were interpreted to represent Cretaceous peak P-T conditions. Metamorphic fabrics are entirely annealed.

**Further reading:** Koroknai et al. (1996).

**Stop no. 33. Acherlabach section. Periadriatic fault.**

*Location: OEK 196 Obertilliach. Lower Archerlabach brook ca. 2 km SE of Liesing. Follow road ca. 1.5 km east of Liesing towards bridge 919 over Gail river.*

F. NEMES, F. NEUBAUER

The Archerlabach brook exposes a ca. 400 m long N-S trending section across the E-W-trending Periadriatic Lineament (Fig. Xy). It represents the best and a complete exposure of the Periadriatic fault. From N to the S the Archerlabach section includes (Figs. 14, 15):

**1) Gailtal Metamorphic Complex:** Diaphthoritic garnet-bearing micaschists of the Gailtal Metamorphic Complex form the northern edge of the Periadriatic Lineament. The micaschists are well recrystallized under peak metamorphic conditions and include only a few features of retrogression, like chloritization along scarce fault planes. The subvertical foliation trends E. This mylonite is characterised by plastic deformation of minerals, shows evidence of internal grain rotation and grain size reduction. The occurrence of chloritized garnet and biotite, but also new grown fine-grained mica on shear planes indicates diaphthoritic overprint. Main features are well defined quartz bands and mica layers, and a granoblastic quartz fabric.

Also phyllonites are associated with micaschists in the Gailtal metamorphic Complex, and are characterised by plastic and cataclastic deformation. The strongly foliated fabric consists mainly of layers marked by sericite chlorite and quartz bands.

**2) Fault gouge:** A 40 m thick package of fault gouge indicating plastic deformation under semi-ductile conditions is one of the main deformation features in the cross section. This gouge is a paste-like rock material formed in a fault zone with less than 30% fragments (e.g., Groshong, 1988).

Development of calcirites is characterised by the occurrence of fault gouges and up to 30 m wide cataclastic bodies. The development of ultracataclasites is restricted to cataclastic bodies. All lithologies in the Archerlabach cross section are affected by cataclastic deformation, including micaschists from the Gailtal Metamorphic Complex, sandstones of the Gröden Formation and tonalites.

The fault gouges are of variable origin, the subhorizontal stretching lineation plunges gently to the east and indicates ductile to semi-ductile deformation in a strike-slip regime. Macrofabrics are characterised by tectonic deformation caused a planar fabric in unconsolidated material. Axial-plane mineral foliations are often found and also broken, rough slabs parallel to the foliation. These fault gouges have usually fine-grained matrix and a major component of clast orientation.

These rocks may have suffered large strain rates. These rocks are characterised by the presence of stylolites and solution cleavages, but relatively undeformed material in a clast-bearing matrix. Boudins are located between ductile layers and result from strain in the stiffer layers.

**3. Gröden Formation:** Sandstones of the Gröden Fm. and chlorite schists are folded in large isoclinal folds with subvertical axial plane and fold axes oriented parallel to the strike of the Periadriatic Lineament. These structures indicate massive N-S directed shortening perpendicular to the fault and lengthening of the rocks in strike-slip direction. The deformation in these sandstones is characterised by planar fabrics and broken elongated clasts parallel to the foliation. These deformed sandstones have a fine-grained matrix and a major component of preferred clast orientation.

Boudins are usually located between strongly foliated schists and are barrel-shaped in cross sections with veins forming the top and end of the barrel. The macroscopic features of these dark red sandstones and fine conglomerates are ductilely deformed conglomerate components, elongated components bedded in red-grey matrix. The foliation strikes E-W and is clearly developed in areas adjacent to the tonalitic body. The contact to the tonalites and adjacent rocks is clearly reflected by S-C fabrics and other strike-slip related structures.

**4. Chlorite schists:** Chlorite schists and black phyllites are interbedded between cataclastic tonalites and ductile deformed fault gouges. They are strongly affected by brittle deformation which is indicated by steep thrusts, backthrusts and oblique dextral strike-slip faults. The chlorite schists are derived from the adjacent tonalite and show cataclastic fabrics indicated by brittle fracturing, showing also often evidence of grain-size reduction and internal clast rotation. Deformation caused a well-developed planar fabrics, mineral shape foliations and asymmetrical kink bands.

**5. Tonalite:** The tonalite suite dips to the S, and is partly overthrust by black slates (Carnic Alps). The tonalites have a preferred orientation and planar subvertical. This is mainly characterised by parallel lengthened and recrystallized quartz grains with undulose extinction. Plagioclase shows post-crystallisation deformation with banded twin lamellae. The dynamically developed banding in the tonalites is presented by S-C fabrics and augen-like texture. Regarding the planar anisotropies in the rocks, these are a secondary formation due a strong deformation event. This is also indicated by the generally tectonic contact of the tonalitic bodies to the country rocks and post-magmatic semi-ductile deformation in tonalites and country rocks. Adjacent rocks were also deformed during the ductile deformation on tonalites and country rocks were mainly overprinted by low grade metamorphism.

The tonalites show clearly cataclastic macrofabrics showing also often evidence of grain-size reduction. The most distinctive textural features in cataclasites are grain fracture and grain size reduction. Grain sizes within the matrix are reduced to sizes of 5-25  $\mu\text{m}$ , larger fragments may be rounded.

**6. Black slate:** The black slates from the Carnic Alps show steep foliation and large isoclinal folds with axes parallel to the strike of the fault zone. Asymmetrical kink bands and symmetrical crenulations occur as macroscale deformation in unlithified slates. In these black slates often microlaminations and grain fabrics occur. This fissility of shale is significantly enhanced by fine-scale interbedding of clay bands, as the fissility of slate may have been caused

by closely spaced lamellae of different compositions. Dark banded phyllites are involved in massive cataclastic deformation which is expressed especially by S-C fabrics.

**Further reading:** Nemes (1997).

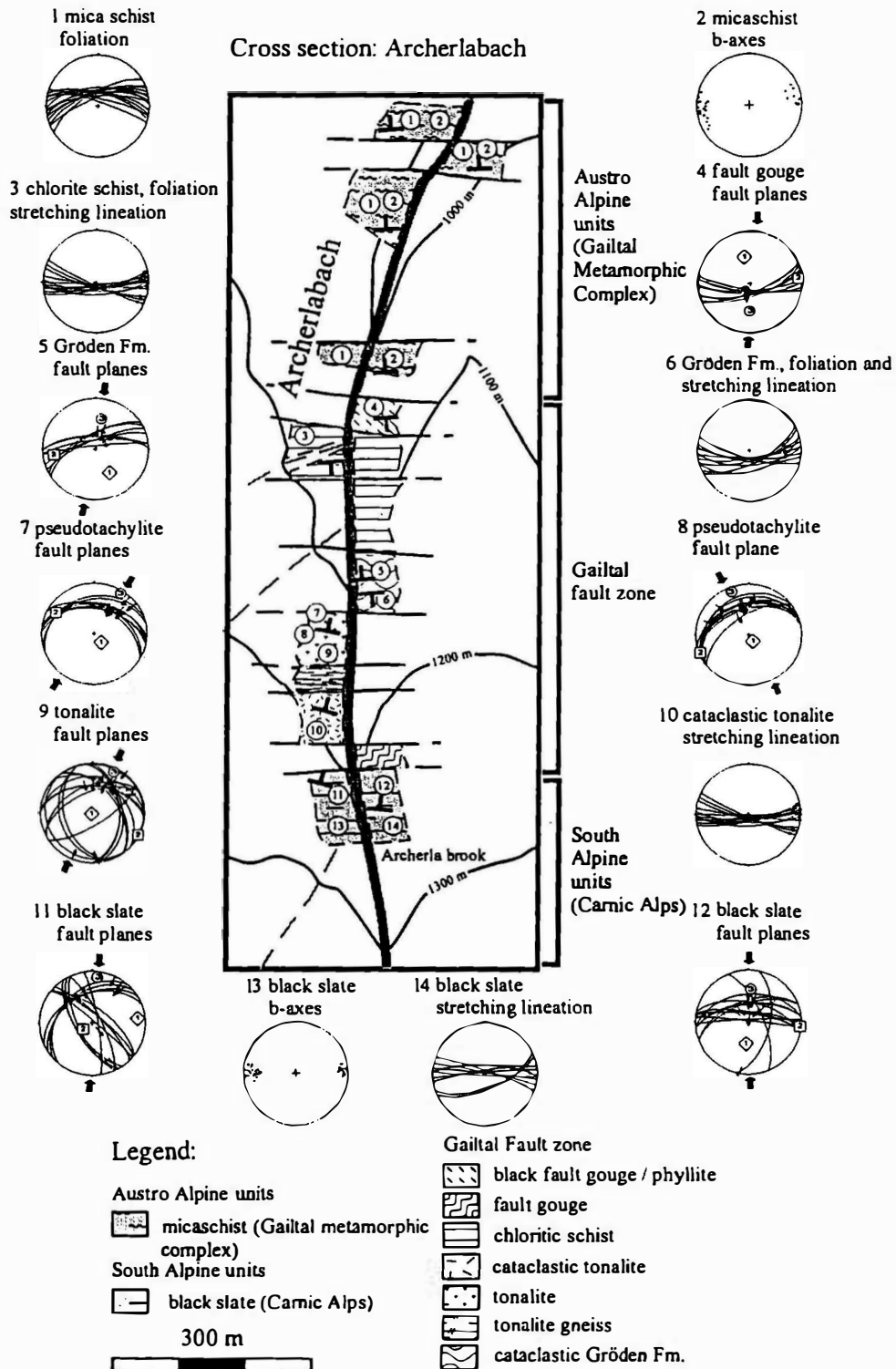


*Fig. 16. Map of the Archerla brook displaying a section through the entire Periadriatic fault (from Nemes, 1997).*

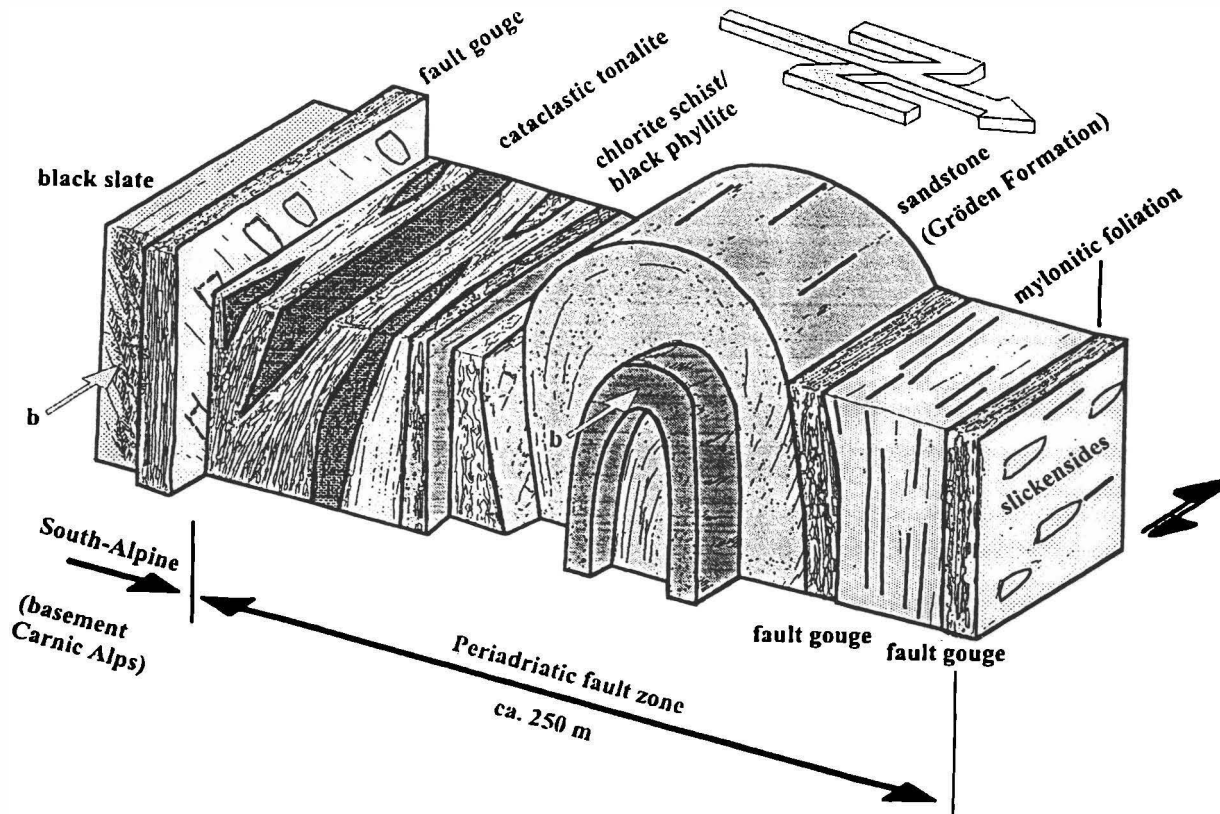


Fig. 17. Schematic diagram displaying structures exposed within the Archerlabach section.

**Stop 32. Tröpolach: Eder Limestone mit Alpine ductile fabrics along the Periadriatic fault**

*Location: OEK 198 Weißbriach. Road cut on Naßfeld road, ca. 200 metres S to Oselitzen near Tröpolach.*

F. NEMES, F. NEUBAUER

The outcrop exposes Steeply dipping. E-trending Eder limestone (metamorphic), actually a mylonite with a prominent foliation and a subhorizontal stretching lineation. The mylonite is interpreted to represent an expression of Oligocene deformation along the Periadriatic fault.

**Further reading:** Läufer et al. (1997); Nemes (1997).

**Stop no. 33. Hochwipfl Group**

*Location: OEK 198 Weißbriach. East Oselitzen river bed, below curve/bridge of Naßfeld road, ca. 700 metres S to Oselitzen near Tröpolach.*

D. MADER, F. NEUBAUER

The outcrop exposes greyish to dark siltstones and graywackes of the Hochwipfl Group (Early Carboniferous). The Hochwipfl Group is interpreted to represent the infilling of a synorogenic flysch basin on top of the Devonian carbonate platform.

**Further reading:** Mader (1998).

**Stop 34. Walking tour from saddle between Gartnerkofel and Garnitzenberg. Middle Triassic, Permian and Late Carboniferous of the Southalpine unit**

*Location: OEK 198 Weißbriach. Walking tour down from the saddle between Gartnerkofel and Garnitzenberg.*

A walking tour down from the top station of the cable-car down to Naßfeld saddle allows to study Middle and Lower Triassic, Permian and Late Carboniferous formations. The section starts with massive Ladinian Schlern Dolomite, shallow water deposits,

**References**

- Becker, B., The Structural Evolution of the Radstadt Thrust System, Eastern Alps, Austria - Kinematics, Thrust Geometries, Strain Analysis, Diss., Univ. Tübingen, 76, 1993.
- Behrmann, J.H., Zur Kinematik der Kontinentkollision in den Ostalpen, Geotekt.Forsch., 76, 1-180, 1990.
- Bernoulli, D., and Jenkyns, H.C., 1970, A Jurassic Basin: The Glasenbach Gorge, Salzburg, Austria. Verh. Geol. Bundesanst., 1970, 504-531.
- Böhm, F., and Brachert, T.C., 1993, Deep-water stromatolites and Frutexites Maslov from the Early and Middle Jurassic of S-Germany and Austria. Facies, 28, 145-168.
- Böhm, F., Dommergues, J.L., and Meister, C., 1995, Breccias of the Adnet Formation: indicators of a Mid-Liassic tectonic event in the Northern Calcareous Alps (Salzburg, Austria). Geol. Rundschau, 84, 272-286.
- Clar, E. 1965. Zum Bewegungsbild des Gebirgsbaues der Ostalpen. Zeitschr. Deutsch. Geol. Ges., 116, 267-291.
- Cliff, R.A., 1981. Pre-Alpine History of the Pennine Zone in the Tauern Window, Austria: U-Pb and Rb-Sr Geochronology. Contrib. Mineral. Petrol., 17, 262-266.
- Cliff, R.A. and Cohen, A., 1980. Uranium-lead isotope systematics in a regionally metamorphosed tonalite from the Eastern Alps. Earth Planet. Sci. Lett., 50, 211-218.

- Cliff, R.A., Norris, R.J., Oxburgh, E.R. and Wright, R.C., 1971. Structural, Metamorphic and Geochronological Studies in the Reißbeck and the Southern Ankogel Groups, the Eastern Alps. *Jb. Geol. Bundesanst.*, 114, 121-272.
- Cliff, R.A., Droop, G.T.R. and Rex, D.C., 1995. Alpine metamorphism in the south-east Tauern Window, Austria. U. heating, cooling and uplift rates. *J. Metam. Geol.*, 3, 403-415.
- Decker, K., Meschede, M. and Ring, U., 1993. Fault slip analysis along the northern margin of the Eastern Alps (Molasse, Helvetic nappes, North and South Penninic flysch, and the Northern Calcareous Alps). *Tectonophysics*. 223, 291-312.
- Egger, H., 1990. Zur paläogeographischen Stellung des Rhenodanubischen Flysches (Neokom-Eozän) der Ostalpen. *Jb. Geol. Bundesanst.*, 133, 147-155.
- Egger, H., 1992. Zur Geodynamik und Paläogeographie des Rhenodanubischen Flysches (Neokom - Eozän) der Ostalpen. *Z. dt. geol. Ges.*, 143, 51-65.
- Egger, H., 1995: Die Lithostratigraphie der Altlengbach-Formation und der Anthering Formation im Rhenodanubischen Flysch (Ostalpen, Penninikum). *N. Jb. Geol. Paläont. Mh.*, 196, 69-91.
- Egger, H., 1996: Geologische Karte der Republik Österreich 1 : 50.000, 66 Gmunden. Geologische Bundesanstalt, Wien.
- Egger, H., 1997. Das sinstrale Innsbruck-Salzburg-Amstetten-Blattverschiebungssystem: ein weiterer Beleg für die miozäne laterale Extrusion der Ostalpen. *Jb. Geol. Bundesanst.*, 140, 47-50.
- Egger, H., Lobitzer, H., Polesny, H. and Wagner, L.R., 1997: Cross section through the oil and gas-bearing Molasse Basin into the Alpine units in the area of Salzburg, Austria. AAPG Vienna '97, Field Trip Notes, Trip no. 1, 104 p., Vienna.
- Elsner, R., 1991. Geologie des Tauern-Südostrandes und geotektonische Konsequenzen, *Jahrb. Geol. Bundesanst.*, 134, 561-645.
- Exner, Ch., 1980. Geologie der Hohen Tauern bei Gmünd in Kärnten. *Jahrb. Geol. Bundesanst.*, 123, 343-410.
- Exner, Ch., 1982. Geologie der zentralen Hafnergruppe (Hohe Tauern). *Jahrb. Geol. Bundesanst.*, 125, 51-154.
- Faupl, P. and Tollmann, A., 1979. Die Roßfeldschichten: Ein Beispiel für Sedimentation im Bereich einer tektonisch aktiven Tiefseerinne aus der kalkalpinen Unterkreide. *Geol. Rundschau*, 68, 93-120.
- Finger, F. and Steyrer, H., 1988. Granite-types in the Hohe Tauern (Eastern Alps, Austria) –Some aspects on their correlation to Variscan plate tectonic processes. *Geodynamica Acta*, 2, 75-87.
- Fischer, A.G., and Garrison, R.E., 1967, Carbonate lithification on the seafloor. *J. Geol.*, 75, 488-496.
- Freimüller, St., 1998. Die strukturelle Entwicklung der Rhenodanubischen Flischzone zwischen Attersee und Traunsee, Oberösterreich. MSc thesis, University of Salzburg.
- Frimmel, H., 1986. Isotopengeologische Hinweise für die paläogeographische Nachbarschaft von Gurktaler Decke (Oberostalpin) und dem Altkristallin, östlich der Hohen Tauern (Österreich). Schweiz. Mineral. Petrogr. Mitt., 66, 193-208.
- Frimmel, H., 1988. Metagranitoide am Westrand der Gurktaler Decke (Oberostalpin) - Genese und paläotektonische Interpretation. *Jahrb. Geol. Bundesanst.*, 131, 575-592.
- Fritz, A. and Boersma, M., 1984. Beitrag zur Oberkarbonflora der Königstuhl-Nordwand, Aufsammlung Dr. E. Ebermann. - *Carinthia II*, 174/94, 267-286.
- Fritz, A., Boersma, M. and Krainer, K., 1990. Steinkohlenzeitliche Pflanzenfossilien aus Kärnten. *Carinthia U, Sonderheft 49*, 1-189.
- Garrison, R.E. and Fisher, A.G., 1969. Deep-water limestones and radiolarites of the Alpine Jurassic. *Soc. Econ. Paleont. Mineral. Spec. Publ.*, 14, 20-55.
- Genser, J. and Neubauer, F., 1989. Low angle normal faults at the eastern margin of the Tauern window (Eastern Alps). *Mitt. Österr. Geol. Ges.*, 81(1988), 233-248.
- Genser, J., 1992. Struktur- Gefüge- und Metamorphoseentwicklung einer kollisionalen Plattengrenze: Das Beispiel des Tauernostrandes (Kärnten/Österreich). Unpubl. Diss. Univ. Graz, 379 pp.
- Germann, K., 1972, Verbreitung und Entstehung Mangan-reicher Gesteine im Jura der Nördlichen Kalkalpen. *Tschermaks Mineral. Petrogr. Mitt.*, 17, 23-150.
- Giese, U., 1988. Lower Paleozoic volcanic evolution at the northwestern border of the Gurktal nappe Upper Austroalpine eastern Alps. *Schweiz. Mineral. Petrogr. Mitt.* 68, 381-396.

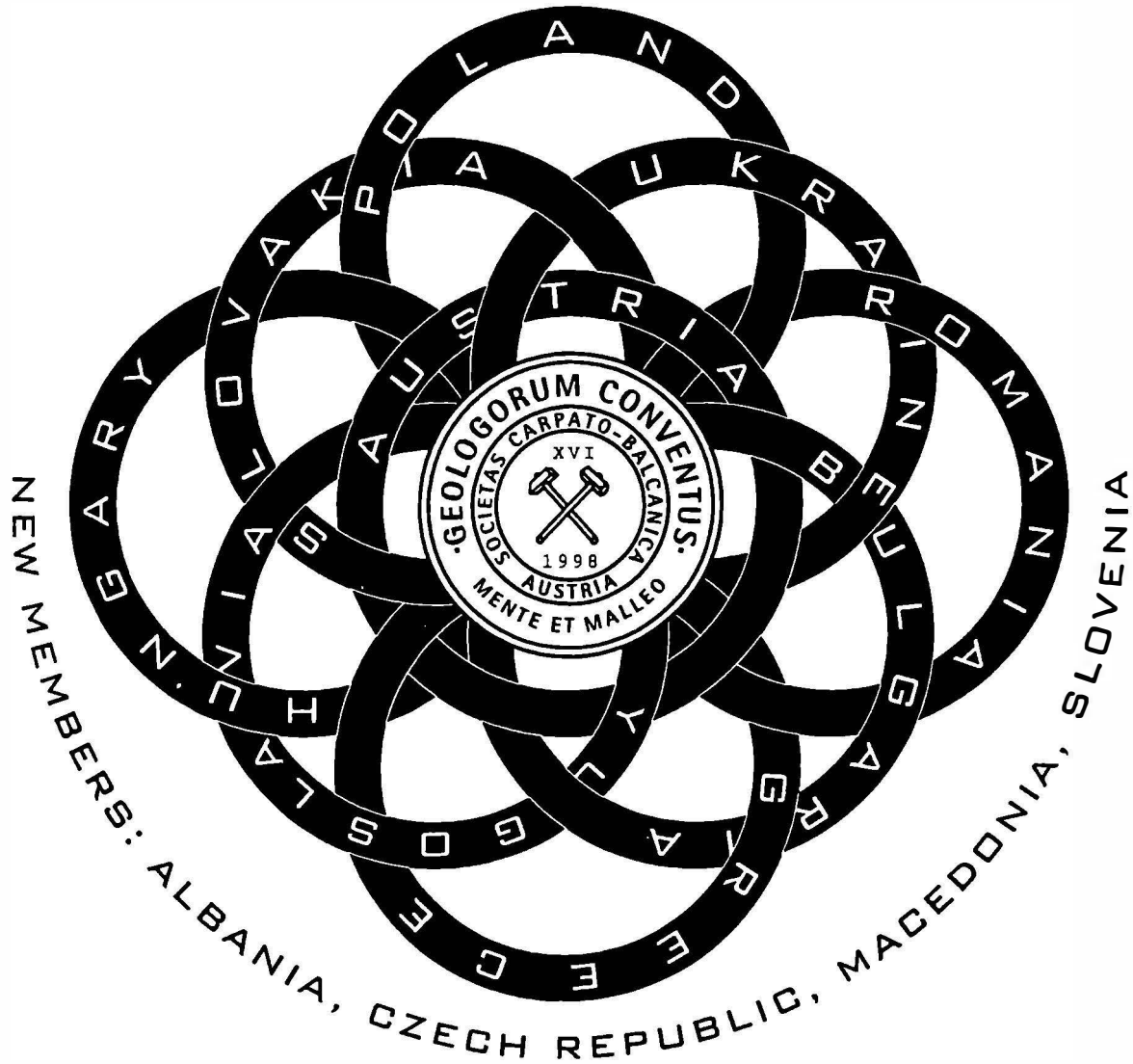
- Groshong, R.H., 1988. Low-temperature deformation mechanisms and their interpretation. *Geol. Soc. Amer. Bull.*, 100, 1329-1360.
- Gosen, W. von, 1989. Gefügeentwicklungen, Metamorphosen und Bewegungen der ostalpinen Baueinheiten zwischen Nockgebiet und Karawanken (Österreich). *Geotekt. Forsch.*, 72, 1-247
- Hallam, A., 1967. Sedimentology and palaeogeographic significance of certain red limestones and associated beds in the Lias of the Alpine region. *Scottish J. Geol.*, 3, 195-220.
- Hawkesworth, C.J., 1976. Rb/Sr geochronology in the Eastern Alps. *Contrib. Mineral Petrol.*, 54, 225-244.
- Heinisch, H. and Sprenger, W., 1988. Mehrphasige Deformation und Pseudotachylitbildung im Gailtalkristallin und am Periadriatischen Lineament zwischen Sillian und Kötschach-Mauthen (Osttirol/Kärnten, Österreich). *Erlanger Geol. Abh.*, 116, 41-52.
- Heizmann, P., 1985. Kakirite, Kataklastite, Mylonite - Zur Nomenklatur der Metamorphite mit Verformungsgefügen. *Ecl. Geol. Helv.*, 78, 273-286.
- Holub, B., 1988. Geologie, Petrologie und Intrusionsfolge der Zentralgneise im Großelendtal (Hochalm-Ankogel-Gruppe, Kärnten). Unpubl. PhD thesis Univ. of Salzburg.
- Holub, B. and Marschallinger, R., 1989. Die Zentralgneiße im Hochalm-Ankogel-Massiv (östliches Tauernfenster) Teil I: Petrographische Gliederung und Intrusionsfolge. *Mitt. Österr. Geol. Ges.*, 81, 5-31.
- Hudson, J.D., and Jenkyns, H.C., 1969. Conglomerates in the Adnet Limestones of Adnet (Austria) and the origin of the 'Scheck'. *N. Jb. Geol. Paläont. Mh.*, 1969, 552-558.
- Jenkyns, H.C., 1974. Origin of red nodular limestones (Ammonitico Rosso, Knollenkalke) in the Mediterranean Jurassic: a diagenetic model. In: K.J., Hsü, and H.C., Jenkyns (eds.), *Pelagic Sediments: on Land and under the Sea. Spec. Publ. Intern. Assoc. Sediment.*, 1, 249-271.
- Jurgan, H., 1969. Sedimentologie des Lias der Berchtesgadener Kalkalpen. *Geol. Rundsch.*, 58, 464-501.
- Krainer, K., 1984. Sedimentologische Untersuchungen an permischen und untertriadischen Sedimenten des Stangalm-Mesozoikums (Kärnten/Österreich). *Jahrb. Geol. Bundesanst.*, 127, 159-179.
- Krainer, K., 1987. Das Perm der Gurktaler Decke: eine sedimentologische Analyse. *Carinthia II*, 177/97, 49-92.
- Krainer, K., 1989a. Molassesedimentation im Oberkarbon der Ostalpen am Beispiel der Stangnock Formation am NW-Rand der Gurktaler Decke (Österreich). *Zentralbl. Geol. Paläont. Teil 1*, 1988, 807-820.
- Krainer, K., 1989b. Die fazielle Entwicklung der Oberkarbonsedimente (Stangnock Formation)
- Kruhl, J.H., 1993. The P-T-d development at the basement-cover boundary in the north-east Tauern Window (Eastern Alps): Alpine continental collision. *J. metamorphic Geol.*, 11, 31-47.
- Kurz, W., Neubauer, F. and Genser, J., 1996. Kinematics of Penninic nappes (Glockner Nappe and basement-cover nappes) in the Tauern Window (Eastern Alps, Austria) during subduction and Penninic-Austroalpine collision. *Ecl. geol. Helv.*, 89, 573-605.
- Läufer, A., 1996. Variscan and Alpine tectonometamorphic evolution of the Carnic Alps (Southern Alps) - Structural analysis, Illite crystallinity, K-Ar and Ar-Ar geochronology. - *Tübinger Geowiss.Arb.*, Reihe A, Bd. 26, 1-126.
- Läufer, A., Frisch, W., Steinitz, G. and Loeschke, J., 1997. Exhumed fault-bounded blocks along the Periadriatic lineament: the Eder unit (Carnic Alps, Austria). *Geol. Rundschau*, 86, 612-626.
- Leiss, O., 1988. Die Kontrolle des Sedimentationsgeschehens und der Biofazies durch evolutive orogentische Prozesse in den Nördlichen Kalkalpen am Beispiel von Gosauvorkommen (Coniac-Santon). *Documenta Naturae*, 43, 1-95.
- Loeschke, J., 1989. Lower Paleozoic volcanism of the Eastern Alps and its geodynamic implications. *Geol. Rdsch.*, 78, 599-616.
- Mader, D., 1998. <sup>40</sup>Ar/<sup>39</sup>Ar dating of detrital white mica and provenance analyses of Palaeozoic sandstones in the Carnic Alps. Unpubl. MSc. thesis Fac. of Science, University of Salzburg, pp. 98, Salzburg.
- Marschallinger, R. and Holub, B., 1991. Die Zentralgneise im Hochalm-Ankogel-Massiv (östliches Tauernfenster) Teil II: Geochemische und zirkontypologische Charakteristik. *Mitt. Österr. Geol. Ges.*, 82, 19-48.

- Mauritsch, H.J., and Frisch, W., 1978, Paleomagnetic Data from the Central Part of the Northern Calcareous Alps, Austria. *J. Geophysics*, 44, 623-637.
- Meschede, M. and Decker, K., 1992: Störungsflächenanalyse entlang des Nordrandes der Ostalpen - ein methodischer Vergleich. *Z. dt. Geol. Ges.*, 144, 419-433.
- Nemes, F. (1996): Kinematics of the Periadriatic Fault in the Eastern Alps - evidence from structural analysis, fission track dating and basin modelling. - unpubl. Ph.D. thesis, Naturwissenschaftliche Fakultät, University of Salzburg, 225 pp., Salzburg.
- Neubauer, F., ed., 1992. ALCAPA Field Guide - The eastern Central Alps of Austria. 245 p., IGP/KFU Graz, Graz.
- Neubauer, F. and Genser, J., 1990. Architektur und Kinematik der östlichen Zentralalpen - eine Übersicht. *Mitt. naturwiss. Ver. Steiermark*, 120, 203-219.
- Neubauer, F. and Pistotnik, J., 1984. Das Altpaläozoikum und Unterkarbon des Gurktaler Deckensystems (Ostalpen) und ihre paläogeographischen Beziehungen. *Geol. Rdsch.*, 73, 149-174.
- Neubauer, F. and Schweigl, J., 1996. Von den Nördlichen Kalkalpen zur Molassezone in der Umgebung von Salzburg. *Exkursionsführer 6. Symposium für tektonik, Strukturgeologie und Kristallingeologie 14.-15. April 1996*, p. 1-33, Salzburg.
- Piller, W., Kleemann, K. and Friebe, J.G., 1991. Middle Miocene Reefs and related facies in Eastern Austria. VI. International Symposium on Fossil Cnidaria including Archaeocyatha and Porifera, Münster 1991, Excursion B4 Guidebook, 47 pp.
- Pistotnik, J., 1974. Zur Geologie des NW-Randes der Gurktaler Masse (Stangalm-Mesozoikum, Österreich). *Mitt. Geol. Ges. Wien*, 66/67 (1973/74), 127-141.
- Pistotnik, J., 1976. Ein Transgressionskontakt des Stangalm-Mesozoikums. *Carinthia II*, 166/86, 127-131.
- Plöching, B. (ed.), 1987, Geologische Karte der Republik Österreich 1:50000, Blatt 94, Hallein. Geologische Bundesanstalt / Wien.
- Plöching, B. (ed.), 1982, Geologischer Karte der Republik Österreich 1:50000, 95 St. Wolfgang im Salzkammergut. Geologische Bundesanstalt / Wien.
- Plöching, B., 1983, Salzburger Kalkalpen. 144 pp., Gebrüder Bornträger / Stuttgart.
- Prey, S. (ed.), 1969. Geologische Karte der Umgebung der Stadt Salzburg, 1:50000. Geologische Bundesanstalt / Wien.
- Ratschbacher, L. and Neubauer, F., 1989. West-directed decollement of Austro-Alpine cover nappes in the eastern Alps: geometrical and rheological considerations. *Geol. Soc. Spec. Publ.*, 45, 243-262.
- Ratschbacher, L., Frisch, W., Neubauer, F., Schmid, S.M. and Neugebauer, J., 1989. Extension in a compressional orogen: the eastern Alps. *Geology*, 17: 404-407.
- Ratschbacher, L., Schmid, S.M., Frisch, W. and Neubauer, F., 1990. Reply on the Comment of S.R. Wallis to "Extension in compressional orogenic belts: the eastern Alps. *Geology*, 18, 675-676.
- Schlöser, H., Kullmann, J. and Loeschke, J., 1990. Korallen-führendes Unterkarbon auf der Brunnachhöhe (Nockgebiet, Gurktaler Decke, (Österreich). *Carinthia II*, 180/100: 643-650.
- Schmidt, M. (1992): Amphibole composition in tonalite as a function of pressure: an experimental calibration of the Al-in-hornblende barometer. *Contrib. Mineral. Petrol.*, 110, 304-310.
- Schönlaub, H.P., ed., 1997. IGCP - 421 Inaugural Meeting Vienna, Guidebook. *Ber. Geol. Bundesanst.*, 1-134.
- Sprenger, W. and Heinisch, H., 1992. Late Oligocene to Recent brittle transpressive deformation along the Periadriatic Lineament in the Lesach Valley (Eastern Alps): remote sensing and paleostress-analysis. - *Annales Tectonicae*, 6, 134-149.
- Stock, P., 1989. Zur antithetischen Rotation der Schieferung in Scherbandgefügen - ein kinematisches Deformationsmodell mit Beispielen aus der südlichen Gurktaler Decke (Ostalpen). *Franfurter Geowiss. Arb.*, A7, 1-155.
- Sylvester, A.G., 1988. Strike-slip faults. *Geol. Soc. Am. Bull.*, 8, 1666-1703.
- Tenčov, Y., 1978. Carboniferous flora from Brunnacherhöhe, Kärnten, Austria. *Geologica Balcanica*, 8, 105-110.



- Theiner, U., 1987. Das Kristallin der NW-Nockberge. Eine kristallingeologische Neuuntersuchung. Unpubl. PhD thesis University of Vienna, 153 pp.
- Tollmann, A., 1975. Die Bedeutung des Stangalm-Mesozoikums in Kärnten für die Neugliederung des Oberostalpins in den Ostalpen. N. Jb. Geol. Paläont. Mh., 150, 19-43.
- Tollmann, A., 1976, Analyse des klassischen nordalpinen Mesozoikums. 580 pp., Deuticke / Wien.
- Unzog, W. (1989): Schertektonik im Gailtalkristallin und an seiner Begrenzung. - unpubl. Ph.D. thesis, Karl-Franzens-University Graz, 204 pp., Graz.
- Vavra, G. and Frisch, W., 1989: Pre-Variscan back-arc and island arc magmatism in the Tauern Window (Eastern Alps). Tectonophysics, 169, 271-280.
- Venturelli, G., Thope, R.S., Dal Piaz, G.V. Del Moro, A., and Potts, P.J., 1984. Petrogenesis of calc-alkaline, shoshonitic and associated ultrapotassic Oligocene volcanic rocks from the Northwestern Alps, Italy. - Contr. Min. Pet., 86, 209-220.
- Venturini, C. (1990): Geologia delle Alpi Carniche centro-orientali. Museo Friul. Stor. Nat., 36, 1-220.
- von Blanckenburg, F. and Davies, J.H., 1995. Slab breakoff: A model for syncollisional magmatism and tectonics in the Alps. Tectonics, 14, 120-131.
- Wagreich, M., Böhm, F. and Lobitzer, H., 1996. Exkursion B1 - Sedimentologie des kalkalpinen Mesozoikums in Salzburg und Oberösterreich (Jura, Kreide). Berichte Geol. Bundesanst., 33, 1-59.
- Wang, X. and Neubauer, F., 1998. Orogen-parallel strike-slip faults bordering metamorphic core complexes: the Salzach-Enns fault zone in the Eastern Alps. J. Struct. Geol., 20, 799-818.
- Wise, D.U., Dunn, D.E., Engelder, J.T., Geiser, P.A., Hatcher, R.D., Kish, S.A., Odom, A.L. and Schamel, S., 1984. Fault related rocks: Suggestions for terminology. Geology, 12, 391-394.

# CARPATHIAN-BALKAN GEOLOGICAL ASSOCIATION



## XVI CONGRESS VIENNA/AUSTRIA

AUGUST 30<sup>TH</sup> - SEPTEMBER 2<sup>ND</sup>, 1998  
UNIVERSITY OF VIENNA, GEOCENTER

